ISSN 2500-316X (Online)

RUSSIAN TECHNOLOGICAL JOURNAL

РОССИЙСКИЙ ТЕХНОЛОГИЧЕСКИЙ ЖУРНАЛ

Information systems.
Comruter sciences.
Issues of information security

Multiple robots (robotic centers) and systems.
Remote sensing and non-destructive testing

Modern radio engineering and telecommunication systems

Micro- and nanoelectronics.
Condensed matter physics

Analytical instrument engineering and technology

Mathematical modeling

Economics of knowledge-intensive and high-tech enterprises and industries.
Management in organizational systems

Product quality management. Standardization

Philosophical foundations of technology and society

12+
www.rtj-mirea.ru

МИРЭА
Российский технологический университет

9(5) 2021

ISSN 2500-316X (Online)

RUSSIAN TECHNOLOGICAL JOURNAL

РОССИЙСКИЙ ТЕХНОЛОГИЧЕСКИЙ ЖУРНАЛ

- Information systems. Computer sciences. Issues of information security
- Multiple robots (robotic centers) and systems. Remote sensing and non-destructive testing
- Modern radio engineering and telecommunication systems
- Micro- and nanoelectronics. Condensed matter physics
- Analytical instrument engineering and technology
- Mathematical modeling
- Economics of knowledge-intensive and high-tech enterprises and industries. Management in organizational systems
- Product quality management. Standardization
- Philosophical foundations of technology and society

- Информационные системы. Информатика. Проблемы информационной безопасности
- Роботизированные комплексы и системы. Технологии дистанционного зондирования и неразрушающего контроля
- Современные радиотехнические и телекоммуникационные системы
- Микро- и наноэлектроника. Физика конденсированного состояния
- Аналитическое приборостроение и технологии
- Математическое моделирование
- Экономика наукоемких и высокотехнологичных предприятий и производств. Управление в организационных системах
- Управление качеством продукции. Стандартизация
- Мировоззренческие основы технологии и общества

Russian Technological Journal
2021, Vol. 9, No. 5

Russian Technological Journal
2021, том 9, № 5

https://www.rtj-mirea.ru

МИРЭА
Российский технологический университет

https://doi.org/10.32362/2500-316X

ISSN 2500-316X (Online)

Russian Technological Journal 2021, Vol. 9, No. 5

Publication date September 30, 2021.

The peer-reviewed scientific and technical journal highlights the issues of complex development of radio engineering, telecommunication and information systems, electronics and informatics, as well as the results of fundamental and applied interdisciplinary researches, technological and economical developments aimed at the development and improvement of the modern technological base.

Periodicity: bimonthly.
The journal was founded in December 2013. The titles were «Herald of MSTU MIREA» until 2016 (ISSN 2313-5026) and «Rossiiskii tekhnologicheskii zhurnal» from January 2016 until July 2021 (ISSN 2500-316X).

Founder and Publisher:
Federal State Budget
Educational Institution
of Higher Education
«MIREA – Russian Technological University»
78, Vernadskogo pr., Moscow, 119454 Russia.

**The journal is included into the List of peer-reviewed science press of the State Commission for Academic Degrees and Titles of Russian Federation.
The Journal is included in RSL (Russian State Library), Russian citation index, elibrary, Socionet, Directory of Open Access Journals (DOAJ), Directory of Open Access Scholarly Resources (ROAD), Google Scholar, Open Archives Initiative, Ulrich's International Periodicals Directory.**

Registration Certificate ПИ № ФС 77 - 81733, issued in August 19, 2021 by the Federal Service for Supervision of Communications, Information Technology, and Mass Media of Russia.

ISSN 2500-316X (Online)

Russian Technological Journal 2021, том 9, № 5

Дата опубликования 30 сентября 2021 г.

Научно-технический рецензируемый журнал освещает вопросы комплексного развития радиотехнических, телекоммуникационных и информационных систем, электроники и информатики, а также результаты фундаментальных и прикладных междисциплинарных исследований, технологических и организационно-экономических разработок, направленных на развитие и совершенствование современной технологической базы.

Периодичность: один раз в два месяца.
Журнал основан в декабре 2013 года. До 2016 г. издавался под названием «Вестник МГТУ МИРЭА» (ISSN 2313-5026), а с января 2016 г. по июль 2021 г. под названием «Российский технологический журнал» (ISSN 2500-316X).

Учредитель и издатель:
федеральное государственное бюджетное
образовательное учреждение
высшего образования
«МИРЭА – Российский технологический университет»
119454, РФ, г. Москва, пр-т Вернадского, д. 78.

Журнал входит в Перечень ведущих рецензируемых научных журналов ВАК РФ, в которых должны быть опубликованы основные научные результаты диссертаций на соискание ученой степени кандидата наук и доктора наук, индексируется в РГБ, РИНЦ, elibrary, Соционет, Directory of Open Access Journals (DOAJ), Directory of Open Access Scholarly Resources (ROAD), Google Scholar, Open Archives Initiative, Ulrich's International Periodicals Directory.

Свидетельство о регистрации СМИ ПИ № ФС 77 - 81733 от 19.08.2021 г. выдано Федеральной службой по надзору в сфере связи, информационных технологий и массовых коммуникаций (Роскомнадзор).

https://www.rtj-mirea.ru

Editorial Board

Редакционная коллегия

Contents

Содержание

Russian Technological Journal. 2021;9(5):7–13 ISSN 2500-316X (Online)

Information systems. Computer sciences. Issues of information security

Информационные системы. Информатика. Проблемы информационной безопасности

UDC 658
https://doi.org/10.32362/2500-316X-2021-9-5-7-13

RESEARCH ARTICLE

The structure of the local detector of the reprint model of the object in the image

Alexander A. Kulikov @

MIREA – Russian Technological University, Moscow, 119454 Russia
@ Corresponding author, e-mail: tibult41@gmail.com

Abstract. Currently, methods for recognizing objects in images work poorly and use methods that are intellectually unsatisfactory. The existing identification systems and methods do not completely solve the problem of identification, namely, identification in difficult conditions: interference, lighting, various changes on the face, etc. To solve these problems, a local detector for the reprint model of the object in the image is developed and described. A transforming autocoder (TA), a model of a neural network, has been developed for a local detector. This neural network model is a subspecies of the general class of neural networks of reduced dimension. The local detector is able, in addition to determining the modified object, to determine the original shape of the object as well. A special feature of TA is the representation of image sections in a compact form and the evaluation of the parameters of the affine transformation. The transforming autocoder is a heterogeneous network (HS) consisting of a set of networks of smaller dimension, called a capsule. Artificial neural networks should use local capsules that perform some rather complex internal calculations on their inputs, and then encapsulate the results of these calculations in a small vector of highly informative outputs. Each capsule learns to recognize an implicitly defined visual object in a limited area of viewing conditions and deformations, and it outputs both the probability that the object is present in its limited area, and a set of «instance parameters» that can include the exact pose, lighting, and deformation of the visual object relative to an implicitly defined canonical version of this object. The main advantage of capsules that output instance parameters is a simple way to recognize entire objects by recognizing their parts. The capsule can learn to display the pose of its visual object in a vector that is linearly related to the «natural» representations of the pose that are used in computer graphics. There is a simple and highly selective test for whether visual objects represented by two active capsules A and B have the correct spatial relationships for activating a higher-level capsule C. The transforming auto-encoder solves the problem of identifying facial images in conditions of interference (noise), changes in illumination and angle.

Keywords: neural network, image recognition, pattern recognition, identification model

• **Submitted:** 25.03.2021 • **Revised:** 31.03.2021 • **Accepted:** 26.05.2021

For citation: Kulikov A.A. The structure of the local detector of the reprint model of the object in the image. *Russ. Technol. J.* 2021;9(5):7–13. https://doi.org/10.32362/2500-316X-2021-9-5-7-13

Financial disclosure: The author has no a financial or property interest in any material or method mentioned.

The author declares no conflicts of interest.

НАУЧНАЯ СТАТЬЯ

Структура локального детектора модели репринта объекта на изображении

А.А. Куликов @

МИРЭА – Российский технологический университет, Москва, 119454 Россия
@ *Автор для переписки, e-mail: tibult41@gmail.com*

Резюме. Задача распознавания объектов на изображениях является актуальной в настоящее время, поскольку существующие системы и методы не решают полностью проблему идентификации в сложных условиях: помехи, освещение, различные изменения на лице и т.д. С целью решения этой задачи разработан и описан локальный детектор для модели репринта объекта на изображении. Для локального детектора разработан трансформирующий автокодер (ТА) – модель нейронной сети. Данная модель является подвидом общего класса нейронных сетей снижения размерности. Локальный детектор способен, помимо определения измененного объекта, также определить и изначальную форму объекта. Особенностью ТА является представление участков изображения в компактном виде и проведение оценки параметров аффинной трансформации. Трансформирующий автокодер представляет собой гетерогенную сеть (ГС), состоящую из множества сетей меньшей размерности, называемых капсулами. Искусственные нейронные сети должны использовать локальные капсулы, которые выполняют некоторые довольно сложные внутренние вычисления на своих входах, а затем инкапсулируют результаты этих вычислений в небольшой вектор высокоинформативных выходов. Каждая капсула учится распознавать неявно определенный визуальный объект в ограниченной области условий просмотра и деформаций. Она выводит как вероятность того, что объект присутствует в своей ограниченной области, так и набор «параметров экземпляра», которые могут включать точную позу, освещение и деформацию визуального объекта относительно неявно определенной канонической версии этого объекта. Главное преимущество капсул, выводящих параметры экземпляра, заключается в простом способе распознавания целых объектов путем распознавания их частей. Капсула может научиться выводить позу своего визуального объекта в вектор, линейно связанный с «естественными» представлениями позы, которые используются в компьютерной графике. Существует простой и высокоселективный тест на то, имеют ли визуальные объекты, представленные двумя активными капсулами, правильные пространственные отношения для активации капсулы более высокого уровня. Трансформирующий автокодер решает проблему идентификации лицевых изображений в условиях помех (шумности), изменения освещенности и ракурса.

Ключевые слова: нейронная сеть, распознавание изображений, распознавание образов, модель идентификации

• **Поступила:** 25.03.2021 • **Доработана:** 31.03.2021 • **Принята к опубликованию:** 26.05.2021

Для цитирования: Куликов А.А. Структура локального детектора модели репринта объекта на изображении. *Russ. Technol. J.* 2021;9(5):7–13. https://doi.org/10.32362/2500-316X-2021-9-5-7-13

Прозрачность финансовой деятельности: Автор не имеет финансовой заинтересованности в представленных материалах или методах.

Автор заявляет об отсутствии конфликта интересов.

INTRODUCTION

Existing systems and methods for object recognition in images do not completely solve the problem of identification, specifically the identification under complex conditions: interference, illumination, changes in faces, changes in wide-angle shooting, etc. Presently, employing sets of nonlinear functions for activation of used neurons represents a laborious and inaccurate process. This statement—supported by a large number of publications [1–13] devoted to this problem—says that the problem is topical and is not solved yet. Corresponding methods, algorithms, and systems either require high computational power, or employing a programmed, continuously operating memory device in “clever” cameras that leads to growth in expenses of the entire system.

LOCAL DETECTOR

To solve the above problem of identification of facial images (and not only those), a local detector (LD) is developed for the model of the object reprint in the image [14]. LD is an elementary unit of the model of the object reprint (MOR) in the image. For the local detector, a transforming autocoder (TA)—the model of a neural network—has been developed. This model represents a subtype of a general class of neural networks of reduced dimension. Besides identification of a changed object, LD is capable of determining initial shape of the object. One of the features of TA is its ability represent parts of the image in a compact form and evaluate the parameters of affine transformation.

The transforming autocoder represents a heterogeneous network (HN) that consists of a set of lower dimensions—capsules.

Definition/Features of a capsule:

- All capsules of the transforming autocoder have the same structure.
- Each capsule encapsulates the visualization of the object's image.

TA is a neural network with the ability to learn, for which a "method of reverse propagation of the error" is directly employed. Input values of the autocoder are used for normalization. For the neural network under consideration, the function has a simple form $c = f(x) = x$. When using a transforming autocoder, it is additionally necessary to apply the restriction of "bottle neck" in one of layers with lower number of neurons than that in the input layer.

Thus, the neurons within such a type of the layer represent a reprint of data. As distinguished from the main components' method, using a set of layers of a transforming auto-coder and nonlinear functions of activation of neurons is compact and accurate.

Here is an example. When a set of data (an image in our case) is delivered to an input and is represented as a set of small images having the size $x \in R^{28*28=784}$, then their reprint can be represented as a hidden layer having the size of the order of 30, that is $c = f(x) = R^{30}$. In each capsule, there is one crucial neuron with values (0, 1), that corresponds to the fact that the object is in the image.

Some systems of computer imaging make use of histograms of oriented gradients as "visual words" and simulate spatial distributions of those elements with the help of a rough spatial pyramid. Such methods can correctly recognize objects without correct knowledge of their location—the ability that is used to diagnose the human's brain damage. Artificial neural networks make use of schemes of weight distribution with manual encoding to reduce the number of free parameters and reach a local translational invariant by subsampling the activation of local pools of translated replicas of the same core. After several stages of subsampling in a converging network, high-level objects have greater uncertainty in their poses.

Artificial neural networks should employ local capsules, which perform some rather complex internal calculations at their inputs, and then encapsulate the results of those calculations in a small vector of highly informative outputs. Each capsule learns to recognize implicitly the determined visual object within a limited region of views and deformations. The capsule's outputs are the probabilities for the object to occupy its limited region and a set of "parameters of a copy" that can include accurate pose, illumination and deformation of a visual object relatively implicitly determined canonical version of this object. When a capsule operates as needed, the probability of presence of a visual entity represents a local invariant; it does not change when the entity moves over the set of possible realizations in encapsulated limited region. The parameters of the copy are "equivariantly": as viewing conditions and motions of the object change over the external set, the parameters of the copy change by the same value since they represent internal coordinates of the object in the external set [1].

One of major advantages of capsules delivering explicit parameters of a copy consists in a simple way of recognizing entire objects by recognizing their parts. If a capsule can learn to deliver a pose of its virtual object to a vector, that is linearly coupled with an used in computer graphics "natural" representation of a pose, there is a simple and highly selective test for checking of whether visual objects (represented by two active capsules A and B) have accurate spatial relationship for activating a capsule of higher level C. Let us suppose that output data of capsule A represented by matrix $\mathbf{T}_A$ that yields the transformation of coordinates between a canonical visual entity and the actual copy of that entity determined by capsule A. If $\mathbf{T}_A$ is multiplied by a functional of coordinates transformation "a part–to a whole" $\mathbf{T}_{AC}$, which couples canonical visual entities A and C, then a predicted matrix $\mathbf{T}_C$ can be obtained. In a similar way, we can use $\mathbf{T}_B$ and $\mathbf{T}_{BC}$ for obtaining another prognosis. If these predictions agree well, then the copies determined by capsules A and B are in correct spatial relationship enabling to activate capsule C; the average value of the prediction informs us of how the greater visual entity—represented by C—transforms relatively canonical visual entity C. For example, if A is a mouth and B is a nose, then each of them can predict the position of the face. If these predictions coincide, then both the mouth and the nose must be in a correct spatial relation to form a face. An interesting feature of this approach for recognizing a form is that the relation "a whole–to a part" is invariant and is represented by weighting matrices, whereas the ensemble of parameters of a copy of objects and their parts being observed at the given moment is equivariant and is represented by neural activities.

To obtain "a whole–to a part" hierarchy, the capsules, which realize parts of the lowest level in this hierarchy, must extract from intensities of pixels explicit parameters of the pose.

After intensities of pixels have been transformed to output data of the given set of active capsules of the first level, each of them yields explicit representation of the pose of its visual object, visual objects can be recognized with the help of active capsules of lower level.

Let us consider a neural network of direct communication shown in Fig. 1.

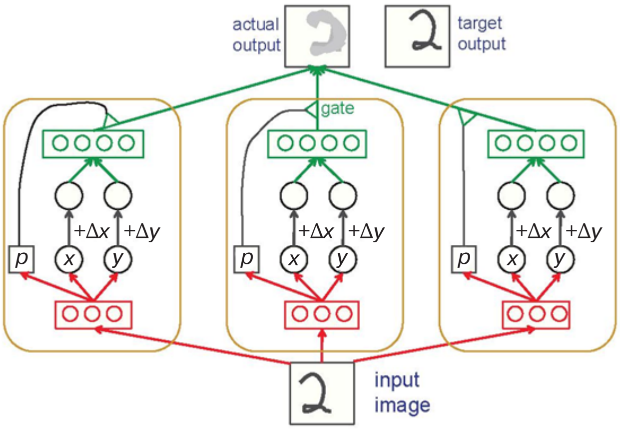

Fig. 1. Three capsules of a transforming autocoder that simulates translations

Each capsule in Fig. 1 has three recognizing blocks and four generating blocks. The weights at connections are learned through reverse propagation of a discrepancy between actual and targeted outputs. The network is determined, and as soon as it is learned it can receive the image as input data and desired shifts Δx and Δy and generate the shifted output. Each capsule has its own logical "recognizing blocks," which act as a hidden layer for the calculation of outputs, which are three numbers, x, y, and p. The capsule will send these outputs to higher levels of the visual system (p is the probability that the visual entity of the capsule is presented in the input image). In its turn, the capsule has its own generators; values $x + \Delta x$ and $y + \Delta y$ being input data for these blocks (where x and y are input and output data for one capsule). The capsules research generative units with projected fields of strong localization (Fig. 2). We describe the state for each of them by the following activation functions:

$$
\begin{aligned}
&H_r = \sigma\left(\mathbf{W}_{xh}x + b_r\right) \in (0,1)^{N_r},\\
&c = \mathbf{W}_{hc}H_r + b_c \in R^2,\\
&c' = c + s \in R^2,\\
&p = \sigma\left(\mathbf{W}_{hp}H_r + b_p\right) \in (0,1),\\
&H_g = \sigma\left(\mathbf{W}_{c'g}c' + b_g\right) \in (0,1)^{N_g},\\
&y = p\mathbf{W}_{hy}H_g \in R^{784}.
\end{aligned}
\tag{1}
$$

Note that if every capsule receives nine real inputs, which are processed as a matrix with 3 × 3 dimension, then TA can be learned to predict complete 2D affine transformation (translation, rotation, scaling, and shift). Transformation matrix $\mathbf{T}$ is applied to the output of capsule A to obtain matrix $\mathbf{T}_A$. Then the elements of $\mathbf{T}_A$ are used as input data for generation blocks when $\mathbf{T}_A$ for the prognosis of targeted output image.

A criterion of rarefaction is supposed to be used as an auxiliary condition. Employing this criterion is effective for TA. Note, that the condition of rarefaction

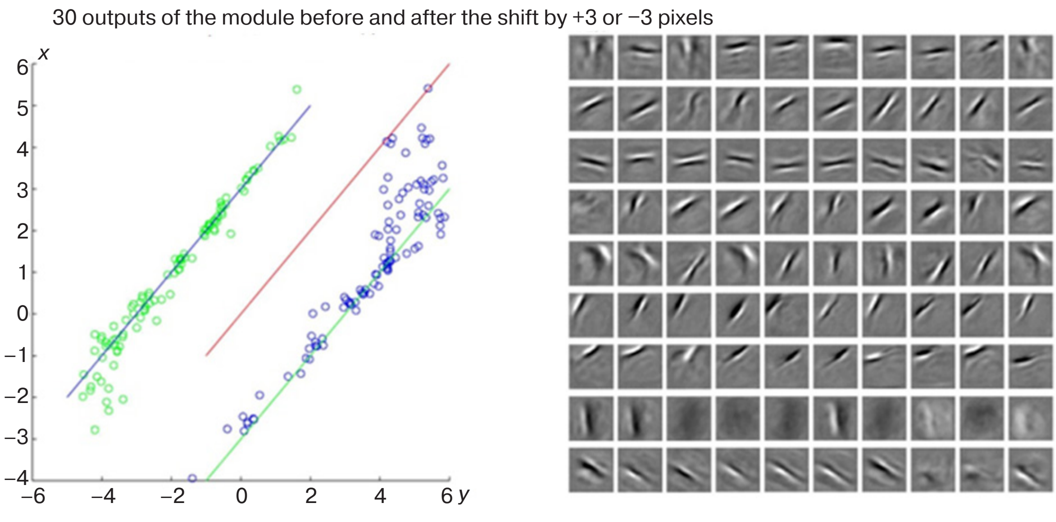

Fig. 2. Shifts in values of x and y

must impose restriction on neurons of a generating and recognizing layer. Therefore, for employing TA as a constituent of the model we should extend a formulation for the transformation beyond the limits of two-dimensional translation. For the rarefaction condition, the information divergence of the facial image identification model already developed by the author is applied. The Kullback–Leibler divergence formula is as follows:

$$S = \sum_{j=1}^{L_n} KL\left(s \,\|\, \hat{s}_j\right) = \sum_{j=1}^{L_n} s \log \frac{s}{\hat{s}_j} + (1-s)\log\frac{1-s}{1-\hat{s}_j}, \qquad (2)$$

where L_n is the number of neurons, $\hat{s}_j = \frac{1}{m}\sum_{i=1}^{m}\left(a_j^{(Ln)} x_j\right)$ is the average value of activation, and s is the rarefaction parameter.

By setting the value of parameter s to be proportionally small, we can limit the average activation of a neuron. Having obtained independent signs, we can also change the impact of this parameter on the operation of the heterogeneous network.

For further optimization of the parameters, it is necessary to employ a price function TA with weights D and v, which can be written as follows:

$$J_s(\mathbf{D},\mathbf{v}) = J(\mathbf{D},\mathbf{v}) + \beta \sum_{i=1}^{L} \sum_{j=1}^{Li} KL\left(s \,\|\, \hat{s}_j\right), \qquad (3)$$

where β is a meta-parameter, **D** and **v** are general matrices of weights.

An additional parameter should be introduced into the algorithm of the error backpropagation. The error determined by the backpropagation method represents an expression for some layer of neuron network l.

$$\delta_i^{(l)} = \left(\left(\sum_{j=1}^{L} \mathbf{W}_{ji}^{(l)} \delta_j^{(l+1)}\right) + \beta\left(-\frac{s}{\hat{s}_j} + \frac{1-s}{1-\hat{s}_j}\right)\right) f'\left(z_i^l\right), \qquad (4)$$

where z_i^l is the argument of a function for activation of the ith neurons in layer l.

This parameter represents the rarefaction criterion. Values s_j depends on D and v as the average activation of neuron j.

As compared to the methods and algorithms investigated in [1–3, 5, 6, 9–13, 15], TA (neural network) has demonstrated the best result in identification of facial images under different shooting conditions. Table 1 shows the results of identification at different angles of shooting.

Table 1. The results of identification for different angles

Angle	POSIT, %	SVM, %	Author's (TA), %
(0°,15°)	82 ± 4	85 ± 2	99 ± 4
(15°, 30°)	80 ± 3	81 ± 3	98 ± 3
(30°, 45°)	79 ± 4	80 ± 4	97 ± 3
(45°, 60°)	81 ± 5	82 ± 4	98 ± 4

Table 2 shows the results of identification for different levels of illumination.

Table 2. The results of identification for different levels of illumination

Illumination, %	POSIT, %	SVM, %	Author's (TA), %
25	35 ± 2	15 ± 2	88 ± 2
50	61 ± 5	47 ± 2	98 ± 2
75	70 ± 2	68 ± 4	98 ± 1
100	99 ± 1	99 ± 1	99 ± 1

Table 3 shows the results of identification under different levels of interferences and noise in the image. We define noise as loosing of the image sharpness with magnification. As for interferences, these are different interferences when producing the image as well as the appearance of additional features in the facial image: glasses, moustache, makeup, etc.

Table 3. The results of identification under different interferences and noise in the image

Parameters	POSIT, %	SVM, %	Author's (TA), %
Noise	84 ± 2	92 ± 2	97 ± 2
Interference	89 ± 5	83 ± 2	99 ± 1

The presented results demonstrate that TA employing a local detector is less responsive to a change in the position of a facial image, illumination, and interference (noise).

CONCLUSIONS

The proposed method can be extended for identification of three-dimensional objects and is promising for analyzing a combination of local spatial structures and hypothetical 3D model of the object. The described LD (the element of the MOR model) solves the problem of the stability of identification of facial images under conditions of interference (noise), change in illumination, and different angles.

REFERENCES

1. Parfinovich S.N. Algorithms of face recognition for identity verification by image. In: *“Molodoi issledovatel’: vyzovy i perspektivy”: sb. mat. CXIV Mezhdunarodnoi nauchno-prakticheskoi konferentsii”* (*Proceedings CXIV International Scientific and Practical Conference “Young Researcher: Challenges and Prospects”*). Moscow: Internauka; 2019, p. 115–163. (in Russ.).
2. Akhmedov A.A., Sagidov G.S., Kurbanismailov G.M. Algorithm of face recognition based on the Viola–Jones method. In: *“Molodoi issledovatel’: vyzovy i perspektivy”: sb. mat. CXVIII Mezhdunarodnoi nauchno-prakticheskoi konferentsii”* (*Proceedings CXVIII International Scientific and Practical Conference “Young Researcher: Challenges and Prospects”*). Moscow: Internauka; 2019, p. 270–274. (in Russ.).
3. Pentland A., Choudhary T. Face recognition for smart environments. *Otkrytye sistemy = Open Systems Publications*. 2000;03 (in Russ.). Available from URL: https://www.osp.ru/os/2000/03/177939
4. Gorelik A.L., Gurevich I.B., Skripkin V.A. *Sovremennoe sostoyanie problemy raspoznavaniya: Nekotorye aspekty* (*The current state of the recognition problem: Some aspects*). Moscow: Radio i svyaz’; 1985. 161 p. (in Russ.).
5. Samal D.I., Frolov I.I. Algorithm of preparation of the training sample using 3D face modeling. *Sistemnyi analiz i prikladnaya informatika = System analysis and applied Information science*. 2016;4:17–23 (in Russ.). Available from URL: https://sapi.bntu.by/jour/article/view/128/105
6. Zavalov R.A., Garaev R.A. Implementation of the Viola–Jones algorithm on a microcontroller with limited resources. *Nauka i obrazovanie segodnya = Science and Education Today*. 2018;6(29):18–23 (in Russ.). Available from URL: https://cyberleninka.ru/article/n/realizatsiya-algoritma-violy-dzhonsa-na-mikrokontrollere-s-ogranichennymi-resursami/viewer
7. Baldin A.V., Eliseev D.V. Multidimensional matrix algebra for adapted data model processing. *Nauka i obrazovanie: nauchnoe izdanie MGTU im. N.E. Baumana = Science and Education of Bauman MSTU*. 2011;7:4 (in Russ.). Available from URL: http://technomag.edu.ru/doc/199561.html
8. Korotkov A. Database index for approximate string matching. In: *Proceedings of the 4th Spring/Summer Young Researchers’ Colloquium on Software Engineering. SYRCoSE ’10*. 2010, p. 136–140. https://doi.org/10.15514/syrcose-2010-4-27
9. Kononykhin I.A., Ezhov F.V., Martynyuk R.A., et al. Implementation of a face recognition and tracking system. *Molodoi uchenyi = Young Scientist*. 2020;28(318):8–12 (in Russ.). Available from URL: https://moluch.ru/archive/318/72492/
10. Hinton G.E., Krizhevsky A., Wang S.D. Transforming auto-encoders. In: Honkela T., Duch W., Girolami M., Kaski S. (Eds.). *Artificial Neural Networks and Machine Learning – ICANN 2011. ICANN 2011. Lecture Notes in Computer Science*. Springer, Berlin, Heidelberg; 2011. V. 6791. P. 44–51. https://doi.org/10.1007/978-3-642-21735-7_6
11. Alghaili M., Li Z., Ali H.A.R. FaceFilter: Face identification with deep learning and filter algorithm. *Scientific Programming*. 2020:1–9. https://doi.org/10.1155/2020/7846264

СПИСОК ЛИТЕРАТУРЫ

1. Парфинович С.Н. Алгоритмы распознавания лиц для верификации личности по изображению. В сб.: «*Молодой исследователь: вызовы и перспективы*»: *сб. мат. CXIV Международной научно-практической конференции*. М.: Интернаука; 2019. С. 155–163.
2. Ахмедов А.А., Сагидов Г.С., Курбанисмаилов Г.М. Алгоритм распознавания лиц на основе метода Виолы – Джонса. В сб.: «*Молодой исследователь: вызовы и перспективы*»: *сб. мат. CXVIII Международной научно-практической конференции*. М.: Интернаука; 2019. С. 270–274.
3. Пентланд А., Чаудхари Т. Распознавание лиц для интеллектуальных сред. *Открытые системы*. 2000;03. URL: https://www.osp.ru/os/2000/03/177939
4. Горелик А.Л., Гуревич И.Б., Скрипкин В.А. *Современное состояние проблемы распознавания: Некоторые аспекты*. М.: Радио и связь; 1985. 161 с.
5. Самаль Д.И., Фролов И.И. Алгоритм подготовки обучающей выборки с использованием 3D-моделирования лиц. *Системный анализ и прикладная информатика*. 2016;4:17–23. URL: https://sapi.bntu.by/jour/article/view/128/105
6. Завалов Р.А., Гараев Р.А. Реализация алгоритма Виолы – Джонса на микроконтроллере с ограниченными ресурсами. *Наука и образование сегодня*. 2018;6(29):18–23. URL: https://cyberleninka.ru/article/n/realizatsiya-algoritma-violy-dzhonsa-na-mikrokontrollere-s-ogranichennymi-resursami/viewer
7. Балдин А.В., Елисеев Д.В. Алгебра многомерных матриц для обработки адаптируемой модели данных. *Наука и образование: научное издание МГТУ им. Н.Э. Баумана.* 2011;7:4. URL: http://technomag.edu.ru/doc/199561.html
8. Korotkov A. Database index for approximate string matching. In: *Proceedings of the 4th Spring/Summer Young Researchers’ Colloquium on Software Engineering. SYRCoSE ’10*. 2010, p. 136–140. https://doi.org/10.15514/syrcose-2010-4-27
9. Кононыхин И.А., Ежов Ф.В., Мартынюк Р.А. и др. Реализация системы распознавания и отслеживания лиц. *Молодой ученый*. 2020;28(318):8–12. URL: https://moluch.ru/archive/318/72492/
10. Hinton G.E., Krizhevsky A., Wang S.D. Transforming auto-encoders. In: Honkela T., Duch W., Girolami M., Kaski S. (Eds.). *Artificial Neural Networks and Machine Learning – ICANN 2011. ICANN 2011. Lecture Notes in Computer Science*. Springer, Berlin, Heidelberg; 2011. V. 6791. P. 44–51. https://doi.org/10.1007/978-3-642-21735-7_6
11. Alghaili M., Li Z., Ali H.A.R. FaceFilter: Face identification with deep learning and filter algorithm. *Scientific Programming*. 2020:1–9. https://doi.org/10.1155/2020/7846264
12. Fitzgerald R.J., Price H.L., Valentine T. Eyewitness identification: Live, photo, and video lineups. *Psychology, Public Policy, and Law*. 2018;24(3):307–325. http://dx.doi.org/10.1037/law0000164
13. Etemad K., Chellapa R. Discriminant Analysis for Recognition of Human Face Images. *Journal of the Optical Society of America A*. 2004;14(8):1724–1733. https://doi.org/10.1364/JOSAA.14.001724

12. Fitzgerald R.J., Price H.L., Valentine T. Eyewitness identification: Live, photo, and video lineups. *Psychology, Public Policy, and Law*. 2018;24(3):307–325. http://dx.doi.org/10.1037/law0000164
13. Etemad K., Chellapa R. Discriminant analysis for recognition of human face images. *Journal of the Optical Society of America A*. 2004;14(8):1724–1733. https://doi.org/10.1364/JOSAA.14.001724
14. Kulikov A.A. The model is a reprint of an object in the image. *Rossiiskii tekhnologicheskii zhurnal = Russian technological journal*. 2020;8(3):7–13 (in Russ.). https://doi.org/10.32362/2500-316X-2020-8-3-7-13
15. Romanenko A.O., Yufryakov A.V. Image blur evaluation for biometric identification. *Nauka i obrazovanie segodnya = Science and Education Today*. 2018;7(30):16–19 (in Russ.). Available from URL: https://cyberleninka.ru/article/n/otsenka-razmytiya-izobrazheniya-dlya-biometricheskoy-identifikatsii/viewer

14. Куликов А.А. Модель репринта объекта на изображении. *Российский технологический журнал*. 2020;8(3):7–13. https://doi.org/10.32362/2500-316X-2020-8-3-7-13
15. Романенко А.О., Юфряков А.В. Оценка размытия изображения для биометрической идентификации. *Наука и образование сегодня*. 2018;7(30):16–19. URL: https://cyberleninka.ru/article/n/otsenka-razmytiya-izobrazheniya-dlya-biometricheskoy-identifikatsii/viewer

About the author

Alexander A. Kulikov, Cand. Sci. (Eng.), Associate Professor, Department of the Tool and Applied Software, Institute of Information Technologies, MIREA – Russian Technological University (78, Vernadskogo pr., Moscow, 119454 Russia). E-mail: tibult41@gmail.com. https://orcid.org/0000-0002-8443-3684

Об авторе

Куликов Александр Анатольевич, к.т.н., доцент, кафедра инструментального и прикладного программного обеспечения Института информационных технологий ФГБОУ ВО «МИРЭА – Российский технологический университет» (119454, Россия, Москва, пр-т Вернадского, д. 78). E-mail: tibult41@gmail.com. https://orcid.org/0000-0002-8443-3684

Translated by E. Shklovskii

Modern radio engineering and telecommunication systems

Современные радиотехнические и телекоммуникационные системы

UDC 004.4:004.7
https://doi.org/10.32362/2500-316X-2021-9-5-14-25

REVIEW ARTICLE

Analysis and evaluation of the effectiveness of methods for ensuring the quality of service for software-defined networks of the standard 5G/IMT-2020

Behrooz Daneshmand @

ITMO University, St. Petersburg, 197101 Russia
@ *Corresponding author, e-mail: daneshmandbehrooz@gmail.com*

Abstract. The quality of service (QoS) in networking is the process of managing network resources to reduce packet loss and to lower network jitter and latency. QoS has been widely used in traditional network and can also be implemented in the 5G standard based on a software-defined network (SDN). A traditional network carries several challenges, such as vendor dependency, the complexity of managing a large network, dynamically changing forwarding policies, and more. Software-defined networking is a new networking strategy designed to address the challenges of a traditional IP network, such as high levels of complexity and inability to adapt to the new quality of service requirements in a timely manner. The fundamental idea behind SDNs compared to the conventional networking paradigm is the creation of horizontally integrated systems through the separation of the control and the data plane while providing an increasingly sophisticated set of abstractions. Recently, various SDN-enabled QoS frameworks have emerged that offer many possibilities for network reconfiguration and high-level definition of policies. QoS requirements for 5G networks have been defined on the basis of three main categories of use cases: extreme mobile broadband (xMBB), massive machine type communications (mMTC) IoT/M2M devices, and highly reliable M2M-communication (ultra-reliable machine-type communications – uMTC). This paper analyzes and surveys the QoS based on the openflow protocol method and QoS based on open-source SDN controllers method in 5G network. In addition, we discuss various architectural issues of open-source SDN controllers network and examine their impact on the QoS. Furthermore, we outline the characteristics of the QoS parameters such as latency, availability, reliability, jitter, and bandwidth in the 5G network. Finally, the article discusses and compares parameters of the QoS in 5G determined by world's leaders in 5G technology.

Keywords: Software-Defined Network, SDN, Quality of Service, 5G/IMT-2020

• **Submitted:** 26.05.2021 • **Revised:** 26.07.2021 • **Accepted:** 28.07.2021

For citation: Behrooz Daneshmand. Analysis and evaluation of the effectiveness of methods for ensuring the quality of service for software-defined networks of the standard 5G/IMT-2020. *Russ. Technol. J.* 2021;9(5):14–25. https://doi.org/10.32362/2500-316X-2021-9-5-14-25

Financial disclosure: The author has no a financial or property interest in any material or method mentioned.

The author declares no conflicts of interest.

ОБЗОР

Анализ и оценка эффективности методов обеспечения качества обслуживания программно-конфигурируемых сетей стандарта 5G/IMT-2020

Данешманд Бехруз Мехди @

Университет ИТМО, Санкт-Петербург, 197101 Россия
@ *Автор для переписки, e-mail: daneshmandbehrooz@gmail.com*

Резюме. Качество обслуживания в сети (QoS) – это процесс управления сетевыми ресурсами для уменьшения потери пакетов, а также уменьшения джиттера и задержки. QoS широко используется в традиционных сетях, а также может быть реализован в стандарте 5G на основе программно-конфигурируемой сети (SDN). Традиционная сеть несет в себе несколько проблем, таких как зависимость от поставщика, сложность управления большой сетью, динамически меняющиеся политики пересылки и многое другое. Программно-конфигурируемая сеть – это новая стратегия, разработанная для решения таких проблем традиционной IP-сети, как высокий уровень сложности и неспособность своевременно адаптироваться к новым требованиям к качеству обслуживания. Фундаментальная идея, лежащая в основе SDN, по сравнению с традиционной сетевой парадигмой, заключается в создании горизонтально интегрированных систем путем разделения уровня управления и данных при обеспечении все более сложного набора абстракций. В последнее время появились различные инфраструктуры QoS с поддержкой SDN, которые предлагают множество возможностей для реконфигурации сети и определения политик на высоком уровне. Требования QoS для сетей 5G были определены на основе трех основных категорий сценариев использования: Extreme Mobile BroadBand (xMBB), Massive Machine Type Communications (mMTC) IoT/M2M-устройства и высоконадежная M2M-связь (сверхнадежная связь машинного типа – uMTC). В статье анализируется и исследуется QoS на основе метода протокола OpenFlow и QoS на основе метода контроллеров с открытым исходным кодом SDN в сети 5G. Обсуждаются различные архитектурные проблемы сети SDN контроллеров с открытым исходным кодом и исследуется их влияние на QoS. Описываются характеристики QoS, такие как задержка, доступность, надежность, джиттер и пропускная способность. Обсуждаются и сравниваются параметры QoS в сети 5G, которые определены мировыми лидерами в данной технологии.

Ключевые слова: программно-конфигурируемая сеть, SDN, качество обслуживания, 5G/IMT-2020

• **Поступила:** 26.05.2021 • **Доработана:** 26.07.2021 • **Принята к опубликованию:** 28.07.2021

Для цитирования: Данешманд Бехруз Мехди. Анализ и оценка эффективности методов обеспечения качества обслуживания программно-конфигурируемых сетей стандарта 5G/IMT-2020. *Russ. Technol. J.* 2021;9(5):14–25. https://doi.org/10.32362/2500-316X-2021-9-5-14-25

Прозрачность финансовой деятельности: Автор не имеет финансовой заинтересованности в представленных материалах или методах.

Автор заявляет об отсутствии конфликта интересов.

INTRODUCTION

The global impact of 4G technology has led to increased use of mobile communications and improved network performance. The implementation of 5G technology will enable to make this momentum greater, offering significant improvements in network performance, including faster connectivity, mobility and bandwidth, and communication with low-delay connectivity. Thus, it opens up new use cases and provides promising applications that can positively influence the development of various industries. The 5G networks can create an ecosystem for technical and business innovation, including vertical markets such as automotive, healthcare, manufacturing, energy, food and agriculture, city management, government, public transportation, media, and more. They offer unlimited mobile broadband access, provide extensive connectivity for everything from human-controlled intelligent devices to sensors and machines, and most importantly, have the ability to support critical machine communications with instant action and ultra-high reliability [1].

The 5G technology for mobile communication first appeared in South Korea in 2020 followed by China, the USA, and the European Union. It is expected that by 2025 there will millions 5G connections. The 5th generation internet will be 5 times faster (with 25 times lesser delay) than the current 4th generation system, and will support up to one million devices per square kilometre. Generally speaking, the basis of 5G Internet relies on the following five technologies: millimetres radio-waves, small cellular networks, MIMO (several inputs and outputs), beam formation, and double-sided bytes. A traditional network bears several problems, such as a dependence on providers, complexity in managing a large network, dynamically changing forwarding policies, and much more. What is more important is that a traditional IP-network is not able timely respond to changes and newly emerged QoS requirements. Such failures are caused mainly by the features of traditional IP-networks, in which a control plane and data plane are vertically connected with each other and implemented in the network devices. To overcome the problems of the existing network, a concept of a programmable network has emerged [2, 3].

Its behaviour is controlled by software called Software Defined Networking (SDN). This network, as distinguished from traditional networks, represents a dynamically developing infrastructure, which controls data plane and control plane in a separate way. Based on Open Networking Foundation (ONF) [4] SDN has three levels, namely: the infrastructure level, control level, and application level [5]. SDN architecture is shown in Fig. 1 and is explained below [4].

- **Infrastructure layer** consists mainly of the transfer elements (for example, physical and virtual switches, routers, and points of wireless access), which represent a data plane.
- **Control layer,** also known as control plane (it is the core of SDN architecture), supports communication between the application level and infrastructure level through open interfaces.
- **Application layer** is mainly developed to meet users'. It consists of business-applications of end-users which use network services.

OpenFlow protocol, supported by ONF, is a fundamental element for developing SDN decisions. OpenFlow is the first of the leading communication interfaces, linking forwarding level and control levels in SDN architecture, enables to control both physically and virtually the forwarding level of network devices (for example, switches and routers). It helps SDN architecture to adapt to a high bandwidth capability, dynamic characters of users' applications, and adjust a network in accordance with different business requirements, and, what is interesting, reduce complexity of management and service.

Many factors affect QoS-based SDN in 5G networks, therefore we will further discuss the QoS parameters, which are defined by the 5G technology world leaders in terms of applicability to such networks. We will present the levels of the high-quality service in the context of the following characteristics: speed

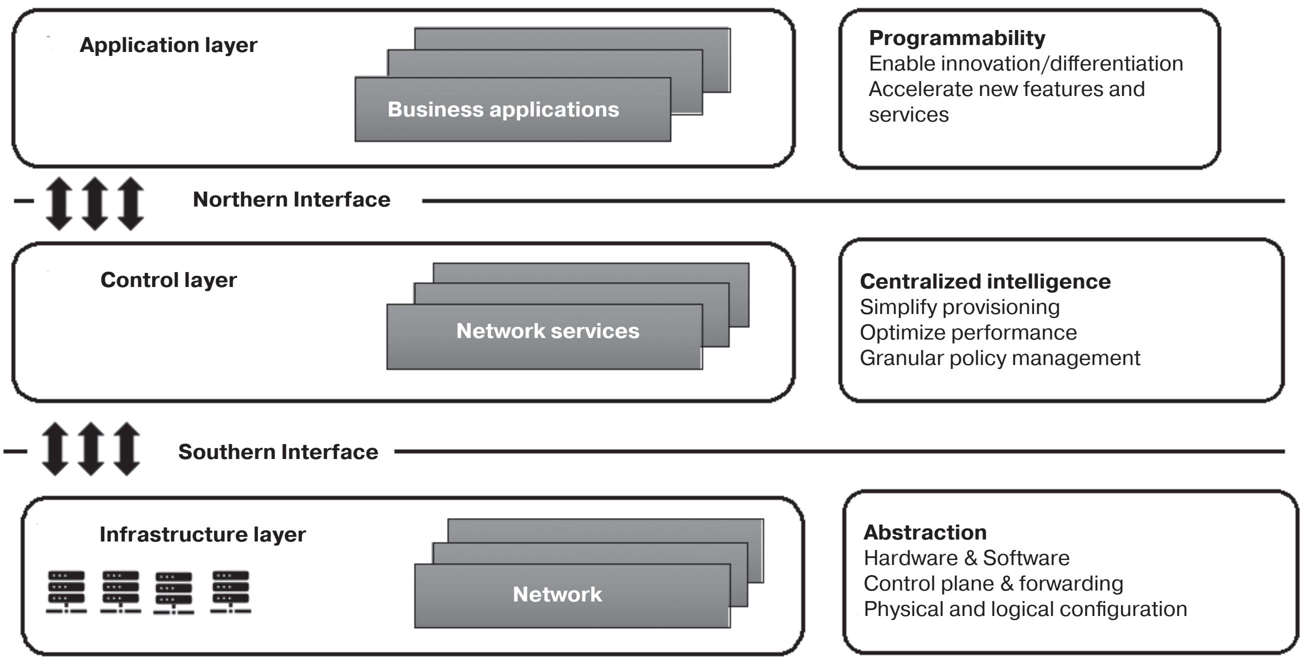

Fig. 1. SDN levels and functions

increase, mobile networks capacity, and growth of wireless devices.

In Section 1, a brief overview of OpenFlow architecture is given followed by two QoS methods based on the OpenFlow protocol and a controller with an open SDN source code. In Section 2, architectural problems in SDN and their influence on QoS are discussed. In Section 3, **Key Performance Indicators (KPI)**, QoS parameters and their influence in the 5G network are given. In Section 4, the QoS parameters for the next generation 5G are analysed and presented in a table.

1. QOS IN OPENFLOW PROTOCOL AND SDN CONTROLLERS WITH OPEN SOURCE CODE

A. OpenFlow architecture and QoS-based OpenFlow protocol

OpenFlow architecture [6] is the proposal of Clean State initiative for the definition of the open protocol, which sets routing tables in switches; it is the base of SDN architecture in which a user can change the network.

Actually, the OpenFlow (infrastructure level) protocol is a communication interface between controllers and OpenFlow routing planes [7]. It is the first standard communication protocol for SDN media. OpenFlow represents a routing path for the flow of transferring packets along programmable networks. A key advantage of this protocol is that it enables to adjust switches of different manufacturers with the help of controllers. Different versions of OpenFlow are available in SDM media.

OpenFlow architecture offers several advantages:

1) OpenFlow centralized controllers can manage all flow decisions thereby reducing complexity of the switches;
2) central controller can “see” all networks and flows providing global and optimal management of network initialization;
3) OpenFlow switches are relatively simple and reliable since direct decisions are determined by a controller but not a micro-program of the controller.

However, OpenFlow unites two characteristics—a unique controller and simple devices—that leads to scalability problems.

In SDN network with switches and the OpenFlow support, a switch consists of three main parts. The components of the OpenFlow architecture are shown in Fig. 2:

- *Data tables* with an action, related to each record of the flow in order to report the switch how to process the flow.
- *Protected channel,* which links switches with the process of remote control (called the controller), enabling to forward commands and packets between the controller and switches.

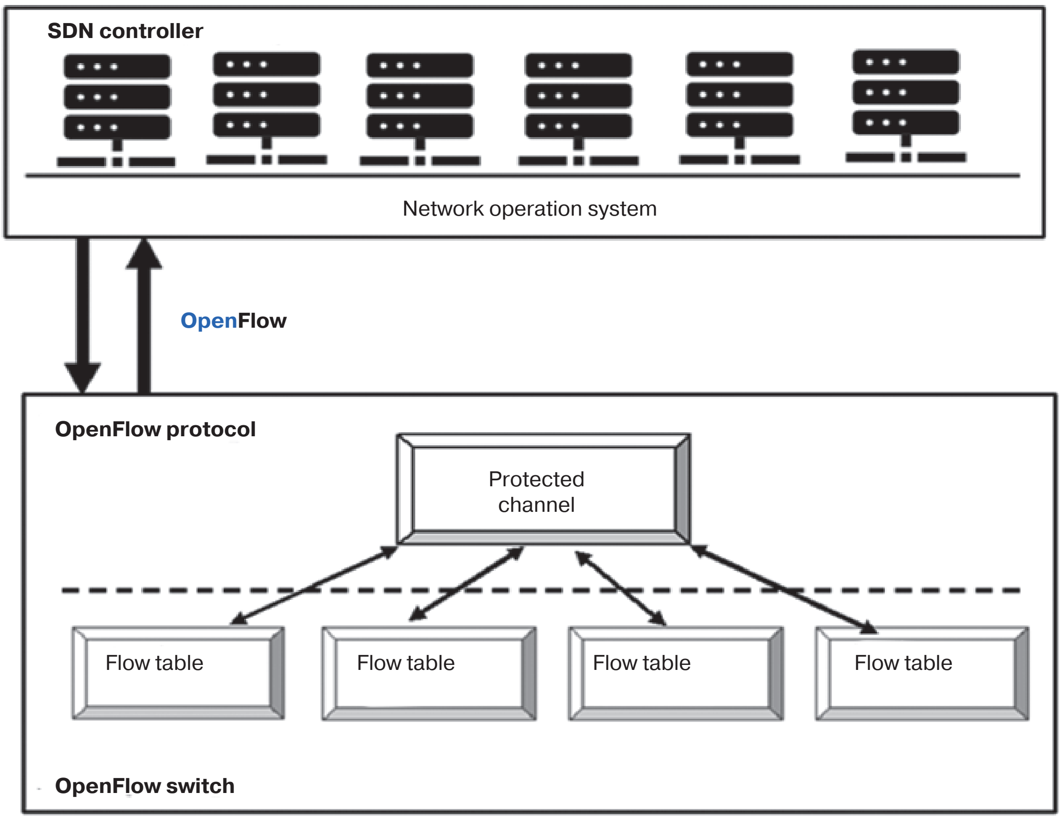

Fig. 2. OpenFlow architecture [8]

- *OpenFlow protocol*, which provides an open and standard method of communication between the controller and switches.

Using OpenFlow protocol, the OpenFlow switch becomes a simple element of the data pathway, which switches packets between ports in a way as defined by the process of remote control.

As the number of OpenFlow switches increases, the use of a single controller for the whole network may become impossible due to several reasons:

1) the number of controlling messages sent to a centralized controller increases with the number of switches;
2) as the network diameter increases some switches will have longer latency for actuation regardless of the controller location [6];
3) the tuning time can increase significantly as the number of switches and the size of the network increase;
4) as the system is limited by the power of the controller's processor, the tuning time may significantly increase with the increase of the number of switches and the network size.

In SDN network for setting a new flow rule, a controller can operate in three modes: Reactive mode, Proactive mode and Hybrid mode [9].

Reactive mode. In the reactive regime, when a new packet arrives to a network device (for example, a switch), the switch executes in its flow tables a search for the flow rule. If no coincidence with a flow is found, the switch (using C-DPI) forwards it to the controller so that the controller decides how to process the packet. After the controller has processed the packet according to the network policies, it creates and forwards the flow record for setting on the network device. Future flows corresponding to this record based on the attribute of the title of the packet will be processed in accordance with the matching rule.

Proactive mode. In the proactive mode, the flows recordings are tuned in switches flows tables before new flows arrive to switches. When a packet arrives to the switch, the latter already "knows" how to process this packet. In this case the switch does not participate in any process of the flow rules tuning.

Hybrid mode. In the hybrid mode, the controller makes use of advantages of both reactive and proactive modes. It is quite possible that network administrators set in advance certain flow records in the devices of data planes, while the switch(s) reactively change (remove/renew) them or even add new flow records based on incoming traffic.

While the proactive mode calls for some worries about invective usage of the switch memory, the reactive mode provides more flexible and dynamic medium for controllers and switches.

B. QoS on the basis of SDN controller with open initial code

The controller throughput is the main issue of OpenFlow architecture. A controller can support a limited number of flow adjustments per second. Software-defined networks employ two types of controllers: centralized and distributed. Classification of different controllers divided into two categories is described in Table 1 [10, 11].

Table 1. Classification of SDN controllers

Types of controllers			
Centralized		**Distributed**	
Centralized controllers implement all of the control plane logic in one place. In such a controller, a single server takes over all actions at the control level. The main advantage of such controllers is the simplicity and manageability since they provide the only one control point. However, their drawback is the scalability problem as each server has limited capacity for the operation with data plane devices. The QoS support in the SDN network became possible due to the component of the centralized logic SDN controller.		The distributed controller has no scalability issues and has the advantage of high performance under heavy traffic loads.	
Controllers	Programming Language	Controllers	Programming Language
NOX	Python	ONOS	Java
POX	Python	Runos	C++
RYU	Python	Hyperflow	C++
Beacon	Java	Onix	C, Python
Maestro	Java	SMaRtLight	Java
FloodLight	Java	OpenMUL	C
OpenDaylight	Java		
Meridian	Java		

In controllers with the open source code the parameters of the service quality include the following ones: reliability, scalability, sequence, and load balance.

2. ARCHITECTURE PROBLEMS IN SDN AND THEIR INFLUENCE ON THE QOS

2.1. Centralized administration

In the SDN medium a switch is separated by controllers and a dump switch. Moreover, all controllers and switches are active for the large network. The design of controllers and their locations remain the subject of research with the aim to improve the network throughput. Other factors—such as flexibility, scalability, delay, safety, and compatibility—are also important for increasing the network throughput [7, 12, 13].

In large-scale SDN networks several controllers are deployed to balance the traffic load and achieve high quality of service [14]. As the number of controllers grows, the concept of centralized management changes. Different controllers can have different functions; therefore, their central administration becomes more difficult [13].

2.2. Network scalability

Due to the presence of several program controllers it can be easily scaled up. However QoS can doubt the scalability because of the load balancing between controllers [13, 14].

2.3. Inconsistency among the controllers

Because there are several controllers in the network, the main problem is the synchronization of information about the state of the network in SDN. This problem is known as the consensus problem [13]. Due to a complex realization and growing delay the consensus approaches do not job. When designing several controllers, it is important to provide matching between them.

2.4. Controller placement

Implementation of only one controller in a software-defined network has many advantages, such as centralized management, checking and monitoring the whole network with the help of only one node. But at the same time such an approach brings the problems of reliability and scalability [13]. As the network grows, these problems worsen throughput. The problem of placing controllers has been known since 2012. In order to reduce the delay of service data and increase total throughput, it is necessary to place in the network an optimal number of controllers at a proper distance [15]. In large-scale networks when deploying the controllers two important issues are being considered: how many controllers are required in the networks, and where should these controllers be placed. Although these are undetermined polynomial-complex problems, they have to be solved for deployment of several controllers [13].

2.5. Controller communication protocol

In a distributed network it is necessary to have several controllers; they directly affect QoS of the SDN network. Therefore, an efficient data interchange between controllers is required. For communication between controllers an interface "eastbound-westbound" is needed, therefore in an SDN network a standard protocol must be developed for such communication. Currently, the global network supports Border Gateway Protocol (BGP) for "eastbound-westbound" interfaces [12].

2.6. Planning deployment of several controllers

QoS can be better at the expense of employing several controllers, but it is necessary to plan ahead the load of various controllers in order to avoid their overload. In this case, the main problem is how to balance the load fast.

3. THE ANALYSIS OF QOS IN DIFFERENT SDN CONTROLLERS

There exist lots of free as well as commercially available SDN controllers. A range of functions of the controllers are suitable for different applications. Descriptions of three SDN controllers are given in Table 2 as examples.

In addition to QoS in controllers, the QoS index is influenced by programming parameters, including QoS in the OpenFlow protocol. Each new version of the OpenFlow specification contains some features with minor and significant changes compared to the previous ones, so QoS varies from version to version.

4. FROM KPI TO QOS IN THE 5G/IMT-2020 NETWORK

The fifth generation network (5G/IMT-2020) is the latest iteration of cellular technology designed to dramatically increase the speed and responsivity of wireless networks. According to [19], the technological goals of 5G are the following indicators: 1000 times more mobile traffic, 10 to 100 times higher transmission speed for users, 10 to 100 times more users, 10 times longer battery life in M2M mass communications, 5x reduction of E2E (end-to-end) delay.

Table 2. Examples of SDN controllers

Controllers	Analyzation and Description of Controllers
OpenDaylight	OpenDaylight (ODL) is a modular open platform for customizing and automating networks of any size and scale. The OpenDaylight Project arose out of the SDN movement, with a clear focus on network programmability. The ODL project includes support for all SDN platforms, including OpenFlow, Open VSwitch (OVS) Database (OVSDB), NETCONF, SNMP, BGP and applications (e.g., DDoS Protection and Virtualization Coordinator), which complement each other to compose a complete reference controller platform for heterogeneous networks. The OpenDaylight Controller exposes open northbound APIs, which are used by applications. These applications use the controller to collect information about the network, run algorithms to conduct analytics, and then use the OpenDaylight Controller to create new rules throughout the network. Packet Cable MultiMedia (PCMM), presented in ODL-Lithium, provides an interface to control and management service flow for CMTS network elements. A service flows constitute a DOCSIS data path between a CMTS and a subscriber's cable modem (CM) guaranteed application specific quality of service (QoS), known as Dynamic Quality of Service (DQoS). PCMM offers (MSOs) the ability to deliver new services using existing cable infrastructure. OVSDB is another southbound protocol for managing and configuring queues in switches and virtual switches. Here is another add-on to the ODL reservation module that aims to provide low-level resource reservations that provide users with network connectivity, bandwidth, and ports for a specific allotted time [2, 9, 16].
ONOS	The open network operating system (ONOS) controller is an operating system (OS) that is designed to help network service providers build carrier-grade SDNs architected for high scalability, availability, and performance. Among the service providers contributing to the ONOS initiative are AT&T, NTT Communications, and SK Telecom. Vendors contributing to ONOS include Cisco, Ericsson, Intel, NEC, Ciena, and Huawei. Likewise, ON.Lab and ONOS partners have found multiple use cases for the OS. ONOS supports the OpenFlow mechanism, and accordingly, the existing switches rarely implement ONOS. Thus, the ONOS platform provides limited QoSs because this implementation supports the functionality of the OpenFlow set_queue. To improve QoS, ONOS libraries have implemented the Set Queue Instruction function, namely, top-level instruction [2, 9, 17].
Floodlight	Floodlight Controller (Java-based) is an SDN controller developed by an open community of developers, many of which from Big Switch Networks are used with the OpenFlow protocol to orchestrate traffic flows in an SDN environment. The Floodlight controller implements a QoS module that provides functionality such as stream deletion, stream insertion, and some policies for handling QoS. These modules are implemented in OpenFlow, version 1.0. The QoS is at its infancy when it comes to OpenFlow. The OpenFlow 1.0 provides a user with a way to simply push the QoS state to switches that support these features. These modules seek to tackle "enqueue" and "SET-NW-ToS" actions. The static flow pusher API calls this "set-ToS-bits." spec includes ways in which one can set the network type of service on a flow, as well as enqueue the packets matching the flow to a specific queue on a specific port. In the Floodlight Northbound interface, module QueuePusher generates the messages for queue configurations for creating, reading, updating, and deleting functions to manage the Open vSwitches [18].

The 5G concept consists of three general services:

1. **eMBB (Enhanced Mobile Broadband).** This requires large capacity, high speed, and dynamic bandwidth allocation. While high speed helps to upload and download video content faster in gigabyte sizes, the bandwidth can be provisioned on demand for ultra high definition (UHD) video, virtual reality, augmented reality, and more.
2. **uRLLC (Ultra Reliable Low Latency Communication).** These services require high reliability, high availability, and low latency. High reliability supports critically important services such as connected robotic factories and remote surgery, while low latency makes services such as autonomous vehicles and remotely controlled drones a reality.
3. **mMTC (machine type mass communication).** This class of service is characterized by high throughput, high speed and dynamic bandwidth allocation and is best suited for Internet of Things (IoT) services such as smart cities serving billions of "things" and "devices" with densities of up to one million per square kilometre [27].

These three generic services should be seen as baseline characteristics covering 5G user scenarios. Key performance indicators (KPIs/KPIs), which, from the point of view of the end user, are used as a basis for assessing the effectiveness of specific scenarios are shown in Table 3.

Most of today's popular applications and applications scenarios will continue within frames of 5G, with KPIs/KPIs and QoS further applying.

Key performance indicators for 5G technology are shown in Fig. 3 [20]:

Table 3. 5G performance characteristics required for each ITU[1] use scenario

eMBB	uRLLC	mMTC
Peak data transfer rate: from 10 to 20 Gbit/s; minimum data transfer rate: 100 Mbit/s	Provides hypersensitive connections	Supports high device density (10^6 per km^2)
Increases traffic capacity/throughput by 100 times	Provides less than 1 ms air interface latency	Supports long rang and low data rate (1–100 Kbit/s)
Supports macro and small cells	Ultra-reliable and affordable with five nines (99.999% of the time)	Takes advantage of ultra-low cost M2M
Supports high mobility of about 500 km/h	Provides data transfer rates from low to medium (50 Kbit/s–10 Mbit/s)	Provides battery life up to 10 years for IoT
Improves network energy savings by 100 times	Provides high speed mobility	Provides asynchronous access

[1] International Telecommunication Union.

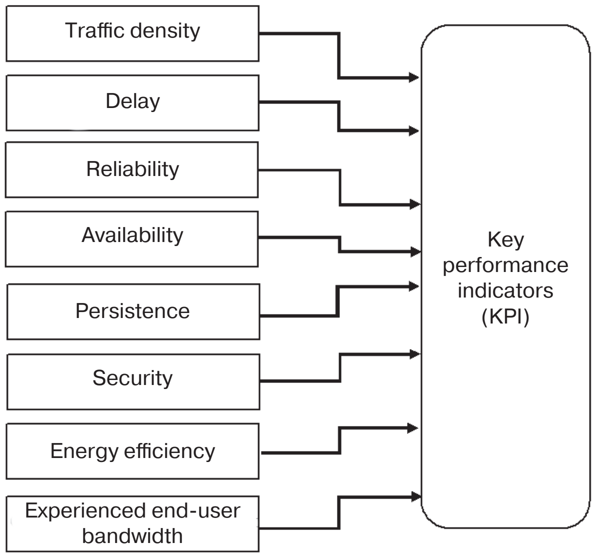

Fig. 3. KIE/KPI for 5G/IMT-2020 technology

New technologies, referred to in this article as 5G Key Technology Enablers (KTEs), play a major role in providing QoS in 5G, and SDN alone is not enough for that. To achieve ambitious QoS values, it is necessary to influence all KTEs listed below:

1. Spectrum and massive MIMO (multi-channel input–multi-channel output).
2. Network function virtualization (NFV).
3. Centralized radio access network (C-RAN).
4. Local offloading.
5. Small cells.
6. Software defined networking (SDN).

Figure 4 illustrates the factors that each concept relies on and which QoS requirements contribute to.

Each of the KTE tools creates a new concept in 5G that directly impacts KPEs/KPIs and therefore impacts 5G QoS. New concepts include:

1. Service chaining.
2. New architecture.
3. New air interfaces.
4. Slicing network.
5. Function allocation and placement.
6. Flexible control.

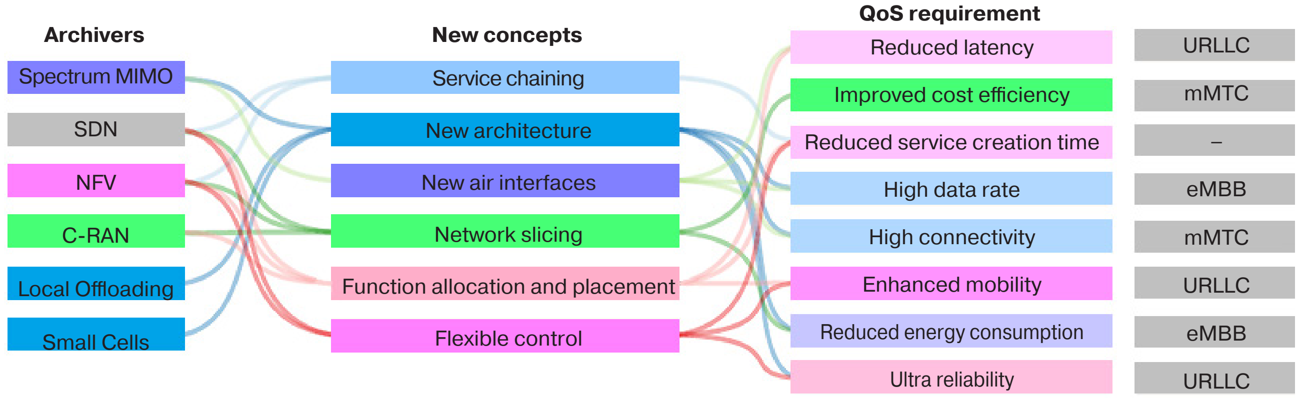

Fig. 4. New concepts, means of implementation and requirements for QoS of the fifth generation (5G)

5. QOS FOR THE NEXT GENERATION OF 5G NETWORKS

The 5G technology should significantly improve service quality in terms of network data volume and service types. There is a huge worldwide effort to define a new 5G architecture with initiatives such as 5G infrastructure public-private partnership (5G-PPP) and the METIS project in Europe [21]; IMT-2020 (5G) in Russia [22]; 5G America in America [23]; IMT-2020 (5G) PG3 in China [24]; The 5G Forum in Korea [25, 26], and the Fifth Generation Mobile Promotion Forum (5GMF) in Japan [26]. The promised values for 5G QoS parameters are shown in Table 4 [28].

Table 4. Promised values for 5G QoS parameters

Speed/throughput	10 Gbit/s, target to 20 GB/s
End-to-end latency	1–10 ms
Network availability	Stretched to 100%
Reliability	Block Error Rate is 0.00001 in an 1-ms period
Jitter	10–100 µs
Bandwidth	100 Kbit/s to several hundred Mbit/s

Table 5 shows the QoS parameters for the basic driving principles of 5G technology.

Within the framework of the METIS project, 12 scenarios for the use of 5G networks have been identified [19]. In the Virtual Reality Office use scenario test, end users should be able to achieve at least 5 GB/s data rates in 20% of office spaces, such as real desks during 99% of busy hours. In all of the above initiatives, the latency between devices (D2D) is less than 5ms. Highest 5G availability and reliability requirements are 100% and 99.999%, respectively, for all initiatives.

Energy consumption, as it can be seen from the table, is an important parameter in 5G technology. This parameter is 10 to 100 times better than that in the previous generation of networks. Another parameter that affects the quality of service is the ratio of packets lost due to errors when receiving data packets IP—Packet Error Loss Rate (PELR). The packet loss rate requirement for video broadcasting in 5G networks is 10^{-9}. For M2M services, the quality will also be determined by the fraction of packets lost during reception. The PELR requirement for M2M service with guaranteed quality of service in 5G networks is 10^{-7}. Another important parameter that determines the QoS requirements in a fifth generation network is the overall packet delay budget (PDB), which is generated at the radio-interface RAN and is considered as the maximum packet delay with a control level of 98%.

CONCLUSIONS

The emergence and implementation of 5G technology is based on remarkably improved key indicators in mobile networks, including end-to-end QoS. A software-configured SDN is an attractive research area for network communications and is also an integral part of the 5G network. SDN promises to provide a powerful way to implement end-to-end quality of service QoS in today's communications networks.

In the 5G technology, customer satisfaction poses many new challenges for the operator. Reliability and scalability are key QoS issues in a programmable network. The article analyzes the QoS method based on the OpenFlow protocol and the QoS method based on open source SDN controllers in the network. The problems of SDN-based architecture and their influence on the parameters of QoS are studied, and key indicators of performance in 5G/IMT-2020 networks are overviewed. In addition, other parameters are analysed for improving QoS in the next generation network: bandwidth, latency, jitter, and losses.

Table 5. QoS parameters for the basic driving principles of 5G technology

QoS	5G-PPP/ METIS	5G Americas	IMT-2020 (5G) PG	5G Forum
Experienced user throughput[1]	Depend on use case test[2]	Depend on use case test	Depend on use case test	Depend on use case test
Latency	5 ms (E2E)	5–100x better	1 ms (E2E)	1 ms (E2E)
Availability	≈100%	≈100%	≈100%	≈100%
Energy consumption	10x better	–	100x better	1000x better
Reliability	five nines 99.999%	high	five nines 99.999%	hyperhigh

[1] Achievable data rate is available ubiquitously across the coverage area to a device/user

[2] Virtual reality office, dense urban areas, shopping malls, and stadiums should provide 5 Gbit/s in downlink and uplink channels.

REFERENCES

1. View on 5G Architecture – 5G-PPP. Version 3.0. Available from URL: https://5g-ppp.eu/wp-content/uploads/2019/07/5G-PPP-5G-Architecture-White-Paper_v3.0_PublicConsultation.pdf
2. Keshari S.K., Kansal V., Kumar S. A systematic review of quality of services (QoS) in software defined networking (SDN). *Wireless Personal Communications*. 2021;116(3):2593−2614. https://doi.org/10.1007/s11277-020-07812-2
3. Moravejosharieh A.H., Lloret J. Performance analysis of quality of service in software-defined networking. *Network Protocols and Algorithms*. 2019;10(4):1. https://doi.org/10.5296/npa.v10i4.14054
4. Nam Tuan Le, Arif Hossain M., Islam A., Do-yun Kim, Young-June Choi, Yeong Min Jang. Survey of promising technologies for 5G networks. *Mobile Information Systems*. 2016; Article ID 2676589. https://doi.org/10.1155/2016/2676589
5. OpenFlow. OpenFlow Switch Specification. Version 1.5.0. 2014. Available from URL: https://opennetworking.org/wp-content/uploads/2014/10/openflow-switch-v1.5.0.pdf
6. Fernandez M.P. Comparing openflow controller paradigms scalability: reactive and proactive. In: *Proc. IEEE 27th International Conference on Advanced Information Networking and Applications* (*AINA*). 2013, p. 1009−1016. https://doi.org/10.1109/AINA.2013.113
7. Masoudi R., Ghaffari A. Software defined networks: A survey. *Journal of Network and Computer Applications*. 2016;67:1−25. https://doi.org/10.1016/j.jnca.2016.03.016
8. McKeown N., Anderson T., Balakrishnan H., Parulkar G., Peterson L., Rexford J., Shenker S., Turner J. OpenFlow: Enabling innovation in campus networks. *ACM SIGCOMM Computer Communication Review*. 2008;38(2):69−74. https://doi.org/10.1145/1355734.1355746
9. Karakus M., Durresi A. Quality of service (QoS) in software defined networking (SDN): A survey. *Journal of Network and Computer Applications*. 2017;200−218. https://doi.org/10.1016/j.jnca.2016.12.019
10. Paliwal M., Shrimankar D., Tembhurne O. Controllers in SDN: A Review Report. *IEEE Access*. 2018;6:36256−36270. https://doi.org/10.1109/ACCESS.2018.2846236
11. Salman O., Elhajj I.H., Kayssi A., Chehab A. SDN controllers: A comparative study. In: *2016 18th Mediterranean Electrotechnical Conference* (*MELECON*). 2016, p. 1−6. https://doi.org/10.1109/MELCON.2016.7495430
12. Wibowo F.X.A., Gregory M.A., Ahmed K., Gomez K.M. Multi-domain software defined networking: Research status and challenges. *Journal of Network and Computer Applications*. 2017;87:32−45. https://doi.org/10.1016/j.jnca.2017.03.004
13. Zhang Y., Cui L., Wang W., Zhang Y. A survey on software defined networking with multiple controllers. *Journal of Network and Computer Applications*. 2018;103:101−118. https://doi.org/10.1016/j.jnca.2017.11.015

СПИСОК ЛИТЕРАТУРЫ

1. View on 5G Architecture – 5G-PPP. Version 3.0. URL: https://5g-ppp.eu/wp-content/uploads/2019/07/5G-PPP-5G-Architecture-White-Paper_v3.0_PublicConsultation.pdf
2. Keshari S.K., Kansal V., Kumar S. A systematic review of quality of services (QoS) in software defined networking (SDN). *Wireless Personal Communications*. 2021;116(3):2593−2614. https://doi.org/10.1007/s11277-020-07812-2
3. Moravejosharieh A.H., Lloret J. Performance analysis of quality of service in software-defined networking. *Network Protocols and Algorithms*. 2019;10(4):1. https://doi.org/10.5296/npa.v10i4.14054
4. Nam Tuan Le, Arif Hossain M., Islam A., Do-yun Kim, Young-June Choi, Yeong Min Jang. Survey of promising technologies for 5G networks. *Mobile Information Systems*. 2016; Article ID 2676589. https://doi.org/10.1155/2016/2676589
5. OpenFlow. OpenFlow Switch Specification. Version 1.5.0. 2014. URL: https://opennetworking.org/wp-content/uploads/2014/10/openflow-switch-v1.5.0.pdf
6. Fernandez M.P. Comparing openflow controller paradigms scalability: reactive and proactive. In: *Proc. IEEE 27th International Conference on Advanced Information Networking and Applications* (*AINA*). 2013, p. 1009−1016. https://doi.org/10.1109/AINA.2013.113
7. Masoudi R., Ghaffari A. Software defined networks: A survey. *Journal of Network and Computer Applications*. 2016;67:1−25. https://doi.org/10.1016/j.jnca.2016.03.016
8. McKeown N., Anderson T., Balakrishnan H., Parulkar G., Peterson L., Rexford J., Shenker S., Turner J. OpenFlow: Enabling innovation in campus networks. *ACM SIGCOMM Computer Communication Review*. 2008;38(2):69−74. https://doi.org/10.1145/1355734.1355746
9. Karakus M., Durresi A. Quality of service (QoS) in software defined networking (SDN): A survey. *Journal of Network and Computer Applications*. 2017;200−218. https://doi.org/10.1016/j.jnca.2016.12.019
10. Paliwal M., Shrimankar D., Tembhurne O. Controllers in SDN: A review report. *IEEE Access*. 2018;6:36256−36270. https://doi.org/10.1109/ACCESS.2018.2846236
11. Salman O., Elhajj I.H., Kayssi A., Chehab A. SDN controllers: A comparative study. In: *2016 18th Mediterranean Electrotechnical Conference* (*MELECON*). 2016, p. 1−6. https://doi.org/10.1109/MELCON.2016.7495430
12. Wibowo F.X.A., Gregory M.A., Ahmed K., Gomez K.M. Multi-domain software defined networking: Research status and challenges. *Journal of Network and Computer Applications*. 2017;87:32−45. https://doi.org/10.1016/j.jnca.2017.03.004
13. Zhang Y., Cui L., Wang W., Zhang Y. A survey on software defined networking with multiple controllers. *Journal of Network and Computer Applications*. 2018;103:101−118. https://doi.org/10.1016/j.jnca.2017.11.015
14. Karakus M., Durresi A. A survey: Control plane scalability issues and approaches in Software-Defined Networking. *Computer Networks*. 2017;112(7):279−293. https://doi.org/10.1016/j.comnet.2016.11.017

14. Karakus M., Durresi A. A survey: Control plane scalability issues and approaches in Software-Defined Networking. *Computer Networks*. 2017;112(7):279–293. https://doi.org/10.1016/j.comnet.2016.11.017
15. Singh A.K., Srivastava S. A survey and classification of controller placement problem in SDN. *International Journal of Network Management*. 2018;28(2):e–2018. https://doi.org/10.1002/nem.2018
16. OpenDaylight Project. Available from URL: https://www.opendaylight.org
17. ONOS Project. Available from URL: http://onosproject.org
18. Floodlight Project. Available from URL: https://floodlight.atlassian.net/wiki/spaces/HOME/overview?mode=global
19. Scenarios, requirements and KPIs for 5G mobile and wireless system. ICT-317669-METIS/D1.1. May 2013. Available from URL: https://cordis.europa.eu/docs/projects/cnect/9/317669/080/deliverables/001-METISD11v1pdf.pdf
20. Banovic-Curguz N., Ilisevic D. Mapping of QoS/QoE in 5G networks. In: *Proc. 2019 42nd International Convention on Information and Communication Technology, Electronics and Microelectronics* (*MIPRO*). 2019, p. 404–408. https://doi.org/10.23919/MIPRO.2019.8757034
21. 5G-PPP. 5G Vision. The 5G infrastructure public private partnership: The next generation of communication networks and services. Available from URL: https://5g-ppp.eu/wp-content/uploads/2015/02/5G-Vision-Brochure-v1.pdf
22. Concept of creation and development of 5G/IMT-2020 networks in the Russian Federation. (in Russ.). Available from URL: https://digital.gov.ru/uploaded/files/kontseptsiya-sozdaniya-i-razvitiya-setej-5g-imt-2020.pdf
23. 5G Americas. Network Slicing for 5G Networks and Services. Available from URL: https://www.5gamericas.org/network-slicing-for-5g-networks-services/
24. IMT-2020 (5G) Promotion Group and 5G PPP Announce Memorandum of Understanding for 5G. Available from URL: https://5g-ppp.eu/imt-2020-5g-promotion-group-and-5g-ppp-announce-memorandum-of-understanding-for-5g/
25. 5G Vision and Requirements of 5Gforum. Available from URL: https://www.itu.int/dms_pub/itur/oth/0a/06/R0A0600005F0001PDFE.pdf
26. 5GMF White Paper. 5G Mobile Communications Systems for 2020 and Beyond. Available from URL: https://5gmf.jp/wp/wp-content/uploads/2016/09/5GMF_WP101_All.pdf
27. Mohandas R., Aravindhar D.J. An intelligent dynamic bandwidth allocation method to support quality of service in internet of things. *International Journal of Computing*. 2021;20(2):254–261.
28. Hind S., Najib E.K., Fatima L. Towards QoS enhancement in wireless network through SDN. In: *2019 7th Mediterranean Congress of Telecommunications* (*CMT*). 2019, p. 1–5. https://doi.org/10.1109/CMT.2019.8931396
15. Singh A.K., Srivastava S. A survey and classification of controller placement problem in SDN. *International Journal of Network Management*. 2018;28(2):e–2018. https://doi.org/10.1002/nem.2018
16. OpenDaylight Project. URL: https://www.opendaylight.org
17. ONOS Project. URL: http://onosproject.org
18. Floodlight Project. URL: https://floodlight.atlassian.net/wiki/spaces/HOME/overview?mode=global
19. Scenarios, requirements and KPIs for 5G mobile and wireless system. ICT-317669-METIS/D1.1. May 2013. URL: https://cordis.europa.eu/docs/projects/cnect/9/317669/080/deliverables/001-METISD11v1pdf.pdf
20. Banovic-Curguz N., Ilisevic D. Mapping of QoS/QoE in 5G networks. In: *Proc. 2019 42nd International Convention on Information and Communication Technology, Electronics and Microelectronics* (*MIPRO*). 2019, p. 404–408. https://doi.org/10.23919/MIPRO.2019.8757034
21. 5G-PPP. 5G Vision. The 5G infrastructure public private partnership: The next generation of communication networks and services. URL: https://5g-ppp.eu/wp-content/uploads/2015/02/5G-Vision-Brochure-v1.pdf
22. Концепция создания и развития сетей 5G/IMT-2020 в Российской Федерации (Проект). URL: https://digital.gov.ru/uploaded/files/kontseptsiya-sozdaniya-i-razvitiya-setej-5g-imt-2020.pdf
23. 5G Americas. Network slicing for 5G Networks and Services. URL: https://www.5gamericas.org/network-slicing-for-5g-networks-services/
24. IMT-2020 (5G) Promotion Group and 5G PPP Announce Memorandum of Understanding for 5G. URL: https://5g-ppp.eu/imt-2020-5g-promotion-group-and-5g-ppp-announce-memorandum-of-understanding-for-5g/
25. 5G Vision and Requirements of 5Gforum. URL: https://www.itu.int/dms_pub/itur/oth/0a/06/R0A0600005F0001PDFE.pdf
26. 5GMF White Paper. 5G Mobile Communications Systems for 2020 and Beyond. URL: https://5gmf.jp/wp/wp-content/uploads/2016/09/5GMF_WP101_All.pdf
27. Mohandas R., Aravindhar D.J. An intelligent dynamic bandwidth allocation method to support quality of service in internet of things. *International Journal of Computing*. 2021;20(2):254–261.
28. Hind S., Najib E.K., Fatima L. Towards QoS enhancement in wireless network through SDN. In: *2019 7th Mediterranean Congress of Telecommunications* (*CMT*). 2019, p. 1–5. https://doi.org/10.1109/CMT.2019.8931396

About the author

Behrooz Daneshmand, Postgraduate Student, Faculty of Infocommunication Technologies, ITMO University (49–A, Kronverkskii pr., St. Petersburg, 197101 Russia). E-mail: daneshmandbehrooz@gmail.com.

Об авторе

Данешманд Бехруз Мехди, аспирант, факультет инфокоммуникационных технологий Санкт-Петербургского национального исследовательского университета информационных технологий, механики и оптики (197101, Санкт-Петербург, Кронверкский пр-т, д. 49, лит. А). E-mail: daneshmandbehrooz@gmail.com.

Translated by E. Shklovskii

Russian Technological Journal. 2021;9(5):26–35 ISSN 2500-316X (Online)

Modern radio engineering and telecommunication systems

Современные радиотехнические и телекоммуникационные системы

UDC 004.4:004.7
https://doi.org/10.32362/2500-316X-2021-9-5-26-35

RESEARCH ARTICLE

Assessment reliability parameters of the DVB-T2 broadcasting station's equipment with local content insertion

Sergey V. Sai [1, @], Nikolay Yu. Sorokin [1], Olga V. Tissen [2]

[1] *Pacific National University, Khabarovsk, 680000 Russia*
[2] *Russian television and radio broadcasting network, Khabarovsk, 680000 Russia*
[@] *Corresponding author, e-mail: 000493@pnu.edu.ru*

Abstract. Local content modification provided to subscribers of the terrestrial digital television signal is necessary to provide the technical possibility of organizing inserts of local content signals, such as TV programs of regional broadcasters, as well as information on emergency situations. Broadcast multiplexes of federal TV programs are designed for use within the corresponding time zone (A, B, C, D, M). In each time zone, there are a number of regions, in each of which there are local TV and radio companies that produce local content that must be delivered to the subscribers of the whole subject. The task of embedding/modifying content at each remote transmitting station is performed by an inserter or local content insertion device (ETSI TS 102773). The reliability parameters of the restorable system for organizing terrestrial television broadcasting at a remote station with the content modification were calculated in this article. Tables and a graph of the broadcasting system states are presented, on the basis of which, systems of Kolmogorov differential equations are compiled. It was found that additional redundancy organized by connecting the output stream from the RX1 receiver directly to the transmitting device allows for a 2.5-fold increase in the average operating time between failures, as well as an increase in the availability factor by 5.26 percent. All calculations were performed using the *SimInTech* software package. The influence of automatic redundancy of the local content inserter and the transmitter on the occurrence of errors in the stream that affect the quality of the output signal is considered. The relationship between the availability factor and the components of the Quality of Service parameter – SAE, SDE, and SIE is determined.

Keywords: local content insertion, T2-MI stream, multiplex, Quality of Service, terrestrial television broadcasting, redundancy, reliability

• **Submitted:** 18.03.2021 • **Revised:** 12.04.2021 • **Accepted:** 12.07.2021

For citation: Sai S.V., Sorokin N.Yu., Tissen O.V. Assessment reliability parameters of the DVB-T2 broadcasting station's equipment with local content insertion. *Russ. Technol. J.* 2021;9(5):26–35. https://doi.org/10.32362/2500-316X-2021-9-5-26-35

Financial disclosure: The authors have no a financial or property interest in any material or method mentioned.

The authors declare no conflicts of interest.

НАУЧНАЯ СТАТЬЯ

Оценка параметров надежности комплекса оборудования станции эфирного телевещания DVB-T2 с регионализацией контента

С.В. Сай [1, @], Н.Ю. Сорокин [1], О.В. Тиссен [2]

[1] *Тихоокеанский государственный университет, Хабаровск, 680000 Россия*
[2] *Российская телевизионная и радиовещательная сеть, Хабаровск, 680000 Россия*
[@] *Автор для переписки, e-mail: 000493@pnu.edu.ru*

Резюме. Модификация контента, предоставляемого абонентам эфирного цифрового телевизионного сигнала, необходима для обеспечения технической возможности организации врезок сигналов местного наполнения, таких как телепрограммы региональных вещателей или информация территориальных органов ГО ЧС. Вещательные мультиплексы федеральных телепрограмм рассчитаны на использование в рамках соответствующей временной зоны (А, Б, В, Г, М). В каждой временной зоне находится целый ряд регионов, в каждом из которых существуют местные телерадиокомпании, выпускающие контент локального характера, который необходимо доставить до абонентов целого субъекта. Задачу врезки/модификации контента на каждой удаленной передающей станции выполняет инсертер или устройство вставки локального контента (ETSI TS 102773). В статье проведен расчет параметров надежности восстанавливаемой системы организации эфирного телевещания на удаленной станции с учетом модификации контента. Представлены таблицы и граф состояний системы вещания, на основании которых составлены системы дифференциальных уравнений А.Н. Колмогорова. Установлено, что дополнительное резервирование, организованное путем подключения выходного потока с приемника RX1 непосредственно на передающее устройство, позволяет в 2.5 раза повысить среднее время наработки между отказами, а также повысить значение коэффициента готовности на 5.26%. Все расчеты выполнены с использованием программного комплекса *SimInTech*. Рассмотрено влияние автоматического резервирования оборудования врезки контента и передатчика на возникновение ошибок в потоке, влияющих на качество выходного сигнала. Определена взаимосвязь коэффициента готовности и составляющих параметра Quality of Service – SAE, SDE и SIE.

Ключевые слова: регионализация контента, T2-MI поток, мультиплекс, Quality of Service, эфирное телевещание, резервирование, надежность

• **Поступила:** 18.03.2021 • **Доработана:** 12.04.2021 • **Принята к опубликованию:** 12.07.2021

Для цитирования: Сай С.В., Сорокин Н.Ю., Тиссен О.В. Оценка параметров надежности комплекса оборудования станции эфирного телевещания DVB-T2 с регионализацией контента. *Russ. Technol. J.* 2021;9(5):26–35. https://doi.org/10.32362/2500-316X-2021-9-5-26-35

Прозрачность финансовой деятельности: Никто из авторов не имеет финансовой заинтересованности в представленных материалах или методах.

Авторы заявляют об отсутствии конфликта интересов.

GLOSSARY:

DVB-T2—Digital Video Broadcasting–Terrestrial 2
T2-MI—T2 Modulator Interface
PLP—Physical Layer Pipes
QoS—Quality of Service
QoE—Quality of Experience
SAE—Service Availability Error
SDE—Service Degradation Error
SIE—Service Impairment Error

INTRODUCTION

Regional adaptation at the DVB-T2 broadcasting stations may be performed by the use of local content inserters conforming to European Telecommunications Standards Institute specification—ETSI TS 102773. The most popular models are produced by ENENSYS Technologies, France (TxEdge T2), NPP Triada-TV, Russia (TTV-PLPSW-0401) and Nevion, Norway (CP330 T2-Bridge). Part of the main T2-MI stream containing multiplex package services may be updated

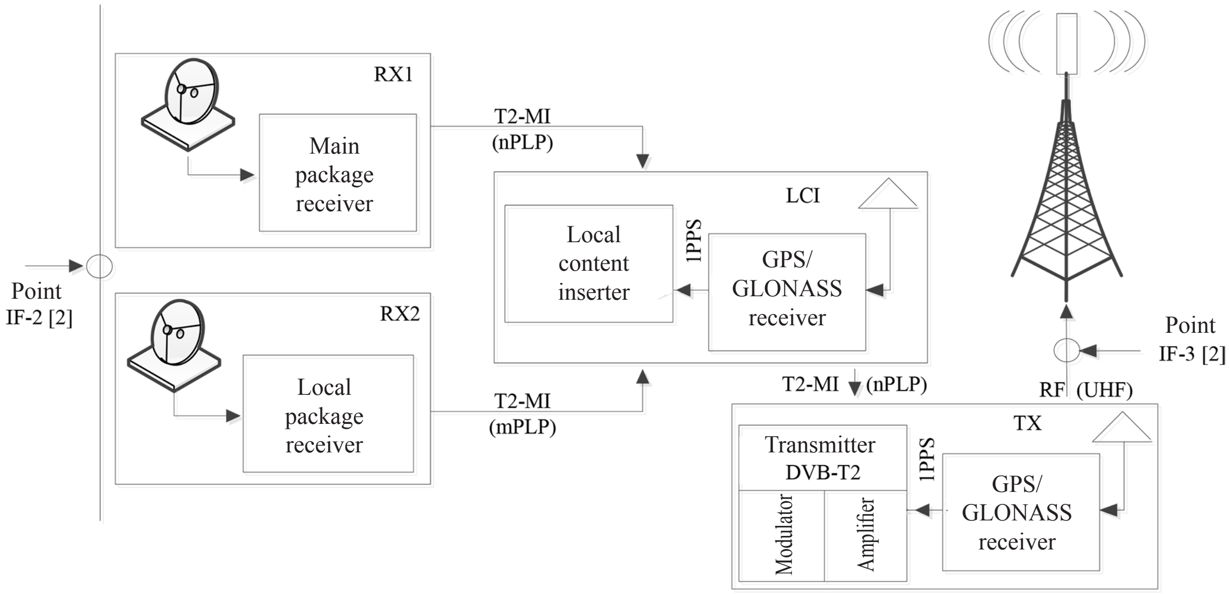

Fig. 1. A scheme for organizing broadcasting at a typical transmitting station

with the local content using PLP substitution. Setting the local content insertion device into operation implies installing an additional equipment to receive local TV channel packages, thus affecting the reliability parameters of the broadcasting system at the station as well as the Quality of Service (QoS) performance index.

According to GOST R 58912-2020 National Standard [1], "*the parameters of the end-to-end transmission of DTV signal at the broadcasting facility are used to assess the distortion of TV signal transmitted from the receiving point at digital transmitting stations before it reaches the land-based (terrestrial) digital TV stations. These parameters characterize the quality of the end-to-end TV signal transmission at two levels:*

- *video and audio quality of experience (QoE);*
- *QoS.*"

The reliability parameters are assessed at point IF-3 (Figure 7.1, Chapter 7 of the Handbook on Organizing Digital Terrestrial Television Broadcasting Networks and Systems Implementation [2]). Throughout the study, the section of broadcasting system within the limits of points IF-2 and IF-3 [2], which hardware is implemented at the remote typical transmitting station, is under consideration. As the paper deals with the transmitting section of a typical transmitting station, it would be reasonable to rest on the objective QoS assessment, since the direct-to-home receiving path has not been assessed here.

Since both parameters (subjective, QoE along with objective, QoS) are of equal significance, the paper aims at calculating the availability factor and reliability parameters of the broadcasting system as well as at determining the relationship between the availability factor and objective QoS assessment, which could be calculated using hardware for digital data stream control and analysis.

ASSESSMENT OF RELIABILITY PARAMETERS FOR THE TERRESTRIAL BROADCASTING SYSTEM

A scheme for organizing broadcasting including local insertions is generally shown in Fig. 1.

To calculate reliability, this scheme can be represented as two elements connected in parallel (equipment for receiving main RX1 and local RX2 streams) along with two elements connected in series: local content inserter (LCI) and DVB-T2 TX Transmitter.

A scheme for calculating reliability is presented in Fig. 2. In practical use of the broadcasting system with content modification, the source of local (modifying) T2-MI stream is usually not fully interchangeable with the source of the main one.

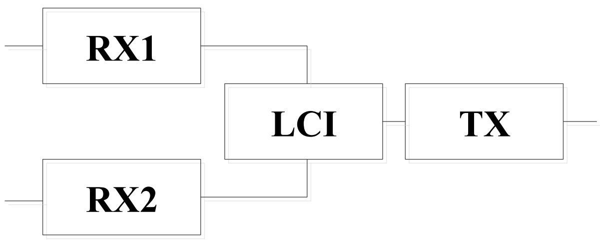

Fig. 2. A scheme for calculating reliability

Therefore, the following calculation is performed specifically for the case, when the system is operable with functioning of either both sources (i.e., insertion is performed), or only the main one (the signal of the main T2-MI package is transmitted without local insertion [3]). In this case, the local source would not replace the main one when the latter fails [4].

It would be ineffective to use the coefficient method for calculating reliability parameters in determining the availability of the broadcasting system, since a unit of equipment is considered as the system element. That means the implementation of hardware and software complex as a single facility, while there is no initial data on the coefficients of conditions and loads as well as on the basic failure and recovery rates for the modern equipment under consideration. Also, according to the analysis of the equipment documentation [5–7], there is no data on an average operating time between failures or other reliability parameters which would allow calculating the system availability factor. In this regard, the dynamic modeling method applying the system of differential equations of A.N. Kolmogorov [8] is used in this paper.

Conditions for calculating reliability parameters for the scheme shown in Fig. 2 may be characterized as follows:

1) the broadcasting system is recoverable, i.e., the failed component can be recovered and further used;
2) two or more components cannot fail simultaneously [8];
3) only one component can be recovered at a time [8];
4) RX1 and RX2 units are not interchangeable, and the system is operable with functioning of either RX1, or both RX1 and RX2. Here, it should be considered that different content may be broadcasted. The system is inoperable when either RX1, or both RX1 and RX2 fails; however, when these units are simultaneously operable, the insertion is performed;
5) the unit that is not actually operating cannot pass into the failure state;
6) the inoperable state of the system means the absence of broadcasting signal, but since the paper considers a remote unattended broadcasting station, the equipment preceding the failed unit remains operable and therefore can also fail, despite the overall inoperable state of the system.

Equipment failure may be characterized by the following conditions [9]:

- for the RX1 and RX2 units: interference effect on the quality of reception and transmission over the delivery channel; hop failure; failure on the side of the data stream formation; hardware and software failures of the receiver; signal errors resulting in broadcasting the output signal by the receiver incorrectly;
- for the LCI unit: hardware and software failure; insertion error; input signal errors preventing substitution; equipment synchronization problems;
- for the TX unit: hardware and software failure; signal errors preventing broadcasting; equipment synchronization problems; T2-MI delay mismatch.

The listed factors are considered when determining actual values of failure and restoration rates for specific equipment separately, calculated on the basis of the equipment operations manual similarly to the method proposed in [9]. Numerical values of failure and recovery rates are the following:

$$\lambda_1 = \lambda_2 = 0.00054;\ \lambda_3 = 0.00226;\ \lambda_4 = 0.00101;$$

$$m_1 = m_2 = 0.082;\ m_3 = 0.038;\ m_4 = 0.038.$$

The failure rate λ_1 and recovery rate m_1 refer to the RX1 unit, while λ_2 and m_2—to the RX2 unit, λ_3 and m_3—to LCI, and λ_4 and m_4—to TX, respectively. Factors affecting the reliability and operability of telecommunication equipment are also given in [10–12].

Table 1. System states when the sources are non-interchangeable

No.	System	RX1	RX2	LCI	TX
1	Operable	Operable	Operable	Operable	Operable
2	Operable	Operable	Failure	Operable	Operable
3	Recovery	Failure	Operable	Inoperable	Inoperable
4	Recovery	Operable	Operable	Failure	Inoperable
5	Recovery	Operable	Operable	Operable	Failure
6	Recovery	Failure	Operable	Failure	Inoperable
7	Recovery	Failure	Failure	Inoperable	Inoperable
8	Recovery	Failure	Operable	Inoperable	Failure
9	Recovery	Operable	Failure	Failure	Inoperable
10	Recovery	Operable	Failure	Operable	Failure
11	Recovery	Operable	Operable	Failure	Failure
12	Recovery	Failure	Failure	Failure	Inoperable
13	Recovery	Operable	Failure	Failure	Failure
14	Recovery	Failure	Failure	Inoperable	Failure
15	Recovery	Failure	Operable	Failure	Failure
16	Recovery	Failure	Failure	Failure	Failure

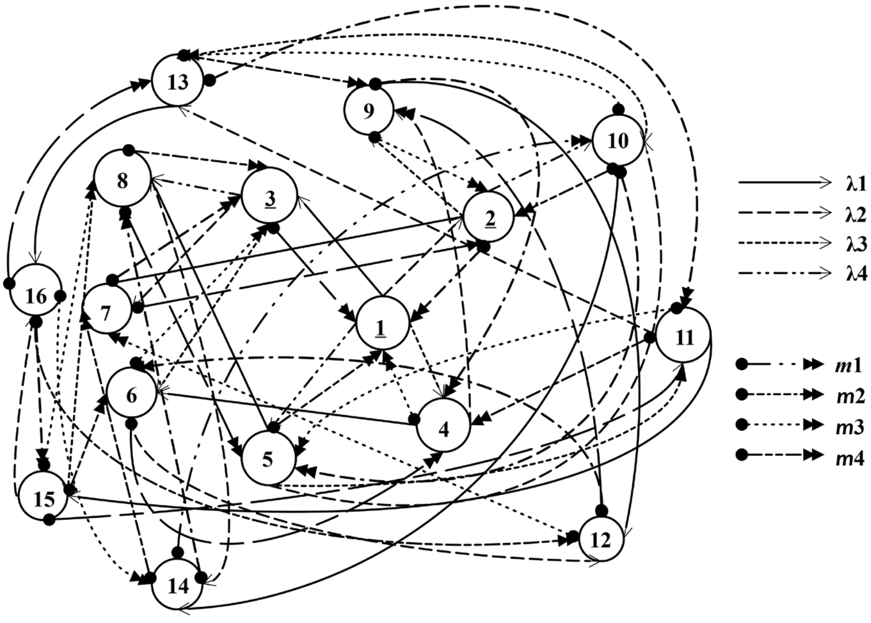

Fig. 3. A transition graph of the broadcasting system states
(the underlined numeration of a state corresponds to the system operability)

Table 1 shows possible states of the broadcasting system shown in Fig. 2. Table 1 demonstrates that when signal sources RX1 and RX2 are non-interchangeable, the system may have only two operable states. Figure 3 shows the transition graph of system states based on the tabled data.

The edges connecting the system states characterize the failure and recovery rates of the system components when transiting from one state to another.

For the resulting graph, the system of Kolmogorov differential equations may be written in the following general form:

$$\frac{d}{dx}p_i(t) = \\ = \left(\sum_{j,k} p_j(t)m_k + \sum_{j,k} p_j(t)\lambda_k\right) - p_i(t)\left(\sum_k m_k + \sum_k \lambda_k\right), \quad (1)$$

where $p_i(t)$ are values of the system state probabilities and $i \in [1, 2, ...16]$ are the numbers of states according to Table 1 and points of graph (Fig. 3). In Eq. (1), the first summand describes edges comprising the vertex number i, while the second summand describes outcoming edges. For example, the equation for the state with number 3 may be written as follows:

$$\frac{d}{dx}p_3(t) = (\lambda_1 p_1(t) + m_3 p_6(t) + \\ + m_2 p_7(t) + m_4 p_8(t)) - p_3(t)(\lambda_2 + m_1),$$

and other 16 equations have been derived in the same way.

The availability factor K_{AF1} is defined as follows:

$$K_{\text{AF1}}(t) = \sum_{i \in E^+} p_i(t) = p_1(t) + p_2(t).$$

The downtime rate K_{DT1} may be written as follows:

$$K_{\text{DR1}}(t) = \sum_{i \in E^-} p_i(t) = p_3(t) + p_4(t) + p_5(t) + \\ + p_6(t) + p_7(t) + p_8(t) + p_9(t) + p_{10}(t) + p_{11}(t) + \\ + p_{12}(t) + p_{13}(t) + p_{14}(t) + p_{15}(t) + p_{16}(t).$$

The failure stream is calculated as the sum of the products of failure rates and state probabilities during system transition from operable to non-operable state [8], as follows:

$$w_1 = \lambda_3 p_1 + \lambda_4 p_1 + \lambda_4 p_2 + \lambda_3 p_2 + \lambda_1 p_2 + \lambda_1 p_1.$$

The recovery stream is defined as the sum of the products of recovery rates and state probabilities during system transition from non-operable to operable state [8], as follows:

$$q_1 = m_4 p_5 + m_3 p_4 + m_4 p_{10} + m_1 p_7 + m_1 p_3 + m_3 p_9.$$

Based on calculations performed using *SimInTech* software [1], the steady-state availability factor amounts to 0.9144 while the downtime rate is 0.086. Steady-state values of the failure and recovery fluxes are equal to 0.0035, i.e., $w_1 = q_1 = 0.0035$.

The average time between failures in terms of nominal units may be written as follows [8]:

$$T_1 = {}^{K_{\text{AF1}}}\!/_{w_1} = {}^{0.9144}\!/_{0.0035} = 261.26 \text{ units},$$

while the average time to recovery may be written in the following way [8]:

$$T_1^{\text{rec}} = {}^{K_{\text{DT1}}}\!/_{q_1} = {}^{0.086}\!/_{0.0035} = 24.57 \text{ units}.$$

According to GOST R 58020-2017 National Standard, the integral availability factor of the digital terrestrial television broadcasting network (from broadcasting of the Russian federal company to the bounders of the coverage area with normalized parameters) should amount at least to 0.9985 for broadcasting zones A and B. This value involves only calculations based on the reliability parameters of specific products/equipment provided by the manufacturer either with the availability factor value, or with the value of time between failures. These parameters are laid down by the manufacturer and are justified only by the software stability of a particular device, hardware quality, the ability to operate at different ambient temperatures, etc., that is, how long the device can operate performing its functions under other ideal external conditions.

It should be noted here that the paper deals with the reliability of the equipment at a typical unattended remote broadcasting station, rather than of the entire network, so the values of availability factors differ from those given in GOST National Standards. According to [14], "*the requirements to K_{AF} of the most mass network elements (for example, unattended radio transmitting television stations with low power transmitters) can be lower due to the fact that they provide service to isolated small towns*."

RELIABILITY OF THE BROADCASTING SCHEME USING NON-INTERCHANGABLE SOURCES WITH ADDITIONAL REDANDUNCY

If the scheme shown in Fig. 2 is supplemented by connecting the output of the main stream source to the input of the transmitting device bypassing the modification system, then the number of operable states of the system may certainly increase.

Figure 4 shows a scheme of redundant connection.

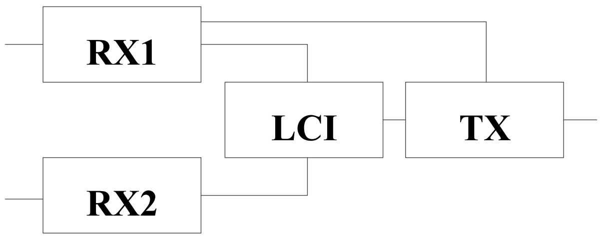

Fig. 4. A scheme with additional redundancy for calculating reliability

In case the insertion unit fails, the signal from RX1 is transmitted directly to TX, as well as the unmodified signal is broadcasted, but when the transmitting station operates in a single-frequency mode, a difference in time delays between the signal which has not passed LCI unit at the considered station and the signal which has passed LCI unit at the neighboring single-frequency zone station may occur. This, as well as the fact that broadcasting an unmodified signal may also represent an abnormal operating mode, should be considered when actually using the broadcasting network.

System states are shown in Table 2, whence it follows that under the given conditions there become more operable system states than in Table 1. The transition graph of the system states is plotted in the same way as

Table 2. States of broadcasting system with additional redundancy

No.	System	RX1	RX2	LCI	TX
1	Operable	Operable	Operable	Operable	Operable
2	Operable	Operable	Failure	Operable	Operable
3	Recovery	Failure	Operable	Inoperable	Inoperable
4	Operable	Operable	Operable	Failure	Operable
5	Recovery	Operable	Operable	Operable	Failure
6	Recovery	Failure	Operable	Failure	Inoperable
7	Recovery	Failure	Failure	Inoperable	Inoperable
8	Recovery	Failure	Operable	Inoperable	Failure
9	Operable	Operable	Failure	Failure	Operable
10	Recovery	Operable	Failure	Operable	Failure
11	Recovery	Operable	Operable	Failure	Failure
12	Recovery	Failure	Failure	Failure	Inoperable
13	Recovery	Operable	Failure	Failure	Failure
14	Recovery	Failure	Failure	Inoperable	Failure
15	Recovery	Failure	Operable	Failure	Failure
16	Recovery	Failure	Failure	Failure	Failure

the graph for the system without redundancy, therefore, it is not presented in the paper for the sake of brevity.

The system of differential equations based on data given in Table 2 may be also created using Eq. (1).

Thus, the availability factor is defined as follows:

$$K_{\mathrm{AF2}}(t)=\sum_{i\in E^{+}} p_i(t)=p_1(t)+p_2(t)+p_4(t)+p_9(t),$$

while the downtime rate may be written in the following way:

$$K_{\mathrm{DT2}}(t)=\sum_{i\in E^{-}} p_i(t)=p_3(t)+p_5(t)+p_6(t)+$$
$$+p_7(t)+p_8(t)+p_9(t)+p_{10}(t)+p_{11}(t)+$$
$$+p_{12}(t)+p_{13}(t)+p_{14}(t)+p_{15}(t)+p_{16}(t).$$

The failure stream may be defined as follows:

$$w_2=\lambda_4 p_1+\lambda_4 p_2+\lambda_1 p_1+\lambda_4 p_4+\lambda_1 p_4+$$
$$+\lambda_1 p_9+\lambda_4 p_9+\lambda_1 p_2,$$

while the recovery stream may be written in the following way:

$$q_2=m_4 p_5+m_4 p_{10}+m_1 p_7+m_1 p_3+m_1 p_6+$$
$$+m_4 p_{11}+m_1 p_{12}+m_4 p_{13}.$$

In steady-state mode, the availability factor calculated for this broadcast scheme using *SimInTech* environment amounts to 0.967, the steady-state value of the failure stream as well as the recovery stream is 0.0015, i.e., at $t\to\infty$, $w_1=q_1=0.0015$. The steady-state downtime design rate is 0.032.

The average time between failures may be written in nominal units in the following way:

$$T_2={K_{\mathrm{AF2}}}/{w_2}={0.967}/{0.0015}=644.67\ \text{units},$$

while the average time to recovery may be written as follows:

$$T_2^{\mathrm{rec}}={K_{\mathrm{DT2}}}/{q_2}={0.032}/{0.0015}=21.33\ \text{units}.$$

Thus, the following conclusions have been drawn from the research.

When using direct non-standard redundancy, the availability factor of the broadcasting system at a typical transmitting station with content modification is 5.26% higher than that of a similar scheme without redundancy.

Conversion to the physical time shows that the redundancy allows reducing the equipment downtime by 19 days, 4 hours and 47 minutes per year.

With the equipment recovery time being almost equal, the average time between failures for the system with redundancy is 2.5 times higher than for that without redundancy, which corresponds to a longer operability interval for the complete set of equipment at a typical transmitting station.

It should be noted that the calculated availability factors for the set of equipment at the remote transmitting station are practical, not regulatory values been determined for the worst-case scenario with allowance for the influence of possible external factors. In the paper, the probability of all the assumed faults happening to the equipment during the considered period is taken as one unit (worst-case scenario); however, this probability may be much lower in actual use.

RELATION OF THE AVAILABILITY FACTOR AND QOS COMPONENTS

According to the Guidelines on Measurements for Digital Terrestrial Television Broadcasting Systems [15], developed by the International Telecommunication Union (ITU), QoS is characterized by the following three main parameters:

- Service Availability Error (SAE);
- Service Degradation Error (SDE);
- Service Impairments Error (SIE).

The numerical values for these parameters are determined on the basis of the data stream analysis for certain errors of the first, second or third priority, according to ETSI TS 101290. Based on formulas for calculating the parameters given in [15], it may be assumed that in steady-state mode $SAE\to 0$, $SDE\to 0$, $SIE\to 0$. For the considered case with additional redundancy, the steady-state mode is defined at $t\in[225;\infty)$.

Thus, the quality of service could be also assessed in a steady-state mode only. The considered scheme for organizing broadcasting with additional redundancy has two automatic recovery points for digital stream:

- redundancy in LCI unit during the system transition from state 1 to state 2 and from state 5 to state 10 and back;
- redundancy in TX unit during the system transition from state 1 to state 4 and from state 2 to state 9 and back.

Automatic redundancy for TX implies switching from the main source of digital data stream (LCI device) to the redundant one (receiver of the federal signal RX1) in the event of a certain number of errors in the stream or complete absence of packages within a specified time. Automatic redundancy for LCI implies transition from the insertion mode when both streams from RX1 and RX2 are used to broadcasting only the basic T2-MI version from RX1 when errors occur in local digital stream. Reverse switching is possible when the main source is recovered and a specified number of correct packages are available. The absence of the main stream packages or errors during the waiting time when transiting to redundancy results in QoS decrease, in particular by SAE and SDE parameters (TS_sync_loss, PAT_error, PMT_error, PCR_error). Depending on the conditions of redundant switching, the decrease in QoS by these parameters causes short-term absence of the image on the subscriber receiver screen, image pixelation and typical image splitting into blocks. Also, redundancy may result in content replacement in the service subjected to modification by the main scheme. Reverse switching to the main source is less problematic, since it occurs in the absence of errors, but can also cause a decrease in QoS, in particular by SIE parameter (Continuity_count_error, Transport_error), which at a single occurrence can be unnoticed by the subscriber's subjective perception, except for changing the content of the modified channel. Moments of automatic redundancy for the system under consideration refer to the transient mode and are limited to time interval $t \in (0;225)$, so the percentage of time providing a subscriber with the signal of a given quality may be directly characterized by the availability factor, i.e., with an appropriate QoS for a selected time period.

CONCLUSIONS

Calculations of reliability parameters for LCI system at a typical DVB-T2 transmitting station using the system of differential equations of Kolmogorov have determined that at practically equal time of equipment recovery with and without additional redundancy, the average operating time between failures of the system with redundancy is 2.5 times higher than of that without redundancy, which corresponds to a longer interval of operability of the entire typical TV broadcasting complex as well as to a less impact on QoS parameter. In addition, a decrease in QoS is conditioned by switching the equipment to redundant sources in case of automatic redundancy due to the absence of T2-MI stream packages during waiting time, as well as during reverse switching to the normal operational scheme in case the main source of the signal is recovered.

Authors' contribution. All authors equally contributed to the research work.

REFERENCES

1. *Televidenie veshchatel'noe tsifrovoe. Sistema efirnogo nazemnogo tsifrovogo televizionnogo veshchaniya vtorogo pokoleniya DVB-T2. GOST R* 58912-2020. (*Digital video broadcasting. Second generation of digital terrestrial television broadcasting system DVB-T2. GOST R* 58912-2020). Moscow: Standartinform; 2020. 73 p. (in Russ.).
2. *Handbook on Digital Terrestrial Television Broadcasting Networks and Systems Implementation*. (Eds.). Dosch Ch., Hemingway D., Sami W. Switzerland: ITU-R; 2016. 318 p. Available from URL: https://www.itu.int/dms_pub/itu-r/oth/0a/07/R0A0700003B0001PDFE.PDF
3. ETSI TS 102773 V1.4.1 (2016-03) DVB. Modulator Interface (T2-MI) for a second generation digital terrestrial television broadcasting system (DVB-T2). France: 2016. Available from URL: http://www.etsi.org/deliver/etsi_ts/102700_102799/102773/01.04.01_60/ts_102773v 010401p.pdf
4. Kukharskaya O.V., Savin E.Z. Physical features of replacement of information contents in the digital stream for DVB-T2. *Uspekhi sovremennoi radioelektroniki = Achievements of Modern Radioelectronics*. 2017;6:55–63 (in Russ.).
5. *Ustroistvo vstavki lokal'nogo kontenta TTV-PLPSW-0401. Rukovodstvo po ekspluatatsii* (*Local content inserter TTV-PLPSW-0401: user manual*). Novosibirsk: NPP Triada-TV; 2017. (in Russ.). Available from URL: https://triadatv.ru/upload/iblock/d08/ip_mi_kommutator_rukovodstvo.pdf

СПИСОК ЛИТЕРАТУРЫ

1. *Телевидение вещательное цифровое. Система эфирного наземного цифрового телевизионного вещания второго поколения DVB-T2. ГОСТ Р* 58912-2020. М.: Стандартинформ; 2020. 73 с.
2. *Handbook on Digital Terrestrial Television Broadcasting Networks and Systems Implementation*. (Eds.). Dosch Ch., Hemingway D., Sami W. Switzerland: ITU-R; 2016. 318 p. URL: https://www.itu.int/dms_pub/itu-r/oth/0a/07/R0A0700003B0001PDFE.PDF
3. ETSI TS 102773 V1.4.1 (2016-03) DVB. Modulator Interface (T2-MI) for a second generation digital terrestrial television broadcasting system (DVB-T2). France, 2016. URL: https://www.etsi.org/deliver/etsi_ts/102700_102799/102773/01.04.01_60/ts_102773v010401p.pdf
4. Кухарская О.В., Савин Е.З. Физические особенности замещения информационного контента в цифровом потоке для DVB-T2. *Успехи современной радиоэлектроники*. 2017;6:55–63.
5. *Устройство вставки локального контента TTV-PLPSW-0401. Руководство по эксплуатации*. Новосибирск: НПП Триада-ТВ; 2017. URL: https://triadatv.ru/upload/iblock/d08/ip_mi_kommutator_rukovodstvo.pdf
6. CP330 T2-Bridge PLP Replacer User's Manual. Norway: Nevion; 2015. URL: https://techex.co.uk/pdf/t-vips/cp330.pdf
7. TxEdge T2 DVB-T2 Local adapter. France: Enensys Technologies, 2019. URL: https://www.enensys.com/wp-content/uploads/2017/04/TxEdgeT2-datasheet-A.pdf

6. *CP330 T2-Bridge PLP Replacer User's Manual*. Norway: Nevion, 2015. Available from URL: https://techex.co.uk/pdf/t-vips/cp330.pdf
7. TxEdge T2 DVB-T2 Local adapter. France: Enensys Technologies, 2019. Available from URL: https://www.enensys.com/wp-content/uploads/2017/04/TxEdgeT2-datasheet-A.pdf
8. Kholodnykh P.V. *Nadezhnost' informatsionno-upravlyayushchikh sistem: metodicheskoe posobie* (*Reliability of information management systems*). St Petersburg: Sankt-Peterburgskii politekhnicheskii universitet Petra Velikogo; 2015. 49 p. (in Russ.). Available from URL: http://saiu.icc.spbstu.ru/media/files/staff/Kholodnykh/metod_reliablity4.pdf
9. Tissen O.V., Livashvili A.I. Reliability evaluation method for DVB-T2 systems on typical transmitter stations. *Journal of Communications Technology and Electronics*. 2020;65(7):826−834. https://doi.org/10.1134/S106422692007013X
[Tissen O.V., Livashvili A.I. Metodika rascheta parametrov nadezhnosti sistemy tsifrovogo televeshchaniya standarta DVB-T2 na tipovoi peredayushchei stantsii. *Radiotekhnika i elektronika = Journal of Communications Technology and Electronics*. 2020;65(7):695−704 (in Russ.).]
10. Borovikov S.M., Tsyrel'chuk I.N., Troyan F.D. *Raschet pokazatelei nadezhnosti radioelektronnykh sredstv* (*Calculation of indicators of reliability of radio-electronic means*). Minsk: BGUIR; 2010. 71 p. (in Russ.). Available from URL: https://www.bsuir.by/m/12_108786_1_72356.pdf
11. Postnikov I.N. Calculation of the characteristics of the reliability of the telecommunication system. In: *Prospects for the development of information technology*. *Telecommunication systems and computer networks*. 2013. (in Russ.). Available from URL: https://cyberleninka.ru/article/n/raschet-harakteristik-nadezhnosti-telekommunikatsionnoy-sistemy/viewer
12. Gromov Yu.Yu., Ivanova O.G., Mosyagina N.G., Nabatov K.A. *Nadezhnost' informatsionnykh system* (*Reliability of information systems*). Tambov: Izdatel'stvo GOU VPO TGTU; 2010. 88 p. (in Russ.). Available from URL: https://tstu.ru/book/elib/pdf/2010/gromov.pdf
13. Software SimInTech v2.20.10.28. Unified Register of Russian Programs No. 2379. Available from URL: https://project797652.turbo.site/page363830#93279bd3-2068-4a20-a89e-b4c17ae80365
14. Leibov A., Maizul's R., Shavdiya Yu. Standardization of reliability indicators of digital television broadcasting networks. *Broadcasting. Televidenie i radioveshchanie*. 2014;3 (in Russ.). Available from URL: http://broadcasting.ru/articles2/Regandstan/normirovanie-pokazateley-nadezhnosti-setey-tsifrovogo-televizionnogo-veschaniya
15. Report ITU-R BT.2389-0. Guidelines on measurements for digital terrestrial television broadcasting systems. ITU-R. Switzerland: ITU-R; 2016.

8. Холодных П.В. *Надежность информационно-управляющих систем: методическое пособие*. СПб: Санкт-Петербургский политехнический университет Петра Великого; 2015. 49 с. URL: http://saiu.icc.spbstu.ru/media/files/staff/Kholodnykh/metod_reliablity4.pdf
9. Тиссен О.В., Ливашвили А.И. Методика расчета параметров надежности системы цифрового телевещания стандарта DVB-T2 на типовой передающей станции. *Радиотехника и электроника*. 2020;65(7):695−704. https://doi.org/10.31857/S003384942007013X
10. Боровиков С.М., Цырельчук И.Н., Троян Ф.Д. *Расчет показателей надежности радиоэлектронных средств*. Минск: БГУИР; 2010. 71 с. URL: https://www.bsuir.by/m/12_108786_1_72356.pdf
11. Постников И.Н. Расчет характеристик надежности телекоммуникационной системы. В сб.: *Перспективы развития информационных технологий. Телекоммуникационные системы и компьютерные сети*. 2013. URL: https://cyberleninka.ru/article/n/raschet-harakteristik-nadezhnosti-telekommunikatsionnoy-sistemy/viewer
12. Громов Ю.Ю., Иванова О.Г., Мосягина Н.Г., Набатов К.А. *Надежность информационных систем*. Тамбов: Изд-во ГОУ ВПО ТГТУ; 2010. 88 с. URL: https://tstu.ru/book/elib/pdf/2010/gromov.pdf
13. Программное обеспечение SimInTech v2.20.10.28. Единый реестр Российских программ № 2379. URL: https://project797652.turbo.site/page363830#93279bd3-2068-4a20-a89e-b4c17ae80365
14. Лейбов А., Майзульс Р., Шавдия Ю. Нормирование показателей надежности сетей цифрового телевизионного вещания. *Broadcasting. Телевидение и радиовещание*. 2014;3. URL: http://broadcasting.ru/articles2/Regandstan/normirovanie-pokazateley-nadezhnosti-setey-tsifrovogo-televizionnogo-veschaniya
15. Report ITU-R BT.2389-0. Guidelines on measurements for digital terrestrial television broadcasting systems. ITU-R. Switzerland: ITU-R; 2016.

About the authors

Sergei V. Sai, Dr. Sci. (Eng.), Head of the Department of Computer technology, Pacific National University (136, Tikhookeanskaya ul., Khabarovsk, 680000 Russia). E-mail: 000493@pnu.edu.ru. Scopus ID 14042260800, https://orcid.org/0000-0002-4506-1857

Nikolay Yu. Sorokin, Cand. Sci. (Eng.), Vice-Rector, Pacific National University (136, Tikhookeanskaya ul., Khabarovsk, 680000 Russia). E-mail: 004040@pnu.edu.ru. Scopus ID 26325081400, https://orcid.org/0000-0002-2044-7534

Olga V. Tissen, Engineer, FGYP RTRN «Far eastern regional center» (7A, Pavlovicha ul., Khabarovsk, 680000 Russia). E-mail: kuharskaya_olga_1991@mail.ru. https://orcid.org/0000-0002-6666-1907

Об авторах

Сай Сергей Владимирович, д.т.н., заведующий кафедрой «Вычислительная техника», Тихоокеанский государственный университет (680000, Россия, Хабаровск, ул. Тихоокеанская, д. 136). E-mail: 000493@pnu.edu.ru. Scopus ID 14042260800, https://orcid.org/0000-0002-4506-1857

Сорокин Николай Юрьевич, к.т.н., проректор, Тихоокеанский государственный университет (680000, Россия, Хабаровск, ул. Тихоокеанская, д. 136). E-mail: 004040@pnu.edu.ru. Scopus ID 26325081400, https://orcid.org/0000-0002-2044-7534

Тиссен Ольга Владимировна, инженер средств радио и телевидения филиала ФГУП РТРС «Дальневосточный РЦ» (680000, Россия, Хабаровск, ул. Павловича, д. 7А). E-mail: kuharskaya_olga_1991@mail.ru. https://orcid.org/0000-0002-6666-1907

Translated by K. Nazarov

Russian Technological Journal. 2021;9(5):36–44 ISSN 2500-316X (Online)

Micro- and nanoelectronics. Condensed matter physics

Микро- и наноэлектроника. Физика конденсированного состояния

UDC 537.621
https://doi.org/10.32362/2500-316X-2021-9-5-36-44

RESEARCH ARTICLE

Towards a model of chain-by-chain magnetization of a granular medium: a variant of magnetic diagnostics of chains of spheres

Anna A. Sandulyak,
Daria A. Sandulyak @,
Yurij O. Gorpinenko,
Vera A. Ershova,
Alexander V. Sandulyak

MIREA – Russian Technological University, Moscow, 119454 Russia
@ Corresponding author, e-mail: d.sandulyak@mail.ru

Abstract. In addition to information on the magnetic parameters of inhomogeneous magnetics, in particular, granular magnetics usually studied within the framework of the quasi-continuous medium model, it is of no less interest to obtain information from the standpoint of the model, when the object of study is the characteristic elements of an inhomogeneous magnetic. According to the well-proven model of selective magnetization of a granular medium, the elements that make up this medium are chains of granules—straight and sinuous, always manifesting themselves in the direction of its magnetization. They perform the function of conductor channels of the generated magnetic flux through the granular medium. As a result, it is a kind of branched «bundle» of conductor channels. For any of the chains of granules, for example, granules-balls of radius R, conceptually significant are the magnetic parameters of its conditional cores with radius $r \leqslant R$, and these parameters, first of all, the magnetic permeability of quasi-continuous cores and magnetic induction in them, for different (in r) cores are variable, which requires appropriate magnetic diagnostics. To clarify the magnetic parameters of the conditional cores of a chain of granules-balls, as a physically self-sufficient element of a granular medium (i.e., in accordance with the model of chain-link magnetization of such a medium), it is practical to make measuring magnetic flux sensors in the core as circular sensors surrounding the contact point of granules-balls, however, not as traditional wire loops, but as circuits on thin printed circuit boards (with mounting holes) placed between adjacent balls. Based on the obtained data of the magnetic flux in cores of different radii r (r/R = 0.2–0.9) of a chain of spheres with a radius of R = 20 mm, the values of the magnetic flux density B in them, as well as their magnetic permeability μ, were determined when the chain is magnetized in the solenoid by a field of strength from 4.8 to 54.5 kA/m. It is shown that with formal thickening of the cores, the values of B and μ decrease due to a decrease in the volume of the ferromagnet in the core, and for the limiting core ($r/R \to 1$), i.e., for the chain as a whole, they correspond to the values of B and μ for a poly-ball backfill medium.

Keywords: magnetization of a chain of spheres, conditional cores, contours-sensors of magnetic flux, magnetic induction and permeability

• **Submitted:** 23.03.2021 • **Revised:** 30.03.2021 • **Accepted:** 25.05.2021

For citation: Sandulyak A.A., Sandulyak D.A., Gorpinenko Y.O., Ershova V.A., Sandulyak A.V. Towards a model of chain-by-chain magnetization of a granular medium: a variant of magnetic diagnostics of chains of spheres. *Russ. Technol. J.* 2021;9(5):36–44. https://doi.org/10.32362/2500-316X-2021-9-5-36-44

Financial disclosure: The authors have no a financial or property interest in any material or method mentioned.

The authors declare no conflicts of interest.

НАУЧНАЯ СТАТЬЯ

К модели поцепочного намагничивания гранулированной среды: вариант магнитной диагностики цепочек шаров

А.А. Сандуляк,
Д.А. Сандуляк @,
Ю.О. Горпиненко,
В.А. Ершова,
А.В. Сандуляк

МИРЭА – Российский технологический университет, Москва, 119454 Россия
@ Автор для переписки, e-mail: d.sandulyak@mail.ru

Резюме. Кроме информации о магнитных параметрах неоднородных, в частности гранулированных, магнетиков, обычно изучаемых в рамках модели квазисплошной среды, не меньший интерес представляет получение информации с позиций модели, когда объект изучения – характерные элементы неоднородного магнетика. Согласно хорошо зарекомендовавшей себя модели избирательного намагничивания гранулированной среды такими элементами, из которых состоит эта среда, являются цепочки гранул – прямые и извилистые, всегда проявляющие себя в направлении ее намагничивания. Они выполняют функцию проводников-каналов генерируемого магнитного потока сквозь гранулированную среду, вследствие чего она представляет собой своеобразный разветвленный «жгут» проводников-каналов. Для любой же из цепочек гранул, например, гранул-шаров радиусом R концептуально значимыми являются магнитные параметры ее условных сердцевин радиусом $r \leqslant R$. Эти параметры, прежде всего, магнитная проницаемость квазисплошных сердцевин и магнитная индукция в них, для разных (по r) сердцевин вариабельны, что требует соответствующей магнитной диагностики. Для выяснения магнитных параметров условных сердцевин цепочки гранул-шаров как физически самодостаточного элемента гранулированной среды (т.е. в соответствии с моделью поцепочного намагничивания такой среды), измерительные датчики магнитного потока в сердцевине практично выполнять в виде круговых датчиков, окружающих точку контакта гранул-шаров, но не традиционных петель из провода, а контуров на тонких печатных платах с посадочными отверстиями, помещаемых между смежными шарами. На основании полученных данных магнитного потока в разных по радиусу r сердцевинах (r/R = 0.2–0.9) цепочки шаров радиусом R = 20 мм определены значения магнитной индукции B в них, а также их магнитной проницаемости μ при намагничивании цепочки в соленоиде полем напряженностью от 4.8 до 54.5 кА/м. Показано, что при формальном утолщении сердцевин значения B и μ снижаются ввиду уменьшения объема ферромагнетика в сердцевине, а для предельной сердцевины ($r/R \to 1$), т.е. для цепочки в целом они ожидаемо соответствуют значениям B и μ для полишаровой среды-засыпки.

Ключевые слова: намагничивание цепочки шаров, условные сердцевины, контуры-датчики магнитного потока, магнитная индукция и проницаемость

• **Поступила:** 23.03.2021 • **Доработана:** 30.03.2021 • **Принята к опубликованию:** 25.05.2021

Для цитирования: Сандуляк А.А., Сандуляк Д.А., Горпиненко Ю.О., Ершова В.А., Сандуляк А.В. К модели поцепочного намагничивания гранулированной среды: вариант магнитной диагностики цепочек шаров. *Russ. Technol. J.* 2021;9(5):36–44. https://doi.org/10.32362/2500-316X-2021-9-5-36-44

Прозрачность финансовой деятельности: Никто из авторов не имеет финансовой заинтересованности в представленных материалах или методах.

Авторы заявляют об отсутствии конфликта интересов.

INTRODUCTION: TO THE ROLE OF CHAINS OF GRANULES IN THE MAGNETIZATION OF A GRANULAR MEDIUM

The problem of investigation of the magnetic properties of various heterogeneous magnets, in particular, composites, suspensions, powders, granular packings, etc. [1–13], is typically considered to be more complex than the conventional problem of study of the magnetic properties of homogeneous (continuous) magnets. However, in most instances, the former problem is reduced to the determination of the same magnetic characteristics as those of continuous magnets. In this case, the magnetic parameters of an essentially quasi-continuous magnet being explored are often referred to as effective parameters.

Along with such information, i.e., that obtained from the standpoint of this macromodel as characterizing one or another heterogeneous magnet as a whole, it is important to obtain information on its "local" magnetic parameters from the point of view of a sort of a micromodel. And the preferred objects of investigation should be characteristic elements, including composite ones, of a heterogeneous medium of one or another type the micromodel magnetic parameters of which enable one to directly arrive at the macromodel magnetic parameters of the entire heterogeneous magnet.

In particular, such a solution was implemented for quite a widely used type of heterogeneous magnets—granular medium [13–16]. An original model of selective magnetization of a granular medium was used to show that a crucial role in the magnetization is played by such elements of the granular medium as chains of granules, straight and sinuous, which always respond in the direction of the magnetization of this medium. They act as channels that conduct the generated magnetic flux, and the crucial role of these constituent elements of the granular medium, which functions as a bundle of conducting channels, is suggested by the similarity of the field dependences of the magnetic flux density of an individual chain of granules and the entire granular medium [13–16].

DEVELOPMENT OF THE APPROACH TO MAGNETIC DIAGNOSTICS OF A CHAIN OF SPHERICAL GRANULES (BALLS)

According to the discussed model [13–16], for any chain of granules, e.g., spherical granules (balls) of radius R, conceptually significant are the magnetic parameters of their conditional cores of radius $r \leq R$, of course, as quasi-continuous magnets. Such parameters, first of all, their magnetic permeability and magnetic flux density at different core radii r are variable because of the difference in magnetic reluctance, which is due to the difference in volume of the gap between the surfaces of the neighboring granules and, consequently, the difference in metal volume in the cores. For the limiting core ($r \to R$), these parameters are virtually equal to those of the entire granular medium, which suggests the existence of expected relationships between the micromodel and macromodel parameters.

The variability of the magnetic parameters of different cores in a chain of balls was demonstrated by both calculations, and direct magnetic diagnostics of the field within the wedgelike space between balls of a chosen chain of balls [13–16]. Such diagnostics is known to be quite difficult to perform in small spaces; therefore, an efficient variant of it is to measure the magnetic fluxes (microfluxes) Φ through microwebermeter-connected concentric circular loops of different radii $r \leq R$, surrounding the point of contact of balls. Such loop sensors are located between the neighboring balls in the middle part of the chain of balls being magnetized. Inserting the loop sensors in so small a space between the balls, which converges as the point of contact of the balls is approached, one can measure the magnetic fluxes Φ through the cores of even relatively small relative radius r/R, especially if the balls in the chosen chain have large radius R, and the loops are made of sufficiently thin wire.

This approach was improved [17, 18] to avoid difficulties in meeting requirements for such sensors, especially the ones that should be inserted between balls and, therefore, have to be made of very thin wire. For example, it is necessary to ensure a strictly circular shape of the sensor, concentricity in the case of using a system of sensors of different radii, and localization of the sensor or a system of sensors in the plane of symmetry of the interball space to prevent the possible displacement of their centers relative to the point of contact of the balls. As applied to the problem under consideration, in which chain of balls 1 (Fig. 1) is magnetized in, e.g., solenoid 2, these requirements are sufficiently completely satisfied by sensor 3, which is a thin flat printed circuit board with a conducting circular loop or a system of concentric loop sensors on it. Each of the loops has a small break to connect the free terminals to the microwebermeter.

The printed circuit board ensures the strict shape of the loop sensor or each of the loop sensors in a system, namely, a geometrically perfect circle on a flat surface. It also (easily) ensures the localization of the loop sensor or a system of the concentric loop sensors in the plane of symmetry of the space between the balls being magnetized, in which such a printed circuit board is placed without fear for the possible displacement of the center of the loop or the system of the loops relative to the point of contact of the balls. For this purpose, there is a hole at the center of the printed circuit board, which is concentric to the loop sensor or the system of the loop sensors. As follows from the corresponding geometric constraints [17, 18], depending on the radius R of the chosen balls and the thickness δ of the thin printed circuit board, the seat diameter d_0 of the hole should be $d_0 = [\delta(4R - \delta)]^{0.5}$.

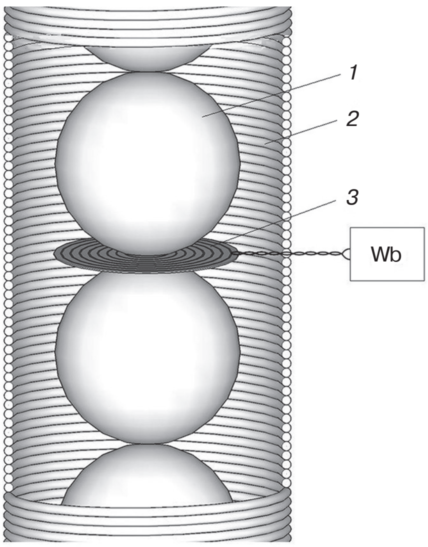

Fig. 1. Chain of balls *1* being magnetized in the field of solenoid *2* with microwebermeter-connected circular loop sensors *3* located on a thin printed circuit board placed between the balls

DATA ON THE MAGNETIC FLUX THROUGH THE CORES OF BALLS: MAGNETIC FLUX DENSITY AND PERMEABILITY

Figure 2a illustrates the results of measuring the magnetic microflux Φ through the loop sensors [17] and, hence, through the cores of the corresponding radius r of balls of a radius of R = 20 mm in a chain as a family of field dependences at various relative radii r/R. The data were obtained for quite a long chain of balls—14 ones—to minimize the demagnetization factor, the magnetizing field strength range was H = 4.8–54.5 kA/m, and the relative core radius range was r/R = 0.2–0.9.

Figure 2a shows that, with increasing H, Φ monotonically increases, and the higher H, the slower this increase, which is particularly noticeable at relatively small r/R. The larger the radius r of a core, the higher the magnetic flux Φ through it (Fig. 2a), which is more clearly demonstrated by a relative family of dependences of Φ on r/R at various H (Fig. 2b).

Using the experimental Φ values (Fig. 2), it is easy to find the magnetic flux density B through each of the quasi-continuous cores of radius r and sectional area πr^2 as $B = \Phi/\pi r^2$, and also the magnetic permeability μ of the corresponding cores as $\mu = B/\mu_0 H = \Phi/\pi r^2 \mu_0 H$, where $\mu_0 = 4\pi \cdot 10^{-7}$ H/m is the vacuum permeability. Figures 3 and 4 present the data on B and μ for the cores of different r/R as families of dependences of B and μ on H, respectively; from these dependences, families of no less informative dependences of B and μ on r/R (at different H) were obtained and are also shown in Figs. 3 and 4, respectively.

Figure 3a shows that, with increasing magnetic field strength H, the magnetic flux density B through each of the cores monotonically increases, but the higher H, the less intense this increase (as for Φ in Fig. 2a), which is best seen at small r/R. The larger the core radius r, the lower the magnetic flux density B through it (Fig. 3a): this is better observed in the dependences of B on r/R at various H (Fig. 3b).

The magnetic permeability μ of the corresponding (in r/R) cores decreases with increasing H (Fig. 4a). As for B (Fig. 3), the larger the radius r of a core, the lower its permeability μ (Fig. 4). This can be seen already from the relative positions of the curves of the dependences of μ on H (Fig. 4a), and also from the decreasing trends of the dependences of μ on r/R at various H (Fig. 4b), which were obtained from the dependences in Fig. 4a.

The observed (Figs. 3, 4) decrease in B and μ with increasing radius r of conditional cores (the relative radius r/R of which ranges from $r/R \to 0$ to $r/R = 1$) is caused by the decrease in the volume fraction γ of the ferromagnetic metal in the growing core. For example, using the relationship between γ and r/R [17]:

$$\gamma = \frac{2}{3}\left[\sqrt{1-(r/R)^2} + \frac{1-\sqrt{1-(r/R)^2}}{(r/R)^2}\right], \quad (1)$$

the key parameters, namely the magnetic flux density B and the magnetic permeability μ, which are presented in

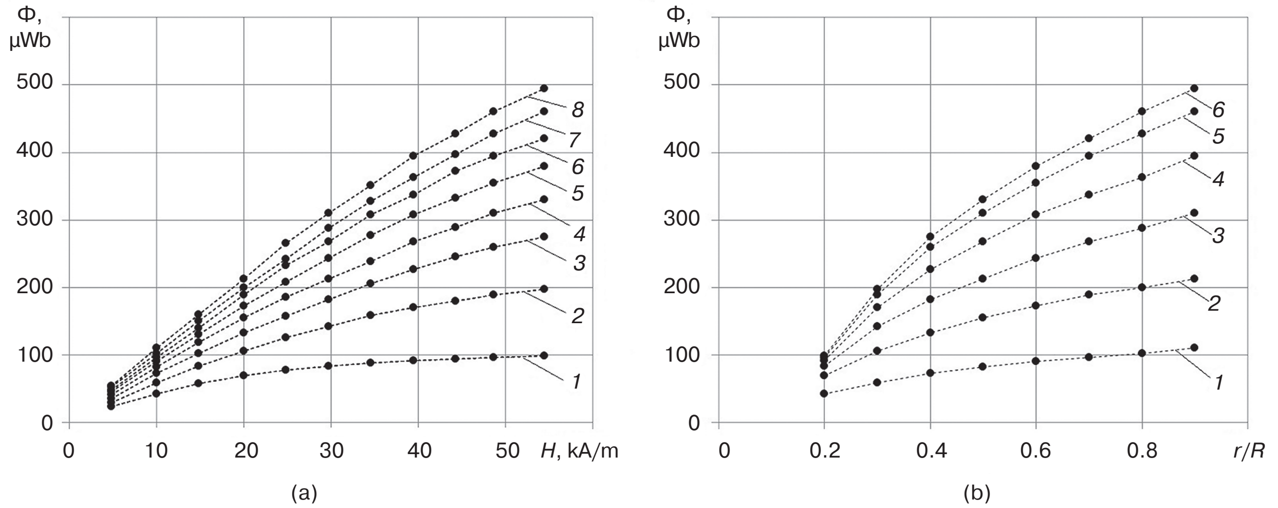

Fig. 2. Dependences of the magnetic microflux Φ through the loop sensors surrounding the cores of radius *r* of balls of a radius of *R* = 20 mm in a chain on (a) the magnetic field strength *H* at *r*/*R* = (*1*) 0.2, (*2*) 0.3, (*3*) 0.4, (*4*) 0.5, (*5*) 0.6, (*6*) 0.7, (*7*) 0.8, and (*8*) 0.9 and (b) on the relative core radius *r*/*R* at *H* = (*1*) 10, (*2*) 20, (*3*) 29.7, (*4*) 39.5, (*5*) 48.7, and (*6*) 54.5 kA/m

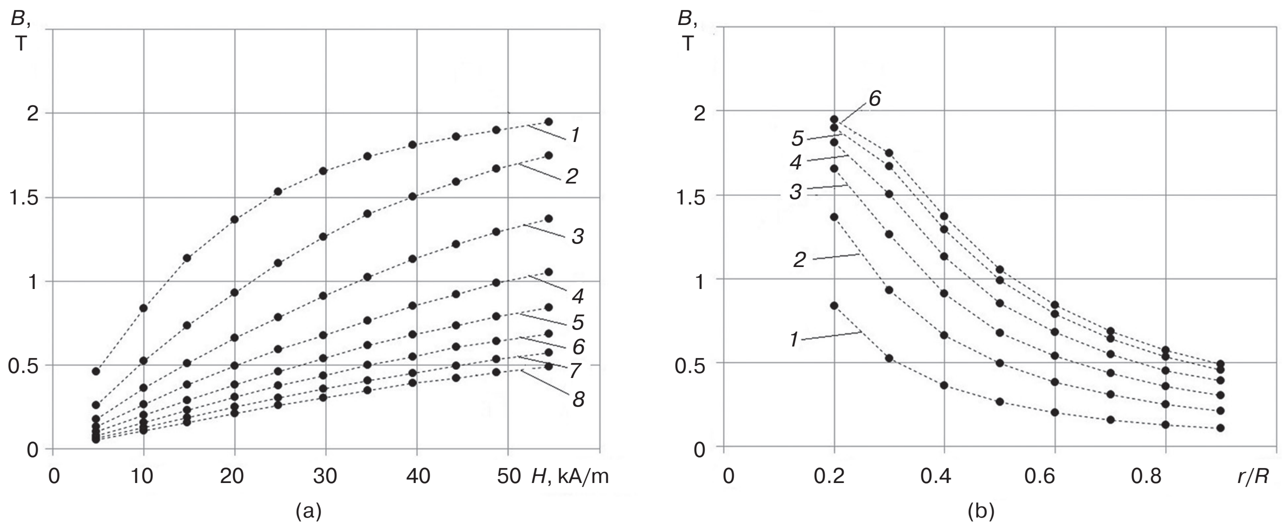

Fig. 3. Dependences of the magnetic flux density *B* in the cores of balls of a chain on (a) the magnetic field strength *H* and (b) the relative core radius *r*/*R*. The notation is as in Fig. 2

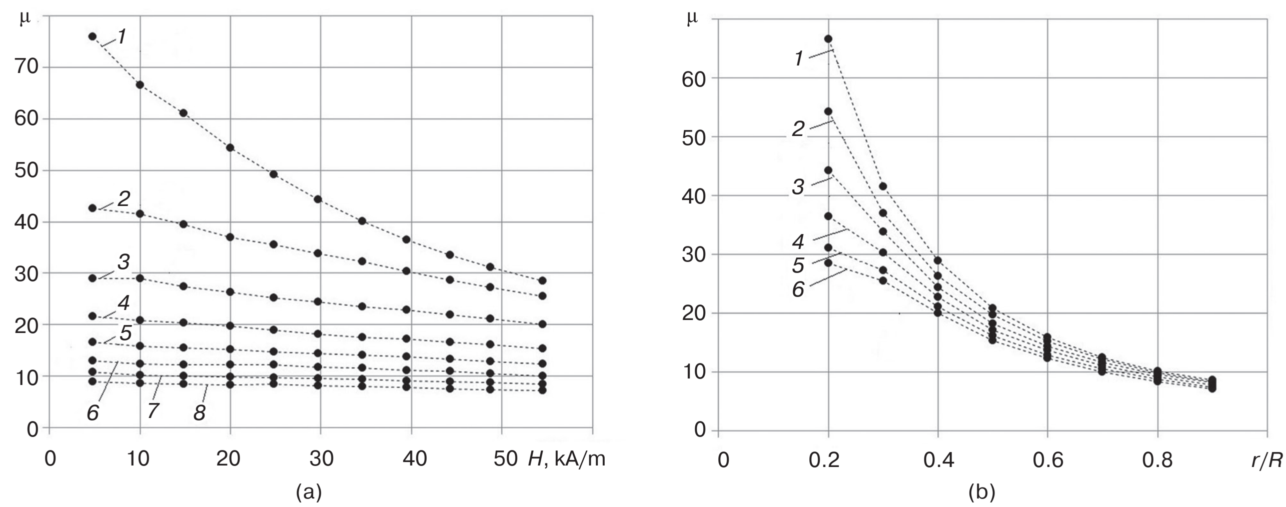

Fig. 4. Dependences of the magnetic permeability μ of the cores of balls of a chain on (a) the magnetic field strength *H* and (b) the relative core radius *r*/*R*. The notation is as in Fig. 2

Figs. 3b and 4b, respectively, as functions of r/R, can be represented as functions of γ (Fig. 5) to demonstrate the role of such a hidden parameter as volume fraction γ of metal in the cores of balls in a chain.

An analysis of these, quite informative, trends of the dependences of B and μ on γ in Fig. 5 toward increasing γ shows that the role of γ is particularly significant at $\gamma = 0.9–0.95$, i.e., as $\gamma \to 1$ (and, correspondingly, $r/R \to 0$). Here, the increase in B and μ is definitely steep, and these quantities tend to approach the B and μ values that are characteristic of the material of the balls. No less informative are the trends of the dependences of B and μ on γ in Fig. 5 toward decreasing γ, down to the values $\gamma \to 0.67$ (i.e., $r/R \to 1$), which are characteristic of the chain of balls. This allows one to test the validity of the conceptual assumption of the magnetization model that the magnetic properties of a chain of balls and a ball-packed medium should be similar. In particular, this can be tested by comparing the field dependences of B and/or μ in the chain and the packing.

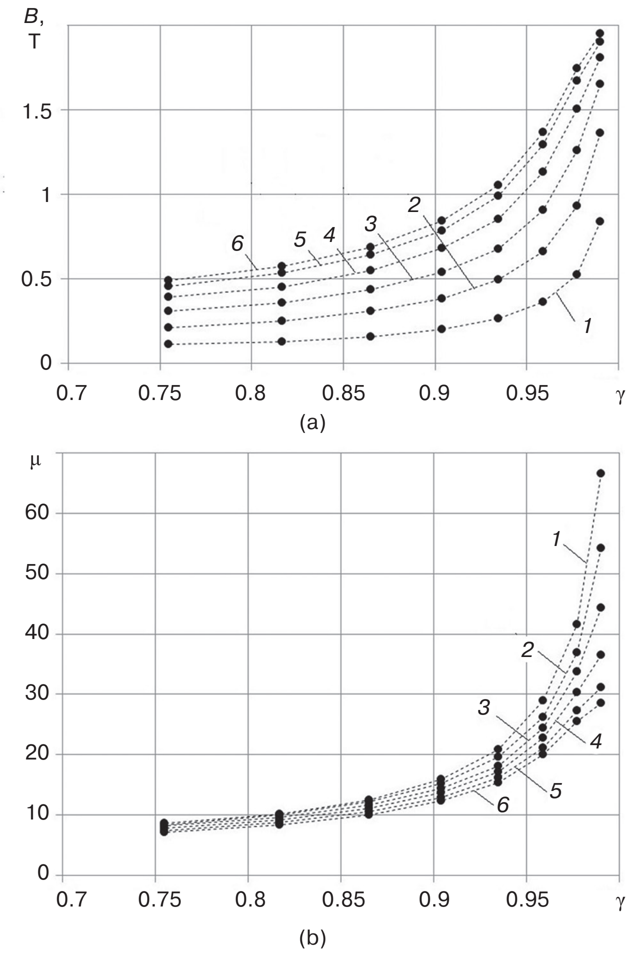

Fig. 5. Dependences demonstrating the effect of the volume fraction γ of metal in the conditionally separated, different in radius r, cores of balls in a chain on (a) the magnetic flux density B in them and (b) their magnetic permeability μ according to the data in Figs. 3 and 4 using relationship (*1*) between γ and r/R

The field dependences of the magnetic flux density B and permeability μ for a chain of balls can be obtained using the data in Fig. 5. In the experiments [17], the maximum relative radius of loop sensor (and their surrounding conditional cores of balls in a chain) was $r/R = 0.9$ (i.e., $\gamma = 0.755$ in Fig. 5); nonetheless, a reliable estimate of the B and μ values up to the required value $r/R = 1$, i.e., to $\gamma = 0.67$, is easy to make. The trends of the dependences of B and μ on γ toward decreasing γ, being near-self-similar at $\gamma < 0.755$ (or, what is the same, at $r/R > 0.9$) (Fig. 5), can readily be extrapolated to the left to $\gamma = 0.67$, i.e., to $r/R = 1$. It is easy to see that the differences of then extrapolated values of B and μ from the B and μ values at $\gamma = 0.755$ (i.e., at $r/R = 0.9$) are quite insignificant (Fig. 5).

This makes it possible to represent the field dependences of the magnetic flux density B and permeability μ for a chain of balls (Fig. 6, curves *1*) using the extended data: at $\gamma = 0.755–0.67$ (i.e., at $r/R = 0.9–1.0$). For the above-proposed comparison, Fig. 6 also presents the published [13] field dependences of B and μ for a ball-packed medium (curves *2*). One can see that, to within virtually a constant, the compared field dependences of both the magnetic flux density B (Fig. 6a, curves *1*, *2*), and the permeability μ (Fig. 6b, curves *1*, *2*) agree with each other. This confirms that a chain of granules is a physically self-sufficient element (in the composition of a bundle of similar elements) of a granular medium, which is actually responsible for the magnetization of this medium.

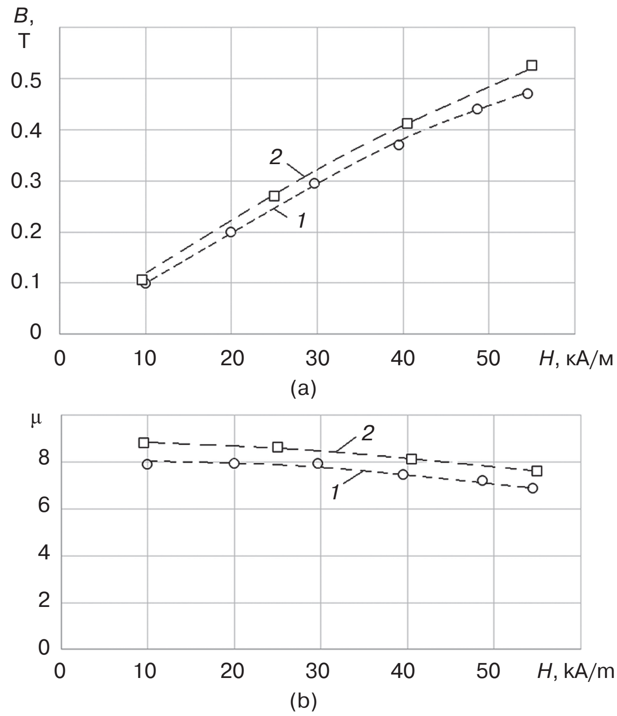

Fig. 6. Field dependences of the (a) magnetic flux density B and (b) permeability μ of (*1*) a chain of balls (its virtually limiting core at $r/R = 0.9–1.0$) and (*2*) a ball-packed medium

CONCLUSIONS

One of the concepts of the well-proven model of chain-by-chain magnetization of a granular medium is the crucial role of such constituting elements of the granular medium as chains of granules, straight and sinuous, which always respond in the direction of the magnetization of this medium. They function as channels that conduct the generated magnetic flux; i.e., the granular medium is a sort of a bundle of these elements. Conceptually significant are the magnetic parameters of the conditional cores of different radii r of granules in a chain, first of all, their magnetic permeability and magnetic flux density. These parameters can be determined from the results of measurements made by magnetic flux sensors designed as concentric circular conducting loops of different radii $r \leq R$, surrounding the point of contact of the balls, that are produced on thin printed circuit boards placed in the plane of symmetry of the space between the contacting balls. The analysis was made of the results of measuring the magnetic fluxes through different (in relative radius $r/R = 0.2-0.9$) cores of balls of a radius of $R = 20$ mm in a chain at a magnetizing field strength in the range 4.8–54.5 kA/m. It was shown that, with formally thickening cores, the values of the magnetic flux density and the permeability decrease because of the decrease in the volume fraction of ferromagnet in the core; and in the limiting core ($r/R \to 1$), i.e., the entire chain, they agree with the values of the magnetic flux density and the permeability of the ball-packed medium. This confirms the corresponding results of the model of chain-by-chain magnetization of a granular medium.

Acknowledgments. This research was supported by the Ministry of Science and Higher Education of the Russian Federation (project 0706-2020-0024) and the program of the President of the Russian Federation for state support of young scientists (project MK-807.2020.8).

Authors' contribution. All authors equally contributed to the research work.

REFERENCES

1. Mishima F., Terada T., Akiyama Y., Izumi Y., Okazaki H., Nishijima S. Research and development of superconducting magnetic separation system for powdered products. *IEEE Transactions on Applied Superconductivity*. 2008;18(2):824–827. https://doi.org/10.1109/TASC.2008.920830
2. Eskandarpour A., Iwai K., Asai S. Superconducting magnetic filter: Performance, recovery, and design. *IEEE Transactions on Applied Superconductivity*. 2008;19(2):84–95. https://doi.org/10.1109/TASC.2009.2014567
3. Bai K., Casara J., Nair-Kanneganti A., Wahl A., Carle F., Brown E. Effective magnetic susceptibility of suspensions of ferromagnetic particles. *Journal of Applied Physics.* 2018;124(12):123901. https://doi.org/10.1063/1.5041750
4. Birčáková Z., Kollár P., Weidenfeller B., Füzer J., Fáberová M., Bureš R. Reversible and irreversible DC magnetization processes in the frame of magnetic, thermal and electrical properties of Fe-based composite materials. *Journal of Alloys and Compounds*. 2015;645:283–289. https://doi.org/10.1016/j.jallcom.2015.05.121
5. Kollár P., Birčáková Z., Vojtek V., Füzer J., Bureš R., Fáberová M. Dependence of demagnetizing fields in Fe-based composite materials on magnetic particle size and the resin content. *Journal of Magnetism and Magnetic Materials.* 2015;388:76–81. https://doi.org/10.1016/j.jmmm.2015.04.008
6. Strečková M., Füzer J., Kobera L., Brus J., Fáberová M., Bureš R., Kollár P., Lauda M., Medvecký L., Girman V., Hadraba H., Bat'kova M., Bat'ko I. A comprehensive study of soft magnetic materials based on FeSi spheres and polymeric resin modified by silica nanorods. *Materials Chemistry and Physics.* 2014;147(3):649–660. https://doi.org/10.1016/j.matchemphys.2014.06.004

СПИСОК ЛИТЕРАТУРЫ

1. Mishima F., Terada T., Akiyama Y., Izumi Y., Okazaki H., Nishijima S. Research and development of superconducting magnetic separation system for powdered products. *IEEE Transactions on Applied Superconductivity*. 2008;18(2):824–827. https://doi.org/10.1109/TASC.2008.920830
2. Eskandarpour A., Iwai K., Asai S. Superconducting magnetic filter: Performance, recovery, and design. *IEEE Transactions on Applied Superconductivity*. 2008;19(2):84–95. https://doi.org/10.1109/TASC.2009.2014567
3. Bai K., Casara J., Nair-Kanneganti A., Wahl A., Carle F., Brown E. Effective magnetic susceptibility of suspensions of ferromagnetic particles. *Journal of Applied Physics.* 2018;124(12):123901. https://doi.org/10.1063/1.5041750
4. Birčáková Z., Kollár P., Weidenfeller B., Füzer J., Fáberová M., Bureš R. Reversible and irreversible DC magnetization processes in the frame of magnetic, thermal and electrical properties of Fe-based composite materials. *Journal of Alloys and Compounds*. 2015;645:283–289. https://doi.org/10.1016/j.jallcom.2015.05.121
5. Kollár P., Birčáková Z., Vojtek V., Füzer J., Bureš R., Fáberová M. Dependence of demagnetizing fields in Fe-based composite materials on magnetic particle size and the resin content. *Journal of Magnetism and Magnetic Materials.* 2015;388:76–81. https://doi.org/10.1016/j.jmmm.2015.04.008
6. Strečková M., Füzer J., Kobera L., Brus J., Fáberová M., Bureš R., Kollár P., Lauda M., Medvecký L., Girman V., Hadraba H., Bat'kova M., Bat'ko I. A comprehensive study of soft magnetic materials based on FeSi spheres and polymeric resin modified by silica nanorods. *Materials Chemistry and Physics.* 2014;147(3):649–660. https://doi.org/10.1016/j.matchemphys.2014.06.004

7. Kanhe N.S., Kumar A., Yusuf S.M., Nawale A.B., Gaikwad S.S., Raut S.A., Bhoraskar S.V., Wu S.Y., Das A.K., Mathe V.L. Investigation of structural and magnetic properties of thermal plasma-synthesized $Fe_{1-x}Ni_x$ alloy nanoparticles. *Journal of Alloys and Compounds*. 2016;663:30−40. https://doi.org/10.1016/j.jallcom.2015.11.190
8. Pal S.K., Bahadur D. Shape controlled synthesis of iron–cobalt alloy magnetic nanoparticles using soft template method. *Materials Letters*. 2010;64(10):1127−1129. https://doi.org/10.1016/j.matlet.2010.01.086
9. Moore R.L. Development and test of concentration scaled demagnetization in effective media theories of magnetic composites. *Journal of Applied Physics*. 2019;125(8):085101. https://doi.org/10.1063/1.5053791
10. Périgo E.A., Weidenfeller B., Kollár P., Füzer J. Past, present, and future of soft magnetic composites. *Applied Physics Reviews*. 2018;5(3):031301. https://doi.org/10.1063/1.5027045
11. Moore R.L. Development of a volume fraction scaling function for demagnetization factors in effective media theories of magnetic composites. *AIP Advances*. 2019;9(3):035107. https://doi.org/10.1063/1.5078736
12. Nakamura T., Tsutaoka T., Hatakeyama K. Frequency dispersion of permeability in ferrite composite materials. *Journal of Magnetism and Magnetic Materials*. 1994;138(3):319−328. https://doi.org/10.1016/0304-8853(94)90054-X
13. Sandulyak A.V. *Magnitno-fil'tratsionnaya ochistka zhidkostei i gazov* (*Magnetic and filtration purification of liquids and gases*). Moscow: Khimiya; 1988. 136 p. (in Russ.). Available from URL: https://dlib.rsl.ru/viewer/01001440011#?page=136
14. Sandulyak A.V., Sandulyak A.A., Ershova V.A. On the model of channel-by-channel magnetization of a granular medium (with a radial permeability profile of a quasi-continuous channel). *Technical Physics*. 2009;54(5):743−745. https://doi.org/10.1134/S1063784209050235
[Sandulyak A.V., Sandulyak A.A., Ershova V.A. On the model of channel-by-channel magnetization of a granular medium (with a radial permeability profile of a quasi-continuous channel). *Zhurnal tekhnicheskoi fiziki = Technical Physics*. 2009;79(5):140−142 (in Russ.).]
15. Sandulyak A.V., Sandulyak A.A., Ershova V.A. Magnetization curve of a granulated medium in terms of the channel-by-channel magnetization model (new approach). *Doklady Physics*. 2007;52(4):179–181. https://doi.org/10.1134/S1028335807040027
[Sandulyak A.V., Sandulyak A.A., Ershova V.A. Magnetization curve of a granulated medium in terms of the channel-by-channel magnetization model (new approach). *Doklady Akademii nauk = Doklady Physics.* 2007;413(4):469−471 (in Russ.).]
16. Sandulyak A.A., Sandulyak D.A., Ershova V.A., Sandulyak A.V. Ferrous Material Fill: Magnetization Channels, Layer-by-Layer and Average Permeability, Element-to-Element Field. In book: *Analysis and Modelling of Advanced Structures and Smart Systems*. 2017;81:191−210. https://doi.org/10.1007/978-981-10-6895-9_9

7. Kanhe N.S., Kumar A., Yusuf S.M., Nawale A.B., Gaikwad S.S., Raut S.A., Bhoraskar S.V., Wu S.Y., Das A.K., Mathe V.L. Investigation of structural and magnetic properties of thermal plasma-synthesized $Fe_{1-x}Ni_x$ alloy nanoparticles. *Journal of Alloys and Compounds*. 2016;663:30−40. https://doi.org/10.1016/j.jallcom.2015.11.190
8. Pal S.K., Bahadur D. Shape controlled synthesis of iron–cobalt alloy magnetic nanoparticles using soft template method. *Materials Letters*. 2010;64(10):1127−1129. https://doi.org/10.1016/j.matlet.2010.01.086
9. Moore R.L. Development and test of concentration scaled demagnetization in effective media theories of magnetic composites. *Journal of Applied Physics*. 2019;125(8):085101. https://doi.org/10.1063/1.5053791
10. Périgo E.A., Weidenfeller B., Kollár P., Füzer J. Past, present, and future of soft magnetic composites. *Applied Physics Reviews.* 2018;5(3):031301. https://doi.org/10.1063/1.5027045
11. Moore R.L. Development of a volume fraction scaling function for demagnetization factors in effective media theories of magnetic composites. *AIP Advances*. 2019;9(3):035107. https://doi.org/10.1063/1.5078736
12. Nakamura T., Tsutaoka T., Hatakeyama K. Frequency dispersion of permeability in ferrite composite materials. *Journal of Magnetism and Magnetic Materials*. 1994;138(3):319−328. https://doi.org/10.1016/0304-8853(94)90054-X
13. Сандуляк А.В. *Магнитно-фильтрационная очистка жидкостей и газов*. М.: Химия; 1988. 136 с. URL: https://dlib.rsl.ru/viewer/01001440011#?page=136
14. Сандуляк А.В., Сандуляк А.А., Ершова В.А. К вопросу о модели поканального намагничивания гранулированной среды (с радиальным профилем проницаемости квазисплошного канала). *Журнал технической физики*. 2009;79(5):140−142.
15. Сандуляк А.В., Сандуляк А.А., Ершова В.А. Кривая намагничивания гранулированной среды с позиций модели поканального намагничивания (новый подход). *Доклады Академии наук.* 2007;413(4):469−471.
16. Sandulyak A.A., Sandulyak D.A., Ershova V.A., Sandulyak A.V. Ferrous Material Fill: Magnetization Channels, Layer-by-Layer and Average Permeability, Element-to-Element Field. In book: *Analysis and Modelling of Advanced Structures and Smart Systems*. 2017;81:191−210. https://doi.org/10.1007/978-981-10-6895-9_9
17. Сандуляк А.В., Горпиненко Ю.О., Полисмакова М.Н., Сандуляк Д.А., Сандуляк А.А. Магнитный поток и индукция в сердцевинах намагничиваемых цепочек шаров. *Международный научно-исследовательский журнал*. 2020;96(6−1):96−110. https://doi.org/10.23670/IRJ.2020.96.6.017
18. Горпиненко Ю.О., Сандуляк А.В., Полисмакова М.Н., Сандуляк Д.А., Сандуляк А.А., Харин А.С. Устройство для измерения магнитного поля: Патент RU 2737024. Заявка № 2020116795. Дата публикации 24.11.2020.

17. Sandulyak A.V., Gorpinenko Y.O., Polismakova M.N., Sandulyak D.A., Sandulyak A.A. Magnetic flow and induction in the hearts of magnetizable ball chains. *Mezhdunarodnyj nauchno-issledovatel'skij zhurnal = International Research Journal*. 2020;96(6−1):96−110 (in Russ.). https://doi.org/10.23670/IRJ.2020.96.6.017
18. Gorpinenko Y.O., Sandulyak A.V., Polismakova M.N., Sandulyak D.A., Sandulyak A.A., Kharin A.S. Ustroystvo dla izmerenija magnitnogo polya (Magnetic field measuring device): RU Pat. 2737024. Publ. 24.11.2020. (in Russ.).

About the authors

Anna A. Sandulyak, Dr. Sci. (Eng.), Professor, Department of Instruments and Information-Measuring Systems, Institute of Integrated Safety and Special Instrument Engineering, MIREA – Russian Technological University (78, Vernadskogo pr., Moscow, 119454 Russia). E-mail: anna.sandulyak@mail.ru. Scopus Author ID 7004032043, https://orcid.org/0000-0002-5111-6092

Daria A. Sandulyak, Cand. Sci. (Eng.), Senior Science Master, Laboratory of Magnetic Control and Material's Separation, MIREA – Russian Technological University (78, Vernadskogo pr., Moscow, 119454 Russia). E-mail: d.sandulyak@mail.ru. Scopus Author ID 36621369400, https://orcid.org/0000-0003-4269-6133

Yurij O. Gorpinenko, Postgraduate Student, Department of Instruments and Information-Measuring Systems, Institute of Integrated Safety and Special Instrument Engineering, MIREA – Russian Technological University (78, Vernadskogo pr., Moscow, 119454 Russia). E-mail: gorpinenko1991@mail.ru.

Vera A. Ershova, Cand. Sci. (Eng.), Associate Professor, Senior Science Master, Laboratory of Magnetic Control and Material's Separation, MIREA – Russian Technological University (78, Vernadskogo pr., Moscow, 119454 Russia). E-mail: v.ershova@mail.ru. Scopus Author ID 36771249600, https://orcid.org/0000-0002-8210-4721

Alexander V. Sandulyak, Dr. Sci. (Eng.), Professor, Department of Instruments and Information-Measuring systems, Institute of Integrated Safety and Special Instrument Engineering, MIREA – Russian Technological University (78, Vernadskogo pr., Moscow, 119454 Russia). E-mail: sandulyak@mirea.ru. Scopus Author ID 57194504434, https://orcid.org/0000-0001-7605-2702

Об авторах

Сандуляк Анна Александровна, д.т.н., профессор, кафедра «Приборы и информационно-измерительные системы» Института комплексной безопасности и специального приборостроения, ФГБОУ ВО «МИРЭА – Российский технологический университет» (119454, Россия, Москва, пр-т Вернадского, д. 78). E-mail: anna.sandulyak@mail.ru. Scopus Author ID 7004032043, https://orcid.org/0000-0002-5111-6092

Сандуляк Дарья Александровна, к.т.н., с.н.с., лаборатория магнитного контроля и разделения материалов, ФГБОУ ВО «МИРЭА – Российский технологический университет» (119454, Россия, Москва, пр-т Вернадского, д. 78). E-mail: d.sandulyak@mail.ru. Scopus Author ID 36621369400, https://orcid.org/0000-0003-4269-6133

Горпиненко Юрий Олегович, аспирант, кафедра «Приборы и информационно-измерительные системы» Института комплексной безопасности и специального приборостроения, ФГБОУ ВО «МИРЭА – Российский технологический университет» (119454, Россия, Москва, пр-т Вернадского, д. 78). E-mail: gorpinenko1991@mail.ru.

Ершова Вера Александровна, к.т.н., с.н.с., лаборатория магнитного контроля и разделения материалов, ФГБОУ ВО «МИРЭА – Российский технологический университет» (119454, Россия, Москва, пр-т Вернадского, д. 78). E-mail: v.ershova@mail.ru. Scopus Author ID 36771249600, https://orcid.org/0000-0002-8210-4721

Сандуляк Александр Васильевич, д.т.н., профессор, кафедра «Приборы и информационно-измерительные системы» Института комплексной безопасности и специального приборостроения, ФГБОУ ВО «МИРЭА – Российский технологический университет» (119454, Россия, Москва, пр-т Вернадского, д. 78). E-mail: sandulyak@mirea.ru. Scopus Author ID 57194504434, https://orcid.org/0000-0001-7605-2702

Translated by V. Glyanchenko

Mathematical modeling

Математическое моделирование

UDC 519.857
https://doi.org/10.32362/2500-316X-2021-9-5-45-56

RESEARCH ARTICLE

Two-stage spline-approximation in linear structure routing

Dmitry A. Karpov,
Valery I. Struchenkov @

MIREA – Russian Technological University, Moscow, 119454 Russia
@ *Corresponding author, e-mail: str1942@mail.ru*

Abstract. In the article, computer design of routes of linear structures is considered as a spline approximation problem. A fundamental feature of the corresponding design tasks is that the plan and longitudinal profile of the route consist of elements of a given type. Depending on the type of linear structure, line segments, arcs of circles, parabolas of the second degree, clothoids, etc. are used. In any case, the design result is a curve consisting of the required sequence of elements of a given type. At the points of conjugation, the elements have a common tangent, and in the most difficult case, a common curvature. Such curves are usually called splines. In contrast to other applications of splines in the design of routes of linear structures, it is necessary to take into account numerous restrictions on the parameters of spline elements arising from the need to comply with technical standards in order to ensure the normal operation of the future structure. Technical constraints are formalized as a system of inequalities. The main distinguishing feature of the considered design problems is that the number of elements of the required spline is usually unknown and must be determined in the process of solving the problem. This circumstance fundamentally complicates the problem and does not allow using mathematical models and nonlinear programming algorithms to solve it, since the dimension of the problem is unknown. The article proposes a two-stage scheme for spline approximation of a plane curve. The curve is given by a sequence of points, and the number of spline elements is unknown. At the first stage, the number of spline elements and an approximate solution to the approximation problem are determined. The method of dynamic programming with minimization of the sum of squares of deviations at the initial points is used. At the second stage, the parameters of the spline element are optimized. The algorithms of nonlinear programming are used. They were developed taking into account the peculiarities of the system of constraints. Moreover, at each iteration of the optimization process for the corresponding set of active constraints, a basis is constructed in the null space of the constraint matrix and in the subspace – its complement. This makes it possible to find the direction of descent and solve the problem of excluding constraints from the active set without solving systems of linear equations. As an objective function, along with the traditionally used sum of squares of the deviations of the initial points from the spline, the article proposes other functions taking into account the specificity of a particular project task.

Keywords: route, horizontal and vertical alignment, spline, dymanic programming, objective function, restrictions

• **Submitted:** 25.01.2021 • **Revised:** 14.03.2021 • **Accepted:** 12.07.2021

For citation: Karpov D.A., Struchenkov V.I. Two-stage spline-approximation in linear structure routing. *Russ. Technol. J.* 2021;9(5):45–56. https://doi.org/10.32362/2500-316X-2021-9-5-45-56

Financial disclosure: The authors have no a financial or property interest in any material or method mentioned.

The authors declare no conflicts of interest.

НАУЧНАЯ СТАТЬЯ

Двухэтапная сплайн-аппроксимация в компьютерном проектировании трасс линейных сооружений

Д.А. Карпов,
В.И. Струченков @

МИРЭА – Российский технологический университет, Москва, 119454 Россия
@ *Автор для переписки, e-mail: str1942@mail.ru*

Резюме. В статье компьютерное проектирование трасс линейных сооружений рассматривается как задача сплайн-аппроксимации. Принципиальной особенностью соответствующих проектных задач является то, что план и продольный профиль трассы состоят из элементов заданного вида. В зависимости от типа линейного сооружения используются отрезки прямых, дуги окружностей, парабол второй степени, клотоид и др. В любом случае результатом проектирования является кривая, состоящая из нужной последовательности элементов заданного вида. В точках сопряжения элементы, как правило, имеют общую касательную, а в наиболее сложном случае – и общую кривизну. Подобные кривые принято называть сплайнами. В отличие от других применений сплайнов в проектировании трасс линейных сооружений приходится учитывать многочисленные ограничения на параметры элементов сплайна, возникающие из необходимости соблюдения технических нормативов с целью обеспечения нормальной эксплуатации будущего сооружения. Технические ограничения формализуются в виде системы неравенств. Главная отличительная особенность рассматриваемых проектных задач состоит в том, что число элементов искомого сплайна неизвестно и должно быть определено в процессе решения задачи. Это обстоятельство принципиально усложняет задачу и не позволяет применить для ее решения математические модели и алгоритмы нелинейного программирования, так как неизвестна размерность задачи. В статье предлагается двухэтапная схема сплайн-аппроксимации плоской кривой, заданной последовательностью точек, при неизвестном числе элементов сплайна и наличии ограничений на параметры его элементов. На первом этапе определяется число элементов сплайна и приближенное решение задачи аппроксимации. Используется метод динамического программирования. На втором этапе выполняется оптимизация параметров элементов сплайна. Используются алгоритмы нелинейного программирования, разработанные с учетом особенностей системы ограничений. При этом на каждой итерации процесса оптимизации для соответствующего набора активных ограничений строится базис в нуль-пространстве матрицы ограничений. Это позволяет найти направление спуска и решить вопрос об исключении ограничений из активного набора без решения систем линейных уравнений вообще, а в наиболее сложных случаях – решая линейные системы малой размерности. В качестве целевой функции наряду с традиционно используемой суммой квадратов отклонений аппроксимируемых точек от сплайна в статье предлагаются другие функции с учетом специфики конкретной проектной задачи.

Ключевые слова: трасса, план и продольный профиль, сплайн, динамическое программирование, целевая функция, ограничения

• **Поступила:** 25.01.2021 • **Доработана:** 14.03.2021 • **Принята к опубликованию:** 12.07.2021

Для цитирования: Карпов Д.А., Струченков В.И. Двухэтапная сплайн-аппроксимация в компьютерном проектировании трасс линейных сооружений. *Russ. Technol. J.* 2021;9(5):45–56. https://doi.org/10.32362/2500-316X-2021-9-5-45-56

Прозрачность финансовой деятельности: Никто из авторов не имеет финансовой заинтересованности в представленных материалах или методах.

Авторы заявляют об отсутствии конфликта интересов.

INTRODUCTION

A linear structure is a structure the ground position of which is determined by the axis of the structure, which is called the route. Among linear structures are roads and railways, pipelines of various purposes, channels, water conduits, etc. A route is a three-dimensional curve, which is conventionally represented by two plane curves: the plan and the longitudinal profile.

The plan of a route is its projection on the *XOY* plane, and the longitudinal profile is the graph of the function $Z(s)$, where s is the length of the curve in plan as calculated from a given initial point. The longitudinal profile is a developed view of the vertical surface passing through the route.

Design of the longitudinal profile of a structure of any type can be considered as the construction of a spline consisting of elements of a given shape. This spline should have the minimum (in a given meaning) deviation from the initial broken line, which is the ground profile in the case of design of new structures and is the profile of the existing structure in the case of design a reconstruction.

The simplest spline of the first order is the grade line of the longitudinal profile of a railway. In this case, the problem is to convert the initial broken line (ground profile) to another broken line that satisfies a variety of constraints: on the slopes of elements and the differences of the slopes of neighboring elements, on the minimum length of elements, and on the height at some points and in some zones [1, 2]. Because the design slopes are small, the length of an element and the difference of the abscissas of its ends virtually coincide; therefore, the difference of the slopes of neighboring elements is equated with the angle of rotation, and the slope is identified with the angle between the element and the abscissa axis.

Meanwhile, the number of elements of the sought spline is unknown. This fact and also numerous constraints distinguish significantly the considered design problem of spline approximation from problems solved in spline theory and its applications [3–5], where the number of spline knots and their abscissas are considered to be given, and constraints are typically absent.

In a simplified formulation, the problem of seeking the optimal spline as a broken line at an unknown number of elements under constraints was solved in the last century as applied to the design of the longitudinal profile of new railways [6, 7].

The problem was solved in two stages. At the first stage, the initial ground profile was converted to a broken line comprising short elements under all the constraints, except the constraint on the length of an element. The developers of the first designing algorithms called such a profile the chain [6].

At the second stage, the chain was converted to the grade line under all the constraints, including those on the length of elements.

In a realistic formulation as applied to design under rugged terrain and complex geology conditions, the problem was solved on a BESM-4 computer by nonlinear programming. The corresponding program gained a wide practical use despite a long computational time because of the extremely low computational speed of this and subsequent computer models (Minsk 32, ES 1020, and others) of the last century [1].

In CAD systems, highly popular in Russia, which were developed by international companies [8–10], and their Russian [11] and Belarusian [12] analogs, the computer is used to solve auxiliary problems, rather than to elaborate the optimal design solutions. In these systems, a spline approximation problem is solved "through the eyes"; i.e., the designer should specify some information that completely determines a sought line. At best, he or she considers several of the theoretically infinitely many possible solutions.

At the present time, the mathematical model, algorithm, and previously developed designing programs should be improved because of changes in the technical specifications for design of high-speed railways. The first order spline should be replaced by a spline comprising line segments and circular arcs, the number of which remains unknown.

A similar spline is also used in designing big-inch pipelines.

In designing the longitudinal profile of roads, a problem arises to seek a parabolic spline of the second order [13] with the above specific features. This problem was solved by nonlinear programming [13].

A spline with circular arcs is used as an alternative to a spline with parabolas in designing the longitudinal profile of roads and also the plane of the routes of various linear structures [14].

The study aimed to analyze the above design problems from a single theoretical standpoint as problems of spline approximation and to present the key stages and specific features of their solution algorithms.

1. FORMULATION OF A PROBLEM OF CIRCULAR ARC SPLINE APPROXIMATION AND ITS FORMALIZATION

Let us consider a problem of designing a longitudinal profile using straight-line elements conjugated to circular arcs.

In the case of redesigning, the initial profile is the profile of the existing structure. If a new structure is designed, the initial profile is the ground profile. The chain longitudinal profile (Fig. 1, dashed line), which can be constructed using the existing designing programs [14], is used to find the number of spline elements. The lengths of elements of the chain need not be equal, but the abscissas of its knots and the abscissas of the knots of the initial broken line coincide.

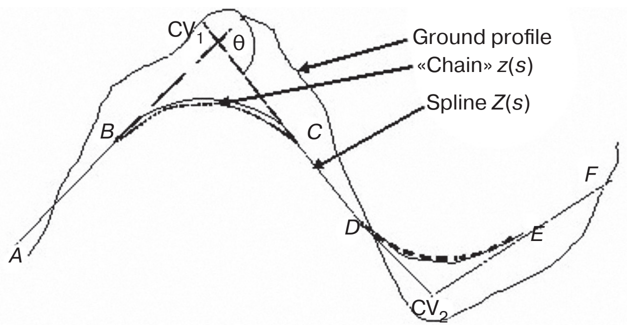

Fig. 1. Spline with circular arcs

Thus, we have the broken line $z(s)$, which should be converted with minimum deviations to the spline $Z(s)$ consisting of line segments conjugated to circular arcs (Fig. 1).

There are the following constraints:

(1) on the slopes I_j of the straight-line spline elements: $-I_{\min} \le I_j \le I_{\max}$, $j = 1, 2, \ldots, N - 1$, where N is the number of spline knots (vertices of the sought broken line, hereinafter referred to as control vertices (CVs)). Actually, this is a constraint on the first derivative of the function $Z(s)$;

(2) on the radii (curvature) of the convex and concave inscribed curves: $1/R_{\text{convex}} \le 1/R_j \le 1/R_{\text{concave}}$, $j = 1, 2, \ldots, N$, $R_{\text{convex}} < 0$, and $R_{\text{concave}} > 0$;

(3) on the lengths of the circular arcs (BC, DE in Fig. 1): $L_{\text{arc},j} \ge L_{\text{arc,min}}$;

(4) on the lengths of the straight-line inserts between the curves (CD in Fig. 1): $L_{\text{ins},j} \ge L_{\text{ins,min}}$.

Additional constraints can be imposed on the ordinates of some points (height constraints at points of intersection of water conduits, other communications, and so on).

Objective function

Equal deviations in different directions from the initial line can often be nonequivalent. Therefore, the conventional minimization of the sum of the squared deviations at given points (also with different weights) is inappropriate.

In designing new roads, the total cut-and-fill quantity can be taken to be the objective function at this stage. The construction costs can be taken to be the objective function if the cut and fill does not give rise to a relationship between elements, which arises if the earth removed from cuts is used to construct fills and requires one to consider the grade line as a whole [14] as in nonlinear programming. At the stage of the conversion of the initial broken line (the chain or the existing profile) to a spline of a necessary type, the ordinate deviations (working marks) are small (about 0.5 m [14]), which allows one to use simplified efficiency criteria because the purpose of this stage is to determine the number of elements and their approximate positions, i.e., construct the initial approximation for nonlinear programming.

In redesigning of the longitudinal profile of a road, at this stage, it is expedient to use modeling functions, which take into account specific features of a problem.

For example, in designing the longitudinal profile during redesigning railways by straight-line elements without taking into account circular curves, which were inscribed into the found line, smooth modeling function $F(h)$ (a spline of the second order with the defect 1) was successfully used (Fig. 2). Here, h is the working mark, i.e., the difference of the ordinates of the sought and initial splines: $h(s) = Z(s) - z(s)$. The h_0 and Δ values and the parameters of the elements of $F(h)$ were found from the existing and designed depths of ballast (H_{ex} and H_{des}, respectively), and the rail and tie heights.

$\Delta = \max(0, H_{\text{ex}} - H_{\text{des}})$, and the portions of the graph of $F(h)$ represent (*1*) filling up of ballast, (*2*) cutting of ballast, and (3) cutting of roadbed.

At $\Delta = 0$, portion *2* of the graph of $F(h)$ is absent. If the existing and designed heights of rails and toes are equal, we have $h_0 = 0$.

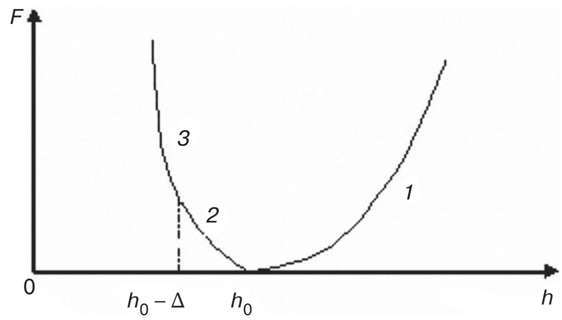

Fig. 2. Modeling function

The $F(h_i)$ values were calculated at the knots of the initial spline, and the objective function had the form

$$\min \Phi(\mathbf{h}) = \sum_{1}^{k} v_i F(h_i), \tag{1}$$

where the coefficients v_i are equal to the half-sums of the lengths of its adjacent elements. Similar modeling functions were used in redesigning the longitudinal profile of roads using parabolic splines [13].

If the objective function is the cut-and-fill quantity, then $F(h_i)$—the cross-sectional area at the ith point—remains piecewise quadratic and corresponds to the calculation of the volume as an integral using the trapezoidal rule.

2. SPLINE APPROXIMATION BY DYNAMIC PROGRAMMING

Dynamic programming under a number of conditions [15–20] makes it possible to create algorithms of several-step construction of the optimal route of motion of a certain system from a given initial state to a final state by solving same-type problems at each of the steps, which are simpler than the initial problem [21]. Variants of reaching one and the same state by various ways are considered to be comparable, and in each state, only the best (according to a chosen criterion) variant remains.

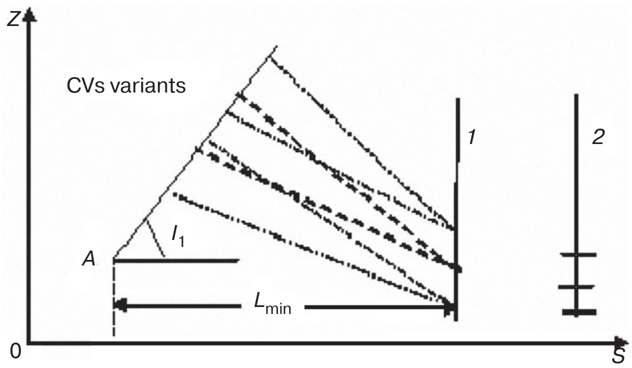

Fig. 3. First step of algorithm

The key concept of dynamic programming is the state of a system, which, for our problem, we define as a pair of two items: one is a point in a straight-line element of a spline, such that beginning with this point a circular arc can be constructed or a straight line can be continued, and the other is the angle between this element and the *OS* (abscissa) axis. The initial state (point *A* and slope I_1 in Fig. 3) is considered to be given.

With respect to the knots of the initial spline (the broken line $z(s)$), a variation grid at a given step is constructed (points in verticals *1* and *2* in Fig. 3). At each of these points, proceeding from the slope of the initial spline, angles with the *OS* axis (search sector) are assigned. The step of assignment of points and angles in the verticals, and the numbers of steps in the vertical and angular directions at each of the points are the initial parameters of an algorithm of seeking the design spline and are specified before calculation. If necessary, the calculation can initially be performed at large increments and then, using the obtained solution, at smaller increments. This is a common trick to reduce the computational time in dynamic programming, which was successfully used in parabolic spline approximation [13, 14].

The first vertical was chosen to be the one spaced apart from the initial point *A* (in abscissas) at distance L_{min}, which is given under constraints 3 and 4 on the lengths of curves and straight-line inserts. In addition, distance L_{max} is given as the sum of the maximum length of the curve and the length of the straight-line insert. Dynamic programming is performed using the angles of rotation (Fig. 1) and the coordinates of their vertices.

In seeking the first curve of the design spline, the left-hand side of the angle is given (the point *A* and the angle I_1). The points in each vertical within the range from L_{min} to L_{max} together with the directions assigned at each of the points constitute the possible variants of the right-hand side of the first angle of rotation (Fig. 3) and determine the corresponding variants of the first CV. For each variant, using the minimum radius of a convex or concave curve (depending on the sign of the angle of rotation), the possibility of satisfying all the constraints is analyzed, and only the variants for which all the constraints are met are retained. Further, it is considered whether or not the radius of the inscribed arc can be increased without violation of constraints using the difference of the slopes of the adjacent elements of the initial spline that are within the angle under consideration. The radius is chosen such that the value of the objective function for the corresponding CV is minimum.

At the first step of comparing paths and rejecting variants, one and the same state is not reached. Each of the allowed states of the first step together with the corresponding values of the objective function (the cost to reach the initial state), the CV coordinates, the radius, and the angle of rotation are stored in memory.

General step of algorithm

The knots of the initial spline are considered such that the abscissas (and the corresponding verticals) of which are within the range from $S_A + 2L_{min}$ to $S - L_{min}$, where *S* is the abscissa of the end of the profile. For each vertical, a sequential analysis is made of all the preceding knots that are no less than L_{min} and no more than L_{max} apart from the vertical and of the straight lines passing through them. For each intersection, the same operations as at the first step are sequentially performed. The difference is that, in the considered state (the right-hand side of the angle, line *BC* in Fig. 4), there may be many intersections with the sides of the preceding angles that originate from one or different CVs (the points A_i and A_{i+1} in Fig. 4). As at the first step, only the joints that satisfy the constraints are considered and compared. As a result, each state in each vertical (the point *C* and the angle) is reached by either one variant, or none. For each of such variants, additionally stored in memory are the point and the direction (the point A_i and the angle A_iB with the abscissa axis in Fig. 4) corresponding to the left-hand side of the angle; i.e., for each new state, the relationship with the best of the preceding states is memorized.

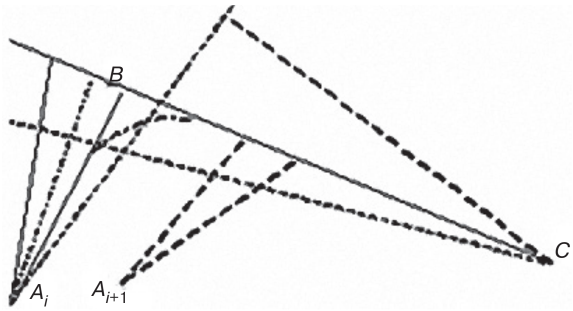

Fig. 4. Comparison and rejection of variants

Last step of algorithm

At the last step, the right-hand side of the angle of rotation is known. These are the final point and the angle determining the final direction. The same operations as at the general step are carried out, and a comparison of the allowable joints determines the minimum value of the objective function. The optimal spline and its parameters are restored by a turn over memorized ties, which is typical for dynamic programming [21, 22].

Of course, one can also consider several final directions and points and perform the same operations for each of them with subsequent selection of the best variant.

The use of the algorithm encountered difficulties in handling long line segments. This gave rise to small angles of rotation. Depending on a specific problem, either such angles are not allowed at all, or curves are not inscribed in them (e.g., in designing low-type roads). In the former case, instead of two intersecting straight lines, one straight line can be formed (using the terminal points) in the course of the exhaustion of variants. But because the algorithm is intended only for the construction of the initial assumption, such transformations were made only for the obtained spline to avoid excessive complications. This is also justified by the fact that not nearly all such intersections at small angles are contained in the final solution.

3. OPTIMIZATION OF SPLINE PARAMETERS

The design line is completely determined by the coordinates of the vertices of the angles of rotation and the radii of the inscribed circles, which are found by dynamic programming (Fig. 5).

To start with, we consider the CV abscissas constant, i.e., analyze the possibility of optimization of the position of the spline by moving CVs along fixed verticals. Because the slopes are small (no more than several tens of permille), the lengths of the sides of each angle are considered to be equal to the difference of the CV abscissas, which are invariable. Since the initial and final points and the directions at them are given, the ordinates of the first and last CVs cannot change. Therefore, the variables are only Z_j, j = 1, 2, …, n, the ordinates of the CVs being varied (their number is $n = N - 2$), and the radii R_j of the inscribed curves. The given boundary conditions are taken into account by the calculation of the limiting values of the slopes, I_1 and I_n, and then the ordinates, Z_1 and Z_n [14].

To obtain a nonlinear programming problem with objective function $\Phi(\mathbf{h})$ (1), one should express in terms of these variables the working marks at the knots of the initial broken line, i.e., the difference of the ordinates of the design spline and the initial broken line ($B'B''$ in Fig. 5), and all the constraints.

In designing the longitudinal profile of new roads, the objective function corresponds to the minimum cost of construction of subgrade and artificial structures. The corresponding models are the same as in the case of using parabolic splines in codesigning the longitudinal and transverse profiles with taking into account the earth mass distribution [14].

If there are such expressions, the calculation of the gradient of objective function (1) reduces to the simple recalculation of derivatives [14] because the ordinates of the points (D and B in Fig. 5) in straight-line elements depend linearly on the CV ordinates. Because the slopes are small, the angle of rotation is considered to be equal to the difference of the adjacent slopes (ΔI_j in Fig. 5).

This enables one to express, with sufficient accuracy, the deviations of the points of the curve from the corresponding points of the straight lines (CC'' and BB'' in Fig. 5), i.e., the corrections to the working marks calculated from the sides of the angle or rotation ("of a boom").

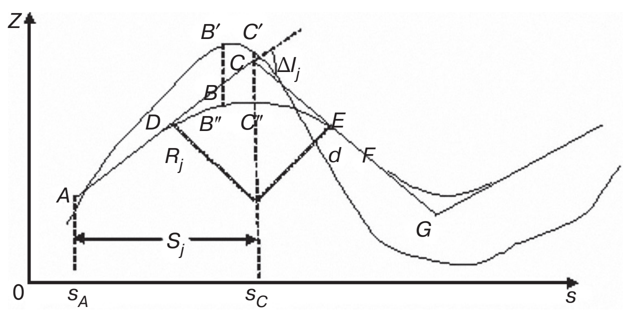

Fig. 5. To the recalculation of derivatives in the presence of circular arcs

In Fig. 5, $CC'' = \delta_j = R_j\Delta I_j^2/8$; $BB'' = \delta_B = \delta_j - t_B\Delta I_j/2 + t_B^2/(2R_j)$, where $t_B = |s_C - s_B|$ is the difference of the abscissas of the CV and the point in the curve; $\Delta I_j = I_{j+1} - I_j$, where $I_j = (Z_j - Z_{j-1})/S_j$, Z_j are unknown design marks of the vertices of the angles of rotation, and S_j are the differences of the abscissas, which differ insignificantly from the lengths of the sides of the angles; and $s_C - s_A = S_j \approx AC$.

Instead of the constraints on the difference of the slopes, there are constraints on the minimum lengths of the curves, $R_j\Delta I_j \geq L_{j,\min}$, and on the minimum length of the straight-line insert, i.e., the sum $CE + FG$ (Fig. 5), should meet the condition

$$R_j\Delta I_j/2 + R_{j+1}\Delta I_{j+1}/2 + L_{\text{ins, min}} \leq S_{j+1}, j = 1, 2, ..., n. \quad (2)$$

Here, $L_{\text{ins,min}}$ is a given minimum length of the straight-line inset, and n is the number of CVs.

At small ΔI_j, to change the length of the straight-line insert by 10 m, it is required to change the radius by 1000 m and more, which can hardly be done by optimizing a spline constructed by dynamic programming. Therefore, condition (2) can be simplified by eliminating the relationship between the variables for the adjacent CVs using the spline obtained at the first stage as the initial approximation.

This can be done by making the following operations:

1. Calculate all the $T_j = R_j\Delta I_j/2$ (in design practice, they are called tangents).
2. Calculate all the straight-line inserts $d_j = S_j - (T_{j-1} + T_j)$, $j = 2, \ldots, n$, and $c_j = d_j - L_{\text{ins,min}}$ ("store").
3. If $d_j = L_{\text{ins,min}}$, then T_{j-1} and T_j are fixed as the maximum values of $R_{j-1}\Delta I_{j-1}/2$ and $R_j\Delta I_j/2$. The fixed values are not further changed.
4. Sequentially consider the straight-line inserts in ascending order, beginning with the smallest d_k. The values $T_{k-1} + T_k$ can be increased by $c_k = d_k - L_{\text{ins,min}}$ without risking a violation of the constraint on the straight-line insert at the neighboring elements. If the maximum values of $R_{k-1}\Delta I_{k-1}/2$ and $R_k\Delta I_k/2$ are not yet fixed, then $T_{k-1} + c_k/2$ and $T_k + c_k/2$, respectively, are taken as their maximum values. The values c_{k-1} and c_{k+1} are decreased by $c_k/2$. If the value T_{k-1} is fixed, then $\max(R_k\Delta I_k/2) = T_k + c_k$ and c_{k+1} are decreased by c_k. If the value T_k is fixed, then $\max(R_{k-1}\Delta I_{k-1}/2) = T_{k-1} + c_k$.
5. Let us proceed to step 3 and continue the process until there are unfixed maximum values of $R_j\Delta I_j/2$. If necessary, the positions of the initial and final points of the profile are taken into account, and the maximum values of $R_1\Delta I_1/2$ and $R_n\Delta I_n/2$ are corrected (decreased).

Bearing in mind that $R_j\Delta I_j$ is the length of the jth curve and $L_{\text{cur,min}}$ is its minimum value, and denoting the calculated maximum values of $R_j\Delta I_j$ as $L_{j,\max}$, we obtain the system of two-sided inequalities

$$L_{\text{cur,min}} \leq R_j\Delta I_j \leq L_{j\,\max}, j = 1, 2, ..., n.$$

Let us convert this system of nonlinear inequalities to a linear system by change of variables from radii to curvatures $\sigma_j = 1/R_j$. The constraint on $L_{j,\max}$ is $\Delta I_j \leq L_{j,\max}\sigma_j$ at $R_j > 0$ and $L_{j,\max}\sigma_j \leq \Delta I_j$ at $R_j < 0$. The constraint on $L_{\text{cur,min}}$ is $L_{\text{cur,min}}\sigma_j \leq \Delta I_j$ at $R_j > 0$ and $\Delta I_j \leq L_{\text{cur,min}}\sigma_j$ at $R_j < 0$.

The signs of R_j are known; hence, we have the linear system of the form

$$\alpha_j\sigma_j \leq \Delta I_j \leq \sigma_j\beta_j, j = 1, 2, ..., n. \quad (3)$$

At $R_j > 0$, $\beta_j = L_{j,\max}$ and $\alpha_j = L_{\text{cur,min}}$. At $R_j < 0$, conversely, $\beta_j = L_{\text{cur,min}}$ and $\alpha_j = L_{j,\max}$.

The algorithm of solving the nonlinear programming problem of finding $\min\Phi(\mathbf{x})$, where $\mathbf{x}$ is the vector of unknowns and $\Phi(\mathbf{x})$ is the objective function, under linear constraints $\mathbf{Ax} \leq \mathbf{b}$ consists of the following steps:

1. Construction of an allowable initial approximation.
2. Calculation of antigradient $\mathbf{f}$.
3. Construction of active constraint matrix $\mathbf{A}_k$ and descent direction $\mathbf{p}$.
4. Check of conditions of termination of calculation.

If the length of the descent vector exceeds given ε, then go to step 5, else check the possibility of eliminating constraints from the active set. If there are no such constraints, then the process is over, else exclude one of the constraints and go to step 3.

5. Search for a step in the direction of the descent as the minimum of the steps to the boundary and to the minimum point. In this case, a one-dimensional minimum search problem is solved.
6. Transition to a new point. Further, if the antigradient at the new point has already been calculated in the search for a step, then go to step 3, else go to step 2.

In the general case, the algorithm ensures a hit of the vicinity of the local minimum point. Therefore, it is important to obtain a good initial approximation by dynamic programming.

There are two key steps: the construction of the descent direction and the elimination of constraints from the active set [22–24]. The problem can be solved using standard algorithms, which require solving systems of linear equations (matrix inversion) at each iteration. For example, the projection of the gradient at the kth iteration can be calculated from the Rosen formula:

$$\mathbf{p} = (\mathbf{E} - \mathbf{A_k}(\mathbf{A_k}\mathbf{A_k^T})^{-1}\mathbf{A_k})\mathbf{f}.$$

To solve the question of the elimination of constraints from the active set, the vector $\mathbf{u} = (\mathbf{A_k}\mathbf{A_k^T})^{-1}\mathbf{A_k}\mathbf{f}$, should be calculated, for which the matrix $\mathbf{A_k}\mathbf{A_k^T}$. should be inverted.

Instead of this, let us consider the possibility of constructing the descent direction using the simple structure of the system of constraints [25]. For this purpose, it is necessary to be capable of constructing a basis in the null space of the matrix $\mathbf{A}_k$ for any active set, which was implemented in the program of spline optimization as a broken line without inscribed curves [14].

For example, if the basis matrix **C** has already been constructed, then the descent vector has the form $\mathbf{p} = \mathbf{CC^Tf}$, where **f** is the antigradient.

Constraints (3) contain additional variables σ_j, but the previously constructed basis vectors [25] can also be converted for this system.

If, in our problem, a certain variable z_j is contained in none of the active constraints, then $p_j = f_j$. The presence of such free points enables one to divide the profile into legs of independent construction of basis vectors and the corresponding components of the descent vector. For example, for system (3) of active constraints on the straight-line insert in the range of CVs from the $(m + 1)$th to the $(m + r - 1)$th (Fig. 6), the variables are z_{m-1}, z_m, …, z_{m+r-1}, z_{m+r} and σ_m, σ_{m+1}, …, σ_{m+r-1}; and the free variables are z_{m-2} and z_{m+r+1}.

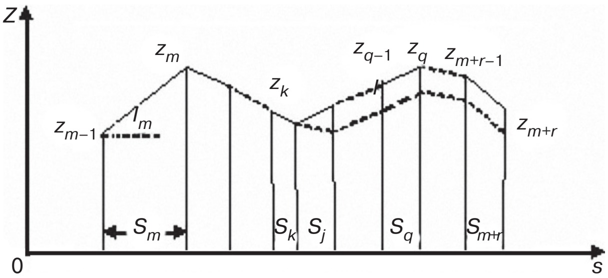

Fig. 6. Example of construction of basis vectors

The active constraints are the following:

$$\begin{aligned} &-\Delta I_m + \alpha_m \sigma_m \le 0, \\ &-\Delta I_{m+1} - \beta_{m+1}\sigma_{m+1} \le 0, \\ &\ldots \\ &-\Delta I_{m+r-1} - \alpha_{m+r-1}\sigma_{m+r-1} \le 0. \end{aligned} \tag{4}$$

This system in the variable ordinates has the form:

$$\begin{aligned} &-1/S_m\, z_{m-1} + (1/S_m + 1/S_{m+1})\, z_m - \\ &-1/S_{m+1}\, z_{m+1} + \alpha_m \sigma_m \le 0, \\ &-1/S_{m+1}\, z_m + (1/S_{m+1} + 1/S_{m+2})\, z_{m+1} - \\ &-1/S_{m+2}\, z_{m+2} - \beta_{m+1}\sigma_{m+1} \le 0, \\ &\ldots \\ &-1/S_{m+r-1}\, z_{m+r-2} + (1/S_{m+r-1} + 1/S_{m+r}) \times \\ &\times z_{m+r-1} - 1/S_{m+r}\, z_{m+r} - \alpha_{m+r-1}\sigma_{m+r-1} \le 0. \end{aligned} \tag{5}$$

The sought basis vectors should convert the inequalities of this system to equalities and be linearly independent. For example, the vector $\mathbf{c_1} = (1\ 1\ \ldots\ 1\ 1\ 0\ 0\ 0)^{\mathrm{T}}$ ($r + 2$ units and r zeros) shifts all the CVs along the ordinate axis without changing slopes and radii. Obviously, the difference of the adjacent slopes and the curvature also remain unchanged.

If all slopes are increased equally, e.g., by 1 (i.e., if a rotation with the center at the $(m - 1)$th CV is made) without changing radii, then the constraints of system (4) and its corresponding system (5) remain active. Therefore, the vector $\mathbf{c_2} = (0\ \ S_m\ \ S_m + S_{m+1}\ \ S_m + S_{m+1} + S_{m+2}\ \ldots\ S_m + S_{m+1} + S_{m+2} + S_{m+r}\ \ 0\ \ldots\ 0)^{\mathrm{T}}$ can also be included in the sought basis. Another r basis vectors are obtained by making rotations about the mth, $(m + 1)$th, …, and $(m + r - 1)$th CVs chosen sequentially as the centers of rotation, changing the right-hand slopes by 1, and compensating the change in the difference of the slopes at the center of rotation by changing the corresponding curvature: (6).

The linear independence of the obtained vectors follows from their construction method.

If, in such a leg, a certain curve σ_j takes the limiting value, then the corresponding component of the descent vector is zero, σ_j is excluded from the variables taken into account in constructing the basis, and the vector corresponding to the change in this variable is not included in the basis.

If the limiting value is taken by the slope of a certain element I_k, then the vector $\mathbf{c}_1$ remains in the basis, but the vectors corresponding to the rotations about the centers at CV_j ($j = m - 1, m, \ldots, k - 1$) change this slope and are not included in the basis.

New basis vectors are constructed by searching through the CVs, beginning with the $(k - 1)$th to the mth, if $k > m$. The center of rotation is taken to be the $(k - 1)$th CV, but the left-hand part is rotated, so that all the left-hand slopes gain equal increments. The difference of the slopes changes only at the $(k - 1)$th CV by 1, which is compensated by changing the $(k - 1)$th curvature. The basis vector is obtained:

$$\mathbf{c} = (s_{k-1} + s_{k-2} + \ldots + s_m\quad s_{k-1} + s_{k-2} + \ldots + s_{m+1}\ \ldots\ s_{k-1} + s_{k-2}\quad s_{k-1}\quad 0 \ldots 0\ \ 0 \ldots 1/\delta \ldots 0 \ldots 0)^{\mathrm{T}},$$

where $\delta = \alpha_{k-1}$ or $\delta = \beta_{k-1}$, depending on the sign of σ_{k-1}.

$$\begin{aligned} &\mathbf{c_3} = (0\ 0\ S_{m+1}\ \ S_{m+1} + S_{m+2} \ldots S_{m+1} + S_{m+2} + \ldots + S_{m+r}\qquad 1/\alpha_m\ \ 0\quad \ldots\ 0)^{\mathrm{T}}, \\ &\mathbf{c_4} = (0\ 0\ 0\quad S_{m+2}\quad \ldots S_{m+2} + S_{m+3}\ \ldots\ S_{m+2} + S_{m+3} + \ldots + S_{m+r}\ \ 0\quad 1/\beta_{m+1} \ldots 0)^{\mathrm{T}}, \\ &\ldots \\ &\mathbf{c_{r+2}} = (0\ 0\ 0\quad 0\quad \ldots\quad 0\quad \ldots\qquad S_{m+r}\ \ 0\ \ldots\ 0\ 1/\alpha_{m+r-1})^{\mathrm{T}}. \end{aligned} \tag{6}$$

If the limiting slope is not the last one, then vertices k, $k + 1$, …, $m + r - 1$ are sequentially taken to be the centers of rotation (Fig. 6), the right-hand part is rotated, and the corresponding basis vector is constructed with the compensation of the change in the difference of the slopes at the center of rotation.

If the limiting slope is the slope of the initial element, then only the rotation of the right-hand part and the motion only to the right are considered. Similarly, if the limiting slope is the slope of the last element, then only left-hand part of the profile is rotated, and the CVs are tested only to the left.

If the limiting value is also taken by the qth slope ($q > k + 1$), then the basis vectors are constructed to the left of the $(k – 1)$th CV and to the right of the qth CV, as for the only limiting slope. If $q = k + 1$, then it is sufficient, else the basis vectors should also be constructed for $k < j < q$. For this purpose, sequentially, beginning with $j = k + 1$ and to $j = q – 1$, all the components of the basis vector are $\mathbf{c}_i = 0$ at $i < j$ and $\mathbf{c}_i = 1$ at $i \geq j$. In this case, only the slope I_j changes, and the constraints are violated at the $(j – 1)$th and jth CVs. They are compensated by changing σ_{j-1} and σ_j in view of the fact that the increments $\Delta I_j = 1/S_j$ and $\Delta I_{j+1} = -1/S_j$. The next basis vector is constructed.

$$\mathbf{c} = (0 ... 0 \underset{j}{1} ... \underset{m+r}{1}\ 0 ... 0 \underset{m+r+j-1}{-1/(\delta_{j-1}S_j)}\ 1/(\delta_j S_j)\ 0 ... 0)^{\mathrm{T}}.$$

If, at some j of $k < j < q$, the curvature σ_j is limiting, then the number of basis vectors is decreased by 1, and in constructing each of them, ΔI_j is retained, and the violation of the difference of the slopes at other CVs is compensated using the curvature at the CVs with the nonlimiting curvature values.

If the leg under active constraints of type (3) contains more than two limiting slopes in, the basis vectors are constructed similarly.

If two legs of the considered form share one common CV to which an inactive constraint of type (3) corresponds, then, for these legs, the basis vectors are constructed as for an integral whole. But for the basis vector obtained by the rotation with the center at this CV, the curvature is not required to be changed. If two legs have no common CVs, then they are considered separately.

To satisfy the conditions for the fixed initial and final points and directions, these conditions are converted to constraints of the form $z_{1,\ \min} \leq z_1 \leq z_{1,\ \max}$ and $z_{n,\ \min} \leq z_n \leq z_{n,\ \max}$ [25].

If some of them becomes active, then the shift vector is not included in the basis. If an active constrain of type (3) is imposed at CV_1 or CV_n, then the vector of rotation with the center at these points is constructed with the compensation of the difference of the slopes by changing the corresponding curvature.

The height constraints at points in the inscribed curves are nonlinear and have to be taken into account by penalty functions [25].

To solve the question of the possibility of eliminating a constraint from the active set, it is necessary to construct vector **g** that violates this and only this constraint. If (**f, g**) < 0, the constraint is excluded. For active constraints of type (3), this is a basis vector, but without compensation at the center of rotation. And if the corresponding curvature is limiting, then it is necessary to construct vector **g** as a basis vector with compensation. If it does not violate the curvature constraint and (**f, g**) > 0, then the curvature constraint can be excluded. For the active constraint on the slope I_k (Fig. 6), such a vector is obtained by allowing the rotation of the right-hand part of the leg with the center at the $(k - 1)$th CV, which was not used in the construction of the basis, with the compensation of the change in ΔI_{k-1}.

If the active set does not contain constraints of type (3), then the question of the possibility of eliminating such constraints from the active set is solved quite simply [25].

CONCLUSIONS

The proposed method to construct the basis enables one to solve the problem of optimization of parameters of a spline with circular arcs and at variable CV abscissas obtained at the first stage. This question, as well as the optimization of parameters of a spline that is not a one-to-one function, which often takes place in designing the plan of road routes, requires a separate consideration.

As was determined as far back as the 1970s–1980s [1, 26], using adequate mathematical models and correct optimization algorithms yielded a significant economic effect. The Profil, Profil-r, Profil-2a, and Profil-2r systems, which were used at that time on slow (by modern standards) computers for designing the longitudinal profile of roads and railways [1, 26], are currently not used, first of all, because of the absence of entities interested in reducing the cost estimate of construction and reconstruction by improving project quality. These systems were replaced by foreign-made CAD systems, which accelerated the processes of preparation and release of numerous drawings and other project documents. However, these systems do not include designing programs. In an expert designer's apt words, they are "convenient drawing tools with no signs of optimization." On the other hand, both updated old systems of longitudinal profile design, and new programs of route plan design solve complex problems of optimization and visualization of computer design solutions, but they cannot completely replace the used foreign-made interactive-design CAD systems.

The point is that designing systems are developed "by inertia," as a personal initiative, without funding sources; therefore, they do not contain subsystems of preparation and release of drawings and various output documents.

The emerging trend toward artificial intelligence in other sciences and technologies gives promise that designing programs will also be in demand in routing of linear structures, which will significantly reduce the labor and money inputs in construction by using intelligent design systems.

Authors' contribution. All authors equally contributed to the research work.

REFERENCES

1. Struchenkov V.I. The use of mathematical optimization methods and a computer in the design of the longitudinal profile of railways; B.K. Malyavskii (Ed.). *Seriya: Trudy Vsesoyuznogo nauchno-issledovatel'skogo instituta transportnogo stroitel'stva = Series: Proceedings of the All-Union Scientific Research Institute of Transport Construction*. Iss. 101. Moscow: Transport; 1977. 169 p. (in Russ.).
2. Struchenkov V.I. Computer technologies in line structure routing. *Rossiiskii tekhnologicheskii zhurnal = Russian Technological Journal*. 2017;5(1):29–41 (in Russ.). https://doi.org/10.32362/2500-316X-2017-5-1-29-41
3. Ahlberg J.H., Nilson E.N., Walsh J.L. The theory of splines and their applications. Academic press; 1967. 296 p. [Alberg J., Nilson E., Walsh J. *Teoriya splainov i ee prilozheniya* (*The theory of splines and their applications*). Moscow: Mir; 1972. 312 p. (in Russ.).]
4. Khakimov B.V. *Modelirovanie korrelyatsionnykh zavisimostei splainami na primerakh v geologii i ekologii* (*Modeling of correlation dependences by splines on examples in geology and ecology*). St. Petersburg: Neva; 2003. 144 p. (in Russ). ISBN 5-7654-2951-3
5. Dierckx P. *Curve and Surface fitting with splines*. Oxford University Press; 1995. 285 p.
6. Mikhalevich V.S., Bykov V.I., Sibirko A.N. To the question of designing the optimal longitudinal profile of the road. *Transportnoe stroitel'stvo = Transport Construction*. 1975;6:39–40 (in Russ.).
7. Kosmin V.V., Struchenkov V.I., Fradkov E.B. Computer design of the longitudinal profile of the road. *Transportnoe stroitel'stvo = Transport Construction*. 1971;4:38–42 (in Russ.).
8. Bentley Rail Track. Available from URL: https://www.bentley.com/-/media/1EA2B937CB5B42BEA5EAE802620C0BA3.ashx
9. CARD/1. Available from URL: http://card-1.ru/
10. Autodesk. Available from URL: https://www.architect-design.ru/autodesk/autocad/
11. Topomatic Robur. Available from URL: http://www.topomatic.ru/
12. Credo-Dialog. Available from URL: https://credo-dialogue.ru/
13. Struchenkov V.I. The use of parabolic splinees in CAD of linear structures. *Rossiiskii tekhnologicheskii zhurnal = Russian Technological Journal*. 2018;6(1):40–51 (in Russ). https://doi.org/10.32362/2500-316X-2018-6-1-40-52
14. Struchenkov V.I. *Metody optimizatsii trass v SAPR lineinykh sooruzhenii* (*Methods for route optimization in CAD of linear structures*). Moscow: Solon-Press; 2014. 271 p. (in Russ). ISBN 978-5-91359-139-5

СПИСОК ЛИТЕРАТУРЫ

1. Струченков В.И. Использование математических методов оптимизации и ЭВМ при проектировании продольного профиля железных дорог; под ред. Б.К. Малявского. Серия: *Труды Всесоюзного научно-исследовательского института транспортного строительства.* Вып. 101. М.: Транспорт; 1977. 169 с.
2. Струченков В.И. Компьютерные технологии в проектировании трасс линейных сооружений. *Российский технологический журнал*. 2017;5(1):29–41. https://doi.org/10.32362/2500-316X-2017-5-1-29-41
3. Альберг Дж., Нильсон Э., Уолш Дж. *Теория сплайнов и ее приложения*: пер. с англ. М.: Мир; 1972. 312 с.
4. Хакимов Б.В. *Моделирование корреляционных зависимостей сплайнами на примерах в геологии и экологии*. СПб.: Нева; 2003. 144 с. ISBN 5-7654-2951-3
5. Dierckx P. *Curve and Surface fitting with splines*. Oxford University Press; 1995. 285 p.
6. Михалевич В.С., Быков В.И., Сибирко А.Н. К вопросу проектирования оптимального продольного профиля дороги. *Транспортное строительство*. 1975;6:39–40.
7. Космин В.В., Струченков В.И., Фрадков Е.Б. Проектирование продольного профиля дороги на ЭВМ. *Транспортное строительство*. 1971;4:38–42.
8. Bentley Rail Track. URL: https://www.bentley.com/-/media/1EA2B937CB5B42BEA5EAE802620C0BA3.ashx
9. CARD/1. URL: http://card-1.ru/
10. Autodesk. URL: https://www.architect-design.ru/autodesk/autocad/
11. Topomatic Robur. URL: http://www.topomatic.ru/
12. Credo-Dialog. URL: https://credo-dialogue.ru/
13. Струченков В.И. Использование параболических сплайнов в САПР линейных сооружений. *Российский технологический журнал.* 2018;6(1):40–52. https://doi.org/10.32362/2500-316X-2018-6-1-40-52
14. Струченков В.И. *Методы оптимизации трасс в САПР линейных сооружений*. М.: Солон-Пресс; 2015. 272 с. ISBN 978-5-91359-139-5
15. Лежнев А.В. *Динамическое программирование в экономических задачах*. М.: Бином; 2016. 285 с. ISBN 5-94774-344-2
16. Cavagnari G., Marigonda A., Piccoli B. Generalized dynamic programming principle and sparse mean-field control problems. *Journal of Mathematical Analysis and Applications*. 2020;481(1):123437. https://doi.org/10.1016/j.jmaa.2019.123437
17. He S., Shin H.-S., Tsourdos A. Computational guidance using sparse Gauss-Hermite quadrature differential dynamic programming. *IFAC-PapersOnLine*. 2019;52(12):13–18. https://doi.org/10.1016/j.ifacol.2019.11.062

15. Lezhnev A.V. *Dinamicheskoe programmirovanie v ekonomicheskikh zadachakh* (*Dynamic programming in economic problems*). Moscow: Binom; 2016. 176 p. (in Russ). ISBN 5-94774-344-2
16. Cavagnari G., Marigonda A., Piccoli B. Generalized dynamic programming principle and sparse mean-field control problems. *Journal of Mathematical Analysis and Applications*. 2020;481(1):123437. https://doi.org/10.1016/j.jmaa.2019.123437
17. He S., Shin H.-S., Tsourdos A. Computational guidance using sparse Gauss-Hermite quadrature differential dynamic programming. *IFAC-PapersOnLine*. 2019;52(12):13−18. https://doi.org/10.1016/j.ifacol.2019.11.062
18. Fayaed S.S., Fiyadh S.S., Khai W.J., Ahmed A.N., Afan H.A., Ibrahim R.K. Improving dam and reservoir operation rules using stochastic dynamic programming and artificial neural network integration model. *Sustainability*. 2019;11(19):5367. https://doi.org/10.3390/su11195367
19. Işik H., Sintunavarat W. An investigation of the common solutions for coupled systems of functional equations arising in dynamic programming. *Mathematics*. 2019;7(10):977. https://doi.org/10.3390/math7100977
20. Karpov D.A., Struchenkov V.I. Dynamic Programming as a Method of Spline Approximation in the CAD Systems of Linear Constructions. *Rossiiskii tekhnologicheskii zhurnal* = *Russian Technological Journal*. 2019;7(3):77−88 (in Russ.). https://doi.org/10.32362/2500-316X-2019-7-3-77-88
21. Karpov D.A., Struchenkov V.I. *Metody i algoritmy resheniya prikladnykh zadach diskretnoi optimizatsii* (*Methods and algorithms for solving applied discrete optimization problems*). Moscow: Solon-Press; 2020. 201 p. (in Russ.). ISBN 978-5-91359-399-3
22. Kochenderfer M., Wheeler T. *Algorithms for Optimization*. The MIT Press; 2019. 521 p.
[Kokhenderfer M., Uiler T. *Algoritmy optimizatsii*. Moscow: Vil'yams; 2020. 528 p. (in Russ.). ISBN 978-5-907144-76-7]
23. Chernorutskii I.G. *Metody optimizatsii. Komp'yuternye tekhnologii* (*Optimization methods. Computer technologies*). St. Petersburg: BHV-Petersburg; 2011. 370 p. (in Russ.). ISBN 978-5-9775-0784-4
24. Ovchinnikov V.A. *Modeli i metody diskretnoi optimizatsii* (*Models and methods of discrete optimization*). Moscow: MGTU im. N.E. Baumana; 2019. 278 p. (in Russ.). ISBN 978-5-7038-5105-0
25. Struchenkov V.I. *Prikladnye zadachi optimizatsii* (*Applied optimization problems*). Moscow: Solon-Press; 2016. 314 p. (in Russ.). ISBN 978-5-91359-191-3
26. Karikh Yu.S. Evaluation of existing longitudinal profile design methods. In: Collection of works of GiprodorNII: *Improving the economic efficiency of investment in the construction, repair and maintenance of roads*. Moscow: Izdanie GiprodorNII; 1976. P. 105−112. (in Russ.).

18. Fayaed S.S., Fiyadh S.S., Khai W.J., Ahmed A.N., Afan H.A., Ibrahim R.K. Improving dam and reservoir operation rules using stochastic dynamic programming and artificial neural network integration model. *Sustainability*. 2019;11(19):5367. https://doi.org/10.3390/su11195367
19. Işik H., Sintunavarat W. An investigation of the common solutions for coupled systems of functional equations arising in dynamic programming. *Mathematics*. 2019;7(10):977. https://doi.org/10.3390/math7100977
20. Карпов Д.А., Струченков В.И. Динамическое программирование как метод сплайн- аппроксимации в САПР линейных сооружений. *Российский технологический журнал*. 2019;7(3):77−88. https://doi.org/10.32362/2500-316X-2019-7-3-77-88
21. Карпов Д.А., Струченков В.И. *Методы и алгоритмы решения прикладных задач дискретной оптимизации*. М.: Солон-Пресс; 2020. 201 с. ISBN 978-5-91359-399-3
22. Кохендерфер М., Уилер Т. *Алгоритмы оптимизации*. М.: Вильямс; 2020. 528 с. ISBN 978-5-907144-76-7
23. Черноруцкий И.Г. *Методы оптимизации. Компьютерные технологии*. СПб.: БХВ-Петербург; 2011. 370 с. ISBN 978-5-9775-0784-4
24. Овчинников В.А. *Модели и методы дискретной оптимизации.* М.: МГТУ им. Н.Э. Баумана; 2019. 278 с. ISBN 978-5-7038-5105-0
25. Струченков В.И. *Прикладные задачи оптимизации*. М.: Солон-Пресс; 2016. 314 с. ISBN 978-5-91359-191-3
26. Карих Ю.С. Оценка существующих методов проектирования продольного профиля. В сб. трудов ГипродорНИИ. Вып. 17. *Повышение экономической эффективности капиталовложений в строительство, ремонт и содержание автомобильных дорог*. М.: Издание ГипродорНИИ; 1976. С. 105−112.

About the authors

Dmitry A. Karpov, Cand. Sci. (Eng.), Head of the General Informatics Department, Institute of Cybernetics, MIREA – Russian Technological University (78, Vernadskogo pr., Moscow, 119454 Russia). E-mail: karpov@mirea.ru. https://orcid.org/0000-0003-3734-7182

Valery I. Struchenkov, Dr. Sci. (Eng.), Professor, General Informatics Department, Institute of Cybernetics, MIREA – Russian Technological University (78, Vernadskogo pr., Moscow, 119454 Russia). E-mail: srt1942@mail.ru. https://orcd.org/0000-0002-9801-7454

Об авторах

Карпов Дмитрий Анатольевич, к.т.н., заведующий кафедрой общей информатики Института кибернетики, ФГБОУ ВО «МИРЭА – Российский технологический университет» (119454, Россия, Москва, пр-т Вернадского, д. 78). E-mail: karpov@mirea.ru. https://orcid.org/0000-0003-3734-7182

Струченков Валерий Иванович, д.т.н., профессор, кафедра общей информатики Института кибернетики, ФГБОУ ВО «МИРЭА – Российский технологический университет» (119454, Россия, Москва, пр-т Вернадского, д. 78). E-mail: srt1942@mail.ru. https://orcid.org/0000-0002-9801-7454

Translated by V. Glyanchenko

Micro- and nanoelectronics. Condensed matter physics

Микро- и наноэлектроника. Физика конденсированного состояния

UDC 544.2
https://doi.org/10.32362/2500-316X-2021-9-5-57-66

RESEARCH ARTICLE

Evaporation of a liquid sessile droplet subjected to forced convection

Anna E. Korenchenko [1, @],
Anna A. Zhukova [2]

[1] MIREA – Russian Technological University, Moscow, 119454 Russia
[2] Sechenov First Moscow State Medical University, Moscow, 105043 Russia
[@] Corresponding author, e-mail: korenchenko@mirea.ru

Abstract. The experiments on measuring the evaporation rate of liquid sessile droplets into air show that the rate of evaporation increases in the presence of forced convection flows. However, data on the effect of convection on the evaporation process is often contradictory and should be clarified. The paper presents a numerical analysis of evaporation from the surface of a water droplet subjected to forced convection in the gas phase. The drop is located on a smooth horizontal isothermal substrate; the mode with constant contact angle is considered. The form of the drop has axial symmetry, the same for the velocities and pressure. Forced convection compatible with the symmetry conditions are represented by flows directed downward along the axis of the system and diverging along the sides near the drop and the substrate. The mathematical model is constructed for evaporation controlled by diffusion in the gas phase and takes into account surface tension, gravity, and viscosity in both media, buoyancy and Marangoni convection. The results indicate the existence of the mutual influence of liquid and gaseous media. Thus, a drop vibrates under the influence of movements in the atmosphere, which generates a density wave in the gas: the drop "sounds". The magnitude of the velocity in a liquid is 50 times less than the characteristic velocity in air. It is found that the evaporation rate does not change in the presence of forced convection flows, which contradicts most of the experimental works. The reason for the discrepancies is supposed to be the appearance of nonequilibrium conditions at the boundary of the condensed phase, under which the evaporation regime ceases to be diffusional.

Keywords: evaporation, diffusion, sessile droplet, forced convection, mathematical modeling

• **Submitted:** 21.01.2021 • **Revised:** 01.03.2021 • **Accepted:** 12.07.2021

For citation: Korenchenko A.E., Zhukova A.A. Evaporation of a liquid sessile droplet subjected to forced convection. *Russ. Technol. J.* 2021;9(5):57–66. https://doi.org/10.32362/2500-316X-2021-9-5-57-66

Financial disclosure: The authors have no a financial or property interest in any material or method mentioned.

The authors declare no conflicts of interest.

НАУЧНАЯ СТАТЬЯ

Испарение жидкой лежащей капли в условиях вынужденной конвекции

А.Е. Коренченко [1, @],
А.А. Жукова [2]

[1] *МИРЭА – Российский технологический университет, Москва, 119454 Россия*
[2] *Первый Московский государственный медицинский университет имени И.М. Сеченова, Москва, 105043 Россия*
[@] *Автор для переписки, e-mail: korenchenko@mirea.ru*

Резюме. Результаты экспериментов по измерению скорости испарения с поверхности жидкой лежащей капли в воздух указывают, что конвективные потоки над поверхностью увеличивают скорость испарения. Однако данные относительно того, в какой мере конвекция влияет на процесс испарения, сильно разнятся, часто противоречивы и требуют уточнения. В работе проведен численный анализ испарения с поверхности капли воды в нейтральный газ – воздух в присутствии конвективных течений в газовой фазе. Капля располагается на горизонтальной, гладкой, изотермической подложке, рассмотрена мода с постоянным углом смачивания. Задача решена в осесимметричном приближении, течения вынужденной конвекции, совместимые с условиями симметрии, представлены потоками, направленными вниз вдоль оси системы и расходящимися по сторонам вблизи капли и подложки. Математическая модель учитывает влияние сил поверхностного натяжения, тяготения и вязкости в обеих средах, возможную свободную гравитационную конвекцию в газовой и жидкой средах, конвекцию Марангони в капле и построена для испарения, контролируемого диффузией в газовой фазе. Получены результаты, свидетельствующие о взаимном влиянии жидкой и газовой сред: капля колеблется под влиянием движений в атмосфере, что порождает волну плотности в газе: колеблющаяся капля «звучит». Величина скорости в жидкой среде в 50 раз меньше характерной скорости в воздухе. Обнаружено, что скорость испарения не изменяется в присутствии течений вынужденной конвекции, что противоречит большинству экспериментальных работ. Предположительная причина расхождений заключается в возникновении неравновесных условий на границе конденсированной фазы, при которых режим испарения перестает быть диффузионным.

Ключевые слова: испарение, диффузия, лежащая капля, вынужденная конвекция, численное моделирование

• **Поступила:** 21.01.2021 • **Доработана:** 01.03.2021 • **Принята к опубликованию:** 12.07.2021

Для цитирования: Коренченко А.Е., Жукова А.А. Испарение жидкой лежащей капли в условиях вынужденной конвекции. *Russ. Technol. J.* 2021;9(5):57–66. https://doi.org/10.32362/2500-316X-2021-9-5-57-66

Прозрачность финансовой деятельности: Никто из авторов не имеет финансовой заинтересованности в представленных материалах или методах.

Авторы заявляют об отсутствии конфликта интересов.

INTRODUCTION

Evaporation of liquid from the surface of droplets is a part of the water cycle, is often encountered in everyday life, and is therefore actively studied theoretically and experimentally [1–6]. For surface evaporation of water, it was experimentally determined that convective air flows over the surface sometimes accelerate the evaporation, and that the evaporation is the more intense, the lower is the ambient humidity φ. However, the published data on the extent to which these phenomena affect the evaporation rate differ widely and are sometimes contradictory. For example, experimental studies of evaporation from the flat surface of water in the presence of convective flows showed an increase in the evaporation rate, which was characterized differently: as either linear in flow velocity V [7], or described by a polynomial of the third degree [8], or proportional to $\sim V^{3/2}$ [9], whereas numerical calculations indicated that the effect of convection on the evaporation rate is weak [2, 10]. The dependence of the evaporation rate on the difference between the saturated vapor pressure over the surface (p_{vs}) and the partial vapor pressure in the surrounding air (p_{v0}) was experimentally described by a formula of the form $(p_{vs} - p_{v0})^n$, where the Dalton approximation predicted $n = 1$ [10], Tang and Etzion [7], and Al-Shammiri [9] obtained the n values smaller than 1, Boetler et al. [12] and Pauken et al. [13] calculated the n values larger than 1, and Jodat and Moghiman [8] proposed an expression relating n to the air flow velocity. Also different are opinions on the role of free convection in evaporation. Guéna et al. [14] experimentally investigated the evaporation rate from the surface of sessile and hanging water droplets and obtained equal values of the evaporation rate, which suggested the absence of the effect of gravitational convection in the gas phase. However, Kelly-Zion et al.'s in their experiments determined [15] that the evaporation rate from the surface of a sessile droplet is four times higher than that calculated for diffusion-controlled evaporation. Obviously, these contradictions are due to the fact that the conditions of the experiments [7–15] differed, but the reasons why the action of the same factors on evaporation brings about different responses are unclear.

Investigation of evaporation from the surface of a droplet requires one to take into account a lot of possible physical phenomena. For example, evaporation causes cooling of the droplet, which is generally nonuniform. This leads to a nonuniformity of the saturated vapor concentration over the surface, and also can lead to thermocapillary convection in the bulk of the droplet. Description of evaporation under gravity can be complicated by free convection in both the gas and the liquid media. Any external perturbations, mechanical or thermodynamic, can cause free vibrations of the droplet [16] and probably influence the evaporation. The main purpose of our studies is to numerically analyze the evaporation from the surface of a sessile droplet into a neutral gas. The calculations took into account the effect of the surface tension, gravity, and viscosity in both media, the possible free gravitational convection in the gas and liquid phases, and the Marangoni convection in the droplet. The effect of gravity on the shape of the droplet was also taken into account, and consideration was made

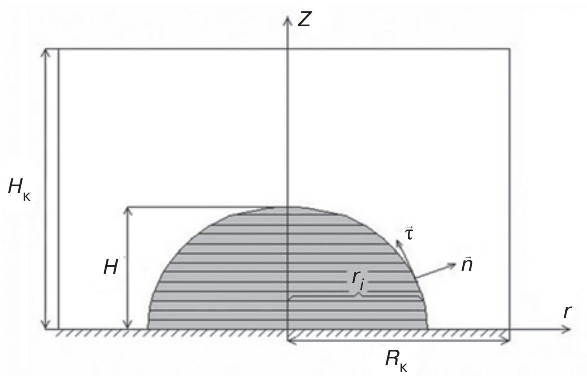

Fig. 1. Experimental design

of the movements of the surface of the droplet that are unrelated to the displacement of the droplet because of the decrease in the volume. We perform our analysis step by step; in this work, the effect of forced convection on the evaporation rate, the shape of the droplet, and the motion of its boundaries.

1. DESCRIPTION OF MATHEMATICAL MODEL

1.1. Design of computer experiment and notation

Let us consider a liquid droplet lying on a horizontal surface, and let R be the radius of a spherical droplet of the same volume. The sessile droplet is in the atmosphere of a neutral noncondensable gas. The problem is solved in an axisymmetric assumption by the finite-difference method. The sizes of the computational space by far exceed the droplet radius: $R_{cs}, H_{cs} \gg R$ (Fig. 1 is sketchy, not to scale). A difference scheme is constructed as follows [16]: (1) the computational space at $z \le H$ is divided into horizontal layers so that the droplet is sliced into layers of equal thickness h_z with radius r_i; (2) the computational space in the gas above the droplet (at $z > H$) is also divided into horizontal layers of thickness, which may exceed h_z (not shown in Fig. 1); and (3) the computational space is divided into vertical layers (not shown in Fig. 1). Because of the complex shape of the subject of computation, the computational grid near the boundary of the droplet thickens to more accurately represent the shape of the boundary. The boundary of the droplet is given by a set of points (ih_z, r_i) connected by line segments.

The following notation is introduced: ρ_l is the density of the liquid; ρ_0, T_0, and p_0 are the density, temperature, and pressure of the gas at the boundaries of the computational space, respectively; T_s is the temperature of the substrate; ν_l and ν_g are the kinematic viscosities of the liquid and the gas, respectively; η_l and η_g are their dynamic viscosities; κ_l and κ_g are their thermal conductivities; c_l and c_g are their specific heat capacities; M_l and M_g are their molar masses; β_l is the thermal expansion coefficient of the liquid; D is the diffusion coefficient of the vapor in air; λ is the heat of evaporation; σ_{lg}, σ_{gs}, and σ_{ls} are the surface tensions at the liquid–gas, gas–solid, and liquid-solid interfaces, respectively. The subscripts l, g, and v refer to the liquid, the gas, and the vapor, respectively.

1.2. The main approximations of the model

It is assumed that the liquid is incompressible and Newtonian, the neutral gas and its mixture with the vapor are ideal gases, and the substrate is smooth and isothermal. The evaporation is assumed to be slow; therefore, over the surface of the liquid, there is an equilibrium saturated vapor. A two-dimensional problem is considered under the assumption of the axial symmetry of the droplet, the flows, and the vapor pressure, temperature, and concentration distributions in the absence of flows of the media in the azimuthal direction.

1.3. Equations and boundary conditions

The conservation equations for the liquid in the droplet are written as follows:

$$\frac{\partial \vec{\mathbf{V}}}{\partial t}+\left(\vec{\mathbf{V}}\cdot\vec{\nabla}\right)\vec{\mathbf{V}}=-\frac{1}{\rho_l}\vec{\nabla}P+\nu_l\vec{\nabla}^2\vec{\mathbf{V}}-\vec{\mathbf{g}}\beta_l\left(T-T_s\right), \quad (1)$$

$$\vec{\nabla}\cdot\vec{\mathbf{V}}=0, \quad (2)$$

$$\frac{\partial T}{\partial t}+\vec{\nabla}\left(\vec{\mathbf{V}}T\right)=\frac{\kappa_l}{\rho_l c_l}\vec{\nabla}^2 T. \quad (3)$$

Here, P is the excess of the pressure over the hydrostatic pressure in the liquid; $\vec{\mathbf{V}}=\{V_r, V_z\}$ and T are the velocity and temperature distributions, respectively; and $\vec{\mathbf{g}}$ is the acceleration of gravity. The buoyance in Eq. (1) is taken in to account in the Boussinesq approximation.

The behavior of the gas is described by the following equations:

$$\frac{\partial \vec{\mathbf{V}}}{\partial t}+\left(\vec{\mathbf{V}}\cdot\vec{\nabla}\right)\vec{\mathbf{V}}=-\frac{1}{\rho}\vec{\nabla}p+\frac{\eta_g}{\rho}\vec{\nabla}^2\vec{\mathbf{V}}-\vec{\mathbf{g}}, \quad (4)$$

$$\frac{\partial \rho}{\partial t}+\vec{\nabla}\left(\rho\vec{\mathbf{V}}\right)=0, \quad (5)$$

$$\frac{\partial T}{\partial t}+\vec{\nabla}\left(\vec{\mathbf{V}}T\right)=\frac{\kappa_g}{\rho c_g}\vec{\nabla}^2 T, \quad (6)$$

$$\frac{\partial C}{\partial t}+\vec{\nabla}\left(\vec{\mathbf{V}}C\right)=D\vec{\nabla}^2 C. \quad (7)$$

System (4)–(7) is supplemented with the equation of state of the vapor–gas mixture:

$$p=\frac{\rho R_g T}{M},\ M=\left(\frac{C}{M_l}+\frac{1-C}{M_g}\right)^{-1}. \quad (8)$$

Here, p, ρ, and M are the pressure, density, and molar mass of the mixture, respectively; C is the mass fraction of the vapor; and R_g is the universal gas constant.

The upper and lateral boundaries of the computational space are the unperturbed gas medium with given vapor mass fraction C_0, density ρ_0, pressure p_0, and temperature T_0.

At the gas–substrate interface, the impermeability, constant temperature, and no-slip conditions are specified.

At the liquid–gas interface S_{lg}, the following conditions are set [17]:

1) The partial vapor pressure p_{vs} is equal to the saturated vapor pressure of the liquid at the temperature of the surface and with taking into account the curvature $K(z)$ and the presence of the neutral gas:

$$p_{vs}=p_{v\infty}+\frac{\rho_{v\infty}}{\rho_l-\rho_{v\infty}}\left(-\sigma_{lg}K+p\right),$$

where $p_{v\infty}$ and $\rho_{v\infty}$ are the pressure and density of the vapor over the flat surface of the liquid $(K=\infty)$, respectively; $p_{v\infty}$ is calculated as $p_{v\infty}=6.112e^{17.62\left(T_s-273\right)/\left(T_s-29.88\right)}$ [18]; and $p(z)$ is the air pressure over the surface of the droplet. The curvature is calculated from the expression $K\left(z_i\right)=R_{1i}^{-1}+R_{2i}^{-1}$; here, R_{1i} and R_{2i} are the radii of normal cross sections of the droplet, which are calculated from geometric considerations [16]. The mass fraction of the vapor over the surface of the droplet is found as

$$C_s=\frac{p_{vs}M_l}{\rho_s R_g T_s}, \quad (9)$$

where ρ_s is the density of the gas–vapor mixture over the surface of the droplet.

2) The normal component of the velocity of the gas medium over the surface of the droplet is determined by the Stefan condition:

$$(1-C_s)\cdot\left(\vec{\mathbf{V}}\cdot\vec{n}-V_{S_{lg}}\right)-D\frac{\partial(1-C)}{\partial n}=0. \quad (10)$$

Condition (10) is written in a frame of reference in which the interface is immovable and describes the diffusion-controlled evaporation: the diffusion air flow to the surface should be compensated for a convective flow from the surface; $V_{S_{lg}}$ is the velocity of the liquid–gas interface in a laboratory frame of reference.

3) The discontinuous change in the normal component of the tension at S_{lg} is described by the Laplace equation

$$\vec{n}\boldsymbol{T}\vec{n}\Big|_l-\rho_l\left(\vec{V}_l\cdot\vec{n}-V_{S_{lg}}\right)^2-$$
$$-\left(\vec{n}\boldsymbol{T}\vec{n}\Big|_g-\rho\left(\vec{V}_g\cdot\vec{n}-V_{S_{lg}}\right)^2\right)=\sigma_{lg}K, \quad (11)$$

where the components of the tension tensor $\boldsymbol{T}$ are written as $T_{ij} = -p\delta_{ij} + \eta\left(\partial u_i/\partial x_j + \partial u_j/\partial x_i\right)$, and δ_{ij} is the Kronecker delta.

4) The discontinuous change in the tangential component of the tension is equal to the tangential component of the surface tension gradient:

$$\vec{n}\boldsymbol{T}\vec{\tau}\big|_{\mathrm{l}} - \rho_{\mathrm{l}}\vec{V}_{\mathrm{l}}\cdot\vec{\tau}\left(\vec{V}_{\mathrm{l}}\cdot\vec{n} - V_{S_{\mathrm{lg}}}\right) -$$
$$-\left(\vec{n}\boldsymbol{T}\vec{\tau}\big|_{\mathrm{g}} - \rho\vec{V}_{\mathrm{g}}\cdot\vec{\tau}\left(\vec{V}_{\mathrm{g}}\cdot\vec{n} - V_{S_{\mathrm{lg}}}\right)\right) = -\left|\frac{d\sigma}{dT}\right|(\nabla T)_{\tau}. \quad (12)$$

Equation (12) assumes a linear dependence of the surface tension on temperature:

$$\sigma = \sigma_0 - \left|\frac{d\sigma}{dT}\right|\left(T - T_{\mathrm{g}}\right).$$

5) The tangential components of the velocity and the temperature at the interface is continuous:

$$V_{\mathrm{l}}\big|_{\tau} = V_{\mathrm{g}}\big|_{\tau}, \quad (13)$$

$$T_{\mathrm{l}} = T_{\mathrm{g}}. \quad (14)$$

6) The heat flux experiences a discontinuous change because of the absorption of the latent heat of evaporation:

$$-k_{\mathrm{l}}\frac{\partial T}{\partial n}\bigg|_{\mathrm{l}} + \rho_{\mathrm{l}}c_{\mathrm{l}}T_{\mathrm{l}}\cdot\left(\vec{\mathbf{V}}_{\mathrm{l}}\cdot\vec{n} - V_{S_{\mathrm{lg}}}\right) -$$
$$-\left(-k_{\mathrm{g}}\frac{\partial T}{\partial n}\bigg|_{\mathrm{g}} + \rho c_{\mathrm{g}}T_{\mathrm{g}}\cdot\left(\vec{\mathbf{V}}_{\mathrm{g}}\cdot\vec{n} - V_{S_{\mathrm{lg}}}\right)\right) = \dot{m}\cdot\lambda. \quad (15)$$

In Eq. (15), the local mass flux on the surface is expressed as

$$\dot{m} = \rho_{\mathrm{l}}\cdot\left(\vec{\mathbf{V}}_{\mathrm{l}}\cdot\vec{n} - V_{S_{\mathrm{lg}}}\right) =$$
$$= \rho C\cdot\left(\vec{\mathbf{V}}_{\mathrm{g}}\cdot\vec{n} - V_{S_{\mathrm{lg}}}\right) - \rho D\frac{\partial C}{\partial n} = \rho\cdot\left(\vec{\mathbf{V}}_{\mathrm{g}}\cdot\vec{n} - V_{S_{\mathrm{lg}}}\right). \quad (16)$$

The velocity of the interface is found from Eqs. (10) and (16) is written as

$$V_{S_{\mathrm{lg}}} = \left(\rho_{\mathrm{l}}\vec{V}_{\mathrm{l}}\cdot\vec{n} - \rho\vec{V}_{\mathrm{g}}\cdot\vec{n}\right)\Big/\left(\rho_{\mathrm{l}} - \rho\right)\Big|_{S_{\mathrm{lg}}}. \quad (17)$$

7) The condition at the three-phase boundary has the form

$$\theta_0 = \mathrm{const}, \quad (18)$$

where θ_0 is the equilibrium contact angle: $\cos\theta_0 = \left(\sigma_{\mathrm{gs}} - \sigma_{\mathrm{ls}}\right)/\sigma_{\mathrm{lg}}$.

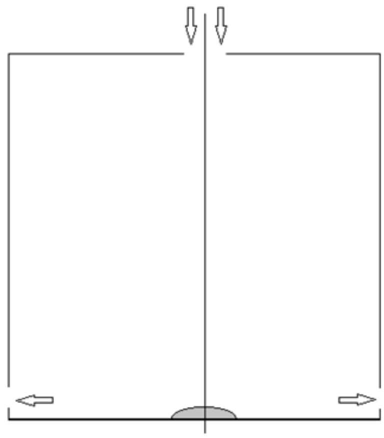

Fig. 2. Computational space (arrows show the air inlet and outlet zones)

To create forced convection flows compatible with the axial symmetry conditions, air is blown through an opening at the top of the computational space and leaves this space through a slot in the lateral walls at the bottom near the substrate (Fig. 2). The gas velocities were chosen so that the amounts of air and the vapor in the bulk remain unchanged during convection.

Equations (1)–(18) are nondimensionalized as follows. Of the parameters of the liquid, the distance is scaled relative to R; the velocity, ν_{l}/R; the pressure, $\rho_{\mathrm{l}}\nu_{\mathrm{l}}^2/R^2$; and time, R^2/ν_{l}. Of the parameters of the gas medium, the distance is scaled relative to R_{cs}; the velocity, U_0; the density, ρ_g; and time, R_{cs}/U_0. The dimensionless variables are hereinafter denoted by tildes.

2. NUMERICAL SOLUTION METHOD

System (1)–(18) was solved by the finite-difference method. Equations (1)–(3) of liquid dynamics were solved by the Gauss elimination method; the equations for the behavior of the gas medium were solved by the Thomas algorithm; and the solutions were joined at the interface using the boundary conditions. The solution procedure was inspired by split-step methods [19]: each time step was divided into a liquid characterization substep and a gas characterization substep, each of the substeps comprising several subsubsteps.

Substep 1: Liquid characterization. The equations for the liquid in the droplet are solved. Substep 1 consists of the following subsubsteps:

- the velocity and pressure distributions in the liquid are calculated by solving Eqs. (1), (2), (11), and (12) by the Gauss elimination method. The values of the velocities in the gas for substituting into Eqs. (11) and (12) are taken from the previous time step;

- the temperature distribution in the droplet is calculated by solving Eqs. (8) and (15). The temperature distribution in the gas and the evaporation intensity $\dot{m}$ are taken from the previous time step.

Substep 2: Gas characterization. Substep 2 consists of the following subsubsteps:

- the velocity distribution in the gas is calculated by solving Eqs. (4), (10), and (13); the normal components of the velocity in the gas near the surface of the liquid are given by the Stefan condition, and the tangential components thereof are continuous. The value of the gas density is taken from the previous time step, and the values of the tangential components of the velocities on the surface of the droplet are taken from substep 1 (liquid characterization);
- the density distribution in the gas is calculated by solving Eq. (5). Near the surface of the droplet, the density of the gas mixture is approximated by a polynomial because there are no physical conditions restricting the value of the density or its derivatives;
- the temperature distribution in the gas is calculated by solving Eqs. (6) and (14);
- the vapor mass fraction distribution in the gas is calculated by solving Eq. (7), in which the vapor mass fraction in the mixture over the surface of the droplet is calculated from formula (9);
- the new shape of the free liquid is calculated from formulas (18) and

$$\tilde{r}_i^{\tilde{t}+\Delta\tilde{t}} = r_i^{\tilde{t}} + \tilde{V}_r\big|_{S_{\mathrm{lg}}} \cdot \Delta\tilde{t}, \quad i = 2,\ m,$$

$$\tilde{z}_i^{\tilde{t}+\Delta\tilde{t}} = i\tilde{h} + \tilde{V}_z\big|_{S_{\mathrm{lg}}} \cdot \Delta\tilde{t}, \quad i = 2,\ m+1.$$

The computational grid is reconstructed at each time step according to the changes in the shape of the droplet. The variables for the liquid and the gas were nondimensionalized differently; therefore, there were several gas characterization substeps per liquid characterization substep.

The described code was tested on test problems [16, 20] and showed good agreement with analytical solutions and experimental results.

All the calculations in this work were performed for the evaporation of a droplet of water into air. The physical characteristics of the liquid are the following: the density is $\rho_{\mathrm{l}} = 1000\ \mathrm{kg/m^3}$, the molar mass is $\mathrm{M_l} = 0.018\ \mathrm{kg/mol}$, the thermal conductivity is $\kappa_{\mathrm{l}} = 0.55\ \mathrm{W/(m \cdot K)}$, the viscosity is $\nu_{\mathrm{l}} = 10^{-6}\ \mathrm{m^2/s}$, the specific heat capacity is $c_{\mathrm{l}} = 4200\ \mathrm{J/(kg \cdot K)}$, the volumetric thermal expansion coefficient is $\beta_{\mathrm{l}} = 1.27 \cdot 10^{-3}\ \mathrm{K^{-1}}$, and the heat of evaporation is $\lambda = 2.26 \cdot 10^6\ \mathrm{J/kg}$. The physical characteristics of the gas are the following: the molar mass is $\mathrm{M_g} = 0.029\ \mathrm{kg/mol}$, the specific heat capacity is $c_{\mathrm{g}} = 720\ \mathrm{J/(kg \cdot K)}$, the viscosity and thermal conductivity of the gas medium in Eqs. (4) and (6) were calculated from formulas of the kinetic theory of gases [21], and the diffusion coefficient of water vapor in air was calculated in an approximation of the hard-sphere model [22]. The temperature of the substrate was $T_{\mathrm{s}} = 293\ \mathrm{K}$. The characteristics of the interfaces are the following: $\sigma_{\mathrm{lg}} = 7.3 \cdot 10^{-2}\ \mathrm{N/m}$, $\sigma_{\mathrm{ls}} - \sigma_{\mathrm{gs}} = 0\ \mathrm{N/m}$, and $\left|\frac{d\sigma}{dT}\right| = 1.7 \cdot 10^{-4}\ \mathrm{N/(m \cdot K)}$. The sizes of the droplet and the computational space are $R = 0.5\ \mathrm{mm}$ and $R_{\mathrm{cs}} = H_{\mathrm{cs}} = 5\ \mathrm{cm}$. The evaporation occurs in dry air: $C_0 = 0$.

The following values of the dimensionless numbers determining the motion in the liquid and the gas. The Marangoni number is $\mathrm{Ma} = 130$, which is sufficient to induce thermocapillary instability in the droplet because this value exceeds the critical value $\mathrm{Ma_{cr}} \approx 80$ (for a liquid film). The Reynolds numbers in the gas ($\mathrm{Re_g} = 115$) and in the liquid ($\mathrm{Re_l} = 0.5$) are relatively low; therefore, in both cases, only laminar flows can occur. The critical Grashof number is $\mathrm{Gr_{cr}} \approx 1000$ (for a liquid in a cylindrical vessel heated from below). This means that free gravitational convection in a droplet with $\mathrm{Gr} = 3.2$ is impossible.

The initial state of the system is the following: the media are at rest at temperature $T = T_{\mathrm{s}} = T_0 = 293\ \mathrm{K}$; the pressure in the gas is $p = p_{\mathrm{g}} = 10^4\ \mathrm{Pa}$; evaporation is absent, as if the droplet is covered with a film, and at time $t = 0$, the film is removed. The initial equilibrium shape of the droplet is calculated by minimizing the mechanical energy [16].

The convergence of the written code was checked by comparing the results obtained on various grids at various time steps, and the parameters of the scheme were chosen to obtain a solution that would be independent of computational step sizes.

3. RESULTS AND DISCUSSION

3.1. Flow patterns in the gas and the liquid

Forced convection flows were given as follows. At the upper boundary of the computational space at $z = H_{\mathrm{cs}}$, there is round opening of radius $R_{\mathrm{air}} = 5\ \mathrm{mm}$, through which dry air is blown (Fig. 2). The flow velocity profile is square: $V_z = U_0\left(1 - r^2/R_{\mathrm{air}}^2\right)$, $U_0 = 0.37\ \mathrm{m/s}$. At the lateral boundary at $r = R_{\mathrm{cs}}$, there is a slot, through which air leaves the computational space; the width of the slot is chosen so the amount of air entering the space is equal to the amount of air leaving the space.

Three cases were calculated:

(1) the evaporation occurs into stagnant air;

(2) in the gas medium, there are forced convention flows, which exist from the initial time throughout the computational time range;

(3) in the gas medium, there are forced convection flows that are similar to those in case 2, with the difference that the former are pulsating; i.e., the state of forced convection as in case 2 is periodically replaced by the state in which the velocities at the inlet and outlet openings become zero. The movements in the gas, unsupported by external forces, rapidly die out.

Figure 3 shows the velocity distribution of the gas–vapor mixture over the droplet in case 2. The convective flow moves down along the axis of the system and diverges over the droplet. The velocities over the surface of the droplet are almost perpendicular to the surface. The component of these velocities that is normal to the surface is a Stefan flow. As Fig. 3 shows, the velocities of the convective flow over the droplet are twice and more as high as the velocity of the Stefan flow. Over the top of the droplet, a stagnant zone is formed where two vertical flows meet: the downward convective flow and the upward Stefan flow.

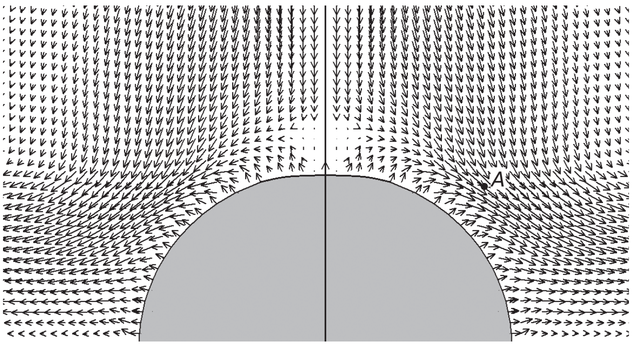

Fig. 3. Velocity distribution in the bulk of the gas near the surface of the droplet under forced convection conditions

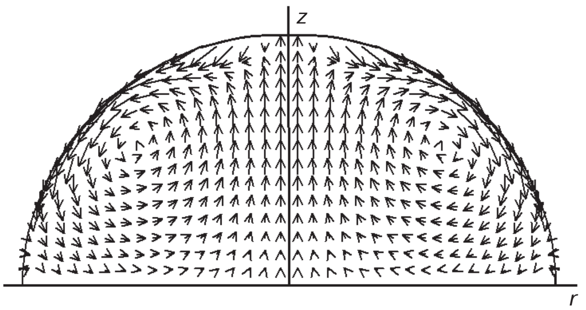

Fig. 4. Velocity distribution in the droplet under forced convection conditions in the gas phase

The convective flows in the gas cause motion inside the liquid. In the droplet, there is a vortex, the flow in which falls down along the surface of the droplet and rises up along the axis (Fig. 4). The velocities in the droplet are much lower than those in the gas. For example, the velocity of the flow in the gas at the point *A* (Fig. 3) is 5 cm/s, whereas the velocity of the flow in the droplet near the surface is about 1 mm/s, i.e., 50 times lower.

Figure 5 presents the time dependence of the deviation of the droplet height from the initial (equilibrium) value in two cases of evaporation: evaporation in the presence of pulsating forced convection flows and evaporation into stagnant air. Figure 5 also illustrates the time dependence of the forced convection velocity U_0; the period of pulsation of the convective flows was 0.5 s. It was determined that the droplet responses to the convection pulses by vibrations at a frequency of ~250 Hz, which is the eigenfrequency of the axisymmetric normal mode of the droplet [16]. Figure 5 shows that the mechanical equilibrium of the droplet is disturbed in both cases, in both the presence and the absence of convective flows. The droplet height in the presence of convective flows is smaller than that in the absence of convection; the difference is ~0.2 µm. This means that the convective flow flattens the droplet. As is seen from Fig. 5, in the stagnation intervals, when there are no convective flows, the droplet height is restored and becomes equal to the height of the droplet evaporating into stagnant air. The free vibrations under convection conditions have lower amplitude than in the absence of it; probably, they are suppressed by the convective flow.

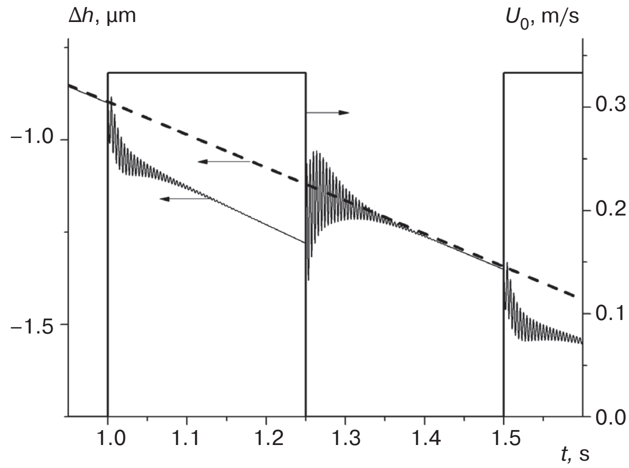

Fig. 5. Time dependence of the deviation of the droplet height at the top from the initial (equilibrium) value in cases 1 (dashed line) and 3 (semibold solid line), and the time dependence of the maximum air velocity in the convective flow (bold solid line)

There is also a feedback effect of the movement on the liquids on the gas. The vibrations of the droplet give rise to a density wave in the gas; i.e., the vibrating droplet emits a sound. The density oscillations are low: their amplitude is about 0.01% of the air density.

3.2. Time dependence of the evaporation rate

Figure 6 shows the time dependence of the evaporation rate *J*, which is the mass of the liquid that leaves the surface of the droplet per unit time. Figure 6 presents three curves, each corresponding to one of the three considered evaporation cases. In the studied evaporation time range, one can see a short (<1 ms) transient process, during which the evaporation rate varies over a wide range. This is related to the nonequlibrium initial state of the system. Then, there is an interval of steady-state evaporation, in which the evaporation rate varies insignificantly—because of the decrease in the surface area of the droplet and in the surface temperature of it under the action of the evaporation. As is seen from Fig. 6, the curves at the stage of steady-state evaporation for different cases coincide with each other so that the difference does not exceed 1%. This confirms the conclusions made by authors of other computational works that the evaporation rate under the considered conditions is independent of the presence of convective flows in the gas phase [2, 10]; however, this contradicts the results of experimental studies of evaporation under forced convection conditions [8, 9, 15].

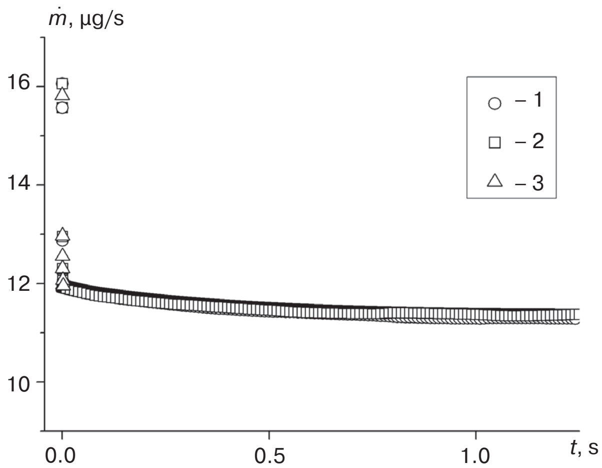

Fig. 6. Time dependence of the evaporation rate from the surface of the droplet in various evaporation cases

It was assumed that this disagreement is due to the fact that, in forced convection experiments, Stefan condition (10) is violated, whereas in numerical calculations, this condition is postulated. It is impossible to directly check whether or not the Stefan condition is valid in the experiment; however, there is indirect evidence that it is invalid. For example, the dependence of the evaporation rate from the surface of a droplet under diffusion control on the contact radius is a linear function [14, 15], and the fact that this condition is invalid suggests that the evaporation is not diffusion-controlled. Thus, the nonequilibrium conditions produced by the action of the convection on the surface of the droplet increase the evaporation rate.

CONCLUSIONS

The evaporation from the surface of a sessile droplet in the presence of forced convection flows in air was numerically studied, and the following results were obtained.

The forced convection in the gas phase affects the shape of the droplet and the flows in it. In the case of pulsating convective flows, the droplet responds to the beginning and end of the convection by vibrations at the eigenfrequency of its normal mode. After the vibrations die out, there is a flow in the droplet, which is caused by the flows in the surrounding air that are tangential to the surface of the droplet.

The curves of the time dependences of the evaporation rates in the cases of the evaporation into stagnant air and in the presence of forced convection flows coincide with each other, which agrees with the results of computational works [2, 10], but contradicts the data of experimental studies [7–9, 15]. It was assumed that this disagreement is due to the appearance of nonequilibrium conditions at the boundary of the condensed phase, under which the evaporation ceases to be diffusion-controlled. Thus, to numerically describe the effect of convection in the gas phase on the evaporation from the surface of a liquid, it is necessary to have a model of the interaction of flows with the matter in the Knudsen layer, at the boundary of which the obtained conditions should be joined with the systems of equations written for bulk regions.

Authors' contribution. All authors equally contributed to the research work.

REFERENCES

1. Borodulin V.Y., Letushko V.N., Nizovtsev M.I., Sterlyagov A.N. Determination of parameters of heat and mass transfer in evaporating drops. *International Journal of Heat and Mass Transfer*. 2017;109:609–618. https://doi.org/10.1016/j.ijheatmasstransfer.2017.02.042
2. Ljung A.-L., Lundström T.S. Evaporation of a sessile water droplet subjected to forced convection in humid environment. *Drying Technology*. 2019;37(1):129–138. https://doi.org/10.1080/07373937.2018.1441866
3. Kontorovich I.I. State of the art and development trends of technical decisions for intensifying evaporation from water surface. *Nauchnyy zhurnal Rossiyskogo NII problem melioratsii = Scientific Journal of Russian Scientific Research Institute of Land Improvement Problems*. 2016;1(21):241–256 (in Russ.).
4. Jeong S.W., Lee D.H. Drying performance of a dishwasher with internal air circulation. *Korean Journal of Chemical Engineering*. 2014;31(9):1518–1521. https://doi.org/10.1007/s11814-014-0194-0
5. Chen Y., Askounis A., Koutsos V., Valluri P., Takata Y., Wilson S.K., Sefiane K. On the effect of substrate viscoelasticity on the evaporation kinetics and deposition patterns of nanosuspension drops. *Langmuir*. 2020;36(1):204–213. https://doi.org/10.1021/acs.langmuir.9b02965
6. Hatte S., Pandey K., Pandey K., Chakraborty S., Basu S. Universal evaporation dynamics of ordered arrays of sessile droplets. *Journal of Fluid Mechanics*. 2019;866:61–81. https://doi.org/10.1017/jfm.2019.105
7. Tang R., Etzion Y. Comparative studies on the water evaporation rate from a wetted surface and that from a free water surface. *Building and Environment*. 2004;39(1):77–86. https://doi.org/10.1016/j.buildenv.2003.07.007
8. Jodat A., Moghiman M. An experimental assessment of the evaporation correlations for natural, forced and combined convection regimes. *Proceedings of the Institution of Mechanical Engineers Part C: Journal of Mechanical Engineering Science*. 2012;226(1):145–153. https://doi.org/10.1177/0954406211413961
9. Al-Shammiri M. Evaporation rate as a function of water salinity. *Desalination*. 2002;150(2):189–203. https://doi.org/10.1016/S0011-9164(02)00943-8
10. Vyatkin G.P., Korenchenko A.E., Izmailov Yu.G. Evaporation of liquids under conditions of free convection. *Doklady Physics*. 1998;43(11):700–702.
11. Dalton J. Experimental essays on the constitution mixed gases: on the force of steam or vapor from water and other liquids in different temperatures, both in a Torricelli vacuum and in air; on evaporation and on the expansion of gases by heat. *Memoirs of the Literary and Philosophical Society of Manchester*. 1802;5:536–602.
12. Boetler L.M.K., Gordon H.S., Griffin J.R. Free evaporation into air of water from a free horizontal quiet surface. *Industrial and Engineering Chemistry*. 1946;38(6):596–600. https://doi.org/10.1021/ie50438a018
13. Pauken M.T., Tang T.D., Jeter S.M., Abdel-Khalik S.I. Novel method for measuring water evaporation into still air. *ASHRAE Transactions*. 1993;99(1):297–300.

СПИСОК ЛИТЕРАТУРЫ

1. Borodulin V.Y., Letushko V.N., Nizovtsev M.I., Sterlyagov A.N. Determination of parameters of heat and mass transfer in evaporating drops. *International Journal of Heat and Mass Transfer*. 2017;109:609–618. https://doi.org/10.1016/j.ijheatmasstransfer.2017.02.042
2. Ljung A.-L., Lundström T.S. Evaporation of a sessile water droplet subjected to forced convection in humid environment. *Drying Technology.* 2019;37(1):129–138. https://doi.org/10.1080/07373937.2018.1441866
3. Конторович И.И. Уровень техники и тенденции развития технических решений для интенсификации испарения с водной поверхности. *Научный журнал Российского НИИ проблем мелиорации*. 2016;1(21):241–256.
4. Jeong S.W., Lee D.H. Drying performance of a dishwasher with internal air circulation. *Korean Journal of Chemical Engineering*. 2014;31(9):1518–1521. https://doi.org/10.1007/s11814-014-0194-0
5. Chen Y., Askounis A., Koutsos V., Valluri P., Takata Y., Wilson S.K., Sefiane K. On the effect of substrate viscoelasticity on the evaporation kinetics and deposition patterns of nanosuspension drops. *Langmuir*. 2020;36(1):204–213. https://doi.org/10.1021/acs.langmuir.9b02965
6. Hatte S., Pandey K., Pandey K., Chakraborty S., Basu S. Universal evaporation dynamics of ordered arrays of sessile droplets. *Journal of Fluid Mechanics*. 2019;866:61–81. https://doi.org/10.1017/jfm.2019.105
7. Tang R., Etzion Y. Comparative studies on the water evaporation rate from a wetted surface and that from a free water surface. *Building and Environment*. 2004;39(1):77–86. https://doi.org/10.1016/j.buildenv.2003.07.007
8. Jodat A., Moghiman M. An experimental assessment of the evaporation correlations for natural, forced and combined convection regimes. *Proceedings of the Institution of Mechanical Engineers Part C: Journal of Mechanical Engineering Science.* 2012;226(1):145–153. https://doi.org/10.1177/0954406211413961
9. Al-Shammiri M. Evaporation rate as a function of water salinity. *Desalination*. 2002;150(2):189–203. https://doi.org/10.1016/S0011-9164(02)00943-8
10. Vyatkin G.P., Korenchenko A.E., Izmailov Yu.G. Evaporation of liquids under conditions of free convection. *Doklady Physics*. 1998;43(11):700–702.
11. Dalton J. Experimental essays on the constitution mixed gases: on the force of steam or vapor from water and other liquids in different temperatures, both in a Torricelli vacuum and in air; on evaporation and on the expansion of gases by heat. *Memoirs of the Literary and Philosophical Society of Manchester*. 1802;5:536–602.
12. Boetler L.M.K., Gordon H.S., Griffin J.R. Free evaporation into air of water from a free horizontal quiet surface. *Industrial and Engineering Chemistry*. 1946;38(6):596–600. https://doi.org/10.1021/ie50438a018
13. Pauken M.T., Tang T.D., Jeter S.M., Abdel-Khalik S.I. Novel method for measuring water evaporation into still air. *ASHRAE Transactions.* 1993;99(1):297–300.
14. Guéna G., Poulard C., Voué M., De Coninck J., Cazabat A.M. Evaporation of sessile liquid droplets. *Colloids and Surfaces A: Physicochemical and Engineering Aspects*. 2006;291(1–3):191–196. https://doi.org/10.1016/j.colsurfa.2006.07.021

14. Guéna G., Poulard C., Voué M., De Coninck J., Cazabat A.M. Evaporation of sessile liquid droplets. *Colloids and Surfaces A: Physicochemical and Engineering Aspects*. 2006;291(1–3):191–196. https://doi.org/10.1016/j.colsurfa.2006.07.021
15. Kelly-Zion P.L., Pursell C.J., Vaidya S., Batra J. Evaporation of sessile drops under combined diffusion and natural convection. *Colloids and Surfaces A: Physicochemical and Engineering Aspects*. 2011;381(1–3):31–36. https://doi.org/10.1016/j.colsurfa.2011.03.020
16. Korenchenko A.E., Beskachko V.P. Oscillations of a sessile droplet in open air. *Physics of Fluids.* 2013;25(11):2106. https://doi.org/10.1063/1.4829025
17. Labuntsov D.A., Yagov V.V. *Mekhanika dvukhfaznykh sistem* (*The Mechanics of Two-Phase Systems).* Moscow: MEI; 2000. 374 p. (in Russ.). ISBN 978-5-383-00036-6
18. *Guide to Meteorological Instruments and Methods of Observation*. Geneva: World Meteorological Organization (WMO); 2008. 681 p. Available from URL: https://www.weather.gov/media/epz/mesonet/CWOP-WMO8.pdf
19. Belotserkovskii O.M. *Chislennoe modelirovanie v mekhanike sploshnykh sred* (*Numerical modeling in mechanics of continuous medium)*. Moscow: Fizmatlit; 1994. 448 p. (in Russ.). ISBN 5-02-014986-1
20. Korenchenko A.E., Malkova J.P. Numerical investigation of phase relationships in an oscillating sessile drop. *Physics of Fluids*. 2015;27(10):2104–2111. https://doi.org/10.1063/1.4932650
21. Matveev A.N. *Molekulyarnaya fizika* (*Molecular Physics)*. Moscow: Mir; 1985. 446 p. (in Russ.).
22. Bird R., Stewart W., Lightfoot E. *Transport Phenomena*. John Wiley & Sons, Inc.; 2002. 687 p.

15. Kelly-Zion P.L., Pursell C.J., Vaidya S., Batra J. Evaporation of sessile drops under combined diffusion and natural convection. *Colloids and Surfaces A: Physicochemical and Engineering Aspects*. 2011;381(1–3):31–36. https://doi.org/10.1016/j.colsurfa.2011.03.020
16. Korenchenko A.E., Beskachko V.P. Oscillations of a sessile droplet in open air. *Physics of Fluids.* 2013;25(11):2106. https://doi.org/10.1063/1.4829025
17. Лабунцов Д.А., Ягов В.В. *Механика двухфазных систем.* М.: МЭИ; 2000. 374 с. ISBN 978-5-383-00036-6
18. *Guide to Meteorological Instruments and Methods of Observation*. Geneva: World Meteorological Organization (WMO); 2008. 681 p. URL: https://www.weather.gov/media/epz/mesonet/CWOP-WMO8.pdf
19. Белоцерковский О.М. *Численное моделирование в механике сплошных сред*. М.: Физматлит; 1994. 448 с. ISBN 5-02-014986-1
20. Korenchenko A.E., Malkova J.P. Numerical investigation of phase relationships in an oscillating sessile drop. *Physics of Fluids*. 2015;27(10):2104–2111. https://doi.org/10.1063/1.4932650
21. Матвеев А.Н. *Молекулярная физика*. М.: Мир; 1985. 448 с.
22. Bird R., Stewart W., Lightfoot E. *Transport Phenomena*. John Wiley & Sons, Inc.; 2002. 687 p.

About the authors

Anna E. Korenchenko, Dr. Sci. (Phys.-Math.), Professor, Department of High Mathematics, Institute of Integrated Safety and Special Instrument Engineering, MIREA – Russian Technological University (78, Vernadskogo pr., Moscow, 119454 Russia). E-mail: korenchenko@mirea.ru. Scopus Author ID 10043443100, https://orcid.org/0000-0002-3413-8855

Anna A. Zhukova, Cand. Sci. (Chem.), Associate Professor, Sechenov First Moscow State Medical University (21, 5 Parkovaya ul., Moscow, 105043 Russia). E-mail: anyazhu@gmail.com. Scopus Author ID 12757009400, https://orcid.org/0000-0003-4511-1882

Об авторах

Коренченко Анна Евгеньевна, д.ф.-м.н., профессор, кафедра высшей математики Института комплексной безопасности и специального приборостроения ФГБОУ ВО «МИРЭА – Российский технологический университет» (119454, Россия, Москва, пр-т Вернадского, д. 78). E-mail: korenchenko@mirea.ru. Scopus Author ID 10043443100, https://orcid.org/0000-0002-3413-8855

Жукова Анна Александровна, к.х.н., доцент, кафедра аналитической, физической и коллоидной химии, Первый Московский государственный медицинский университет им. И.М. Сеченова (105043, Россия, Москва, 5-ая Парковая ул., 21). E-mail: anyazhu@gmail.com. Scopus Author ID 12757009400, https://orcid.org/0000-0003-4511-1882

Translated by V. Glyanchenko

Russian Technological Journal. 2021;9(5):67–83 ISSN 2500-316X (Online)

Mathematical modeling

Математическое моделирование

UDC 519.833, 51-77
https://doi.org/10.32362/2500-316X-2021-9-5-67-83

RESEARCH ARTICLE

Mathematical modeling of some social processes using game-theoretic approaches and making managerial decisions based on them

Kirill E. Krasnikov @

MIREA – Russian Technological University, Moscow, 119454 Russia
@ Corresponding author, e-mail: krasnikovkirill@yandex.ru

Abstract. In this article, using game-theoretic approaches, the human community is modeled as a dynamic system, and the influence of such ethical norms of behavior as egoism and altruism, morality (on the example of the Kant imperative or the Golden Rule of Morality) on the state of this system is investigated, as well as the question of determining the effectiveness of the community depending on the prevailing worldview of its representatives. Using the example of a game model of social choice between two norms of behavior: one generally accepted, but outdated, and the other newone, not yet widespread, but more advanced and progressive, it is shown that communities, among whose representatives a predominantly egoistic worldview prevails, are less likely to innovate and abandon outdated norms of behavior. Conversely, those communities whose representatives share basic ethical principles are more confident and quickly moving to advanced and progressive norms. In conclusion, the paper examines the question of what advantages a community acquires in which purposeful educational and educational activities are conducted, designed to increase the level of morality and morality among its representatives. The results obtained can be used, firstly, as an integral part of the course on the mathematical base of ethics, which could perform the functions of educational work in higher and secondary educational institutions, and, secondly, for the purposes of evaluating the effectiveness of educational work and state planning in this area.

Keywords: game theory, conflict equilibria, behavioral economics

• **Submitted:** 28.12.2020 • **Revised:** 26.05.2021 • **Accepted:** 12.07.2021

For citation: Krasnikov K.E. Mathematical modeling of some social processes using game-theoretic approaches and making managerial decisions based on them. *Russ. Technol. J.* 2021;9(5):67–83. https://doi.org/10.32362/2500-316X-2021-9-5-67-83

Financial disclosure: The author has no a financial or property interest in any material or method mentioned.

The author declares no conflicts of interest.

НАУЧНАЯ СТАТЬЯ

Математическое моделирование некоторых социальных процессов с помощью теоретико-игровых подходов и принятие на их основе управленческих решений

К.Е. Красников @

МИРЭА – Российский технологический университет, Москва, 119454 Россия
@ *Автор для переписки, e-mail: krasnikovkirill@yandex.ru*

Резюме. В статье с помощью теоретико-игровых подходов моделируется человеческое сообщество как динамическая система и исследуется, какое влияние оказывают на состояние этой системы такие этические нормы поведения, как эгоизм и альтруизм, мораль (на примере императива Канта или Золотого правила нравственности), а также изучается вопрос определения эффективности сообщества в зависимости от превалирующего среди его представителей мировоззрения. На примере игровой модели социального выбора между двумя нормами поведения: одной общепринятой, но устаревшей, и другой новой, еще не распространенной, но более передовой и прогрессивной, показывается, что сообщества, среди представителей которых преобладает преимущественно эгоистическое мировозрение, менее склонны к инновациям и отказу от устаревших норм поведения. И наоборот: те сообщества, представители которых разделяют базовые этические принципы, увереннее и быстрее переходят к более передовым и благоприятным для сообщества в целом поведенческим нормам. В заключении работы с помощью модели пороговых значений, определяющих коллективный выбор, исследуется вопрос, какие преимущества приобретает сообщество, в котором ведется целенаправленная воспитательная, просветительская деятельность, призванная повысить уровень морали и нравственности среди его представителей. Полученные результаты могут быть использованы, во-первых, в качестве составной части курса по математическим основам этики, который мог бы исполнять функции воспитательной работы в высших и средних учебных заведениях, а, во-вторых, для целей оценки эффективности проводимой воспитательной работы и государственного планирования в сферах воспитания и образования.

Ключевые слова: теория игр, конфликтные равновесия, моделирование социально-этических норм поведения

• **Поступила:** 28.12.2020 • **Доработана:** 26.05.2021 • **Принята к опубликованию:** 12.07.2021

Для цитирования: Красников К.Е. Математическое моделирование некоторых социальных процессов с помощью теоретико-игровых подходов и принятие на их основе управленческих решений. *Russ. Technol. J.* 2021;9(5):67–83. https://doi.org/10.32362/2500-316X-2021-9-5-67-83

Прозрачность финансовой деятельности: Автор не имеет финансовой заинтересованности в представленных материалах или методах.

Автор заявляет об отсутствии конфликта интересов.

INTRODUCTION

What is the world's driver? "*The world is set in motion by ideas, and the ideas are realized in the world through people*." Since the human community is an example of a dynamic system, its state is determined in each moment in time by some internal and external parameters. For example, while the state of vapour inside a steam engine is determined by pressure and temperature, the state of a human community is determined by dominating in the given community cultural and worldview principles.

These worldview principles are embedded in every member of a community mainly by education and upbringing. Therefore, to establish the state policy in the area of education and culture it is important to investigate and analyze the influence of moral and ethical values on the development of the community.

On September 1, 2020, the State Duma of the Russian Federation adopted amendments of law "On Education in Russian Federation" recommended by the President of the Russian Federation. As a result, the law has determined the concept of youth development as the activity targeted "to the development of an individual, creation of conditions for self-determination and socialization on the basis of sociocultural, moralethical values, and also "*the formation of patriotic feelings and education for citizenship, respectfulness to the memory of Motherland's defenders… to the law and order, to working and older people, mutual respectfulness, careful relation to cultural heritage and traditions of multinational people of Russian Federation, and to the nature*…" [1].

The law also requires middle, middle professional institutions and higher schools to make corresponding changes in their programs on youth development and related educational work during the period of one year (before September 2021).

The following questions arise, however:

- What specifically are these values that should be cultivated in the young generation?
- In what way will these values affect the development of the community as a whole at the time when students—having reached the age of maturity—become fully responsible members of the community?
- And most importantly, how we should evaluate the efficacy youth development that is conducted?

Philosophy and psychology are not the only two domains that can help to get answers to these and other arising questions. It may be surprising, but mathematics, particularly one of its applied branches—the game theory—can do the same.

In this paper, using approaches of the game theory we model the influence of such behavioural norms as egoism and altruism, morality (we understand the latter in terms of Kant Imperative and closely related to it the Golden Rule of Morality) on the process of making decisions by individuals in some human community. We develop a game model of choice between two norms of behaviour: the first of which is generally accepted but less effective, and the second one—new, poorly known but more favourable for the community as a whole once it spreads throughout the community. This model rather indicatively illustrates how dominating among members of a community moral and ethical norms can lead the community either to progress and wellbeing, or, in contrast, to disintegration and degradation.

In Conclusions, an attempt is made to model how youth development and educational work affects the process of making decisions by members of the community that results in a growth (according to a certain law) of the moral level of the community.

Let us briefly overview the results obtained in this area of research by Russian and foreign thinkers.

OVERVIEW OF MODELS OF SOCIOETHICAL BEHAVIOUR BASED ON THEORETICAL APPROACHES OF THE GAME THEORY

Since the time of Adam Smith [2], the founder of economics theory, it has been generally accepted that first and foremost it is an individualistic motif of personal well-being maximisation that is a driving force. Even the term *homo economicus* had appeared—the rational human.

However, even Adam Smith himself had doubted this. For example, in his work "The theory of moral senses" [3] he introduces the notion "sympathy"—the sense which is the attribute of people forcing them to behave sometimes exclusively against their interests.

In the 20th century there appeared a new area of research (*behavioral economics*) that studies the impact of psychological, moral and ethical, cognitive and cultural factors on making a decision. This analysis is highly demanded because it more realistically—than the generally accepted classical yet rather inaccurate *homo economicus* model—takes into account all aspects which affect making a decision by a human.

Because one of the branches of mathematics used for analysis of processes in economics is the game theory, a lot was devoted to model the processes and phenomena, which until recently have been the subject of sociology, philosophy, and psychology.

One of the first attempts to model moral-ethical behavioral norms employing a game theory approach was undertaken by prof. Braithwaite in his lecture in Cambridge in 1955 [4]; ever since similar studies have been conducted on regular basis by different authors.

For example, in his work "Models of Game Theory and Making Decisions in Ethics" [5] Nobel Prize winner J. Harsanyi argues that ethical (moral) behavior is based on the notion of collective rationale that goes beyond the frameworks of a traditional for the game theory concept of maximization of individual or cooperative income: "*The theory of rational behavior in social medium can be divided into game theory and ethics. Game theory applies to two or more individuals, who often have different interests, and who attempt to maximize their (selfish or selfless) interests in a rational way against all other individuals, who also attempt to maximize their (selfish or selfless) interests*" [5].

Harsanyi, in his work "Utilitarianism of rules and the theory of making decisions" [6], applies a fundamental concept of utilitarianism for the creation of a more realistic model of making decisions by individuals in a community. Utilitarianism is the branch of ethics, according to which moral and ethical values of any act are determined by combined utility brought by this act to all individuals for who this act has the influence [7]. In this respect, Harsanyi introduces a function of a social utility, which value for each participant in every point (of each behavioral strategy) is determined by the average value of all participants: $W_i(s) = \frac{1}{N}\sum_{i=1}^{N} U_i(s)$ [5]. The theory of utility is discussed in more detail in [8].

This approach was significantly developed by many experts on behavioral economics and game theory [9–11].

We have to draw attention to the so-called evolutionary game theory, which is the game theory application for the investigation of the development of populations in biology as well as sociology. The feature of this theory is that it analyses, as a rule, repeatable games; therefore, each strategy is evaluated on the basis of whether it is evolutionary stable that is capable of being verified by the time. For example, if applied to biology, different strategies represent genetic traits—inherited by descendants—which determine the behavior of species. Based on evolutionary game theory it was possible to justify—often observable in nature, particularly for social species,—"gentlemen's" and even altruistic behavior that is a behavior for the benefit of species. This in no way agrees with Darwinian assumption that natural selection happens at individual level [12, 13].

With regard to researches conducted by Russian scientists, we refer to work Yu.B. Germeier and I.A. Vatel' "Games with hierarchical vector of interests" [14]. In this work the authors to analyze a problem of distribution of resources between individual and societal needs introduce a notion of "egoism" in relation to the needs of the given community for the case when a participant prefers to spend all means at his possession exclusively for personal objectives ignoring societal interests.

Some ideas proposed by Germeier and Vatel' laid the foundation for a model of compliance of communal and private interests (CCPI-model) [15, 16]. In this model a two-level community is discussed, and similar to [14] the problem of resource distribution between private and community needs is investigated. In [16] participants are divided into two classes depending on whether they prefer to spend resources for personal or communal objectives; these are *individualists* and *collectivists*.

In 2017 in game theory-oriented journal "Games" (Basel, Switzerland) a special edition was issued under the title "Ethics, morality and game theory" [10]. In this edition, a collection of articles of different authors were presented; these articles covered the problem of modeling moral-ethical norms of behavior and their impact on decision making by participants of the game problem.

In "Behavioral strategy of moralists and altruists" [11] in addition to already mentioned types of behavior, based on individualism and collectivism, a third class of participants is introduced. These participants when choosing their own strategy follow Kant Imperative, according to which "*a human has to strive so that his or her goal is to become a part of general law*" [7] or a Golden rule of morale: "*treat people the way you would like they treat you*" [17]. The essence of such behavior if applied to a game theory model means that before choosing a strategy, every participant assumes that with a certain probability all of the participants would choose the same strategy. Therefore, it is the assumption that must be taken into account when making a decision and acting.

Analogously to *homo economicus—rational human* (to name the first class of *participants–individualists*, who are guided exclusively by achieving the maximum of their personal income), the participants of the third class are named in [11] *homo-moralis—moral human*.

This type of behavior can relatively successfully be used to model a dynamic model of social choice between two norms of behavior: the first one which is traditional but less favorable and effective and the second one which is not applied yet by most participants. However, employing the new norm by the vast majority of members of the community under consideration would enable the community as a whole to attain much better results. It is shown that specifically the participants of *homo-moralis* class are able to a certain degree to serve as an example of how to employ the new behavioral norm even though being initially a minority and losers, and thereby leading the community to a fundamentally new qualitative level.

According to [11], since the transit to the new norm may not occur under natural conditions, an educational model is also considered. This model supposes that the level of morale and "consciousness" in the community as a result of some educational activities is enhanced in accordance with a certain law. As a result, a greater number of individuals accept new behavioral norms; the latter is becoming generally accepted by the community and is leading to undoubted progress.

THE MODEL

In this paper, a gaming model with N participants is considered. It is supposed that all participants choose their own strategies from the same set of permissible strategies.

Assumption 1. Let Q be a metric space, G—a compact set:

$$G \overset{\Delta}{=} Q^N = \underbrace{Q \times \ldots \times Q}_{N}.$$

Let continuous functions (a functional) $J_i(q), i = \overline{1, N}, q = (q_1, \ldots, q_N) \in G$ are determined in set G, where q_i is the strategy of the ith player, $q_i \in Q, q^i \overset{\Delta}{=} (q_1, \ldots, q_{i-1}, q_{i+1}, \ldots, q_N)$ are the strategies of the rest $N-1$ players with a fixed strategy, q_i of the ith player, $q^i \in Q^{N-1}$. $J_i(q)$ is the *payoff function* (*functional*) of player i, which determines the size of some benefit or resource gained by the ith participant when choosing strategy q_i while the rest participants choose strategy q^i. Under these conditions $J_i(q), i = \overline{1, N}$ are supposed to be transferable, which means that they can be split and distributed in any way between the players.

Let $J(q) \overset{\Delta}{=} \sum_{k=1}^{N} J_k(q)$ is the total payoff function of all players, $J^i(q) \overset{\Delta}{=} \sum_{k \neq i} J_k(q)$ is the total payoff function of all players but the ith player.

Definition 1. *We will call a game problem for which Assumption 1 is valid a classic game (or Game)* G^{he} *if each of the players when choosing strategy* $q_i \in Q$, *aims to get maximal payoff function* $J_i(q_i, q^i)$.

This a classic problem statement in game theory that models the behavior based on getting exclusively personal benefits. In order to stress that every player maximizes only own payoff function and distinguish it from the model as determined below, we will also call it the model of *participants–individualists* or the *homo economicus* model as it is called in [11].

Alternatively, a class of game problem is considered in which every player supposedly takes into account (with some weighting coefficient) interests of other participants. This statement is modeled by a transition from initially stated problem with a set of payoff functions $\{J_i, i = \overline{1, N}\} = \{J_i\}$, to an auxiliary problem determined by a parametric family of *utility functions* $\{U_i(J_k, \alpha)\} = \{U_i\}$.

Definition 2. *We will call a game problem, satisfying Assumption 1, game* G^{α} *if every player aims to realize maximum of his utility function* U_i, *which is expressed through a payoff function of the given player* $J_i(q)$ *and a total payoff function of the rest players* $J^i(q)$, *as follows:*

$$U_i(q) = (1-\alpha) J_i(q) + \frac{\alpha}{N-1} J^i(q),$$
$$q \in G, \alpha \in \mathbb{R}, \alpha \in \left[0, \frac{N-1}{N}\right], i = \overline{1, N}. \quad (1)$$

Let us use substitution $\beta \overset{\Delta}{=} \alpha \frac{N}{N-1}$. As $\alpha \in \left[0, \frac{N-1}{N}\right]$, $\beta \in [0,1]$, and utility function $U_i(q)$ can be written in the following form:

$$U_i(q) = (1-\beta) J_i(q) + \frac{\beta}{N} J(q), \beta \in [0,1]. \quad (2)$$

The model, written in this form, determined by utility functions (2), can be considered as a public goods game, in which functions $\beta J_i(q)$ determine a contribution of the ith participant to some community needs. Term $(1-\beta) J_i(q)$ determines a part of resources, which a participant holds for his own needs, while sum $\frac{\beta}{N} J(q)$ determines what he gets from the community.

Unlike the first model (of *participants–individualists*) the model given by Definition 2, supposes that there is no direct antagonism between participants, and even the interest of other participants is taken to some degree into account that follows from the form of function (1). Therefore, this model can be called a model of *participants–collectivists.* Note that in a number of publications (for example, in [2, 4, 6]) similar models yet with somewhat different forms of utility functions U_i called the models of *participants–altruists.*

A number of works accomplished by the author are devoted to this model. For example, in [18] it is shown that in the class of *participants–collectivists* G^{α} under a certain degree of cooperation between participants that is modeled by parameter α, total payoff function J becomes the strongest game equilibrium.

When considering the third model, which is predominantly discussed in this paper, note that there is something common in behavioral and decision making patterns, given by Definitions 1 and 2. Both *individualists* and *collectivists* (or *altruists* as they are called in a number of papers) do not care to some degree of means: if the former pursue exclusively a personal interest, the latter with some weighting coefficient care about community's good. Because according to Assumption 1 all participants can use the same set of possible strategies (actions) Q, the players from both classes when choosing a strategy do not take into account what may happen if the rest participants choose the same strategy. However, the participants of the third class—*homo moralis*—as called in [11, 19], do analyze what may happen.

In the basis of the behavioral pattern that corresponds to this class lies a well-known ethical principle—Kant's categorical imperative: "Act so that maxima of your will could be a universal law [20]." A close in its sense principle is known in ethics under the name "Golden rule of morality:" "Treat others as you want to be treated by others" [21].

In [11, 19] this principle is suggested to be modeled in the following way. Let the ith participant supposes that every other player with probability $k_i \in [0,1]$ will choose the same strategy as he does, and with probability $(1 - k_i)$, it is a different strategy. Thus, every player, when choosing strategy $q_i \in Q$, gets known from the probability theory Bernoulli scheme of $N - 1$ trials (corresponding to the rest players). The scheme has two outcomes for the jth trial, $j = \overline{1, N-1}$: jth participant has chosen strategy $q_j = q_i$ or strategy $(q_j \neq q_i)$. Under these assumptions, instead of initial payoff functions, the game is conducted on utility functions, which for every participant represents a mathematical expectation described by binomial distribution.

Definition 3. *We will to call a game problem, which meets Assumption 1, game* G^{hm} *(the game in homo moralis class), every player instead of his initial payoff function* J_i *pursues maximum of utility function* W_i, *defined as mathematical expectation of random value* $J_i(q_i, \tilde{q}^i)$:

$$W_i(q_i, q^i) = \mathbb{E}_{k_i}[J_i(q_i, \tilde{q}^i)],$$
$$q_i \in Q, k_i \in \mathbb{R}, k_i \in [0,1], i = \overline{1, N}, \qquad (3)$$

where $\tilde{q}^i$ is a random $(N - 1)$-dimensional vector with values taken from Q^{N-1}, having the following distribution: exactly $m \in \{0, \ldots, N-1\}$ number of its component with probability $k_i^m (1-k_i)^{N-m-1}$ gets value equal to q_i, the rest components keeping their initial values.

Note that for each m there are $\binom{N-1}{m} \stackrel{\Delta}{=} C_{N-1}^m$ ways to choose m out of $(N - 1)$ components of q^i.

We also note that for $k_i = 0$ only one random vector gets a value with a non-zero (equal to unity—that is total) probability. It means that a random vector gets the only value, namely the one which corresponds to the argument of function W_i. In this case $W_i(q_i, q^i) \equiv J_i(q_i, q^i)$, that is the players from class *homo moralis* with coefficients $k_i = 0$ are actually the *participants–individualists* of the first class G^{he}. It will be demonstrated more clearly in the model of social choice to be considered below.

For example, for a game with three participants the utility function (3) has the form:

$$W_i(q_i, q_j, q_k) = (1-k_i)^2 J_i(q_i, q_j, q_k) + k_i(1-k_i) \times$$
$$\times J_i(q_i, q_i, q_k) + k_i(1-k_i) J_i(q_i, q_j, q_i) + k_i^2 J_i(q_i, q_i, q_i).$$

SOCIAL MODEL OF CHOICE BETWEEN TWO BEHAVIORAL NORMS

Let us illustrate the difference introduced in the previous section between three behavioral patterns using an example of a coordination game. A coordination game implies a class of game problems with pure strategies, in which participants obtain substantially higher gain if they choose equal or corresponding to each other strategy than if they choose different strategies. This class of game problems models life situations for which some new, progressive behavioral norms if employed by few do not have significant influence on community life. Let us assume that separate garbage collection by a small group of enthusiasts does not have a noticeable ecological effect on the environment in the region. However, when such a behavioral strategy becomes a norm and employed by a majority of community members, this kind of garbage utilization can substantially reduce pollution of the environment. If we consider this situation as a game model, then the two strategies emerge before every community member: to act in the old way or to use new behavioral models.

As an example of a coordination game with two participants, let us consider the following problem taken from the paper of Edna Ullmann-Margalit "The Emergence of Norms" [22]. Let two gunners in the course of a battle have to choose whether to run away from the enemy or stay and continue to fight. Their gun is in a strategically important mountain pass. If they both stay, the enemy may take the pass, overtake them and take them. If one of the gunners stays but the second one runs away, the brave gunner will be killed and his partner, the aimer, will have enough time to escape for his good. Supposing that the both will attempt to survive, both soldiers have reasons to run away. So each of them has a choice: to run or stay and fight.

Table 1. Payoff matrix of the problem

	Fight	Run
Fight	(2, 2)	(0, 3)
Run	(3, 0)	(1, 1)

Note that coordination games have a lot of applications in economics, described in [5].

Let us now consider a coordination game, representing a model of social choice in the problem of many participants, described in [2]. Let N participants of some community make independently from each other a choice between two behavioral norms (strategies) *A* and *B*; norm *A* being more effective than norm *B* in the sense that if all individuals make a transit to norm *A*, the well-being (in a broad sense) of each participant will be higher than in the case when all participants choose norm *B*. However, norm *B* is commonly adopted, which is why at the beginning of the social model all participants choose norm *B*, while *A* is a new norm for them.

For example, we often see that young people—when in the process of socialization find them in new social groups (classmates, friends, etc.)—takes over from some members of these groups habits which are not always useful. But sometimes we have opposite examples. Suppose a group of acquainted individuals dependent on a harmful habit. If somebody from this group has managed to get rid of this habit, he or she initially experiences discomfort since he or she becomes kind of "a white crow." However, gradually other members of the group begin to follow the example of that individual, and starting from some critical fraction of those who got rid off, others who are still subjected to the harmful habit feel "disapproval." Gradually, the community as a whole begins to change relation to this harmful habit: banning advertisements in mass media is introduced; selling to youngsters is also being banned, etc. This change of attitude in a community and increase in restrictions makes the lives of followers of harmful habits more and more difficult as long as a healthy way of life becomes a norm. This, in its turn, results in the decrease in occurrence of various illnesses, births of healthier children, and strengthening the gene pool. In other words, the transition to a new norm of behavior has a rather positive effect on the development of the community as a whole. A lot of other similar examples can be given to support the above said

Let us clarify under what conditions a community is able to have a transit from less effective old norm *B* to more effective new norm *A*. In order to make this transition we will formulate the described model in terms of a game problem. First, let us consider a steady-state case, and then study dynamic behavior of the model.

Let $q_i \in Q = \{0,1\}$ is the choice of the *i*th participant, where q_i means that norm *A* is chosen, and if $q_i = 0$, then norm *B* is chosen. If the *i*th participant chooses norm *A* and other n_A participants also choose this norm, then the payoff function of the *i*th participant takes the value of $a \cdot n_A$. On the other hand, if a participant chooses *B* and n_B other participants acts the same way, then the value of his utility function equals $b \cdot n_B$. We will suppose that $0 < b < a$.

In the model of *participants-individualist*s G^{he}, the payoff functions have the following form:

$$J_i(q_i, q^i) = aq_i \sum_{\substack{j=1,\\ j\neq i}}^{N} q_j + $$
$$+ b(1-q_i) \sum_{\substack{j=1,\\ j\neq i}}^{N} (1-q_j), q_i \in Q, q^i \in Q^{N-1}. \quad (4)$$

For the model of *participants–collectivists* G^{α} , the payoff function takes the form:

$$U_i(q_i, q^i) = (1-\alpha) J_i(q_i, q^i) +$$
$$+ \frac{\alpha}{N-1} \sum_{\substack{k=1,\\ k\neq i}}^{N} J_k(q_k, q^k), q_i \in Q, q^i \in Q^{N-1}, \quad (5)$$

where J_1 and J_2 are determined by formula (4), $\alpha \in \left[0, \frac{N-1}{N}\right]$ is the parameter that determines to what degree each individual prefers community interests. For $\alpha = 0$ functions (4) and (5) are equivalent to each other: $J_i \equiv U_i$. It is not difficult to realize that both for the players of the first and the second classes independently of the value of coefficient α the problem has (according to Nash) two situations with equal weights—either all participants choose norm *A*: $q = (1,\ldots,1)$, or *B*: $q = (0,\ldots,0)$.

Thus, if norm *B* is considered as generally accepted and each player supposes that the rest will do choose this norm, while the number of players is high enough and a direct cooperation between them is impossible, then in the case of participants pursuing exclusively personal interests, norm *B* remains to be an equilibrium since by acting alone in choosing *A* the player would get nothing.

Similar situation is in players' class G^{α} that takes into account interests of other participants. Even at low values of coefficient α, when $U_i(q) = \frac{1}{N} J(q) = \frac{1}{N} \sum_{k=1}^{N} J_k$, that means that the utility function—which is maximized by every player—is directly proportional to a total payoff function, neither of players wish to step away from less effective norm *B* since the community as a whole will get less if a participant makes transition to norm *A*.

However, the situation changes radically for the players of the third class (*homo moralis*). Utility functions, the maximums of which the players of this class wish to attain, according to Definition 3 have the form of mathematical expectation: $W_i(q) = \mathbb{E}_{k_i}[J_i(q_i, \tilde{q}^i)]$, where $\tilde{q}^i$ is a random vector with such distribution that with probability $\tilde{q}^i$ $k_i^m(1-k_i)^{N-m-1}$ exactly its $m \in \{0,\ldots,N-1\}$ components takes the value equal to q_i, other components retaining their initial values. This distribution looks like the well known from the probability theory binomial distribution, $B_{k_i}^{N-1}$, however the condition applied to the latter is different: namely, $(N-m-1)$ of its component must have their initial values (that is values in point $q \in G$, in which the values of function $W_i(q)$ are determined) unchanged.

Thus, the values of $W_i(q_i, q^i)$ are determined by the expression:

$$W_i(q_i,q^i) = \sum_{m=0}^{N-1}\binom{N-1}{m}k_i^m(1-k_i)^{N-m-1} \times \underbrace{\times [aq_i \cdot (mq_i + \frac{N-1-m}{N-1}\cdot \sum_{\substack{j=1,\\ j\neq i}}^{N} q_j)+}_{I} \underbrace{+ b(1-q_i)(m(1-q_j) + \frac{N-1-m}{N-1}\cdot \sum_{\substack{j=1,\\ j\neq i}}^{N}(1-q_j))],}_{II} \quad (6)$$

where term I corresponds to the case when $q_i = 1$, and term II—when $q_i = 0$. The term with coefficient $\frac{N-1-m}{N-1}$ reflects the situation that the rest players except for those m players, whose strategies are considered equal to q, keep their strategies unchanged.

Once again formula (6) clearly shows a feature that we already mentioned: for $k_i = 0$, $W_i(q_i,q^i) \equiv J_I(q_i,q^i)$, i.e., participants belonging to *homo moralis* with nonzero level of coefficient k_i become *players–individualists*.

If all players choose the strategy A, then the ith participant also gets $(N-1)a$ by choosing A, but if he decides to choose B, his utility function equals to:

$$W_i(0,q^i = (1,\ldots,1)) = b\sum_{m=0}^{N-1}\binom{N-1}{m}k_i^m(1-k_i)^{N-m-1}m. \quad (7)$$

Let us simplify expression (7). Because for $m = 0$ the corresponding term of the series also equals 0, the summation can be performed starting with $m = 1$. As

$$\binom{N-1}{m}m = \frac{(N-1)!}{m!(N-1-m)!}m = \frac{(N-1)(N-2)!}{(m-1)!(N-2-(m-1))!} = (N-1)\binom{N-2}{m-1},$$

expression (7) can be rewritten in the following form:

$$W_i(0,q^i = (1,\ldots,1)) = b(N-1)\sum_{m=1}^{N-1}\binom{N-2}{m-1}k_i k_i^{m-1}(1-k_i)^{N-2-(m-1)} = \{\text{Substitution: } m-1 \overset{\Delta}{=} l\} = b(N-1)k_i\sum_{l=0}^{N-2}\binom{N-2}{l}k_i^l(1-k_i)^{N-2-l} = \{\text{Newton's Binomial Formula}\} = b(N-1)k_i(k_i+(1-k_i))^{N-2} = b(N-1)k_i. \quad (8)$$

If all players choose B, then acting as everyone the ith participant gets $W_i(0,\ldots,0) = (N-1)b$, but when choosing A alone, he gets

$$W_i(1,q^i = (0,\ldots,0)) = a\sum_{m=0}^{N-1}\binom{N-1}{m}k_i^m(1-k_i)^{N-m-1}m = a(N-1)k_i. \quad (9)$$

Thus, for $k_i > \frac{b}{a}$ it happens that $W_i(1,q^i = (0,\ldots,0)) > W_i(0,\ldots,0)$, that is a player with high enough level of coefficient k_i is ready to make a transition to the more effective norm A even if he is alone. It is worth to note that in a homogeneous community, in which all participants have the same level of the coefficient $k_i > \frac{b}{a}$, situation $q = (1,\ldots,1)$, meaning that all participants choose A, appears the only equilibrium as defined by Nash.

A more realistic scenario, however, is the so-called heterogeneous case, when coefficients k_i of all members of the community in question can be different.

THRESHOLD VALUES IN THE MODEL OF HETEROGENEOUS COMMUNITIES

Let us introduce a concept of a *threshold value* to study such heterogeneous communities. Under the threshold value θ_i of the ith participant we will imply the least fraction (of the total number of other participants of the community that have made a transition to norm A) required that the ith participant would have also made a choice in favor of norm A. For example, the ith participant makes a transition to the norm A if he believes that it will be chosen by half of the community, and the jth participant makes so if one third of the community chooses norm *A*. In this case $\theta_i = \frac{1}{2}$, and $\theta_i = \frac{1}{2}$,

We can determine a threshold value $i \in \{1, N\}$ for each number on the basis of the following reasoning. Let the *i*th participant supposes that $\tilde{n} \in \{0, \dots, N-1\}$ other participants will choose norm *A*. Then, the participant's utility function for the case of choosing *B* will take the form:

$$W_i(0, q^i) = b \sum_{m=0}^{N-1} \binom{N-1}{m} k_i^m \times$$
$$\times (1-k_i)^{N-1-m} [\frac{N-1-m}{N-1}(N-\tilde{n}-1)+m] =$$
$$= \overbrace{b \sum_{m=0}^{N-1} \frac{(N-1)!}{m!(N-1-m)!} \cdot \frac{N-1-m}{N-1} k_i^m (1-k_i)^{N-1-m} (N-\tilde{n}-1)}^{I} +$$
$$\underbrace{+ b \sum_{m=0}^{N-1} \binom{N-1}{m} k_i^m (1-k_i)^{N-1-m} m}_{II}.$$

For $m = N - 1$, the corresponding term of series *I* equals 0, therefore the upper limit of the summation can be substituted with $m = N - 2$. According to formula (8) term *II* equals $b(N-1)k_i$, therefore

$$W_i(0, q^i) = b \overbrace{\sum_{m=0}^{N-2} \binom{N-2}{m} k_i^m (1-k_i)^{N-2-m}}^{I} \times$$
$$\times (1-k_i)(N-\tilde{n}-1) + b(N-1)k_i =$$
$$= \{\text{Newton's Binomial Formula applied to } I\} =$$
$$= b \cdot [(1-k_i)(N-\tilde{n}-1) + (N-1)k_i] =$$
$$= b \cdot [(N-\tilde{n}-1) + \tilde{n}k_i].$$

If under the same conditions the *i*th participant chooses norm *A*, he gets

$$W_i(1, q^i) = b \sum_{m=0}^{N-1} \binom{N-1}{m} k_i^m \times$$
$$\times (1-k_i)^{N-1-m} [\frac{N-1-m}{N-1} \cdot \tilde{n} + m] =$$
$$= a \cdot [(1-k_i)\tilde{n} + (N-1)k_i] = a \cdot [\tilde{n} + (N-\tilde{n}-1)k_i].$$

Thus, the *i*th participant will make a choice in favour of norm *A* if $W_i(1, q^i) > W_i(0, q^i)$: $a \cdot [\tilde{n} + (N-\tilde{n}-1)k_i] \geq b \cdot [(N-\tilde{n}-1) + \tilde{n}k_i]$. This condition is equivalent to the following one:

$$\frac{\tilde{n}}{N-1} \geq \frac{b - k_i a}{(a+b)(1-k_i)} \overset{\Delta}{=} \theta_i, \qquad (10)$$

where θ_i is the threshold value, i.e., the minimal fraction of participants who have chosen norm *A*, at which the *i*th participant is also ready to make a choice in favor of norm *A*. Note that when $k_i > \frac{b}{a}$, the threshold value θ_i is negative; this can be interpreted so that for a sufficiently large value of coefficient k_i (determining the level of morality as interpreted in [2]), the *i*th participant is ready to make a transition to a new norm even if he is alone in this decision.

Also note that players with the lowest acceptable level of coefficient $k_i = 0$, the threshold value $\theta_i = \frac{b}{a+b}$. It means that if the fraction of community members who have made a transition to norm *A* exceeds this level, even *players–individualists* make a transition to norm *A*.

To model inhomogeneity of a community relatively a coefficient k_i and correspondingly the threshold value θ_i of each individual, let us consider a distribution function $F(x): \mathbb{R} \to [0,1]$, its values equal to the fraction of the total number of the community members whose threshold value θ_i does not exceed *x*.

If the threshold value θ of some member of the community consider as a random value, that takes some value within interval $\left(-\infty, \frac{b}{a+b}\right]$, then we can consider the function *F*(*x*) as a function of the distribution of the given random value: $F(x) = \mathbf{P}(\theta < x)$, where **P** is a corresponding probability equal to a fraction of the total number of those community members whose threshold value does not exceed *x*.

To find numerical parameters of the distribution of a threshold value at which members of the community are ready to make a transition to a new behavioral norm, we can rely on a special area of statistical research called moral statistics.

Moral statistics covers a broad area of problems related to negative phenomena in a society, such as different kinds of criminality as well as violation of social order and violation of moral-ethical norms. Positive phenomena that characterize morality of the population are also studied by moral statistics; participation of citizens in public organizations on preserving the environment, free donation, participation in rescue services, etc. [23].

For example, if we assume that there is free blood donation at some enterprise or university, then each employee, the enterprise or student has two strategies: to participate in donation (norm *A*), or not (norm *B*). Since it is difficult to formalize the sense of moral satisfaction experienced by a person participating in these activities, finding numerical values of

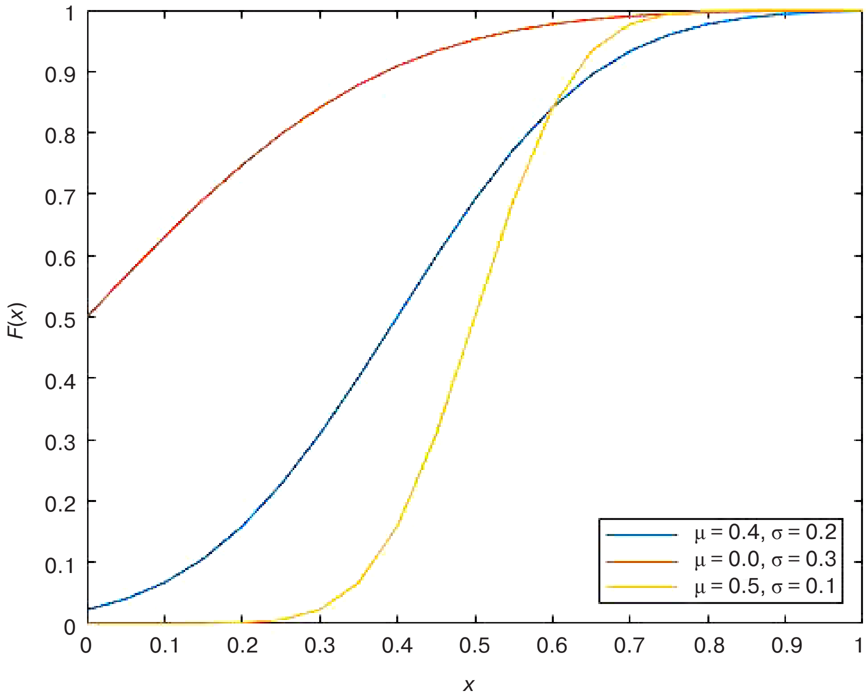

Fig. 1. Distribution function $F(x)$ for threshold value θ_i

coefficients a and b is impossible. However, threshold values, corresponding to the transition from A to B can be found numerically.

To make this, a sociological study among those who came up to donate can be conducted in order to clarify and evaluate the number of their acquaintances who had participated in the donation of blood before they decided to do the same. This will enable us to determine a threshold value for each participant.

Of course, the particular form of a distribution function will be different for each problem. However, because the considered social model is supposedly rely on high enough number of participants, we can take Gaussian function of normal distribution with mathematical expectation μ and dispersion σ^2, where μ and σ are the parameters characterizing a community:

$$F(x) = \frac{1}{\sigma\sqrt{2\pi}} \int_{-\infty}^{x} e^{-(u-\mu)^2/(2\sigma^2)} du.$$

In the above example of blood donation, the average threshold values for all interviewed participants enable to determine mathematical expectation, while mean square deviation determines the dispersion.

The graphs of distribution functions for different parameters μ and σ are shown in Fig. 2. Note that $F(x) = 1$ for $x \geq \frac{b}{a+b}$.

Here, the normal distribution serves as an approach, since in the real world when analyzing social processes, we should take into account a human factor; this is because humans are capable of self-organizing and because they have memory.

A number of contemporary authors (D.O. Zhukov, T.Yu. Khvatova, and others [26, 27]), have researched stochastic dynamics in the social systems based on a cellular automaton; a memory system of participants is taken into account. The memory system is the dependence of a state, in which each participant is present, on the same state in previous moments of time. This model enables via giving initial parameters of a system (for example, the number of contacts between community members) to find a distribution function of threshold values required for the community as a whole to make a transition from one state to another.

Let us analyze the dynamics of a transition between norms A and B.

THE DYNAMICS OF A SOCIAL MODEL

We will analyze the dynamics of a transition of the community members in a certain time interval $[t_0, T]$. We begin our analysis from a model with a discrete time increment Δt, and then will make Δt approaching to zero. Let $N_A(t)$ is the number of community members who choose norm A at time t. We have the following condition: $N_A(t_0) = 0$. Then $\frac{N_A(t)}{N-1}$ gives the fraction of participants making a transition to A at time t. According to the definition of $F(x)$, $F\left(\frac{N_A(t)}{N-1}\right)$ is the fraction of the total number of individuals, whose the threshold value does not exceed $\frac{N_A(t)}{N-1}$. Therefore, the number of individuals making a transition to A at the next moment in time is determined by the following relation: $N_A(t+\Delta t) = F\left(\frac{N_A(t)}{N-1}\right)\cdot N$. If we suppose that the community is large enough, then $N-1 \approx N$. By denoting the fraction of all individuals who have made a transition to norm A at time t as $x(t) \overset{\Delta}{=} \frac{N_A(t)}{N}$, we obtain

$$x(t+\Delta t) = F(x(t)) \qquad (11)$$

or

$$x(t+\Delta t) - x(t) = F(x(t)) - x(t). \qquad (12)$$

It follows from the last expression that if $F(x) > x$, then $x(t)$ and correspondingly $N_A(t)$ increases with time, and if $F(x) < x$, then $N_A(t)$ decreases. If in equality (11) $\Delta t \to 0$, then we obtain a condition for equilibrium: $x(t) = F(x(t))$, at which the number of individuals who have made a transition to norm A stabilizes. The states of the equilibrium correspond to a fixed point in the graph of the function F. These states, however, can be both stable and unstable. To illustrate this feature, let us consider an example.

THE STABILITY OF EQUILIBRIUM STATES

Let us consider a community with the distribution function $F(x)$ of a threshold value θ, shown in Fig. 2. First, we analyze a model with discrete time. According to the initial condition $N_A(t_0) = 0$. Individuals with the negative value of a threshold will be the first to make a transition to norm A, therefore $N_A(\Delta t) = F(0)\cdot N$. In the next moment in time a transition will be made by individuals whose threshold value does not exceed the fraction of participants who chose to make a transition in the previous moment in time. That is $N_A(2\cdot\Delta t) = F\left(\frac{N_A(\Delta t)}{N}\right) = F(F(0))$, and so on. Once $\Delta t \to 0$, we get a continuous process.

Function F, displayed in Fig. 2 has three fixed points and corresponding equilibrium states: point L near zero, points M and P near unity.

The feature of points L and P is that they are stable: if the fraction of the individuals who made a transition to norm A is close to θ_L or θ_P, then it will oscillate closely about these values. Indeed, as shown above, for $x < \theta_L$ $F(x) > x$, therefore, $N_A(t)$ is increasing. And *vice versa*, if $x > \theta_L$. $N_A(t)$ is decreasing.

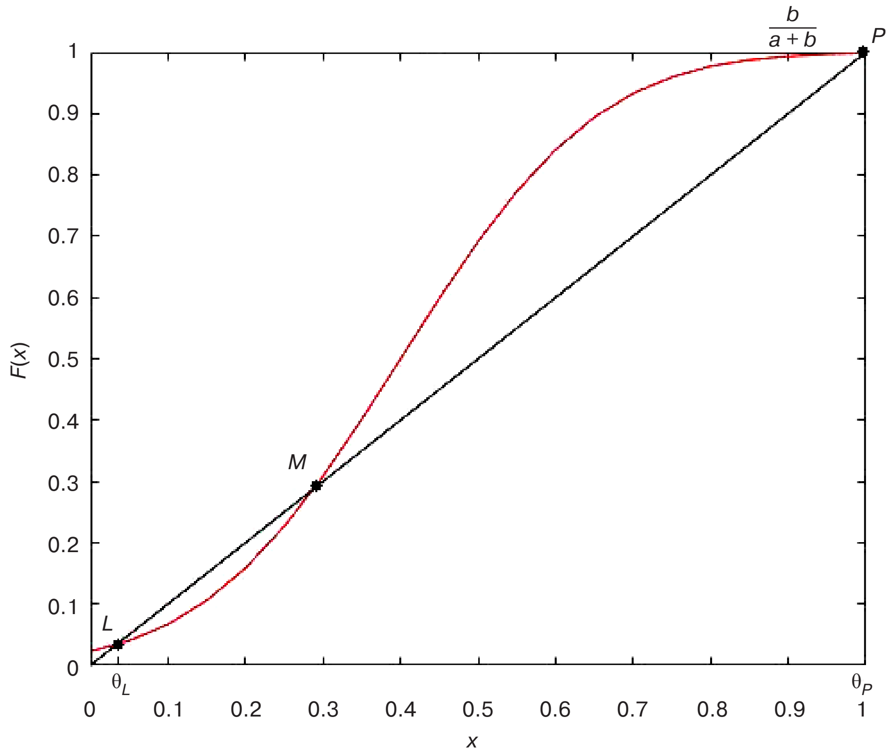

Fig. 2. Distribution function of threshold values with marked points at stable states

The equilibrium point M is unstable: if a fraction of individuals who made a transition to the norm A exceeds θ_M by any negligibly small amount, then $F(x) > x$, and $N_A(t)$ will be growing until the fraction stabilizes at a level corresponding to the nearest equilibrium point $\theta_P = 1$, that will indicate that the community has in general made the transition to the norm A. And vice versa, if fraction $x(t) = \frac{N_A(t)}{N}$ is arbitrary smaller than θ_M, it will continue decreasing until it reaches a stable position near θ_L, that means that the community has "rolled" back to the ineffective norm B. Application of the theory of stability of fixed points to a number of economical, social and biological processes is considered in [28].

Note that for a continuous function of the distribution, the fixed points, in which the equilibrium is reached, will be the points corresponding to changes in the concavity and the convexity of the function. If in a fixed point the function is concave from the left, then the point is stable, if it is convex, it is unstable.

As $F(x) = 1$ at $x > \frac{b}{a+b}$, then the function $F(x)$ is convex for $x \to 1-0$. Therefore the point $x = -1$, corresponding to a scenario when the entire community has made a transition to a new norm A, will always be stable. But if the distribution function F is such that there exists a fixed point with a value less than unity that represents a stable equilibrium, then the community as a whole will never make a transition to a more effective norm, and will be stuck in the vicinity of the nearest to zero equilibrium point.

EDUCATIONAL MODEL

Let us suppose in addition that in a community there is an education program in place. As a result, the moral level in the community increases.

For example, the author knows the fund "For Morality"—The Fund for revival and the development of culture and morality of citizens. The Fund's volunteers along with experienced teachers and scientists with the expertise in education, developed a course of lectures "Morality is the Nation's Strength;" corresponding text book for middle school students was released [29].

The course was approved and supported by experts with reviews from the members of educational enterprises and government of 40 regions across Russia [30], and was also used in facultative classes in middle schools of many regions in Russia [31]. It illustrates a constructive cooperation of the state and society.

One section of the text book titled "Moral traditions of the past is the foundation of modern society" has a subtitle "You will harvest what you seeded". In this section moral-ethical traditions of many peoples are generalized. The essence of these traditions is the necessity for an individual to comprehend a causal relationship between individuals' own actions and their consequences. In other words, before making an action an individual has to think: what happens if others will act towards him or her the same way as the individual is going to act. Will be it good?

Thus, we will consider that behavioral and educational activities contribute in a way that coefficient k_i for each community member increases with time. Of course, the value of coefficient k_i is difficult to formalize, and it is difficult to predict in advance which low it will follow (linearly or nonlinearly). It depends both on the kind of educational activity and on every particular member of a community.

However, we can indirectly estimate the efficacy of educational activity and, correspondingly, the rate of growth of coefficient k_i, based on the rate of change of threshold values θ_i which can be determined by statistical methods that is shown above in the example about blood donation.

Indeed, by differentiating θ_i with respect to k_i in expression (10), we obtain:

$$\frac{\partial\theta_i}{\partial k_i} = \frac{(a+b)(b-a)}{(1-k_i)^2(a+b)^2} < 0,$$

as we assume that $a > b > c$.

Thus, as the coefficient k_i increases, corresponding threshold value θ_i of the ith participant decreases. In other words, the higher the moral level of an individual, the sooner he is ready to a more effective norm A.

This process can be represented in the following form: $\theta_i(t) = \theta_i(t_0) - \phi(t)$, $\phi(t) > 0$, $\frac{\partial\phi}{\partial t} > 0$, $t \in [t_0, T]$. We assume that the function $\phi(t)$ is the same for community members.

We recall that for a fixed state function F is defined as a function of the distribution of a random value θ, which is a threshold value of a randomly chosen community member: $F \overset{\Delta}{=} P(\theta \equiv \theta(t_0) < x)$.

As for the case of the dynamics with education, the function F depends on time; moreover, it is related to its statistical analog in the following way:

$$F(x,t) = P(\theta(t_0) - \phi(t) < x) =$$
$$= P(\theta(t_0) < x + \phi(t)) = F(x + \phi(t)).$$

As $\phi(t) > 0$, the graph of $F(x,t)$ is obtained in every moment in time $t \in [t_0, T]$ from the graph of $F(x)$ through the shifting to the left by a none-negative value $\phi(t)$. This process is illustrated in Fig. 3.

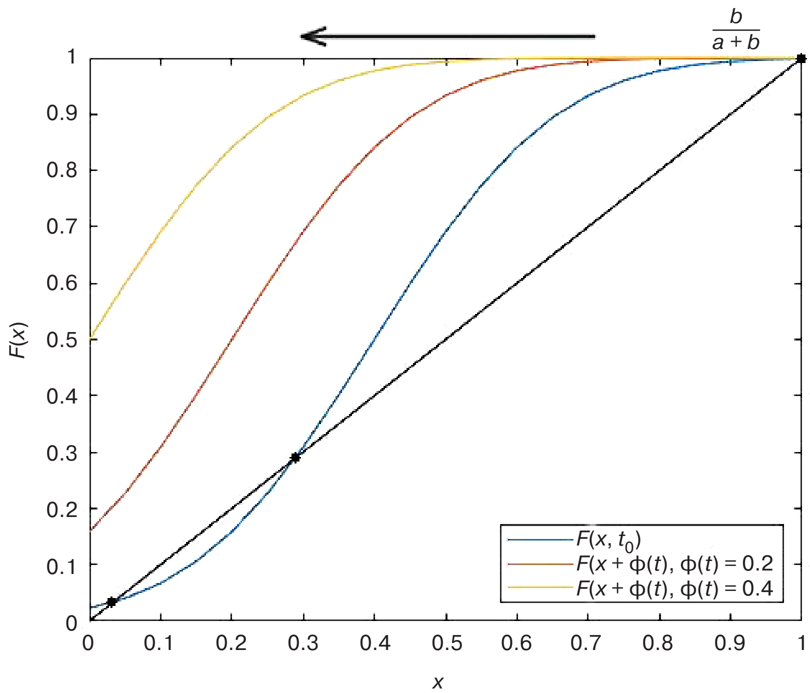

Fig. 3. Change of the distribution function of a threshold value with time in the model with education

Hence, if the distribution $F(x)$ has stable fixed points $x^* < 1$, we can choose such moment in time t', that function $F(x, t')$ will have only one fixed point $x = 1$. Thus, the community, in general, will successfully make a transition to a new norm A.

DISCUSSION

The model of a behavior of individuals, following the principle of morality in the sense of Kant Imperative, developed and presented in a number of papers (for example, [11, 32]), shows an essential difference between the behavior of individuals who we call *homo moralis* and *homo economicus* traditionally studied in papers on the game theory.

Another approach described in the literature is the modeling of collectivism or altruism which supposedly takes into account (with some weighting coefficient) interests of other participants. In a number of publications. For example, in [9, 11], collectivism is modeled so that in a problem with two participants each of them seeks for making maximum of not his initial payoff function $J_i(q)$ but a special utility function $U_i(q) = (1-\alpha)J_i(q) + \alpha J^i(q), \alpha \in [0,1]$, or (as it was generalized for an arbitrary number of participants in [18]) $U_i(q) = (1-\alpha)J_i(q) + \frac{\alpha}{N}\sum_{k=1}^{N} J_k(q), \alpha \in [0,1]$. For a particular case of such a function at $\alpha = 1$ Harsanyi [5] suggested a function in the form $U_i(q) = \frac{1}{N}\sum_{k=1}^{N} J_k(q)$.

There is an essential difference between *homo moralis*, the so-called *individualists* (*homo economicus*), and even *altruists*: while the former (*homo moralis*), when evaluating advantages of the transition of all community members to a new norm of behavior are able to become kind of a catalysis of the process, pioneers, neither *participants–individualists*, no *altruists*, are able play such a role.

This feature allows us to realize that there is some evolutionary stability in this model of behavior that, apparently, can be indirectly confirmed employing methods of evolutionary game theory. As was already mentioned, in this theory repeatable games are accepted for the analysis; and each behavioral strategy can be tested against a success not in one game but in the long run of a number of game situations.

It is exactly the approach that was "taken into service" by American game designer Nicky Case, who created an interactive game that illustrates how different behavioral strategies act in the processes of a repeatable dilemma of a prisoner [33]. The essence of the dilemma is that two players have a choice: to cooperate with or betray a friend. If both players choose to cooperate, they both are on the plus side. But each of them experiences a temptation, because if deception is successful, the one who deceived would get even more than if they cooperated, but the one who was deceived would lose. If both players are tempted and choose to deceive each other, they are punished and get the least favorable game situation.

Nicky Case considered as strategies such behavioral pattern as "naïve"—a type of players who try to continue to cooperate even when they are deceived, "rogues"—who deceive even though others try to cooperate with them, and "imitators"—who begin from cooperation and then just repeat the behavior of the opponent. Then Nicky Case models a society with the help of the so called cellular automaton, in which each cell employs only one of the listed strategies. Interestingly enough that it was cleared out that exactly the last type of behavior—characterized by word "mutuality" which, as Confucius believed, determines the essence of ethical teaching—appears to be the most evolutionary stable.

Nevertheless, based on the above reasoning about the stability of the equilibrium in heterogeneous communities we conclude that under natural conditions a new, more advanced behavioral model may never become a commonly accepted norm. In this case a society is "stuck" in a less effective model of behavior if additional measures are not accepted which favor the growth of a moral level (increase of the coefficient k_i in our model). Such measures, in particular, are educational and social-educational work.

Note, that there is a drawback in the analyzed model: it is difficult to formalize the parameters that were used in the model (for example, the coefficients k_i) that makes it difficult to determine their numerical value necessary for applications.

However, employing different statistical methods [23] will enable us to solve this problem. This makes it possible to use the presented theoretical material, for example, for the evaluation of the efficacy of state-guided work in education of young people and youth development. These are the topics the author is planning to cover in his future works.

CONCLUSIONS

In Conclusions, the investigated social model of the choice between two norms of the behavior enabled to obtain a nontrivial result that the higher the moral level of an individual, the higher the readiness of this individual to make a transition to a more favorable for a community in general behavioral norm. This feature distinguishes such individuals greatly from both the individuals (*individualists*) who seek exclusively for enhancing their personal well-being as well as those (*altruists*) who also take into accountsocietal but momentary interests.

The participants of the *homo moralis* class when choosing their behavioral strategy analyze what happens if the rest members will act the same way as they do. It gives them the opportunity, even though they initially lose, to foresee the advantages of accepting new behavioral patterns as new behavioral norms.

Therefore, we cannot disagree with T.N. Mickushina and M.L. Skuratovskaya [34] arguing that "*the states built on ethical and moral principles had always had economical and political advantage that resulted in prosperity and economic growth*."

With regard to the above said, governmental policy in the area of education and uprising can have significant impact on the rate of economic development because young people educated by employing the best cultural traditions will more effectively cope with challenges and bring new, more advanced communities into life of the society.

REFERENCES

1. O vnesenii izmenenii v Federal'nyi zakon "Ob obrazovanii v Rossiiskoi Federatsii' po voprosam vospitaniya obuchayushchikhsya": Federal'nyi zakon of 31.07.2020, No. 304-FZ (On amendments to the Federal Law "On Education in the Russian Federation 'on the education of students": Federal Law of the Russian Federation of 31.07.2020, No. 304-FZ). (in Russ.). Available from URL: http://www.kremlin.ru/acts/bank/45788
2. Smith A. *An inquiry into the nature and causes of the wealth of nations*. London: W. Strahas & T. Cadell; 1776. 542 p. Reedited: Oxford, UK: Oxford University Press; 1976. 754 p.
3. Smith A. *The theory of moral sentiments*. Strand: A. Millar; 1759. Reedited: Oxford, UK: Oxford University Press; 1759. 412 p.
4. Braithwaite R.B. *Theory of games as a tool for the moral philosopher*. An Inaugural Lecture Delivered in Cambridge on 2 December 1954. Cambridge, UK: Cambridge University Press; 1955. 84 p. Available from URL: https://archive.org/details/theoryofgamesast0000brai

СПИСОК ЛИТЕРАТУРЫ

1. О внесении изменений в Федеральный закон «Об образовании в Российской Федерации по вопросам воспитания обучающихся»: Федеральный закон от 31.07.2020 № 304-ФЗ. URL: http://www.kremlin.ru/acts/bank/45788
2. Smith A. *An inquiry into the nature and causes of the wealth of nations*. London: W. Strahas & T. Cadell; 1776. 542 p. Reedited: Oxford, UK: Oxford University Press; 1976. 754 p.
3. Smith A. *The theory of moral sentiments*. Strand: A. Millar; 1759. Reedited: Oxford, UK: Oxford University Press; 1759. 412 p.
4. Braithwaite R.B. *Theory of games as a tool for the moral philosopher*. An Inaugural Lecture Delivered in Cambridge on 2 December 1954. Cambridge, UK: Cambridge University Press; 1955. 84 p. URL: https://archive.org/details/theoryofgamesast0000brai
5. Harsanyi J.C. Game and decision theoretic models in ethics. In: R.J. Aumann, S. Hart (Eds.). *Handbook of Game Theory with Economic Applications*. Elsevier; 1992. V. 1. Ch. 19. P. 669−707.

5. Harsanyi J.C. Game and decision theoretic models in ethics. In: R.J. Aumann, S. Hart (Eds.). *Handbook of Game Theory with Economic Applications*. Elsevier; 1992. V. 1. Ch. 19. P. 669–707.
6. Harsanyi J.C. Rule utilitarianism and decision theory. *Erkenntnis*. 1977;11:25–53. https://doi.org/10.1007/BF00169843
7. Guseinov A.A. (Ed.). *Istoriya eticheskikh uchenii* (*History of ethical teachings*). Moscow: Akademicheskii proekt; 2015. P. 716–724. (in Russ.).
8. Lyu'is R.D., Raifa Kh. *Igry i resheniya* (*Games and solutions*). Moscow: Izdatel'stvo inostrannroi literatury; 1961. P. 33–67. (in Russ.).
9. Kranz S. Moral norms in a partly compliant society. *Games and Economic Behavior*. 2010;68(1):255–274. https://doi.org/10.1016/j.geb.2009.07.007
10. Alfano M., Rusch H., Uhl M. Ethics, Morality, and Game Theory. *Games*. 2018;9(2):20. https://doi.org/10.3390/g9020020
11. Alger I., Weibull J.W. Strategic behavior of moralists and altruists. *Games*. 2017;8(3):38. https://doi.org/10.3390/g8030038
12. Smith J.M. *Evolution and the theory of games*. Cambridge: Cambridge University Press; 1982. 224 p.
13. Newton J. Evolutionary game theory: A renaissance. *Games*. 2018;9(2):31. https://doi.org/10.3390/g9020031
14. Germeier Yu.B., Vatel' I.A. Games with a hierarchical vector of interests. *Izvestiya AN SSSR. Tekhnicheskaya kibernetika*. 1974;3:54–69 (in Russ.).
15. Gorbaneva O.I., Ugol'nitskii G.A. Price of anarchy and control mechanisms in models of concordance of public and private interests. *Matematicheskaya teoriya igr i ee prilozheniya*. 2015;7(1):50–73 (in Russ.).
16. Gorbaneva O.I. Models of social and private iterests combinining with independed agents. *Matematicheskaya teoriya igr i ee prilozheniya*. 2018;10(4):3–15 (in Russ.).
17. Guseinov A.A. The "golden rule" of morality. *Vestnik Moskovskogo universiteta. Seriya 7. Filosofiya = MSU Vestnik. Series* 7. Philosophy. 1972;4:53–63 (in Russ.).
18. Krasnikov K.E. Modeling of social and ethical principles in terms of game tasks. *Ekonomika: vchera, segodnya, zavtra = Economics: Yesterday, Today and Tomorrow.* 2020;10(2–1):224–240 (in Russ.).
19. Sarkisian R. Team incentives under moral and altruistic preferences: Which team to choose? *Games*. 2017;8(3):37. https://doi.org/10.3390/g8030037
20. Kant I. *Osnovy metafiziki nravstvennosti. Sochineniya v 6 t.* (*Foundations of the metaphysics of morality: in 6 v.*). Moscow: Mysl'; 1965. V. 4. P. 211–310. (in Russ.).
21. Galitskaya Z.I., Il'ina E.Yu., Marchenko O.V., Pavlova G.L. *Nravstvennost' – sila natsii: uchebnoe posobie* (*Morality is the strength of the nation*). Omsk: Fond "Za Nravstvennost'!"; 2016. 212 p. (in Russ.).
22. Ullmann-Margalit E. *The emergence of norms.* Oxford: Oxford University Press; 1977. 206 p.
23. Sobolevskaya M.K., Strekalova S.A. Analysis of indicators of moral statistics in Russia for 2000–2015. *Molodoi uchenyi = Young Scientist*. 2016;20(124):419–421 (in Russ.).
24. Blackman F.F. Optima and limiting factors. *Annals of Botany*. 1905;os–19(2):281–296. https://doi.org/10.1093/oxfordjournals.aob.a089000

6. Harsanyi J.C. Rule utilitarianism and decision theory. *Erkenntnis*. 1977;11:25–53. https://doi.org/10.1007/BF00169843
7. *История этических учений*; под ред. А.А. Гусейнова. М.: Академический проект; 2015. С. 716–724.
8. Льюис Р.Д., Райфа Х. *Игры и решения*. М.: Издательство иностранной литературы; 1961. С. 33–67.
9. Kranz S. Moral norms in a partly compliant society. *Games and Economic Behavior*. 2010;68(1):255–274. https://doi.org/10.1016/j.geb.2009.07.007
10. Alfano M., Rusch H., Uhl M. Ethics, Morality, and Game Theory. *Games*. 2018;9(2):20. https://doi.org/10.3390/g9020020
11. Alger I., Weibull J.W. Strategic behavior of moralists and altruists. *Games*. 2017;8(3):38. https://doi.org/10.3390/g8030038
12. Smith J.M. *Evolution and the theory of games*. Cambridge: Cambridge University Press; 1982. 224 p.
13. Newton J. Evolutionary game theory: A renaissance. *Games*. 2018;9(2):31. https://doi.org/10.3390/g9020031
14. Гермейер Ю.Б., Ватель И.А. Игры с иерархическим вектором интересов. *Известия АН СССР. Техническая кибернетика*. 1974;3:54–69.
15. Горбанева О.И., Угольницкий Г.А. Цена анархии и механизмы управления в моделях согласования общественных и частных интересов. *Математическая теория игр и ее приложения.* 2015;7(1):50–73.
16. Горбанева О.И. Модели сочетания общих и частных интересов независимых агентов. *Математическая теория игр и ее приложения*. 2018;10(4):3–15.
17. Гусейнов А.А. «Золотое правило» нравственности. *Вестник Московского университета. Серия 7. Философия*. 1972;4:53–63.
18. Красников К.Е. Моделирование социально-этических принципов в терминах игровых задач. *Экономика: вчера, сегодня, завтра.* 2020;10(2–1):224–240.
19. Sarkisian R. Team incentives under moral and altruistic preferences: Which team to choose? *Games*. 2017;8(3):37. https://doi.org/10.3390/g8030037
20. Кант И. *Основы метафизики нравственности.* Сочинения в 6 т. М.: Мысль; 1965. Т. 4. С. 211–310.
21. Галицкая З.И., Ильина Е.Ю., Марченко О.В., Павлова Г.Л. *Нравственность – сила нации*: учебное пособие. Омск: Фонд «За Нравственность!»; 2016. 212 с.
22. Ullmann-Margalit E. *The emergence of norms.* Oxford: Oxford University Press; 1977. 206 p.
23. Соболевская М.К., Стрекалова С.А. Анализ показателей моральной статистики России за 2000–2015 гг. *Молодой ученый*. 2016;20(124):419–421.
24. Blackman F.F. Optima and limiting factors. *Annals of Botany*. 1905;os–19(2):281–296. https://doi.org/10.1093/oxfordjournals.aob.a089000
25. Von Bertalanffy L. *Modern theories of development*. Translated and adapted by J.H. Woodger. London: Humphrey Milford; 1933. 232 p.
26. Zhukov D., Khvatova T., Millar C., Zaltcman A. Modelling the stochastic dynamics of transitions between states in social systems incorporating self-organization and memory. *Technological Forecasting and Social Change*. 2020;158:120134. https://doi.org/10.1016/j.techfore.2020.120134

25. Von Bertalanffy L. *Modern theories of development*. Translated and adapted by J.H. Woodger. London: Humphrey Milford; 1933. 232 p.
26. Zhukov D., Khvatova T., Millar C., Zaltcman A. Modelling the stochastic dynamics of transitions between states in social systems incorporating self-organization and memory. *Technological Forecasting and Social Change*. 2020;158:120134. https://doi.org/10.1016/j.techfore.2020.120134
27. Istratov L.A., Smychkova A.G., Zhukov D.O. Modeling group behavior based on stochastic cellular automata with memory and systems of differential kinetic equations with delay. *Vestnik Tomskogo gosudarstvennogo universiteta. Upravlenie vychislitelnaja tehnika i informatika = Tomsk State University Journal of Control and Computer Science*. 2020;51:45‒54 (in Russ.). https://doi.org/10.17223/19988605/51/5
28. Granovetter M. Threshold model of collective behavior. *American Journal of Sociology*. 1978;83:1420‒1443.
29. Vyshel v svet komplekt materialov kursa lektsii "Nravstvennost' – sila natsii". Fond vozrozhdeniya kul'tury, dukhovnosti i nravstvennosti grazhdan "Za nravstvennost'!" (A set of materials for the course of lectures "Morality is the strength of the nation" has been published. Foundation for the revival of culture, spirituality and morality of citizens "For morality!"). 2017. (in Russ.). Available from URL: https://fondzn.org/news/distribution/00207
30. Otvety uchrezhdenii obrazovaniya i gosudarstvennykh organov na kurs lektsii "Nravstvennost' – sila natsii". Fond vozrozhdeniya kul'tury, dukhovnosti i nravstvennosti grazhdan "Za nravstvennost'!" (Responses of educational institutions and government agencies to the course of lectures "Morality is the strength of the nation". Foundation for the revival of culture, spirituality and morality of citizens "For morality!"). 2017. (in Russ.). Available from URL: https://fondzn.org/news/responses
31. Otzyvy i blagodarnosti. Fond vozrozhdeniya kul'tury, dukhovnosti i nravstvennosti grazhdan "Za nravstvennost'!" (Feedback and thanks. Foundation for the revival of culture, spirituality and morality of citizens "For morality!"). 2017. (in Russ.). Available from URL: https://fondzn.org/volunteer/responses
32. Alger I., Weibull J. Homo moralis-preference evolution under incomplete information and assortative matching. *Econometrica*. 2013;81(6):2269‒2302. https://doi.org/10.3982/ECTA10637
33. Case N. Evolyutsiya doveriya (Evolution of trust). Available from URL: https://notdotteam.github.io/trust/
34. Mikushina T.N., Skuratovskaya M.L. The problem of morality and the global crisis of society. In: *The world on the threshold of a new era. As it will be*? *Materials of the II International Scientific and Practical Conference*. Saratov; 2014, p. 74‒79. (in Russ.).

27. Истратов Л.А., Смычкова А.Г., Жуков Д.О. Моделирование социальных процессов группового поведенияна основе стохастических клеточных автоматов с памятью и систем дифференциальных кинетических уравнений с запаздыванием. *Вестник Томского гос. ун-та. Управление, вычислительная техника и информатика*. 2020;51:45‒54. https://doi.org/10.17223/19988605/51/5
28. Granovetter M. Threshold model of collective behavior. *American Journal of Sociology*. 1978;83:1420‒1443.
29. Вышел в свет комплект материалов курса лекций «Нравственность – сила нации». Фонд возрождения культуры, духовности и нравственности граждан «За нравственность!». 2017. URL: https://fondzn.org/news/distribution/00207
30. Ответы учреждений образования и государственных органов на курс лекций «Нравственность – сила нации». Фонд возрождения культуры, духовности и нравственности граждан «За нравственность!». 2017. URL: https://fondzn.org/news/responses
31. Отзывы и благодарности. Фонд возрождения культуры, духовности и нравственности граждан «За нравственность!». 2017. URL: https://fondzn.org/volunteer/responses
32. Alger I., Weibull J. Homo moralis-preference evolution under incomplete information and assortative matching. *Econometrica.* 2013;81(6):2269‒2302. https://doi.org/10.3982/ECTA10637
33. Кэйс Н. Эволюция доверия. 2017. URL: https://notdotteam.github.io/trust/
34. Микушина Т.Н., Скуратовская М.Л. Проблема нравственности и глобальный кризис общества. В сб.: «*Мир на пороге новой эры. Как это будет?*»: материалы II международной научно-практ конф. Саратов; 2014. С. 74‒79.

About the author

Kirill E. Krasnikov, Assistant, Computer Technology Department, Institute of Information Technologies, MIREA – Russian Technological University (78, Vernadskogo pr., Moscow, 119454 Russia). E-mail: krasnikovkirill@yandex.ru. https://orcid.org/0000-0002-2716-0202

Об авторе

Красников Кирилл Евгеньевич, ассистент, кафедра вычислительной техники Института информационных технологий ФГБОУ ВО «МИРЭА – Российский технологический университет» (119454, Россия, Москва, пр-т Вернадского, д. 78). E-mail: krasnikovkirill@yandex.ru. https://orcid.org/0000-0002-2716-0202

Translated by E. Shklovskii

UDC 531.391
https://doi.org/10.32362/2500-316X-2021-9-5-84-94

RESEARCH ARTICLE

Evolution of the rotational motion of a viscoelastic planet with a core on an elliptical orbit

Albina V. Shatina @,
Anastasia V. Starostina

MIREA – Russian Technological University, Moscow, 119454 Russia
@ Corresponding author, e-mail: shatina_av@mail.ru

Abstract. The work is devoted to the study of the evolution of the rotational motion of the planet in the central Newtonian field of forces. The planet is modeled by a body, consisting of a solid core and a viscoelastic shell rigidly attached to it. A limited formulation of the problem is considered, when the center of mass of the planet moves along a given Keplerian elliptical orbit. The equations of motion are derived in the form of a system of Routh equations using the canonical Andoyer variables, which in the unperturbed problem are "action-angle" variables, and have the form of integro-differential equations with partial derivatives. The technique developed by V.G. Vil'ke is used for mechanical systems with an infinite number of degrees of freedom. A system of ordinary differential equations is obtained by the method of separation of motions, which describes the rotational motion of the planet, taking into account the perturbations caused by elasticity and dissipation. An evolutionary system of equations for the "action" variables and slow angular variables is obtained by the averaging method. A phase portrait is constructed that describes the mutual change in the modulus of the angular momentum vector **G** of the rotational motion and the cosine of the angle between this vector and the normal to the orbital plane of the planet's center of mass. A stationary solution of the evolutionary system of equations is found, which is asymptotically stable. It is shown that in stationary motion the angular momentum vector **G** is orthogonal to the orbital plane, and the limiting value of the modulus of this vector depends on the eccentricity of the elliptical orbit. The constructed mathematical model can be used to study the tidal evolution of the rotational motion of planets and satellites. The results obtained in this work are consistent with the results of previous studies in this area.

Keywords: viscoelastic body, Keplerian elliptic orbit, Andoyer variables, averaging method, dissipative evolution of motion

• **Submitted:** 01.03.2021 • **Revised:** 29.03.2021 • **Accepted:** 12.07.2021

For citation: Shatina A.V., Starostina A.V. Evolution of the rotational motion of a viscoelastic planet with a core on an elliptical orbit. *Russ. Technol. J.* 2021;9(5):84–94. https://doi.org/10.32362/2500316X-2021-9-5-84-94

Financial disclosure: The authors have no a financial or property interest in any material or method mentioned.

The authors declare no conflicts of interest.

НАУЧНАЯ СТАТЬЯ

Эволюция вращательного движения вязкоупругой планеты с ядром на эллиптической орбите

А.В. Шатина @,
А.В. Старостина

МИРЭА – Российский технологический университет, Москва, 119454 Россия
@ Автор для переписки, e-mail: shatina_av@mail.ru

Резюме. Работа посвящена исследованию эволюции вращательного движения планеты в центральном ньютоновском поле сил. Планета моделируется телом, состоящим из твердого ядра и жестко прикрепленной к нему вязкоупругой оболочки. Рассматривается ограниченная постановка задачи, когда центр масс планеты движется по заданной кеплеровской эллиптической орбите. Уравнения движения выводятся в форме системы уравнений Рауса с использованием канонических переменных Андуайе, которые в невозмущенной задаче являются переменными «действие-угол» и имеют вид интегро-дифференциальных уравнений с частными производными. Используется методика, разработанная Вильке В.Г. для механических систем с бесконечным числом степеней свободы. Методом разделения движений получена система обыкновенных дифференциальных уравнений, описывающая вращательное движение планеты с учетом возмущений, вызванных упругостью и диссипацией. Методом усреднения получена эволюционная система уравнений относительно переменных «действие» и медленных угловых переменных. Построен фазовый портрет, описывающий взаимное изменение модуля вектора кинетического момента **G** вращательного движения и косинуса угла между этим вектором и нормалью к плоскости орбиты центра масс планеты. Найдено стационарное решение эволюционной системы уравнений, которое является асимптотически устойчивым. Показано, что в стационарном движении вектор кинетического момента **G** ортогонален плоскости орбиты, а предельное значение модуля этого вектора зависит от эксцентриситета эллиптической орбиты. Построенная математическая модель может быть использована для изучения приливной эволюции вращательного движения планет и спутников. Полученные в работе результаты согласуются с результатами ранее проведенных исследований в этой области.

Ключевые слова: вязкоупругое тело, кеплеровская эллиптическая орбита, переменные Андуайе, метод усреднения, диссипативная эволюция движения, метод усреднения

• **Поступила:** 01.03.2021 • **Доработана:** 29.03.2021 • **Принята к опубликованию:** 12.07.2021

Для цитирования: Шатина А.В., Старостина А.В. Эволюция вращательного движения вязкоупругой планеты с ядром на эллиптической орбите. *Russ. Technol. J.* 2021;9(5):84–94. https://doi.org/10.32362/2500-316X-2021-9-5-84-94

Прозрачность финансовой деятельности: Никто из авторов не имеет финансовой заинтересованности в представленных материалах или методах.

Авторы заявляют об отсутствии конфликта интересов.

INTRODUCTION

The motion of a spherically symmetric rigid body relative to the center of mass, which moves in a Keplerian orbit, is a uniform rotation about an axis oriented constantly in an inertial coordinate system. Because none of the bodies of the Solar System is a rigid body, the interaction with the central body, around which a planet revolves, forms bulges on the viscoelastic body of the planet. These bulges tend to align with the planet–central body line. Because of the internal viscous friction, the tidal bulges lag behind and are shifted at a certain angle to the above line. This gives rise to gravitational torque. In addition, the planet is contracted along the axis of rotation. All of this affects the rate of rotation of the planet.

To describe the dynamics of a system, classical tidal theory typically uses the models of rigid body and point particle. The theory is based on various assumptions of the values of tidal bulges and lag angle [1].

To study the tidal evolution of the rotational motion of celestial bodies, V.V. Beletskii proposed a phenomenological model formula for tidal torque [2, 3] based on the model of rigid body for a planet. Later, this formula was confirmed in V.G. Vil'ke's theory of a viscoelastic sphere in a gravitational field [4].

An evolutionary system of equations of the rotational motion of a viscoelastic sphere in a central Newtonian force field in a circular orbit was obtained [5] by the method of separation of motions and averaging [4].

Previously [6], an evolutionary system of equations was derived for the translational–rotational motion of a viscoelastic sphere in the spatial case in the Andoyer–Delaunay variables. For the planets of the Solar System, the rate of evolution of the angular velocity of the proper rotation of a planet is 10^7–10^9 times higher than the rate of evolution of the mean motion in the orbit because their ratio is equal to the ratio of the squares of the radii of the orbit and the planet [4]. In this work, a restricted formulation of the problem was considered, which enabled one to make a more detailed study of the dissipative evolution of the rotational motion of a planet.

In the 1980s–1990s, the rotational motion of a solid body with elastic and dissipative elements was investigated in many works [7–9]. More recently, the tidal evolution of the rotational motion of celestial bodies have been studied using various models of viscoelastic bodies [10, 11].

1. FORMULATION OF THE PROBLEM. EQUATIONS OF MOTION

Let us consider a problem of the motion of a planet relative to the center of mass in a central Newtonian gravitational field. The planet is modeled by a body comprising a rigid core and a viscoelastic shell attached rigidly to the core. In the absence of deformations, i.e., in the natural, undeformed state, the planet occupies region V in the three-dimensional Euclidean space:

$$V = V_0 \cup V_1, \;\; V_0 = \left\{ \mathbf{r} \in E^3 : |\mathbf{r}| \le r_0 \right\},$$
$$V_1 = \left\{ \mathbf{r} \in E^3 : r_0 < |\mathbf{r}| \le r_1 \right\},$$

where r_0 and r_1 are the inner and outer radii of the shell, respectively. Let ρ_0 and ρ_1 be the densities of the core and the viscoelastic shell, respectively, which are assumed to be constant; and m_0 and m_1 are their respective masses.

Let the center of mass of the planet move in a given elliptical orbit. We introduce inertial coordinate system $OXYZ$ with the origin at the attracting center coinciding with one of the foci of the ellipse. Let the OX axis be directed along the radius vector of the perigee; the OZ axis, perpendicular to the plane of the orbit, and the OY axis, so that the unit vectors of the fixed coordinate systems form a right-hand system. To describe the rotational motion of the planet, we introduce moving coordinate system $Cx_1x_2x_3$ and König system of axes $C\xi_1\xi_2\xi_3$ with the origin at the center of mass C of the planet.

The position of point M on the planet in the inertial coordinate system $OXYZ$ is determined by the vector field

$$\mathbf{R}_M(\mathbf{r},t) = \mathbf{R}(t) + \Gamma(t)\big(\mathbf{r} + \mathbf{u}(\mathbf{r},t)\big), \qquad (1.1)$$

$$\mathbf{R}(t) = \frac{1}{m}\int_V \mathbf{R}_M(\mathbf{r},t)\rho dx, \quad \int_{V_1} \mathbf{u} dx = 0, \quad \int_{V_1} \operatorname{rot}\mathbf{u} dx = 0, \; (1.2)$$

where $\mathbf{R}(t)$ is the radius vector of the center of mass of the planet; $\Gamma = \Gamma(t)$ is the operator of transition from the moving coordinate system $Cx_1x_2x_3$ to the König system of axes $C\xi_1\xi_2\xi_3$; $\mathbf{u}(\mathbf{r},t)$ is the elastic displacement vector, which is identically zero for points of the rigid core V_0; $m = m_0 + m_1$; and $\rho = \rho_i$ for $\mathbf{r} \in V_i$, ($i = 0, 1$). Conditions (1.2) uniquely determine the radius vector of the center of mass C of the deformed planet, and also the moving coordinate system $Cx_1x_2x_3$, relative to which the viscoelastic planet does not rotate in the integral sense [4]. In the coordinate system $Cx_1x_2x_3$,

$$\mathbf{u}(\mathbf{r},t) = \big(u_1(\mathbf{r},t),\, u_2(\mathbf{r},t), u_3(\mathbf{r},t)\big), \; \mathbf{r} = \big(x_1, x_2, x_3\big).$$

The problem is solved within a linear model of elasticity theory. The functional of the potential energy of elastic deformations has the form

$$\mathcal{E} = \int_{V_1} \mathcal{E}[\mathbf{u}]dx, \;\; \mathcal{E}[\mathbf{u}] = \alpha_1\left(I_E^2 - \alpha_2 II_E\right), \qquad (1.3)$$

$$\alpha_1 = \frac{E(1-\nu)}{2(1+\nu)(1-2\nu)}, \;\; \alpha_2 = \frac{2(1-2\nu)}{1-\nu},$$
$$\alpha_1 > 0, \;\; 0 < \alpha_2 < 3,$$

$$I_E = \sum_{j=1}^{3} e_{jj}, \;\; II_E = \sum_{k<l}\left(e_{kk}e_{ll} - e_{kl}^2\right),$$
$$e_{kl} = \frac{1}{2}\left(\frac{\partial u_k}{\partial x_l} + \frac{\partial u_l}{\partial x_k}\right), \;\; dx = dx_1 dx_2 dx_3,$$

where E is Young's modulus, and ν is Poisson's ratio of the viscoelastic shell of the planet.

To describe the dissipative properties of the shall of the planet, we use the Kelvin–Voigt model, i.e., assume that the dissipative functional $\mathcal{D}$ is related to functional (1.3) by the expressions

$$\mathfrak{D} = \int_{V_1} \mathfrak{D}[\dot{\mathbf{u}}]dx, \ \mathfrak{D}[\dot{\mathbf{u}}] = \chi\mathcal{E}[\dot{\mathbf{u}}],$$

where $\chi > 0$ is the coefficient of internal viscous friction.

According to the considered restricted formulation of the problem, the center of mass of the problem moves in a Keplerian elliptical orbit, i.e., the radius vector $\mathbf{R}(t)$ of the point C is a given function of time according to the relations

$$\mathbf{R} = R(\cos\vartheta; \sin\vartheta; 0), \quad (1.4)$$

$$R = \frac{a(1-e^2)}{1+e\cos\vartheta}, \ \dot{\vartheta} = \frac{\partial\vartheta}{\partial l}\dot{l} = \frac{(1+e\cos\vartheta)^2}{(1-e^2)^{3/2}}n,$$

$$n = \sqrt{\frac{\gamma}{a^3}}, \ l = n(t-t_0). \quad (1.5)$$

Here, ϑ is the true anomaly; a is the semi-major axis of the orbit; e is the eccentricity; n is the mean motion of the center of mass C of the planet in the orbit; l is the mean anomaly; γ is the standard gravitational parameter ($\gamma = fM_0$, where f is the universal gravitational constant, and M_0 is the mass of the attracting center); and t_0 and t are the initial and current times, respectively.

The kinetic energy of the sphere is represented by the functional

$$T = \frac{1}{2}\int_V \dot{\mathbf{R}}_M^2 \rho dx = \frac{1}{2}\int_V \left[\Gamma^{-1}\dot{\mathbf{R}} + \boldsymbol{\omega}\times(\mathbf{r}+\mathbf{u}) + \dot{\mathbf{u}}\right]^2 \rho dx, \quad (1.6)$$

where $\boldsymbol{\omega}\times(\cdot) = \Gamma^{-1}\dot{\Gamma}(\cdot)$, $\boldsymbol{\omega}$ is the angular velocity of the rotation of the sphere (the coordinate system $Cx_1x_2x_3$). Under conditions (1.2), the functional of the kinetic energy of the viscoelastic sphere takes the form

$$T = \frac{1}{2}m\dot{\mathbf{R}}^2 + \frac{1}{2}\int_V [\boldsymbol{\omega}\times(\mathbf{r}+\mathbf{u})]^2 \rho dx + \int_{V_1} (\boldsymbol{\omega}\times(\mathbf{r}+\mathbf{u}), \dot{\mathbf{u}})\rho_1 dx + \frac{1}{2}\int_{V_1} \dot{\mathbf{u}}^2 \rho_1 dx. \quad (1.7)$$

The potential energy of the gravitational field has the form

$$\Pi = -\gamma\int_V \frac{\rho dx}{\sqrt{(\mathbf{R}+\Gamma(\mathbf{r}+\mathbf{u}))^2}}. \quad (1.8)$$

Because $|\mathbf{R}| \gg |\mathbf{r}+\mathbf{u}|$, the integrand in expression (1.8) can be expanded into a series in powers of $|\mathbf{r}+\mathbf{u}|/R$. Truncating the series after the terms of the second order in $|\mathbf{r}+\mathbf{u}|/R$ and of the first order in $|\mathbf{u}|/R$, we obtain

$$\Pi = -\frac{\gamma m}{R} + \frac{\gamma}{R^3}\int_{V_1} [(\mathbf{r},\mathbf{u}) - 3(\xi,\mathbf{r})(\xi,\mathbf{u})]\rho_1 dx,$$

$$\xi = \Gamma^{-1}\mathbf{R}/R. \quad (1.9)$$

The configurational space of the mechanical system is the direct product $SO(3)\times\mathfrak{B}$, where

$$\mathfrak{B} = \left\{\mathbf{u}:\mathbf{u}\in\left(W_2^1(V_1)\right)^3, \int_{V_1}\mathbf{u}dx = 0, \int_{V_1}\operatorname{rot}\mathbf{u}dx = 0, \mathbf{u}\big|_{|\mathbf{r}|=r_0} = 0\right\},$$

$\left(W_2^1(V_1)\right)^3$ is the Sobolev space [4], and $SO(3)$ is the group of rotations of the three-dimensional Euclidean space. The generalized coordinates $q_1q_2q_3$, which determine the group of rotations $SO(3)$, can be, e.g., the Euler angles.

The components of the angular velocity vector $\boldsymbol{\omega}$ are linear homogeneous functions of the generalized velocities $\dot{q}_i$ $(i=1,2,3)$. Grouping the second-, first-, and zero-degree term of the right-hand side of expression (1.7) that contain the generalized velocities $\dot{q}_i$ $(i=1,2,3)$, one can represent the kinetic energy functional in the form

$$T = T_2 + T_1 + T_0, \quad (1.10)$$

$$T_2 = \frac{1}{2}\int_V [\boldsymbol{\omega}\times(\mathbf{r}+\mathbf{u})]^2 \rho dx, \quad T_1 = \int_{V_1} (\boldsymbol{\omega}\times(\mathbf{r}+\mathbf{u}), \dot{\mathbf{u}})\rho_1 dx,$$

$$T_0 = \frac{1}{2}m\dot{\mathbf{R}}^2 + \frac{1}{2}\int_{V_1} \dot{\mathbf{u}}^2\rho_1 dx. \quad (1.11)$$

Let us obtain the equations of motion of the planet in the form of the Routh equations using the canonical Andoyer variables $(\mathbf{I}, \boldsymbol{\varphi}) = (I_1, I_2, I_3, \varphi_1, \varphi_2, \varphi_3)$ [4, 12] to describe the rotational motion of the coordinate system $Cx_1x_2x_3$ relative to the König axes and the Lagrangian coordinates $u_i(\mathbf{r}, t)$, $i = (1, 2, 3)$ to characterize the deformations of the viscoelastic shell of the planet.

The vector of the angular momentum of the planet about the center of mass is

$$\mathbf{G} = \nabla_\omega T = J[\mathbf{u}]\boldsymbol{\omega} + \mathbf{G}_\mathbf{u}, \quad (1.12)$$

$$J[\mathbf{u}]\boldsymbol{\omega} = \int_V (\mathbf{r}+\mathbf{u})\times[\boldsymbol{\omega}\times(\mathbf{r}+\mathbf{u})]\rho dx,$$

$$\mathbf{G}_\mathbf{u} = \int_{V_1} [(\mathbf{r}+\mathbf{u})\times\dot{\mathbf{u}}]\rho_1 dx. \quad (1.13)$$

Using expression (1.13), the term T_2 of the right-hand side of formula (1.10) is expressed in terms of the inertia tensor $J[\mathbf{u}]$ of the deformed planet as

$$T_2 = \frac{1}{2}(J[\mathbf{u}]\boldsymbol{\omega}, \boldsymbol{\omega}). \quad (1.14)$$

Let us construct the kinetic momentum vector $\mathbf{G}$ at the point C and also construct the plane CMN, which is perpendicular to the vector $\mathbf{G}$ and intersects the plane $C\xi_1\xi_2$ at the straight line CM and the plane Cx_1x_2 at the straight line CN. The variable I_2 is the magnitude of the vector $\mathbf{G}$; and I_1 and I_3 are its projections on the Cx_3 and $C\xi_3$ axes, respectively. The transition from the König system of axes $C\xi_1\xi_2\xi_3$ to the moving coordinate system $Cx_1x_2x_3$ in the Andoyer variables is performed by five successive rotations by angles φ_3, δ_1, φ_2, δ_2, and φ_1 about the $C\xi_3$ axis, the CM axis, the vector $\mathbf{G}$, the CN axis, and the Cx_3 axis, respectively (Fig. 1).

The transition operator Γ in the Andoyer variables is represented as the product of five orthogonal matrices [12]:

$$\Gamma = \Gamma_3(\varphi_3)\Gamma_1(\delta_1)\Gamma_3(\varphi_2)\Gamma_3(\delta_2)\Gamma_3(\varphi_1),$$
$$\cos\delta_1 = I_3/I_2,\ \cos\delta_2 = I_1/I_2,$$

$$\Gamma_3(\varphi_k) = \begin{pmatrix} \cos\varphi_k & -\sin\varphi_k & 0 \\ \sin\varphi_k & \cos\varphi_k & 0 \\ 0 & 0 & 1 \end{pmatrix},$$
$$\Gamma_1(\delta_j) = \begin{pmatrix} 1 & 0 & 0 \\ 0 & \cos\delta_j & -\sin\delta_j \\ 0 & \sin\delta_j & \cos\delta_j \end{pmatrix}.$$

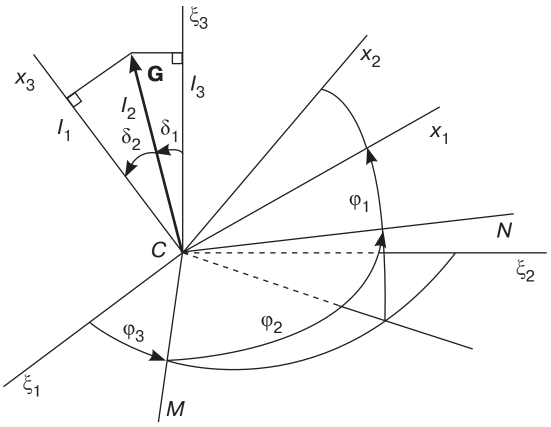

Fig. 1. Andoyer variables

In the coordinate system $Cx_1x_2x_3$,

$$\mathbf{G} = \left(\sqrt{I_2^2 - I_1^2}\sin\varphi_1,\ \sqrt{I_2^2 - I_1^2}\cos\varphi_1, I_1\right), \quad (1.15)$$

$$\xi = \Gamma^{-1}\mathbf{R}/R = \Gamma_3(-\varphi_1)\Gamma_1(-\delta_2)\Gamma_3(-\varphi_2)\times$$
$$\times\Gamma_1(-\delta_1)\Gamma_3(-\varphi_3)(\cos\vartheta, \sin\vartheta, 0)^{\mathrm{T}}. \quad (1.16)$$

It follows from expression (1.12) that

$$\boldsymbol{\omega} = J^{-1}[\mathbf{u}](\mathbf{G} - \mathbf{G}_{\mathbf{u}}). \quad (1.17)$$

Then, from expressions (1.14) and (1.17), the functional T_2 can be represented as

$$T_2 = \frac{1}{2}\left(\mathbf{G} - \mathbf{G}_{\mathbf{u}}, J^{-1}[\mathbf{u}](\mathbf{G} - \mathbf{G}_{\mathbf{u}})\right). \quad (1.18)$$

The Routh functional $\mathfrak{R}$, which depends on the canonical variables $\mathbf{I}$, $\boldsymbol{\varphi}$ and the Lagrangian variables $\dot{\mathbf{u}}, \mathbf{u}$, is defined by the expression

$$\mathfrak{R} = T_2 - T_0 + \Pi + \mathcal{E}[\mathbf{u}], \quad (1.19)$$

where T_2 is given by formula (1.18); and in expression (1.9) for the functional Π of the potential energy of the gravitational field, the vector ξ is given by formula (1.16).

Using expressions (1.11) and (1.18), Routh functional (1.19) can be written as

$$\mathfrak{R} = \frac{I_2^2}{2A} - \frac{1}{A}\left(\mathbf{G}, \int_{V_1}\mathbf{r}\times\dot{\mathbf{u}}\rho_1 dx\right) - \frac{1}{2A^2}\times$$
$$\times(J_1[\mathbf{u}]\mathbf{G}, \mathbf{G}) - \frac{1}{2}m\dot{\mathbf{R}}^2 + \Pi + \mathcal{E}[\mathbf{u}] + \mathfrak{R}^*, \quad (1.20)$$

where A is the moment of inertia of the undeformed planet about the diameter, and $\mathfrak{R}^*$ contains terms of the second and higher orders in the coordinates of the vectors $\mathbf{u}$ and $\dot{\mathbf{u}}$:

$$J_1[\mathbf{u}]\boldsymbol{\omega} = \int_{V_1}\left(\mathbf{r}\times[\boldsymbol{\omega}\times\mathbf{u}] + \mathbf{u}\times[\boldsymbol{\omega}\times\mathbf{r}]\right)\rho_1 dx,$$

$$A = \frac{8\pi}{15}\left[\rho_0 r_0^5 + \rho_1\left(r_1^5 - r_0^5\right)\right].$$

The equations of the rotational motion of the planet in the elliptical orbit are written in the form of the canonical equations in the Andoyer variables and in the form of the d'Alembert–Lagrange variational principle [4]:

$$\dot{I}_k = -\frac{\partial\mathfrak{R}}{\partial\varphi_k},\ \dot{\varphi}_k = \frac{\partial\mathfrak{R}}{\partial I_k},\ k = 1, 2, 3, \quad (1.21)$$

$$\left(-\frac{d}{dt}\nabla_{\dot{\mathbf{u}}}\mathfrak{R} + \nabla_{\mathbf{u}}\mathfrak{R} + \nabla_{\dot{\mathbf{u}}}\mathfrak{D} + \boldsymbol{\lambda}_1, \delta\mathbf{u}\right)_{V_1} +$$
$$+\int_{V_1}\left(\boldsymbol{\lambda}_2, \operatorname{rot}\delta\mathbf{u}\right)dx = 0,\ \forall\delta\mathbf{u}\in(W_2^1(V))^3. \quad (1.22)$$

Here, $\boldsymbol{\lambda}_1$ and $\boldsymbol{\lambda}_2$ are Lagrange's undetermined multipliers generated by conditions (1.2).

2. DEFORMATION OF THE VISCOELASTIC SHELL OF THE PLANET

Let the stiffness of the deformable shell of the planet be high; i.e., the dimensionless parameter $\tilde{\varepsilon} = \omega^2(0)\rho_1 r_1^2 E^{-1}$ be small (where $\omega(0)$ is the magnitude of the initial angular velocity of the planet). Choosing the scales of the dimensional quantities in a certain manner, one can introduce small parameter $\varepsilon = E^{-1}$. As an unperturbed problem, we consider a problem of the motion of a spherically symmetric rigid-body planet in an elliptical orbit. In this case, $\mathbf{u}(\mathbf{r}, t) = 0$, and the parameter ε is assumed to be zero. The equations of the unperturbed motion have the form.

$$\dot{I}_k = 0,\ k = 1,2,3,\ \dot{\varphi}_1 = 0,\ \dot{\varphi}_2 = I_2/A,\ \dot{\varphi}_3 = 0. \quad (2.1)$$

Equations (2.1) describe the uniform rotation of the planet about one of the diameters at the angular velocity $\dot{\varphi}_2 = I_2/A$. At $\varepsilon \neq 0$, according to the method of separation of motions [4], after the damping of the natural vibrations of the viscoelastic sphere, the solution $\mathbf{u}(\mathbf{r}, t)$ is sought as a series of powers of the small parameter ε:

$$\mathbf{u}(\mathbf{r},t) = \varepsilon\,\mathbf{u}_1(\mathbf{r},t) + \varepsilon^2\mathbf{u}_2(\mathbf{r},t) + \cdots \quad (2.2)$$

Lagrange's undetermined multipliers $\boldsymbol{\lambda}_1$ and $\boldsymbol{\lambda}_2$ should also be sought as series of powers of ε:

$$\lambda_1(t) = \lambda_{10}(t) + \varepsilon\lambda_{11}(t) + \cdots,$$
$$\lambda_2(t) = \lambda_{20}(t) + \varepsilon\lambda_{21}(t) + \cdots \quad (2.3)$$

Using expressions (1.20) and (1.9), Eq. (1.22) for the first-approximation function $\mathbf{u}_1(\mathbf{r}, t)$ is transformed to the form

$$\int_{V_1}\left[-\frac{\rho_1}{A}\frac{d}{dt}(\mathbf{G}\times\mathbf{r}) + \frac{1}{2A^2}(\nabla_{\mathbf{u}}J_1[\mathbf{u}]\mathbf{G},\mathbf{G}) - \frac{\gamma\rho_1\mathbf{r}}{R^3} + \frac{3\gamma\rho_1}{R^3}(\xi,\mathbf{r})\xi + \boldsymbol{\lambda}_{10}\right]\delta\mathbf{u}\,dx +$$
$$+\int_{\partial V_1}(\boldsymbol{\lambda}_{20}\times\mathbf{n})\delta\mathbf{u}\,d\sigma - \varepsilon(\nabla_{\mathbf{u}}\mathcal{E}[\mathbf{u}_1 + \chi\dot{\mathbf{u}}_1],\delta\mathbf{u})_{V_1} = 0. \quad (2.4)$$

The derivation of this formula included the use of the divergence theorem in the form:

$$\int_{V_1}\boldsymbol{\lambda}_{20}\,\mathrm{rot}\,\delta\mathbf{u}\,dx = \int_{\partial V_1}(\delta\mathbf{u}\times\boldsymbol{\lambda}_{20})\mathbf{n}\,d\sigma,$$

where ∂V_1 is the boundary of the region V_1, and $\mathbf{n}$ is a normal to ∂V_1.

The variables $(\mathbf{I}, \boldsymbol{\varphi})$ in Eq. (2.4) according to the method of separation of motions are solutions of unperturbed problem (2.1). Therefore, in Eq. (2.4), $\frac{d}{dt}(\mathbf{G}\times\mathbf{r}) = 0.$ Further,

$$(\nabla_{\mathbf{u}}J_1[\mathbf{u}]\mathbf{G},\mathbf{G}) = 2\rho_1 I_2^2\mathbf{r} - 2\rho_1(\mathbf{r},\mathbf{G})\mathbf{G}. \quad (2.5)$$

Successively substituting $\delta\mathbf{u} = \delta\boldsymbol{\alpha}\times\mathbf{r}$ and $\delta\mathbf{u} = \mathbf{a}$, $(\delta\boldsymbol{\alpha}, \mathbf{a} \in E^3)$, into Eq. (2.4) and taking into account that the work done by the elastic and dissipative forces at infinitesimal rotations is zero, we obtain $\boldsymbol{\lambda}_{10} = 0$ and $\boldsymbol{\lambda}_{20} = 0$.

For the last term of the left-hand side of Eq. (2.4), the following equality is valid [4]:

$$\left(\nabla_{\mathbf{u}}\mathcal{E}[\mathbf{u}],\delta\mathbf{u}\right)_{V_1} =$$
$$= \int_{V_1}\nabla\mathcal{E}[\mathbf{u}]\delta\mathbf{u}\,dx + \int_{\partial V_1}\sum_{i=1}^{3}\sigma_{ni}\,\delta u_i\,dx,$$

$$\nabla\mathcal{E}[\mathbf{u}] = -\frac{E}{2(1+\nu)}\left(\frac{1}{1-2\nu}\mathrm{grad}\,\mathrm{div}\,\mathbf{u} + \Delta\mathbf{u}\right),$$

$$\sigma_{ni}[\mathbf{u}] = \frac{E\nu\gamma_i}{(1+\nu)(1-2\nu)}\mathrm{div}\,\mathbf{u} +$$
$$+\frac{E}{2(1+\nu)}\left(\frac{\partial\mathbf{u}}{\partial x_i} + \mathrm{grad}\,u_i,\mathbf{n}\right),$$
$$i = 1,2,3,\ \mathbf{n} = (\gamma_1,\gamma_2,\gamma_3).$$

Thus, the boundary-value problem to determine the first-approximation function $\mathbf{u}_1(\mathbf{r}, t)$ takes the form

$$\varepsilon\nabla\mathcal{E}[\mathbf{u}_1 + \chi\dot{\mathbf{u}}_1] =$$
$$= \rho_1\frac{I_2^2}{A^2}\mathbf{r} - \frac{\rho_1}{A^2}(\mathbf{r},\mathbf{G})\mathbf{G} - \frac{\rho_1\gamma}{R^3}\mathbf{r} + \frac{3\rho_1\gamma}{R^3}(\xi,\mathbf{r})\xi, \quad (2.6)$$

$$\mathbf{u}_1\big|_{|\mathbf{r}|=r_0} = 0,\ \sigma_{ni}\left[\mathbf{u}_1\right]\big|_{|\mathbf{r}|=r_1} = 0,\ i = (1,2,3). \quad (2.7)$$

Boundary conditions (2.7) mean that the movements on the inner boundary of the viscoelastic shell of the planet are zero, and so are the stresses on its outer boundary. The solution of boundary-value problem (2.6)–(2.7) has the form [13, 14]

$$\mathbf{u}_1 = \mathbf{u}_{10} + \mathbf{u}_{11} + \mathbf{u}_{12}, \quad (2.8)$$

$$\mathbf{u}_{10} = \frac{2I_2^2}{3A^2}\rho_1\left(a_1 r^2 + a_2 + \frac{a_3}{r^3}\right)\mathbf{r},$$

$$\mathbf{u}_{11} = \rho_1\left\{p(r_0,r_1,\nu)\left[\frac{I_2^2}{3A^2}\mathbf{r} - \frac{\mathbf{G}}{A^2}(\mathbf{G},\mathbf{r})\right] + \right.$$
$$\left. + q(r_0,r_1,\nu)\left[\frac{I_2^2}{6A^2}r^2 - \frac{1}{2A^2}(\mathbf{G},\mathbf{r})^2\right]\mathbf{r}\right\},$$

$$\mathbf{u}_{12} = -\frac{3\gamma\rho_1}{R^3}\left(1+\frac{3\chi\dot{R}}{R}\right)\times$$
$$\times\left\{p(r_0,r_1,\nu)\left[\frac{1}{3}\mathbf{r}-\xi(\xi,\mathbf{r})\right]+\right.$$
$$\left.+q(r_0,r_1,\nu)\left[\frac{1}{6}r^2-\frac{1}{2}(\xi,\mathbf{r})^2\right]\mathbf{r}\right\}-$$
$$-\frac{3\chi\gamma\rho_1}{R^3}\left\{p(r_0,r_1,\nu)\left[\dot{\xi}(\xi,\mathbf{r})+\xi(\dot{\xi},\mathbf{r})\right]+\right.$$
$$\left.+q(r_0,r_1,\nu)(\xi,\mathbf{r})(\dot{\xi},\mathbf{r})\mathbf{r}\right\}, \qquad (2.9)$$

$$a_1 = -\frac{1+\nu}{5(k+2)}, \quad a_2 = -\frac{a_1 r_1^2\left(4x^5+5k+6\right)}{4x^3+3k+2},$$

$$a_3 = -\frac{a_1 r_1^5 x^3\left((3k+2)x^2-5k-6\right)}{4x^3+3k+2},$$

$$p(r_0,r_1,\nu) = b_1 r^2 + b_2 + \frac{b_3}{r^3}+\frac{b_4}{r^5},$$
$$q(r_0,r_1,\nu) = b_5 + \frac{b_6}{r^5}+\frac{b_7}{r^7},$$

$$k = \frac{2\nu}{1-2\nu}, \quad r = |\mathbf{r}|, \quad x = \frac{r_0}{r_1},$$

$$b_1 = -\frac{(1+\nu)}{\Delta_0}\left\{8(9k+14)x^{10}+80x^7+24(k+1)\times\right.$$
$$\left.\times(5k+11)x^5-5(k+2)(15k+16)x^3+2(3k+8)(5k+4)\right\},$$

$$b_2 = \frac{(1+\nu)r_1^2}{\Delta_0}\left\{8(9k+14)x^{12}+8\left(15k^2+46k+51\right)x^7-\right.$$
$$\left.-\left(63k^2+114k+56\right)x^5+4(3k+8)(4k+3)\right\},$$

$$b_3 = \frac{2(1+\nu)r_1^5 x^3}{\Delta_0}\times$$
$$\times\left\{40x^9-16(k+6)x^7+(21k+16)x^2-10(4k+3)\right\},$$

$$b_4 = \frac{2(1+\nu)(k+1)r_1^7 x^5}{\Delta_0}\times$$
$$\times\left\{24x^7-2(3k+26)x^5+(15k+16)x^2-6(4k+3)\right\},$$

$$b_5 = -\frac{4(1+\nu)(k+1)}{\Delta_0}\times$$
$$\times\left\{60x^7-12(2k+17)x^5+5(3k+26)x^3-2(3k+8)\right\},$$

$$b_6 = 3(k+1)b_3, \; b_7 = -5b_4,$$

$$\Delta_0 = 8(2k+7)(9k+14)x^{10}+200\left(3k^2+8k+7\right)x^7-$$
$$-1008(k+1)^2x^5+25\left(27k^2+56k+28\right)x^3+$$
$$+2(3k+8)(19k+14).$$

In expression (2.9), the time differentiation is performed on the strength of unperturbed system of equations of motion (2.1), and the **G** and ξ values are found from formulas (1.15) and (1.16).

3. PERTURBED SYSTEM OF EQUATIONS OF MOTION

The found solution $\mathbf{u} = \varepsilon\mathbf{u}_1 = \varepsilon(\mathbf{u}_{10} + \mathbf{u}_{11} + \mathbf{u}_{12})$ describes the forced vibrations of the viscoelastic sphere. According to the asymptotic method of separation of motions, this solution should further be substituted into the right-hand sides of Eqs. (1.21) for the "slow" variables after preliminary linearization of them in $\dot{\mathbf{u}}$ and $\mathbf{u}$. This substitution with subsequent calculation of the triple integrals over the spherical layer V_1 gives the perturbed system of equations of the rotational motion of the planet:

$$\dot{I}_1 = -\frac{6\varepsilon\gamma\rho_1^2 D}{A^2R^3}\left(1+3\chi\frac{\dot{R}}{R}\right)\left(\frac{\partial\mathbf{G}}{\partial\varphi_1},\xi\right)(\mathbf{G},\xi)+$$
$$+\frac{6\varepsilon\chi\gamma\rho_1^2 D}{A^2R^3}\left\{\left(\frac{\partial\mathbf{G}}{\partial\varphi_1},\xi\right)(\mathbf{G},\dot{\xi})+\left(\frac{\partial\mathbf{G}}{\partial\varphi_1},\dot{\xi}\right)(\mathbf{G},\xi)\right\}-$$
$$-\frac{6\varepsilon\gamma\rho_1^2 D}{A^2R^3}\left(\frac{\partial\xi}{\partial\varphi_1},\mathbf{G}\right)(\xi,\mathbf{G})-\frac{18\varepsilon\chi\gamma^2\rho_1^2 D}{R^6}\left(\frac{\partial\xi}{\partial\varphi_1},\dot{\xi}\right),$$

$$\dot{I}_j = -\frac{6\varepsilon\gamma\rho_1^2 D}{A^2R^3}\left(\frac{\partial\xi}{\partial\varphi_j},\mathbf{G}\right)(\xi,\mathbf{G})-$$
$$-\frac{18\varepsilon\chi\gamma^2\rho_1^2 D}{R^6}\left(\frac{\partial\xi}{\partial\varphi_j},\dot{\xi}\right), \; j=2,3, \qquad (3.1)$$

$$\dot{\varphi}_1 = \frac{6\varepsilon\gamma\rho_1^2 D}{A^2R^3}\left(1+3\chi\frac{\dot{R}}{R}\right)\left(\frac{\partial\mathbf{G}}{\partial I_1},\xi\right)(\mathbf{G},\xi)-$$
$$-\frac{6\varepsilon\chi\gamma\rho_1^2 D}{A^2R^3}\left\{\left(\frac{\partial\mathbf{G}}{\partial I_1},\xi\right)(\mathbf{G},\dot{\xi})+\left(\frac{\partial\mathbf{G}}{\partial I_1},\dot{\xi}\right)(\mathbf{G},\xi)\right\}+$$
$$+\frac{6\varepsilon\gamma\rho_1^2 D}{A^2R^3}\left(\frac{\partial\xi}{\partial I_1},\mathbf{G}\right)(\xi,\mathbf{G})+\frac{18\varepsilon\chi\gamma^2\rho_1^2 D}{R^6}\left(\frac{\partial\xi}{\partial I_1},\dot{\xi}\right),$$

$$\dot{\varphi}_3 = \frac{6\varepsilon\gamma\rho_1^2 D}{A^2R^3}\left(\frac{\partial\xi}{\partial I_3},\mathbf{G}\right)(\xi,\mathbf{G})+\frac{18\varepsilon\chi\gamma^2\rho_1^2 D}{R^6}\left(\frac{\partial\xi}{\partial I_3},\dot{\xi}\right).$$

Here, $D=\frac{1}{3}k_1(5b_1+b_5)+b_2k_3+\frac{1}{5}k_4(5b_3+b_6)$, $k_1=\frac{4\pi}{35}(r_1^7-r_0^7)$, $k_3=\frac{4\pi}{15}(r_1^5-r_0^5)$, and $k_4=\frac{2\pi}{3}(r_1^2-r_0^2)$.

The variable φ_2 is the fast angular variable, and $\dot\varphi_2\approx I_2/A$. The time differentiation on the right-hand sides of the system of Eqs. (3.2) is performed on the strength of unperturbed system (2.1) and expressions (1.5); i.e.,

$$\dot R=\frac{\partial R}{\partial\vartheta}\dot\vartheta=\frac{ane\sin\vartheta}{\sqrt{1-e^2}},$$

$$\dot\xi=\frac{\partial\xi}{\partial\vartheta}\dot\vartheta+\frac{\partial\xi}{\partial\varphi_2}\dot\varphi_2=\frac{\partial\xi}{\partial\vartheta}\frac{(1+e\cos\vartheta)^2}{(1-e^2)^{3/2}}n+\frac{\partial\xi}{\partial\varphi_2}\frac{I_2}{A}.$$

Here, the vector ξ is defined by formula (1.16) and can be represented as

$$\xi=(\xi_x,\xi_y,\xi_z),$$

$$\xi_x=d_x\cos\varphi_1+d_y\sin\varphi_1,$$

$$\xi_y=-d_x\sin\varphi_1+d_y\cos\varphi_1,\ \xi_z=d_z,$$

$$d_x=\cos\varphi_2\cos(\varphi_3-\vartheta)-\sin\varphi_2\cos\delta_1\sin(\varphi_3-\vartheta),$$

$$d_y=-\sin\varphi_2\cos(\varphi_3-\vartheta)\cos\delta_2-$$
$$-\cos\varphi_2\cos\delta_1\sin(\varphi_3-\vartheta)\cos\delta_2+$$
$$+\sin\delta_1\sin(\varphi_3-\vartheta)\sin\delta_2,$$

$$d_z=\sin\varphi_2\cos(\varphi_3-\vartheta)\sin\delta_2+$$
$$+\cos\varphi_2\cos\delta_1\sin(\varphi_3-\vartheta)\sin\delta_2+$$
$$+\sin\delta_1\sin(\varphi_3-\vartheta)\cos\delta_2.$$

4. EVOLUTIONARY SYSTEM OF EQUATIONS OF MOTION

Next, let us average the right-hand sides of perturbed system (3.1) over the fast angular variables—the Andoyer variable φ_2 and the mean anomaly l—provided that there are no resonances. The averaging procedure is the calculation of the integral

$$\langle *\rangle_{\varphi_2,l}=\frac{1}{(2\pi)^2}\int_0^{2\pi}\int_0^{2\pi}(*)d\varphi_2dl=$$
$$=\frac{1}{(2\pi)^2}\int_0^{2\pi}\int_0^{2\pi}(*)\frac{(1-e^2)^{3/2}}{(1+e\cos\vartheta)^2}d\varphi_2d\vartheta.$$

This gives the evolutionary system of equations of the dynamics of the rotational motion of the viscoelastic planet with then rigid core in the form

$$\dot I_1=\dot I_2\cos\delta_2,$$

$$\dot I_2=-\frac{18\chi\rho_1^2\varepsilon Dn^4}{(1-e^2)^{9/2}}\left\{\frac{I_2}{A}\left[\frac{1}{2}+\frac{3e^2}{4}(1+2\cos^2\varphi_3)+\right.\right.$$
$$+\frac{e^4}{16}(1+4\cos^2\varphi_3)+\cos^2\delta_1\left(\frac{1}{2}+\frac{3e^2}{4}(1+2\sin^2\varphi_3)+\right.$$
$$\left.\left.\left.+\frac{e^4}{16}(1+4\sin^2\varphi_3)\right)\right]-\frac{n\cos\delta_1}{(1-e^2)^{3/2}}\cdot F_2(e)\right\},\qquad(4.1)$$

$$\dot I_3=-\frac{18\chi\rho_1^2\varepsilon Dn^4}{(1-e^2)^{9/2}}\left\{\frac{I_2}{A}\cdot\cos\delta_1\cdot F_1(e)-\frac{n}{(1-e^2)^{3/2}}\cdot F_2(e)\right\},$$

$$\dot\varphi_1=0,\ \dot\varphi_2\approx I_2/A,$$

$$\dot\varphi_3=-\frac{3\rho_1^2\varepsilon DI_2n^2\cos\delta_1}{A^2(1-e^2)^{3/2}}+\frac{9\chi\rho_1^2\varepsilon Dn^4}{A(1-e^2)^{9/2}}\left(\frac{3e^2}{2}+\frac{e^4}{4}\right)\sin2\varphi_3,$$

where $F_1(e)=1+3e^2+\frac{3}{8}e^4$, $F_2(e)=1+\frac{15}{2}e^2+\frac{45}{8}e^4+\frac{5}{16}e^6$.

It follows from the first equation of system (4.1) that the angle between the kinetic momentum vector **G** and the Cx_3 axis is conserved:

$$\cos\delta_2=\frac{I_1}{I_2}=\frac{I_1(0)}{I_2(0)}.$$

The method of separation of motions is based on the physical assumption that the time of damping of the free natural vibrations of the elastic medium at the lowest frequency is longer than the period of these vibrations, but much shorter than the characteristic time of the rigid-body motion [7, 8]. Therefore, the product χn is small ($\chi n\ll1$). Consequently, in the system of Eqs. (4.1), the angular variable φ_3 can be considered fast, and the averaging in φ_3 can be performed. The averaging transforms system (4.1) to the form

$$\dot I_1=\dot I_2\cos\delta_2,$$
$$\dot I_2=-\frac{18\chi\rho_1^2\varepsilon Dn^4}{(1-e^2)^{9/2}}\left\{\frac{I_2}{2A}F_1(e)(1+\cos^2\delta_1)-\frac{n\cos\delta_1}{(1-e^2)^{3/2}}\cdot F_2(e)\right\},$$
$$\dot I_3=-\frac{18\chi\rho_1^2\varepsilon Dn^4}{(1-e^2)^{9/2}}\left\{\frac{I_2}{A}\cdot\cos\delta_1\cdot F_1(e)-\frac{n}{(1-e^2)^{3/2}}\cdot F_2(e)\right\},$$
$$\dot\varphi_1=0,\quad\dot\varphi_2\approx I_2/A,\quad\dot\varphi_3=-\frac{3\rho_1^2\varepsilon DI_2n^2\cos\delta_1}{A^2(1-e^2)^{3/2}}.\qquad(4.2)$$

Let us pass from the variables I_2, I_3 to the dimensionless variables $y=\cos\delta_1=I_3/I_2$, $\omega_0=I_2/An$. Then, from the second and third equations of system

(4.2), the closed autonomous system of differential equations:

$$\dot{y} = -\frac{\varepsilon\Delta}{(1-e^2)^{9/2}} \cdot \frac{(1-y^2)}{\omega_0} \cdot \left\{ \omega_0 \cdot y \cdot F_1(e) - \frac{2F_2(e)}{(1-e^2)^{3/2}} \right\},$$
$$\dot{\omega}_0 = -\frac{\varepsilon\Delta}{(1-e^2)^{9/2}} \cdot \left\{ \omega_0 \cdot (1+y^2) \cdot F_1(e) - \frac{2yF_2(e)}{(1-e^2)^{3/2}} \right\}, \quad (4.3)$$

where $\Delta = 9\chi\rho_1^2 A^{-1} D n^4$.

System (4.3) has an asymptotically stable stationary solution:

$$y = 1, \ \omega_0^* = \frac{F_2(e)}{F_1(e) \cdot (1-e^2)^{3/2}}. \quad (4.4)$$

In the stationary motion, the kinetic momentum vector **G** is orthogonal to the plane of the orbit, and the limiting value of the angular velocity of the proper rotation depends on the eccentricity of the elliptical orbit. Stationary solution (4.4) was previously obtained by Beletskii [2, 3], who modeled a planet by a rigid body and represented the tidal torque by a phenomenological formula.

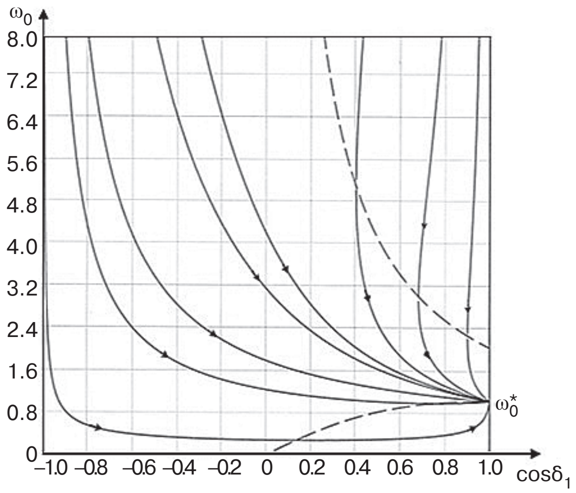

Fig. 2. Phase portrait of the evolutionary system of equations of motion

Figure 2 presents the phase portrait of system (4.3), which was constructed in the Octave environment at $e = 0.05$. The dashed lines are the loci of points at which the integral curves have horizontal and vertical tangent lines. All the integral curves collapse to the same point $(1, \omega_0^*)$. One can distinguish three types of motion: (1) monotonic decrease in the dimensionless angular velocity to a stationary value and monotonic decrease in the angle δ_1 to zero (when the integral curves do not intersect the dashed lines); at points of the straight line $\cos\delta_1 = 0$, there is a transition from the reverse to the direct rotation; (2) monotonic decrease in the angle δ_1 to zero and monotonic decrease in the dimensionless angular velocity to a certain minimum value with subsequent increase to a stationary value (when the integral curves intersect the lower dashed line); and (3) monotonic decrease in the dimensionless angular velocity to a stationary value and monotonic increase in the angle δ_1 to a certain minimum value with subsequent decrease to zero (when the integral curves intersect the upper dashed line).

Previously [15], the methods of separation of motions and averaging were used to study the rotational motion of a satellite with flexible viscoelastic rods in an elliptical orbit.

CONCLUSIONS

In this work, a study was made of the rotational motion of a planet modeled by a body comprising a rigid core and a viscoelastic shell attached rigidly to the core. A system of equations of motion was obtained within the linear theory of elasticity as a system of integro-partial differential equations in the form of Routh equations using the canonical Andoyer variables. The asymptotical method of separation of motions was used to derive a system of sixth-order ordinary differential equations describing the dynamics of the rotational motion of the planet. The averaging method was used to obtain an evolutionary system of equations of motion of the planet in the nonresonance case. It was shown that the motion of the planet tends to a stationary motion, in which the kinetic momentum vector **G** is orthogonal to the plane of the orbit, and its magnitude has a constant value depending on the eccentricity of the elliptical orbit. At zero eccentricity in the stationary motion, the angular velocity of the proper rotation of the planet coincides with the orbital angular velocity, and the axis of rotation of the planet is orthogonal to the plane of the orbit.

The results of this work can be used to investigate the tidal effects of the rotational motion of planets and their satellites.

Authors' contribution. All authors equally contributed to the research work.

REFERENCES

1. Efroimsky M., Williams J.G. Tidal torques. A critical review of some techniques. *Celestial Mechanics and Dynamical Astronomy.* 2009;104:257−289. https://doi.org/10.1007/s10569-009-9204-7
2. Beletskii V.V. *Dvizhenie sputnika otnositel'no tsentra mass v gravitatsionnom pole* (*Satellite motion relative to the center of mass in a gravitational field*). Moscow: MGU; 1975. 308 p. (in Russ.).
3. Beletskii V.V. *Ocherki o dvizhenii kosmicheskikh tel* (*Essays on the motion of cosmic bodies*). Moscow: LKI; 2009. 432 p. (in Russ.). ISBN 978-5-382-00982-7
4. Vil'ke V.G. *Analiticheskaya mekhanika sistem s beskonechnym chislom stepenei svobody: v 2-kh ch.* (*Analytical mechanics of systems with an infinite number of degrees of freedom: in 2 v.*). Moscow: MGU, mekhaniko-matematicheskii fakul'tet; 1997. V. 1. 216 p., V. 2. 160 p. (in Russ.).
5. Vil'ke V.G., Kopylov S.A., Markov Yu.G. Evolution of the rotational motion of a viscoelastic sphere in a central Newtonian field force field. *Journal of Applied Mathematics and Mechanics*. 1985;49(1):24−30. https://doi.org/10.1016/0021-8928(85)90122-4
   [Vil'ke V.G., Kopylov S.A., Markov Yu.G. Evolution of the rotational motion of a viscoelastic sphere in a central Newtonian field force field. *Prikladnaya matematika i mekhanika = Journal of Applied Mathematics and Mechanics*. 1985;49(1):25−34 (in Russ.).]
6. Shatina A.V. Evolution of the motion of a viscoelastic sphere in a central Newtonian field. *Cosmic Research*. 2001;39(3): 282−294. https://doi.org/10.1023/A:1017585722391
   [Shatina A.V. Evolution of the motion of a viscoelastic sphere in a central Newtonian field. *Kosmicheskie issledovaniya = Cosmic Research.* 2001;39(3):303−315 (in Russ.).]
7. Chernous'ko F.L., Akulenko L.D., Leshchenko D.D. *Evolyutsiya dvizhenii tverdogo tela otnositel'no tsentra mass* (*Evolution of motion of a rigid body relative to the center of mass*). Moscow; Izhevsk: Izhevskii institut komp'yuternykh issledovanii; 2015. 308 p. (in Russ.).
8. Chernous'ko F.L. On the motion of solid body with elastic and dissipative elements. *Journal of Applied Mathematics and Mechanics.* 1978;42(1):32−41. https://doi.org/10.1016/0021-8928(78)90086-2
   [Chernous'ko F.L. On the motion of solid body with elastic and dissipative elements. *Prikladnaya matematika i mekhanika = Journal of Applied Mathematics and Mechanics.* 1978;42(1):34−42 (in Russ.).]
9. Sidorenko V.V. The dynamic evolution of a mechanical system with a very rigid linear damper. *Journal of Applied Mathematics and Mechanics*. 1995;59(4):533−539. https://doi.org/10.1016/0021-8928(95)00062-3
   [Sidorenko V.V. The dynamic evolution of a mechanical system with a very rigid linear damper. *Prikladnaya matematika i mekhanika = Journal of Applied Mathematics and Mechanics.* 1995;59(4):562−568 (in Russ.).]
10. Frouard J., Efroimsky M. Precession relaxation of viscoelastic oblate rotation. *Monthly Notices of the Royal Astronomical Society*. 2018;473(1):728−746. https://doi.org/10.1093/mnras/stx2328

СПИСОК ЛИТЕРАТУРЫ

1. Efroimsky M., Williams J.G. Tidal torques. A critical review of some techniques. *Celestial Mechanics and Dynamical Astronomy.* 2009;104:257−289. https://doi.org/10.1007/s10569-009-9204-7
2. Белецкий В.В. *Движение спутника относительно центра масс в гравитационном поле*. М.: Изд-во МГУ; 1975. 308 с.
3. Белецкий В.В. *Очерки о движении космических тел*. М.: Изд-во ЛКИ; 2009. 432 с. ISBN 978-5-382-00982-7
4. Вильке В.Г. *Аналитическая механика систем с бесконечным числом степеней свободы: в 2-х ч*. М.: Изд-во МГУ. Мех.-мат. фак.; 1997. Ч. 1. 216 с., Ч. 2. 160 с.
5. Вильке В.Г., Копылов С.А., Марков Ю.Г. Эволюция вращательного движения вязкоупругого шара в центральном ньютоновском поле сил. *Прикладная математика и механика*. 1985;49(1):25−34.
6. Шатина А.В. Эволюция движения вязкоупругого шара в центральном ньютоновском поле сил. *Космические исследования*. 2001;39(3):303−315.
7. Черноусько Ф.Л., Акуленко Л.Д., Лещенко Д.Д. *Эволюция движений твердого тела относительно центра масс*. М.; Ижевск: Ижевский институт компьютерных исследований; 2015. 308 с.
8. Черноусько Ф.Л. О движении твердого тела с упругими и диссипативными элементами. *Прикладная математика и механика*. 1978;42(1):34−42.
9. Сидоренко В.В. Об эволюции движения механической системы с линейным демпфером большой жесткости. *Прикладная математика и механика*. 1995;59(4):562−568.
10. Frouard J., Efroimsky M. Precession relaxation of viscoelastic oblate rotation. *Monthly Notices of the Royal Astronomical Society*. 2018;473(1):728−746. https://doi.org/10.1093/mnras/stx2328
11. Haus E., Bambusi D. Asymptotic Behavior of an Elastic Satellite with Internal Friction. *Mathematical Physics, Analysis and Geometry.* 2015;18(1): Article No. 14. https://doi.org/10.1007/s11040-015-9184-7
12. Вильке В.Г. *Механика систем материальных точек и твердых тел*. М.: Физматлит; 2013. 268 с. ISBN 978-5-9221-1481-3
13. Лейбензон Л.С. *Краткий курс теории упругости*. М.-Л.: Гостехиздат; 1942. 304 с.
14. Шатина А.В., Шерстнев Е.В. Движение спутника в гравитационном поле вязкоупругой планеты с ядром. *Космические исследования*. 2015;53(2):173–180.
15. Садовникова Е.В., Шатина А.В. Эволюция вращательного движения спутника с гибкими вязкоупругими стержнями на эллиптической орбите. *Российский технологический журнал*. 2018;6(4):89−104. https://doi.org/10.32362/2500-316X-2018-6-4-89-104

11. Haus E., Bambusi D. Asymptotic Behavior of an Elastic Satellite with Internal Friction. *Mathematical Physics, Analysis and Geometry.* 2015;18(1): Article No. 14. https://doi.org/10.1007/s11040-015-9184-7
12. Vil'ke V.G. *Mekhanika sistem material'nykh tochek i tverdykh tel* (*Mechanics of systems of material points and solids*). Moscow: Fizmatlit; 2013. 268 p. (in Russ.). ISBN 978-5-9221-1481-3
13. Leibenzon L.S. *Kratkii kurs teorii uprugosti* (*A Short Course of the Elasticity Theory*). Moscow – Leningrad: Gostekhizdat; 1942. 304 p. (in Russ.).
14. Shatina A.V., Sherstnyov E.V. Satellite motion in the gravitational field of a viscoelastic planet with a core. *Cosmic Research*. 2015;53(2):163–170. https://doi.org/10.1134/S0010952515020082
[Shatina A.V., Sherstnyov E.V. Satellite motion in the gravitational field of a viscoelastic planet with a core. *Kosmicheskie issledovaniya = Cosmic Research*. 2015;53(2):173–180 (in Russ.).]
15. Sadovnikova E.V., Shatina A.V. Evolution of the rotational movement satellite with flexible viscoelastic rods on the elliptic orbit. *Rossiiskii tekhnologicheskii zhurnal = Russian Technological Journal*. 2018;6(4):89–104 (in Russ.). https://doi.org/10.32362/2500-316X-2018-6-4-89-104

About the authors

Albina V. Shatina, Dr. Sci. (Phys.-Math.), Docent, Professor, Department of Higher Mathematics, Institute of Cybernetics, MIREA – Russian Technological University (78, Vernadskogo pr., Moscow, 119454 Russia). E-mail: shatina_av@mail.ru. https://orcid.org/0000-0001-5016-5899

Anastasia V. Starostina, Graduate Student, Senior Lecturer, Department of Higher Mathematics, Institute of Cybernetics, MIREA – Russian Technological University (78, Vernadskogo pr., Moscow, 119454 Russia). E-mail: starostina_a@mirea.ru

Об авторах

Шатина Альбина Викторовна, д.ф.-м.н., доцент, профессор, кафедра высшей математики Института кибернетики ФГБОУ ВО «МИРЭА – Российский технологический университет» (119454, Россия, Москва, пр-т Вернадского, д. 78). E-mail: shatina_av@mail.ru. https://orcid.org/0000-0001-5016-5899

Старостина Анастасия Валерьевна, аспирант, старший преподаватель, кафедра высшей математики Института кибернетики ФГБОУ ВО «МИРЭА – Российский технологический университет» (119454, Россия, Москва, пр-т Вернадского, д. 78). E-mail: starostina_a@mirea.ru

Translated by V. Glyanchenko

UDC 378.1
https://doi.org/10.32362/2500-316X-2021-9-5-95-101

RESEARCH ARTICLE

Influence of the humanitarian environment on improving the quality of training of specialists in a technical university

Olga G. Savka @

MIREA – Russian Technological University, Moscow, 119454 Russia
@ *Corresponding author, e-mail: savka@mirea.ru*

Abstract. The article is devoted to the consideration of the theoretical aspects of the influence of the organization of the humanitarian environment in a technical educational institution on improving the quality of training specialists, increasing their competitiveness in the labor market. The analysis of special literature and generalization of different points of view on the subject of research act as research methods. The humanitarian environment represents a certain content orientation of the educational system of curricula and work programs of disciplines that include the unity of material and spiritual values that are responsible for the formation of students' personality. Each teacher considers this problem in his own way, so the points of view have their own specifics. The humanitarian environment of the university includes a specially organized training system in which a set of specially selected methods and technologies is used to «nurture» a competitive specialist with a set of not only professional, but also personal competencies. The training of specialists in a technical university has its own characteristics related to the further professional implementation of graduates. Students at the stage of training must master special competencies, develop personal qualities, be motivated to study disciplines and master new types of activities. The organization of the humanitarian environment in the organization should be implemented at all levels: university, faculty, at each specific lesson in the study of disciplines, both provided for in the curriculum and extracurricular according to the plan of educational work. For this purpose, it is necessary to maintain and control the interaction of students with all components of the educational environment of a higher educational institution using methods such as: humanitarian technologies, mentoring, organizing a positive psychological climate in the institution, introducing additional educational programs, using active and innovative teaching methods.

Keywords: humanitarian environment, university, humanism, pedagogy, training, personality, self-realization, creative approach

• **Submitted:** 15.07.2021 • **Revised:** 25.08.2021 • **Accepted:** 29.08.2021

For citation: Savka O.G. Influence of the humanitarian environment on improving the quality of training of specialists in a technical university. *Russ. Technol. J.* 2021;9(5):95–101. https://doi.org/10.32362/2500-316X-2021-9-5-95-101

Financial disclosure: The author has no a financial or property interest in any material or method mentioned.

The author declares no conflicts of interest.

НАУЧНАЯ СТАТЬЯ

Влияние гуманитарной среды на повышение качества подготовки специалистов в техническом вузе

О.Г. Савка @

МИРЭА – Российский технологический университет, Москва, 119454 Россия
@ *Автор для переписки, e-mail: savka@mirea.ru*

Резюме. Статья посвящена рассмотрению теоретических аспектов влияния организации гуманитарной среды в образовательном учреждении технической направленности на повышение качества подготовки специалистов и их конкурентоспособности на рынке труда. Проведен анализ специальной литературы и обобщение разных точек зрения на предмет исследования. Гуманитарная среда представляет собой определенную содержательную направленность образовательной системы учебных планов и рабочих программ дисциплин, включающих в себя единство материальных и духовных ценностей, отвечающих за формирование личности студентов. Каждый педагог рассматривает данную проблему в своем ключе, поэтому его точка зрения имеет свою специфику. Гуманитарная среда вуза включает в себя специально организованную систему обучения, в которой применяется комплекс подобранных методов и технологий, позволяющих «взрастить» конкурентоспособного специалиста, обладающего комплексом не только профессиональных, но и личностных компетенций. Подготовка специалистов в техническом вузе имеет свои особенности, связанные с дальнейшей профессиональной реализацией выпускников. Студенты на этапе обучения должны овладеть специальными компетенциями, развить личностные качества, иметь мотивацию к изучению дисциплин и освоению новых видов деятельности. Организация гуманитарной среды в образовательном учреждении должна быть реализована на всех уровнях: вузовском, факультетском, на каждом конкретном занятии по изучению дисциплин, как предусмотренных учебным планом, так и внеучебных, согласно плану воспитательной работы. Для этого необходимо поддерживать и контролировать взаимодействие студентов со всеми компонентами образовательной среды вуза с помощью таких методов, как гуманитарные технологии, наставничество, организация положительного психологического климата в учреждении, введение дополнительных образовательных программ, использование активных и инновационных методов обучения.

Ключевые слова: гуманитарная среда, вуз, педагогика, обучение, личность, профессионализм, самореализация

• **Поступила:** 15.07.2021 • **Доработана:** 25.08.2021 • **Принята к опубликованию:** 29.08.2021

Для цитирования: Савка О.Г. Влияние гуманитарной среды на повышение качества подготовки специалистов в техническом вузе. *Russ. Technol. J.* 2021;9(5):95–101. https://doi.org/10.32362/2500-316X-2021-9-5-95-101

Прозрачность финансовой деятельности: Автор не имеет финансовой заинтересованности в представленных материалах или методах.

Автор заявляет об отсутствии конфликта интересов.

INTRODUCTION

At the current stage of education development, it is extremely important to improve the quality of training of specialists, their personal characteristics, and competitiveness. A promising direction for achieving this goal, in our opinion, is the creation of a special humanitarian environment at the university, which has a huge practical potential. The article analyzed the main aspects of the influence of this environment on improving the quality of training of technical specialists.

It is important to understand that higher professional education is currently undergoing serious changes due to the complete or partial resolution of emerging contradictions. A significant contradiction is the lack of a holistic theoretical concept of higher professional education and the need for society to humanize the education system, which assumes a mutually respectful attitude to each other based on the transfer of social experience into personal experience. However, in many universities, especially of a technical profile, very little attention is paid to the upbringing of a harmonious personality of a future specialist, the primary role belongs to mastering special professional competencies.

The purpose of this study is to analyze the theoretical and methodological aspects of the influence of the humanitarian environment on improving the quality of training specialists in a technical university.

The research methods were as follows: analyzing the various methodological approaches and views on the problem in the current modern literature, and synthesis and generalization of the data obtained.

ANALYSIS OF METHODOLOGICAL APPROACHES TO THE PROBLEM

By analyzing the views of Russian scientists on the concept of the humanitarian educational environment, we can make a preliminary conclusion that without doubt it has an influence on the harmonious formation of the personality of a student, who subsequently will become a specialist and a member of modern society. Next, we will consider different approaches to understanding this definition [1–4].

According to Professor V.L. Kurguzov, humanitarian environment is a certain meaningful humanitarian orientation of the educational system of curricula and work programs of disciplines that include the unity of material and spiritual values responsible for the formation of the personality of students [5].

Doctor of Philological Sciences L.E. Saraskina also reveals the concept of the humanitarian environment in her works. It implies the inclusion of a special educational space in this concept using active teaching methods, with the help of which the basic concepts of the formation, development and realization of personality in the profession are assimilated [6].

The view of Professor R.M. Petruneva is also interesting. It characterizes the humanitarian environment as a complex of pedagogical techniques, technologies and administrative provisions aimed at creating special conditions for the implementation of humanitarian education. It is worth noting that from her point of view, this problem is considered only in the educational sphere, and this is not accidental. This is explained by the fact that it is at the stage of occupational training the personality passes the most important stages of its formation and acquires life norms and values, which will adhere to further [7].

Considering the problem of the organization of the humanitarian environment in a technical university, it is worth noting that it provides for the creation and maintenance of special conditions that contribute to the value-based humanitarian orientation of the student's personality. In this aspect, it is necessary to reflect the most important modern cultural realities, historical traditions in the content of education, in the structure of academic disciplines, as well as in the teaching methods used. Researchers L.G. Viktorova and L.V. Petrov emphasize that, in addition to all the above, it is important to include current achievements of science and technology in the content of education, as well as to rely on the study of accumulated historical experience and cultural traditions [8].

By summarizing the points of view discussed above, it can be noted that the following components can be included in the structure of the humanitarian educational environment: pedagogical activity of a teacher (including planning the content of the studied disciplines, as well as the methods of teaching used); research and extracurricular activities of students (including writing scientific articles, research papers and projects on a required topic and topics interesting to students themselves, as well as taking part in independent works in the studied disciplines and various educational activities, which are necessary for the harmonious development of students' personality); economic and administrative activities of the university's management (regulating the rules of behavior in university and performing the planning of the university's activities, thereby creating optimal conditions for mastering professional competencies).

RESULTS AND DISCUSSION

It is worth noting the special need to create a humanitarian environment of a technical university. This is because the disciplines taught in technical educational institutions are largely removed from the social and cultural components commonly present in humanitarian universities. In such universities, the humanitarian environment is able to be created without compromising the quality of the educational content.

The humanitarian environment at a technical university is designed to ensure that students master the specific competencies necessary to become first-class specialists. In many ways, it is related to an individual's personal qualities, norms, and values. The creation of such an environment can be considered a complex, multicomponent process, which makes implementation problematic without specialized knowledge. During the development of a humanitarian environment, several structural elements can be distinguished: humanitarian elements, general technical and specialized training, modern pedagogical ideas and technologies, and traditions of the university.

In her work, O.L. Kolonitskaya notes that the use of the humanitarian environment in the educational process can significantly improve the quality of professional training of future specialists. However, to achieve this outcome, it is necessary to work comprehensively to create such an environment in a technical university; this includes working at the university, faculty, and subject levels, with implementation of the humanitarian environment in each specific lesson. In addition, the author notes the special role of the administration in this process, with which we cannot disagree [9, 10].

It can be concluded that the humanitarian environment of the university includes an organized training system, which uses a set of individually selected methods and technologies that allow "nurturing" a competitive specialist with a complex of not only professional, but also personal competencies. Also, when organizing this process, it is important to pay attention to the psychological climate in the institution. It should be trusting and favorable for the greatest effectiveness of the formation of the specialist's personality [11].

Under analyzing the possibilities of applying the humanitarian educational environment in a particular lesson, it is impossible not to consider the specifics of the discipline being studied. According to the curriculum, a different number of hours are allocated for each subject, and different competencies are also reinforced. It is important for a teacher to update the presented knowledge, to show their need in the future, whether it is physical culture or a foreign language. All disciplines are interconnected, each of them can have a creative component that will contribute to the student's personal self-development under the supervision of a teacher.

In addition to developing a creative approach to the discipline and the surrounding reality, when choosing the means and methods of teaching, it is important to carry out an individual approach to students, based on their needs and interests. Due to the use of innovative technical means—computer equipment, special programs and websites—it is possible to achieve excellent results of the quality of training. In addition, we should not forget about traditional methods and means of teaching and use them in the educational process.

When implementing the humanitarian educational environment, it is important to organize not only educational, but also extracurricular activities. University events, competitions, meetings, gatherings, group informal communication significantly affects the development of the worldview and the formation of personal qualities of a future specialist. Extracurricular activities should also be regulated and conducted in accordance with the plan of educational work of the university, the direction of training and a specific group. It is not for nothing that much attention has been paid to education recently at all levels of education: school and university. To improve the quality of training of specialists, it is important to accept and maintain the traditions of the university, to instill a certain "image of a student" with a special set of characteristics.

Analyzing all the above, we can generalize and conclude that in order to create and maintain a humanitarian environment in a technical university, it is necessary to support and monitor the interaction of students with all components of the educational environment of a higher educational institution. This can be implemented by applying the following technologies and approaches:

- Special humanitarian teaching technologies (for example, psychotechnologies, anthropopractics)—technologies of creative cooperation between teachers and students. I.V. Bobrysheva describes their application and concludes that it should be based on a number of principles in her writings. Among them, we can distinguish the principle of addressing the real life situation of a student, i.e. the connection of the studied material with the actual and prospective needs and aspirations of the individual; the principle of value-semantic equality, according to which the interaction of the teacher and the student is based on subject-subject relations, mutual respect and equality of positions; the principle of subjectivity, that is, recognition of the value of each person, his identity; the principle of contextuality, implying links between past and present experience and knowledge; the principle of sovereignty, which means non-interference in the personal space of the student, compliance with moral and ethical norms of communication in the "teacher-student" system; the principle of incompleteness, by which we understand the incompleteness of the process of obtaining life experience (socialization) [12, 13].
- Special approaches in the construction of the educational process, such as competence-based, problem-search and cultural approaches. The use of these approaches contributes to the comprehensive development of students' personality, their inculturation, as well as the actualization of existing knowledge about the world.
- Special psychological, social, moral and legal components of the educational process, which guarantees the personal stable development and psychological safety of each student. These components should ensure harmonious relationships between the subjects of the educational process, form students' confidence in the future and their environment [14].
- Systems for the exchange of knowledge and experience among students and teachers within the same university, as well as the development of interuniversity relations. This can be achieved through the organization of a system of mentoring senior courses over junior courses, active supervision of teachers in student groups, coordination of teachers' actions among

themselves; exchange of students studying in similar areas between universities; holding student Olympiads and competitions in the interuniversity space. It is worth noting that this area of work has not yet been sufficiently implemented in many higher educational institutions, but it carries a huge developing potential that will improve the quality of training of future specialists.

- Specially developed additional educational programs that meet the needs of students and modern social realities. Students may be interested in similar areas of training that expand their future professional prospects, which will also increase their competitiveness in the labor market.
- Various methods of intensification and activation of educational, cognitive and creative activities. There are quite a lot of these methods, but they must be chosen based on the characteristics and interests of a particular group and the possibilities of application in the study of the subject. Active teaching methods, problem-based search technologies, a system of mixed and distance learning—all this is at the disposal of the teacher, who must actively use and select working methods.

CONCLUSIONS

Thus, the analysis of scientific literature and our own pedagogical experience allow us to conclude that the creation of a humanitarian educational environment in a technical university is extremely necessary to improve the quality of training specialists. Thanks to specially created conditions, a comprehensive development of the students' personality takes place, a creative and humanitarian view of the surrounding reality is formed. However, to organize a humanitarian environment in a technical university, it is necessary to have the following prerequisites:

- increasing the importance of higher education both for teachers in terms of transferring accumulated experience, and for students who want to become professionals;
- creating special conditions in society and the state that allow the higher education system to develop;
- actualization of the need to create and maintain a humanitarian component in a higher technical educational institution, which allows students to expand their worldview, as well as develop their personal qualities.

From the point of view of functioning, the humanitarian environment of a technical university is the unity of the humanitarian environment from the level of an educational organization to the level of a specific activity, and from the point of view of content, it is a combination of the humanitarian educational environment and a number of necessary auxiliary elements.

Summing up, we can say that a properly organized humanitarian environment in a higher technical educational institution allows you to activate educational and cognitive processes, expand the possibilities of implementing a future specialist, and be based on a creative approach to understanding the surrounding reality. This can be considered a recommendation to higher educational institutions to improve the efficiency of their activities.

REFERENCES

1. Evchenko A.F. Humanitarian environment of a Russian university: problems and prospects. *Zhurnal gumanitarnykh nauk*. 2016;16:32–36 (in Russ.).
2. Martynova E.A. Humanitarian environment of the university as a condition for formation graduate's cultural competence. *Vysshee obrazovanie v Rossii = Higher Education in Russia*. 2013;4:92–95 (in Russ.).
3. Posokhova N.V., Ionov K.A. Development of the humanitarian environment at the university. *Alma Mater* (*Vestnik vysshei shkoly*) = *Alma Mater* (*Higher School Herald*). 2013;5:54–56 (in Russ.).
4. Kovylyaev K.N. Humanitarian environment of high school as factor of formation and development of personality. *Vestnik Moskovskogo universiteta im. S.Yu. Vitte. Seriya 3: Pedagogika. Psikhologiya. Obrazovatel'nye resursy i tekhnologii = Moscow Witte University Bulletin. Series 3: Pedagogy. Psychology. Educational Resources and Technologies.* 2013;1(2):53–58 (in Russ.).

СПИСОК ЛИТЕРАТУРЫ

1. Евченко А.Ф. Гуманитарная среда российского вуза: проблемы и перспективы. *Журнал гуманитарных наук*. 2016;16:32–36.
2. Мартынова Е.А. Гуманитарная среда вуза как условие формирования культурной компетенции выпускника. *Высшее образование в России*. 2013;4:92–95.
3. Посохова Н.В., Ионов К.А. Развитие гуманитарной среды в вузе. *Alma mater* (*Вестник высшей школы*). 2013;5:54–56.
4. Ковыляев К.Н. Гуманитарная среда вуза как фактор формирования и развития личности. *Вестник Московского университет им. С.Ю. Витте. Серия 3: Педагогика. Психология. Образовательные ресурсы и технологии*. 2013;1(2):53–58.
5. Кургузов В.Л. Философия здоровья, гуманитарная культура и образование как детерминанты устойчивого развития. *Проблемы социально-экономического развития Сибири*. 2013;4(14):149–155.

5. Kurguzov V.L. Philosophy of health, humanitarian culture and education as determinants for sustainable development. *Problemy sotsial'no-ekonomicheskogo razvitiya Sibiri = Issues of Social - Economic Development of Siberia*. 2013;4(14):149−155 (in Russ.).
6. Saraskina L.E. *Formation of humanitarian goal-setting of the student's personality at the university*. Thesis. Krasnoyarsk; 1994. 176 p. (in Russ.).
7. Erofeeva M.A. *Pedagogicheskaya sistema professional'noi gotovnosti studentov k gendernomu vospitaniyu shkol'nikov* (*Pedagogical system of students' professional readiness for gender education of schoolchildren*). Moscow: Econ-inform; 2015. 320 p. (in Russ.). ISBN 978-5-9906832
8. Viktorova L.G., Petrova L.V. *Gumanizatsiya i gumanitarizatsiya vysshego obrazovaniya – uslovie formirovaniya gumanitarnogo potentsiala lichnosti intelligenta: monografiya* (*Humanization and humanitarization of higher education – a condition for the formation of a humanitarian personality of an intellectual: monograph*). Krasnoyarsk: Sibirskii gosudarstvennyi tekhnologicheskii universitet; 1999. 45 p. (in Russ.). ISBN 5-8173-0053-2
9. Kolonitskaya O.L. Humanitarian environment is one of the ways to solve the problems of higher professional education. *Molodoi uchenyi = Young Scientist*. 2012;5(40):431−435 (in Russ.).
10. Koval' N.A. Humanitarian environment of the university as a factor in the formation of a specialist. In: *Russia and the East. Learning Society and Social Sustainable Development of the Caspian Region: Proc. III International Scientific Conference*. Astrakhan: ID "Astrakhanskii universitet"; 2005. V. 1, p. 60−64. (in Russ).
11. Wittenbek V.K. Formation of the socio-cultural environment as a condition for the implementation of the competence-based approach of the university. In: *Innovative Development of Russia: Conditions, Contradictions, Priorities. Part 3: Materials of IX International scientific conferences*. Moscow: Moskovskii universitet im. S.Yu. Vitte; 2013, p. 68−75. (in Russ.).
12. Bobrysheva I.V. Humanitarian competence of a teacher as a condition of modern education. *Inform-Obrazovanie = Inform-Education*. 2020;1:15−23 (in Russ.).
13. Andreev A.L. Humanitarian cycle in a technical university and intellectual environments. *Vysshee obrazovanie v Rossii = Higher Education in Russia*. 2015;1:30−36 (in Russ.).
14. Ul'yanova I.V. Formation of the humanistic personality of a PDN employee as an actual factor in the success of his professional activity. *Mezhdunarodnyi zhurnal psikhologii i pedagogiki sluzhebnoi deyatel'nosti = International journal* "*Psychology and Pedagogics Official Activity*". 2018;1:72−77 (in Russ.).
15. Federal'nyi zakon RF ot 29.12.2012 No. 273-FZ "Ob obrazovanii v Rossiiskoi Federatsii" (Federal Law of the Russian Federation of December 29, 2012 No. 273-FZ "On Education in the Russian Federation") (in Russ.). Available from URL: http://www.rg.ru/2012/12/30/obrazovanie-dok.html

6. Сараскина Л.Е. *Формирование гуманитарного целеполагания личности студента в вузе*: дис. … канд. пед. наук. Красноярск; 1994. 176 с.
7. Ерофеева М.А. *Педагогическая система профессиональной готовности студентов к гендерному воспитанию школьников*. М.: Экон-информ; 2015. 320 с. ISBN 978-5-9906832
8. Викторова Л.Г., Петрова Л.В. *Гуманизация и гуманитаризация высшего образования – условие формирования гуманитарного потенциала личности интеллигента*: монография. Красноярск: Сиб. гос. технол. ун-т; 1999. 45 с. ISBN 5-8173-0053-2
9. Колоницкая О.Л. Гуманитарная среда – один из способов решения проблем высшего профессионального образования. *Молодой ученый*. 2012;5(40):431–435.
10. Коваль Н.А. Гуманитарная среда университета как фактор становления специалиста. В сб.: *Россия и Восток. Обучающееся общество и социально-устойчивое развитие Каспийского региона: материалы III Международной научной конференции*. Астрахань: ИД «Астраханский университет»; 2005. Т. 1. С. 60−64.
11. Виттенбек В.К. Формирование социокультурной среды как условие реализации компетентностного подхода в вузе. В сб.: *Инновационное развитие России: условия, противоречия, приоритеты. Часть 3: Материалы IX Международной научной конференции.* М.: Московский университет им. С.Ю. Витте; 2013. С. 68−75.
12. Бобрышева И.В. Гуманитарная компетентность педагога как условие современного образования. *Информ-образование*. 2020;1:15−23.
13. Андреев А.Л. Гуманитарный цикл в техническом вузе и интеллектуальные среды. *Высшее образование в России*. 2015;1:30−36.
14. Ульянова И.В. Формирование гуманистической личности сотрудника ПДН как актуальный фактор успешности его профессиональной деятельности. *Международный журнал психологии и педагогики служебной деятельности.* 2018;1:72−77.
15. Федеральный закон РФ от 29.12.2012 № 273-ФЗ «Об образовании в Российской Федерации». URL: http://www.rg.ru/2012/12/30/obrazovanie-dok.html

About the author

Olga G. Savka, Cand. Sci. (Hist.), Head of the Department of Documentary Studies, History of State and Law, Institute of Management Technologies, MIREA – Russian Technological University (78, Vernadskogo pr., Moscow, 119454 Russia). E-mail: savka@mirea.ru. https://orcid.org/0000-0002-0808-1760

Об авторе

Савка Ольга Геннадьевна, к.и.н., доцент, заведующий кафедрой документоведения, истории государства и права Института технологий управления ФГБОУ ВО «МИРЭА – Российский технологический университет» (119454, Россия, Москва, пр-т Вернадского, д. 78). E-mail: savka@mirea.ru. https://orcid.org/0000-0002-0808-1760

Translated by N. Isaeva

MIREA – Russian Technological University.
78, Vernadskogo pr., Moscow, 119454, Russian Federation.
Publication date September 30, 2021.

«МИРЭА – Российский технологический университет».
119454, РФ, г. Москва, пр-т Вернадского, д. 78.
Дата опубликования 30.09.2021 г.

МИРЭА
Российский
технологический
университет